Model reduction of network systems with structure preservation

Cheng, Xiaodong

Model Reduction of Network Systems with Structure Preservation

Graph Clustering and Balanced Truncation

Xiaodong Cheng

university of groningen

The research described in this dissertation has been carried out at the Faculty of Science and Engineering, University of Groningen, the Netherlands.

The research reported in this dissertation is part of the research program of the Dutch Institute of Systems and Control (DISC). The author has successfully complete the educational program of DISC.

This work was supported by Chinese Scholarship Council (CSC), the Chinese Ministry of Education.

Published by *Ridderprint BV*
Ridderkerk, the Netherlands

Cover picture is designed by starline / Freepik

ISBN (book): 978-94-034-1081-4
ISBN (e-book): 978-94-034-1080-7

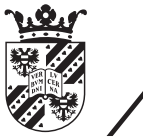

university of groningen

Model Reduction of Network Systems with Structure Preservation

Graph Clustering and Balanced Truncation

PhD thesis

to obtain the degree of PhD at the
University of Groningen
on the authority of the
Rector Magnificus, Prof. E. Sterken,
and in accordance with
the decision by the College of Deans.

This thesis will be defended in public on

Friday 2 November 2018 at 11.00 hours

by

Xiaodong Cheng

born on 10 July 1988
in Anhui, China

Supervisors
Prof. J.M.A. Scherpen
Prof. M. Cao

Assessment committee
Prof. M.K. Camlibel
Prof. H. Sandberg
Prof. P.M.J. Van den Hof

To my family,

Baojie, Zhiyuan,
Zhengwu, Sicui, Xiaojuan

献给我的家人，

妻子宝杰，儿子知远，
父亲成正武，母亲贾思翠，妹妹成小娟

Acknowledgments

It is a pleasure for me to acknowledge the support which I have received during the preparation of this thesis. First of all, I would like express my sincere gratitude to my supervisor Prof. Jacquelien M.A. Scherpen for her thoughtful and patient guidance. She opened the door for me in academia and supported me to go through many difficulties in my research and life. Second, I want to thank my second supervisor Prof. Ming Cao, who has been a good role model, and his advices have greatly improved my PhD experience.

I greatly appreciate the reading committee of this thesis, Prof. Kanat Camlibel, Prof. Henrik Sandberg, and Prof. Paul Van den Hof for their time and effort on evaluating my thesis and providing many constructive comments.

All of my cooperators deserve a very special word of gratitude. Especially, I want to thank Dr. Yu Kawano, Dr. Bart Besselink, Dr. Michele Cucuzzella, Dr. Sebastian Trip, and Dr. Fan Zhang for their excellent collaborations and wonderful friendship. Moreover, I am grateful to Prof. Arjan van der Schaft, Dr. Nima Monshizadeh, Dr. Tudor Ionescu, Dr. Hildeberto Jardón Kojakhmetov, Dr. Pablo Borja, and Petar Mlinarić for their valuable discussions on the topic of this thesis.

My sincere thanks also goes to all of my colleagues and friends in the University of Groningen. Thank you all for making such a pleasant environment for research. I am grateful to my paranymphs, Martijn Dresscher and Yuzhen Qin for the friendship and companion in these years. Many thanks to my Nelson Chan for translating the summary of this thesis into dutch and Alain Govaert for proofreading it. Furthermore, I also want to thank all the other friends I met in Groningen. Because of them, I had many cheerful moments in these four years.

Last but not the least, I would like to thank the support, encouragement and love from my family. This thesis would not have been possible without them.

Xiaodong Cheng
Groningen
September, 2018

Contents

List of symbols and acronyms

CHAPTER 1

Introduction

Due to advancing technology, today's systems tend to be increasingly complex and interconnected. This growing trend is profoundly reshaping the state of the art and future perspectives in engineering. However, meanwhile many challenges arise. With the increasing complexity of networks, system analysis and control design are becoming more difficult. It motivates this thesis which deals with extending the theory of model reduction for control systems to the simplification of dynamic networks. A direct application of classical reduction methods would destroy the interconnection structure of a network, making the obtained reduced-order model not useful for e.g, multi-agent coordination, distributed control and sensor allocation. Thus, the main thread of this research follows the question: how to approximate the model of a dynamic network with a certain accuracy while ensuring the preservation of a network structure?

1.1 Background

Nowadays, booming technologies such as the Internet of things are connecting an enormous number of industrial robots, home appliances, and electronic products embedded with sensors and controllers [171]. There is a clear trend that future systems are becoming more complex and interconnected. In the field of robotics, researchers, inspired by collective intelligence in nature, e.g., swarms of bees, ants, birds, and fish, have designed self-assembling robots [75], that are integrated into far more complex and large-scale systems than before. In [149], the Self-Organizing

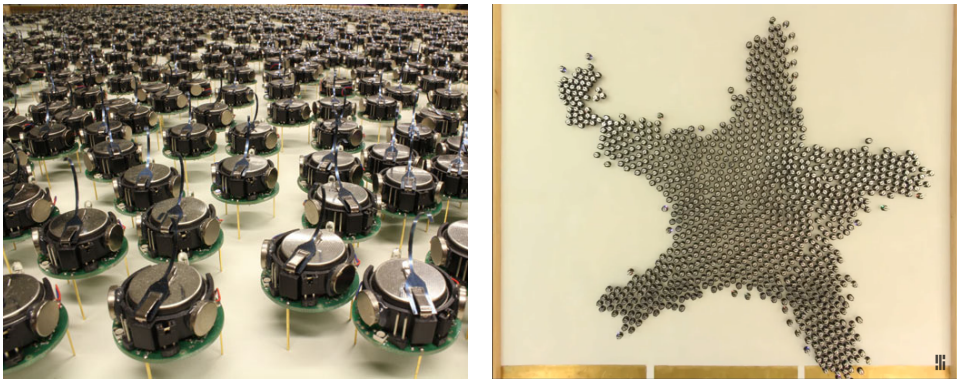

(a) (b)

Figure 1.1: (a) Kilobots designed by Harvard University. These robots are about the size of a coin but can move horizontally on three vibrating legs and communicate with each other via bouncing infrared lights. (b) A swarm of 1024 Kilobots are self-assembling into a complex shape through only local sensing and interactions. (Source: https://spectrum.ieee.org/automaton/robotics/robotics-hardware/a-thousand-kilobots-self-assemble).

Systems Research Group at Harvard University demonstrates a swarm of more than 1000 tiny robots, called Kilobots, which are capable of flexible self-assembly of two-dimensional shapes through programmable local interactions and local sensing, achieving highly complex collective behavior, see Fig. 1.1. The Kilobots communicate with each other by blinking infrared lights on their bodies. By measuring how much the brightness of the infrared light changes, a robot can tell how far away it is from the neighboring robots. Thereby, movements can be made to reach large-scale formations. Large-scale networks of robots have shown a great potential in civil and military applications. For instance, in some disaster rescue missions, a team of drones can search a large area to detect the presence of life via infrared sensors. Power grids are the other applications of complex networks. Modern power grid evolution towards the smart grid integration is certainly expected in the near future. They are experiencing the penetration and integration of a wide array of new electronic devices (e.g., electric cars, autonomous mobile robots), renewable energy sources (e.g., wind farms, solar panels) and distributed control systems [15, 46]. The conventional electricity paradigm, as shown in Fig. 1.2a, is gradually phasing out and superseded by the so-called smart grids, see Fig. 1.2b. The new generation of power networks, improving energy efficiency and optimization of the power supply and demand, however will inevitably become more large-scale and complex,

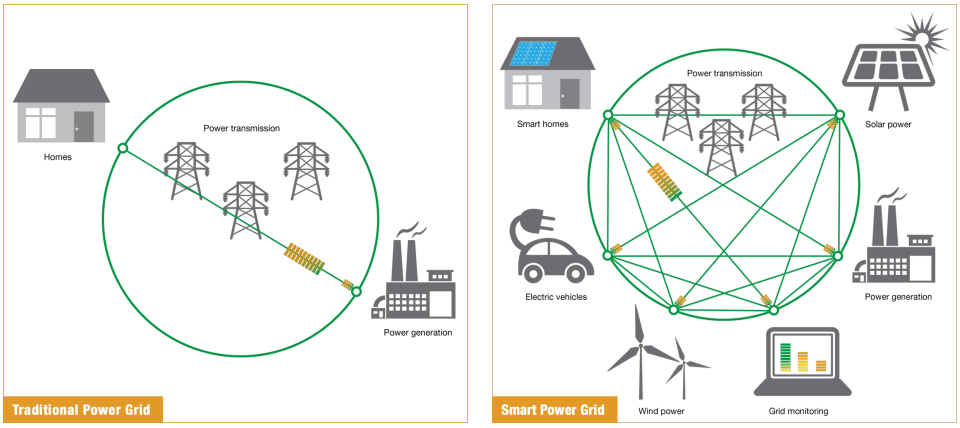

(a) (b)

Figure 1.2: The illustration of the traditional power grids (a) and the future smart power networks (b). The smart grids are equipped with advanced sensing, communication, and control systems that lead to much more complex interactions between electricity providers and consumers. (Source: http://www.news.gatech.edu/features/building-power-grid-future).

with higher variation in the generators, uncertain loads, and denser transmission lines [129, 134, 135].

In real life, systems taking the form of networks are ubiquitous, and the study of such systems have received compelling attention from many disciplines, especially in science and engineering, see e.g., [27, 48, 117, 130, 131, 161] for an overview. Coupled chemical oscillators, cellular and metabolic networks, interconnected physical systems, electrical power grids, see e.g. [12,48,62,79,88,129,163], are only a few examples of systems composed by a number of interconnected dynamical units. To capture the behaviors and properties of dynamic networks, graph theory is often useful. As a network describes the behavior of a collection of interacting dynamical units, a *graph* can interpret the interconnection structure among the dynamical units. In such a graph, *vertices* represent the dynamical units, and *edges* stand for the interactions among them. Using the language of the control community, a dynamical unit in a network is interpreted as a subsystem, or an agent, such that a set of *state* variables, commonly denoted by $x(t)$, can be used to describe the behavior of each unit evolving through time t. Take the multi-robots system in Fig. 1.3 as an example. Each robot in the network is a subsystem, whose states collect its position, velocity, rotation angle and angular velocity. To achieve interactions between the robots, sensors are embedded

Figure 1.3: Mobile robots with Mecanum wheels in DTPA Lap, University of Groningen. With onboard sensors and controllers, each robot can acquire position information of the others and adjust the speed and rotation accordingly to achieve a certain formation.

in each robotic platform in order to measure the relative positions with respect to the others. The acquired information is then delivered to the onboard controller of the robot, and a time-varying command $u(t)$ will be generated by a designed algorithm to control the direction and speed of the wheels. The evolution of state variables of each subsystem depends not only on the values they have at any given time but also on the externally imposed values of the control input signal $u(t)$, resulting in a closed-loop system. In addition, information of the robots is exchanged such that their states are coordinated in order to achieve a team task. In general, a network system is interpreted in a way that multiple subsystems are interacting and showing a form of collective behavior.

Despite that the past few decades have witnessed great progress in understanding and control of complex networks, the exponentially increasing complexity of network systems still poses intense challenges to the management and operation of these systems. For instance, a robotic network composed of a large number of small robots as in Fig. 1.1 can be modeled by a mathematical equation that contains over a thousand state variables. Besides, the immense size and additional interconnections of a power grid may lead to a high-dimensional differential model, which describes the changing states of all the interacting power units. Due to limited computational, accuracy, and storage capabilities, large-scale networks can be extremely difficult for transient analysis, failure detection, distributed controller design, or system simulation. These difficulties are the basic motivation of this research that aims for simplified models of dynamical network systems capturing the main features of the original complex ones. Performing analysis with simplified network models is often meaningful, as we may obtain a clearer understanding of essential structures and properties of complex

networks, avoiding distraction from less important issues. Additionally, simplified models are of lower dimensions, requiring less computational complexity and storage memories. Therefore, they are effective for simulation and prediction of the behaviors of large-scale networks. Moreover, a reduced-order system can be utilized in place of the original complex model for facilitating the design of controllers, which is beneficial since the complexity of a controller is approximately the same as that of the system to be controlled. When working with reduced-order models, it is crucial that the reduction retains the most important characteristics of the original systems. More precisely, the approximation error between a "good" simplified model and the original complex system needs to be small enough. Then, how to find a "good" simplified model for a large-scale network system? This question naturally leads to an important branch in the field of system and control, called model reduction.

1.2 Problem Statement

In this thesis, we investigate model reduction techniques for an important class of networks, namely *consensus networks*, in which subsystems are reaching certain agreements via *diffusive couplings* [145]. Formation control of mobile vehicles, coordination of distributed sensors, or balancing in chemical kinetics can be viewed as different applications of consensus networks [91,92,159]. In a consensus network, the structure of the diffusive couplings among subsystems is commonly captured by a *Laplacian* matrix. Given a complex dynamical network consisting of identical subsystems, the key problem we would like to explore in this thesis is how to construct a simplified network preserving the diffusive couplings, or equivalently how to retain a Laplacian structure in the reduced-order model.

Note that the complexity of a dynamical network comes from two aspects: the large scale of the network (i.e., a large number of subsystems) and the high dimensional integrated subsystems, which then naturally split the key problem of this thesis into three sub-problems:

- How to reduce the size of the network? Specifically, we aim to find a simplified dynamical model that can be interpreted as a dynamical network with a fewer number of diffusively coupled subsystems. This reduced-order network model also captures the main input-output feature and synchronization property of the original network. (Part I)

- How to reduce the complexity of nodal dynamics? Particularly, we aim to find the lower-order approximation of each subsystem while preserving the synchronization property of the overall network. (Chapter 8)

- How to reduce the size of the network and the dimension of individual subsystems in a unified framework? The model reduction problem aims to generate a simplified network model that has reduced-order subsystems and a reduced-size network simultaneously. The obtained model is also desired to achieve a small input-output approximation error. (Chapter 7)

1.3 Literature Review and Contributions

In the past few decades, a variety of theories and techniques of model reduction have been investigated and developed. These techniques can be roughly classified into two categories: Krylov-subspace methods (also known as moment matching) and singular value decomposition (SVD) based approaches [7]. The schemes in the first category can be found in e.g., [8, 10, 64, 69, 71, 82, 153], which are generally developed on the notion of Krylov projectors or interpolation theory. The latter category uses theories of balancing and Hankel operator, including balanced truncation [25, 65, 70, 128, 150, 156, 157], the Hankel Norm Approximation [66, 181] and the Singular Perturbation Approximation [101, 112]. Amongst all the classic reduction methods, balanced truncation is one of the most well grounded and commonly used schemes for control systems. Its theory for stable linear systems can be traced back to early 1980s [128]. The reduction procedure is accomplished with two steps. The first step is called *balancing*, which makes a coordinate transformation to simultaneously diagonalize the *controllability and observability Gramians* of the system and make them equal. Then it is well known that in the new coordinate, the diagonal entries of the Gramians are so-called *Hankel singular values* that indicate the degrees of controllability and observability of the states [128]. The second step is then to truncate the state variables that are relatively difficult to be controlled and observed from the balanced system. From both theoretical and practical viewpoint, the balanced truncation approach is of great importance as it preserves stability and allows for an *a priori* error bound for the approximation error.

Even though the above conventional reduction methods can provide systematic and efficient procedures to generate reduced-order models that well approximate the input-output behavior of original complex systems, the direct application of them to network systems are still restricted as the interconnection topology of a network is completely lost through reduction procedures [85]. Since the conventional methods do not take into account the interconnection structure of a network, the obtained projections will mix the states of vertices and the reduced-order models cannot be interpreted as networks of interconnected subsystems anymore. Such models are not preferable for further analyses and applications of complex networks, including synchronization analysis [53, 107, 129], community and modularity detection [132, 133],

distributed controller design [6,29,108,160], and sensor allocation [104,159]. Thus, for large-scale complex network systems, it is essential to seek for a structure-preserving model reduction scheme such that the reduced-order model can be interpreted as a network of interconnected subsystems.

In the literature, we observe that there exist two directions for model reduction of complex network systems. The first one aims to lower the dimension of the individual subsystem. Representatives are found in e.g., [125,152], where the setup of network models are interconnected higher-dimensional subsystems, and the approximation is applied to each subsystem such that certain properties of the overall network, such as synchronization and stability, are preserved. The second direction for the approximation of large-scale networks is to reduce the complexity of the network topology, i.e., to find a smaller-sized network with fewer vertices to approximate the original network of many vertices. The mainstream methodology to handle such a problem is called *graph clustering* [94,154], which has been widely used in many other fields, including machine learning, data mining, and computer graphics [2,98,114]. In recent years, this methodology has shown its potential to tackle the structure preserving model reduction of dynamic networks. The approach has an insightful physical interpretation of the reduction process: Partition a network into several nonoverlapping clusters and merge the vertices in each cluster into a single vertex, which potentially preserve the essential spatial structure of the network. A preliminary framework is introduced in [87], where the clustering-based model reduction is interpreted as a Petrov-Galerkin approximation. However, it leaves an open question of how to find a "good" clustering such that the reduced-order network systems achieve an accurate approximation. Actually, this is the most difficult part of applying such methods, as finding an optimal clustered network is roughly an NP-hard problem even for static graphs [2,94]. Various methods are proposed to find an appropriate clustering for dynamic networks. The results in [96,124,126] consider the *almost equitable partition* (AEP) as a clustering of the underlying network, and derive an explicit $\mathcal{H}_2$ error expression when a specific output matrix is assumed, but finding AEPs itself is rather difficult and computationally expensive. A combination of the Krylov subspace method with graph clustering is proposed by [121,122], where a reduced-order model is found by the Iterative Rational Krylov Algorithm (IRKA), and then the partition of the network is obtained by the QR decomposition with column pivoting on the projection matrix. [20,21] consider so-called edge dynamics of networks with a tree topology such that the importance of each edge can be characterized. Then, vertices linked by the less important edges are iteratively clustered. Nonetheless, the reduction process and error bound are heavily reliant on the tree topology. An alternative approach is proposed in [84,85] to simplify positive networks. The notion of *reducibility* is introduced, which is characterized by the

uncontrollability of clusters. Merging the reducible clusters leads to a reduced-order model that still maintains the network structural information.

This thesis will discuss two reduction techniques, namely graph clustering, and balanced truncation in Part I and Part II, respectively. The graph clustering approach essentially reduces the complexity of the interconnection structure of a network, i.e., reducing the number of interacting subsystems in the network. However, the method based on balanced truncation can also reduce the dimension of each subsystem.

The clustering-based techniques proposed in this thesis are inspired by early pioneering works in [21, 84, 87, 126]. The model reduction framework is established on Petrov-Galerkin projection, where the projection matrices are constructed using the characteristic matrix of network clustering. The proposed framework results in a reduced Laplacian matrix in the reduced-order model. Thus, it can be employed to structure preserving model reduction of different types of networks, including multi-agent systems, second-order network systems, and directed networks. A novel scheme is proposed to find an appropriate clustering for dynamic networks. Specifically, we describe the behaviors of vertices by the transfer functions mapping from external inputs to individual vertex states and define the dissimilarities of vertices by the norms of the transfer function deviations. Note that in the frequency domain, the behaviors of vertices are invariant to the changes of external input signals, and the dissimilarities only depend on the distribution of input signals and the interconnection structure of the network. In other words, no matter what inputs are injected into the network, the measurement of the dissimilarity between any two vertices remains the same. With the information of dissimilarities of each pair of vertices, algorithms are easily designed to place those vertices with similar behaviors into same clusters. In contrast to [84, 85], where the clustering selection requires an error bound relying on the positivity of the network system, the proposed framework can be applied to more general network systems, which are not limited to positive systems or tree networks. Basically, for any linear networks, transfer functions can be used for characterizing the dissimilarities among vertices. Unlike the reducibility in [84, 85], the dissimilarity is a pairwise notion, which is a meaningful extension and generalization of the definition of distance in static graphs. Owing to the consistency, many existing clustering algorithms in computer graphics and data mining, including hierarchy clustering, K-means clustering, can be adapted to efficiently generate an appropriate clustering for dynamic networks. Another contribution of this thesis is to propose the notion of *pseudo Gramians* that are employed to efficiently evaluate the pairwise dissimilarities and the approximation error between the original and reduced-order network systems. The concepts are feasible for general semistable systems and can be viewed as the generalization of standard Gramians for asymptotically stable systems. Moreover, the pseudo Gramians are characterized by a set of Lyapunov equations.

The second reduction technique that we develop for dynamic networks is based on generalized balanced truncation. As mentioned before, network structures potentially eclipse if applying the standard balanced truncation. However, the generalized version may allow us to maintain a network interpretation. In this thesis, we apply generalized balanced truncation to reduce the dimensions of synchronized Lur'e networks, which are composed of multiple identical Lur'e-type subsystems. The reduction is performed on each individual nonlinear subsystems while the interconnection topology is untouched. By carefully selecting the generalized Gramians, we are able to preserve the robust synchronization property of a Lur'e network. Besides, we propose a framework to simplify networked linear passive systems based on generalized balanced truncation that reduces the complexity of network structures and individual agent dynamics simultaneously. We find that a diagonalizable matrix is similar to a Laplacian matrix if it satisfies a spectral condition, which provides us a network reduction method: we reduce a network by generalized balanced truncation that preserves the spectral condition in the reduced-order model, which then can be reconstructed as a simplified network system only by a coordination transformation.

1.4 Thesis Outline

The remainder of the thesis is structured as follows. Chapters 2 contains important notations and definitions, and provides background information on graph theory and model reduction. The subsequent chapters present methods of model reduction of different dynamical network systems with structure preservation. The methods are proposed in two frameworks, namely the clustering-based projection and generalized balanced truncation.

Chapter 3 proposes a general framework for structure-preserving model reduction of a second-order network system based on graph clustering. The notion of nodal dissimilarity is proposed which characterizes the difference between nodes with second-order dynamics. A greedy hierarchical clustering algorithm is proposed to place those vertices with similar behaviors into the same clusters. The simplified system preserves a second-order form as well as a network structure. Furthermore, this chapter generalizes the definition of Gramians for asymptotically stable systems to semistable systems and based on that, an efficient method to characterize the vertex dissimilarities is developed. The materials in this chapter are based on the conference and journal papers [35, 39, 45].

Chapter 4 applies the clustering-based model reduction to power networks with distributed controllers. The studied system and controller are modeled as second-order and first-order ordinary differential equations, which are coupled as a closed-loop model. By analyzing the influence of disturbances to the power units, we

characterize the behavior of each node (generator or load) in the power network and define a novel notion of dissimilarity between two nodes. The reduction methodology is developed based on separately clustering the generators and loads according to their behavior dissimilarities. The material in this chapter is based on the journal papers [35, 42].

Chapter 5 investigates a model reduction scheme for multi-agent systems, which is a broader class of network system consisting of linear time-invariant subsystems. The dissimilarity is measured based on the output errors of the subsystems with respect to external inputs of the network. The proposed method is to simplify the topology of the network such that the dimension of the system is reduced. A computable bound of the approximation error between the full-order and reduced-order models is provided. This chapter also provides a special result for reduction of networked single integrators. The materials in this chapter are based on the conference and journal papers [33, 34, 36].

Chapter 6 explores a model reduction problem for linear directed network systems, in which the interconnections among the vertices are described by general weakly connected digraphs. The method focuses on selecting a suitable graph clustering to simply the directed graph topology. The concepts of vertex clusterability is proposed to identify feasible clusterings that guarantee the boundedness of the approximation error. The materials in this chapter are based on the conference and journal papers [41, 43].

Chapter 7 studies a novel model order reduction methodology for network systems based on generalized balanced truncation. The network model consists of identical linear passive subsystems. The proposed method then simultaneously reduces the complexity of the network structure and individual agent dynamics, and it preserves the passivity of the subsystems and the synchronization of the network. Moreover, it allows for the *a priori* computation of a bound on the approximation error. The materials in this chapter are based on the conference and journal papers [37, 40].

Chapter 8 applies balanced truncation to a class of nonlinear networks, namely, Lur'e networks. The aim of this chapter is to reduce the complexity of interconnected Lur'e-type subsystems while simultaneously preserving the synchronization property of the network. An LMI condition is established to characterize the robust synchronization of the Lur'e network. Using the maximum and minimal solutions of the LMI, the linear part of each Lur'e subsystem are balanced, leading to a reduced-order Lur'e subsystem. In addition, an *a prior* error bound is provided to compare the behaviors of the full-order and reduced-order Lur'e subsystem. The materials in this chapter are based on the conference paper [44] and journal paper [38].

Finally, Chapter 9 formulates the conclusions of the thesis and makes some suggestions for future work.

1.5 List of Publications

Journal articles

[1] X. Cheng, J. M. A. Scherpen, and F. Zhang, "Reduction of robustly synchronized Lur'e networks with incrementally sector bounded nonlinearities," *Under review*, 2018.

[2] X. Cheng, and J. M. A. Scherpen, "Gramian-based model reduction of directed networks," *Under review*, 2018.

[3] X. Cheng, J. M. A. Scherpen, and B. Besselink "Balanced truncation of networked linear passive systems," *Provisionally accepted by Automatica*, 2018.

[4] X. Cheng, Y. Kawano, and J. M. A. Scherpen, "Model reduction of multi-agent systems using dissimilarity-based clustering," *To appear in IEEE Transactions on Automatic Control*, 2018, doi: 10.1109/TAC.2018.2853578.

[5] X. Cheng and J. M. A. Scherpen, "Clustering approach to model order reduction of power networks with distributed controllers," *To appear in Advances in Computational Mathematics*, 2018, doi: 10.1007/s10444-018-9617-5.

[6] M. Cucuzzella, S. Trip, C. De Persis, X. Cheng, A. Ferrara, and A.J. van der Schaft, "A robust consensus algorithm for current sharing and voltage regulation in DC microgrids," *To appear in IEEE Transactions on Control Systems Technology*, 2018, doi: 10.1109/TCST.2018.2834878.

[7] S. Trip, M. Cucuzzella, X. Cheng, and J. M. A. Scherpen, "Distributed averaging control for voltage regulation and current sharing in DC microgrids," *IEEE Control Systems Letters*, vol. 3, no. 1, pp. 174-179, Jan. 2019. DOI: 10.1109/LCSYS.2018.2857559.

[8] X. Cheng, Y. Kawano, and J. M. A. Scherpen, "Reduction of second-order network systems with structure preservation," *IEEE Transactions on Automatic Control*, vol. 62, pp. 5026-5038, 2017, doi: 10.1109/TAC.2017.2679479.

Conference papers

[1] X. Cheng, L. Yu, J. M. A. Scherpen, "Reduced Order Modeling of Diffusively Coupled Dynamical Networks using Weight Assignments", *Under review*.

[2] L. Chen, M. Cao, C. Li, X. Cheng, Y. Kapitanyuk, "Multi-agent formation control using angle measurements", *Under review*.

[3] S. Trip, R. Han, M. Cucuzzella, X. Cheng, J. M. A. Scherpen, J. M. Guerrero, "Distributed averaging control for voltage regulation and current sharing in DC microgrids: modelling and experimental validation", in *Proceedings of 7th IFAC Workshop on Distributed Estimation and Control in Networked Systems (NecSys)*, Gronigen, The Netherlands, 2018, pp. 242-247.

[4] S. Trip, M. Cucuzzella, C. De Persis, X. Cheng, A. Ferrara, "Sliding modes for voltage regulation and current sharing in DC microgrids," in *Proceedings of 2018 Annual American Control Conference (ACC)*, Milwaukee, The USA 2018, pp. 6778-6783.

[5] X. Cheng and J. M. A. Scherpen, "Robust synchronization preserving model reduction of Lur'e networks," in *Proceedings of 2018 European Control Conference (ECC)*, Limassol, Cyprus, 2018, pp. 2254-2259.

[6] X. Cheng and J. M. A. Scherpen, "A new controllability Gramian for semistable systems and its application to approximation of directed networks," in *Proceedings of 56th IEEE Conference on Decision and Control (CDC)*, Melbourne, Australia, 2017, pp. 3823-3828.

[7] X. Cheng and J. M. A. Scherpen, "Balanced truncation approach to linear network system model order reduction," in *Proceedings of the 20th World Congress of the International Federation of Automatic Control (IFAC World Congress)*, Toulouse, France, 2017, pp. 2506-2511.

[8] X. Cheng and J. M. A. Scherpen, "Introducing network Gramians to undirected network systems for structure-preserving model reduction," in *Proceedings of 55th IEEE Conference on Decision and Control (CDC)*, Las Vegas, The USA, 2016, pp. 5756-5761.

[9] X. Cheng, J. M. A. Scherpen, and Y. Kawano, "Model reduction of second-order network systems using graph clustering," in *Proceedings of 55th IEEE Conference on Decision and Control (CDC)*, Las Vegas, The USA, 2016, pp. 7471-7476.

[10] X. Cheng, Y. Kawano, and J. M. A. Scherpen, "Clustering-based model reduction of network systems with error bounds," in *Proceedings of 22nd International Symposium on Mathematical Theory of Networks and Systems (MTNS)*, Minnesota, The USA, 2016, pp. 90-95.

[11] X. Cheng, Y. Kawano, and J. M. A. Scherpen, "Graph structure-preserving model reduction of linear network systems," in *Proceedings of 2016 European Control Conference (ECC)*, Aalborg, Denmark, 2016, pp. 1970-1975.

1.6 Notations

In this section, we provide the notations that are used throughout this thesis.

Sets

Let $\mathbb{R}$ be the set of real numbers and $\mathbb{R}_+$ as the set of real nonnegative numbers. $\mathbb{R}^n$ and $\mathbb{R}^{n\times m}$ denote the spaces of all n-dimensional vector and $n \times m$ matrices with real elements, respectively. Suppose $\mathbb{W}$ is a subspace of $\mathbb{R}^n$, then $\mathbb{W}^\perp$ denotes the orthogonal complement of $\mathbb{W}$ in $\mathbb{R}^n$. The cardinality of a set $\mathbb{V}$ is denoted by $|\mathbb{V}|$, and $\mathsf{dim}(\mathbb{W})$ represents the dimension of space $\mathbb{W}$.

Vectors and Matrices

For a vector v, we denote its i-th element by v_i, and for a matrix A, we denote its (i, j)-th entry by A_{ij}. A^T and A^H denote the transpose and conjugate transpose of A, respectively. The determinant, trace, rank, image and nullspace of a matrix A are denoted by $\mathsf{det}(A)$, $\mathsf{tr}(A)$, $\mathsf{rank}(A)$, $\mathsf{im}(A)$, and $\mathsf{ker}(A)$, respectively. For a symmetric matrix $A \in \mathbb{R}^{n\times n}$, we write $A \succ 0 (A \prec 0)$ if A is positive (negative) definite . Moreover, $A \succcurlyeq 0 (A \preccurlyeq 0)$ if A is positive (negative) semi-definite. Besides, a real square matrix A is called *generalized negative definite* if its symmetric part $A_s = \frac{1}{2}(A + A^T)$ is negative definite. If A is generalized negative definite, then A is also Hurwitz [57].

The identity matrix of size n is given as I_n , and $\mathbb{1}_n$ denotes an n-entries vector of all ones. The subscript n is omitted when no confusion arises. $\mathbf{e}_i$ is the i-th column vector of an identity matrix, and $\mathbf{e}_{ij} = \mathbf{e}_i - \mathbf{e}_j$. $\mathsf{diag}(v)$ represents a square diagonal matrix with the entries of vector v on the main diagonal, and $\mathsf{blkdiag}(A_1, A_2 \cdots, A_n)$ is a block diagonal matrix with matrices $A_1, A_2 \cdots, A_n$ as its diagonal blocks.

Given two matrices $A \in \mathbb{R}^{m\times n}$ and $B \in \mathbb{R}^{p\times q}$. The Kronecker product of A and B is denoted by

$$A \otimes B = \begin{bmatrix} a_{11}B & \cdots & a_{1n}B \\ \vdots & \ddots & \vdots \\ a_{m1}B & \cdots & a_{mn}B \end{bmatrix} \in \mathbb{R}^{mp\times nq} \tag{1.1}$$

with a_{ij} the (i, j)-th entry of A. Kronecker product, which is widely used for the representation of multiagent systems, has some important properties as follows.

$$(A \otimes B)^{-1} = A^{-1} \otimes B^{-1}$$
$$A \otimes B + A \otimes C = A \otimes (B + C)$$
$$(A \otimes B)(C \otimes D) = (AC) \otimes (BD)$$

CHAPTER 2

Preliminaries

This chapter introduces the necessary concepts used throughout the thesis. In particular, we recapitulate some definitions from graph theory, including Laplacian matrices and graph clustering. Then, some properties of matrices and system norms are reviewed. Subsequently, we introduce the well-known model reduction methodology, balanced truncation.

2.1 Graph Theory

Graphs are naturally describing the interconnection topology among the vertices in dynamical networks. Here, we briefly recapitulate the definitions and fundamental results from graph theory that will be used throughout this thesis. For more details, we refer to e.g., [1, 32, 67, 146, 175, 176].

A finite graph is commonly defined by a pair $\mathcal{G} = (\mathcal{V}, \mathcal{E})$, where $\mathcal{V}$ and $\mathcal{E} \subseteq \mathcal{V} \times \mathcal{V}$ represent the sets of vertices and edges, respectively. Each directed edge $a_{ij} = (i, j) \in \mathbb{E}$ indicates that information flows from vertex j to vertex i. An *undirected path* connecting nodes i_0 and i_n is a sequence of undirected edges of the form (i_{k-1}, i_k), $k = 1, \cdots, n$. Then, an undirected graph $\mathcal{G}$ is *connected* if there is an undirected path between any pair of distinct nodes. In this thesis, we only consider *simple graphs*, i.e., graphs do not contain any self-loops, and all the edges are connecting two distinct vertices. Assume that $|\mathcal{V}| = n$ and $|\mathcal{E}| = n_e$, i.e., the graph $\mathcal{G}$ contains n vertices and n_e edges. Then, denote $\mathscr{W} \in \mathbb{R}^{n \times n}$ as the *weighted adjacency matrix*, whose elements indicate whether pairs of vertices are adjacent or not in $\mathcal{G}$. Specifically, (i, j) entry,

denoted by w_{ij}, is strictly positive if the edge $(j,i) \in \mathcal{E}$, and $w_{ij} = 0$ otherwise. The *degree matrix* of $\mathcal{G}$, denoted by $\mathscr{D} \in \mathbb{R}^{n\times n}$ is a diagonal matrix which contains information about the degree of each vertex, that is the number of edges attached to each vertex. For a simple graph, we have $\mathscr{D} = \mathsf{diag}(\mathscr{W}\mathbb{1}_n)$. Thereby, the Laplacian matrix $L \in \mathbb{R}^{n\times n}$ is defined as

$$L = \mathscr{D} - \mathscr{W} = \mathsf{diag}(\mathscr{W}\mathbb{1}_n) - \mathscr{W}. \tag{2.1}$$

In an undirected graph, $w_{ij} = w_{ji}$, which implies that L is symmetric, and has the following properties, see e.g. [35].

Lemma 2.1. *For a connected undirected graph, the Laplacian matrix L fulfills the following structural conditions:*

- $\mathbb{1}^T L = 0$, *and* $L\mathbb{1} = 0$;
- $L_{ij} \leq 0$ *if* $i \neq j$, *and* $L_{ii} > 0$;
- L *is positive semi-definite with a single zero eigenvalue.*

The Laplacian L is the matrix representation of the graph $\mathcal{G}$. Conversely, a real square matrix can be interpreted as a Laplacian matrix representing a connected undirected graph, if it satisfies the above structural conditions.

The undirected graph Laplacian also can be described by a so-called *incidence matrix* of $\mathcal{G}$, which is defined by $R \in \mathbb{R}^{n\times n_e}$ such that $R_{ij} = 1$ if the edge (i,j) heads to vertex i, -1 if it leaves vertex i and 0 otherwise. For an undirected graph, R can be obtained by assigning each edge with an arbitrary orientation. Then, the Laplacian matrix of an undirected graph $\mathcal{G}$ is given by

$$L = RWR^T, \tag{2.2}$$

where $W \in \mathbb{R}^{n_e\times n_e}$ is the diagonal and positive definite matrix whose diagonal entries represent the weights of edges.

In a directed graph (digraph), w_{ij} is generally not equal to w_{ji}, which means that L may be asymmetric.

Lemma 2.2. *For a directed graph, the Laplacian matrix L has the following characteristics:*

- $L\mathbb{1} = 0$;
- $L_{ij} \leq 0$ *if* $i \neq j$, *and* $L_{ii} > 0$.

If a real square matrix satisfies the above structural conditions, then it can be interpreted as a Laplacian matrix representing a digraph.

Example 2.1. *Examples of undirected and directed graphs are shown in Fig. 2.1. The weighted adjacency matrices of Fig. 2.1a and Fig. 2.1b are*

$$\mathscr{W}_a = \begin{bmatrix} 0 & 2 & 1 & 0 & 0 & 0 \\ 2 & 0 & 2 & 1 & 0 & 0 \\ 1 & 2 & 0 & 0 & 0 & 0 \\ 0 & 1 & 0 & 0 & 0 & 1 \\ 0 & 0 & 0 & 0 & 0 & 3 \\ 0 & 0 & 0 & 1 & 3 & 0 \end{bmatrix}, \; \mathscr{W}_b = \begin{bmatrix} 0 & 0 & 1 & 0 & 0 & 0 \\ 2 & 0 & 0 & 0 & 0 & 0 \\ 0 & 2 & 0 & 0 & 0 & 0 \\ 0 & 1 & 0 & 0 & 0 & 1 \\ 0 & 0 & 0 & 0 & 0 & 3 \\ 0 & 0 & 0 & 1 & 0 & 0 \end{bmatrix},$$

respectively. Considering the degree matrices

$$\mathscr{D}_a = \mathsf{diag}(3, 5, 3, 2, 3, 4), \text{ and } \mathscr{D}_b = \mathsf{diag}(1, 2, 2, 2, 3, 1),$$

we obtain the Laplacian matrices

$$L_a = \begin{bmatrix} 3 & -2 & -1 & 0 & 0 & 0 \\ -2 & 5 & -2 & -1 & 0 & 0 \\ -1 & -2 & 3 & 0 & 0 & 0 \\ 0 & -1 & 0 & 2 & 0 & -1 \\ 0 & 0 & 0 & 0 & 3 & -3 \\ 0 & 0 & 0 & -1 & -3 & 4 \end{bmatrix}, \; L_b = \begin{bmatrix} 1 & 0 & -1 & 0 & 0 & 0 \\ -2 & 2 & 0 & 0 & 0 & 0 \\ 0 & -2 & 2 & 0 & 0 & 0 \\ 0 & -1 & 0 & 2 & 0 & -1 \\ 0 & 0 & 0 & 0 & 3 & -3 \\ 0 & 0 & 0 & -1 & 0 & 1 \end{bmatrix}$$

of the undirected and directed graphs, respectively. Note that the matrix L_a can be also written as $L_a = R_a W_a R_a^T$ with $W_a = \mathsf{diag}(2, 1, 2, 1, 1, 3)$ and the incidence matrix

$$R_a = \begin{bmatrix} 1 & 1 & 0 & 0 & 0 & 0 \\ -1 & 0 & 1 & 1 & 0 & 0 \\ 0 & -1 & -1 & 0 & 0 & 0 \\ 0 & 0 & 0 & -1 & 1 & 0 \\ 0 & 0 & 0 & 0 & 0 & 1 \\ 0 & 0 & 0 & 0 & -1 & -1 \end{bmatrix}. \tag{2.3}$$

Undirected graphs can be regarded as a special class of digraphs. In a directed graph, a directed path is a sequence of edges which connect a sequence of vertices, but with the added restriction that the edges all be directed in the same direction. Digraphs can be categorized as follows.

Definition 2.1. *A digraph $\mathcal{G}$ is **weakly connected** ($\mathcal{G} \in \mathbb{G}_w$) if there exists an undirected path between any $i, j \in \mathbb{V}$. Particularly, if there exists a directed path in each direction between any $i, j \in \mathbb{V}$, $\mathcal{G}$ is **strongly connected** ($\mathcal{G} \in \mathbb{G}_s$). Furthermore, for every pair of vertices $i, j \in \mathbb{V}$, if there exists a vertex $k \in \mathbb{V}$ that can reach i, j by a directed path, $\mathcal{G}$ is **quasi strongly connected** ($\mathcal{G} \in \mathbb{G}_q$).*

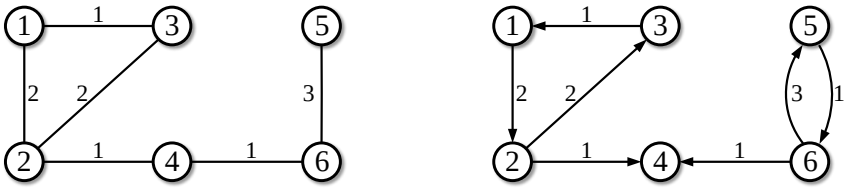

Figure 2.1: (a) An undirected graph with 6 vertices; (b) A directed graph with 6 vertices.

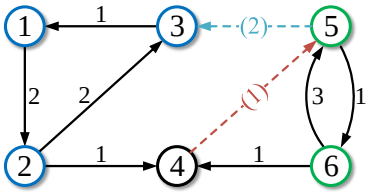

Figure 2.2: Illustration of different categories of digraphs.

These categories can be classified using the following concepts.

Definition 2.2. *A **strongly connected component** (SCC) of a digraph $\mathcal{G}$ is a subgraph in which every vertex is reachable from every other vertex. Any digraph $\mathcal{G}$ can be partitioned into several SCCs. If a SCC only has outflows, it is then called a **leading strongly connected component** (LSCC) [176].*

A digraph $\mathcal{G} \in \mathbb{G}_w$ may contains multiple LSCCs, while $\mathcal{G} \in \mathbb{G}_q$ only has a single LSCC. Generally, we have

$$\mathbb{G}_w \supset \mathbb{G}_q \supset \mathbb{G}_s. \tag{2.4}$$

Example 2.2. *Fig. 2.2 demonstrates different types of digraphs. When only considering the edges indicated by solid arrows, $\mathcal{G} \in \mathbb{G}_w$, and there exist three SCCs in $\mathcal{G}$: $\{1, 2, 3\}$, $\{5, 6\}$ and $\{4\}$, where the first two SCCs are LSCCs. Whereas, after an extra edgea_{45} (dashed arrow (1)) is added, this digraph becomes quasi strongly connected, i.e., $\mathcal{G} \in \mathbb{G}_q$, which contains only two SCCs: $\{1, 2, 3\}$, $\{4, 5, 6\}$, and the first one is the LSCC. Moreover, $\mathcal{G}$ will be strongly connected, when the vertices 2 and 4 are also connected by a_{24} represented by the dashed arrow (2).*

In the last part of this section, we recap the notions of graph clustering and its characteristic matrix from e.g., [67, 126]. Consider a graph $\mathcal{G} = (\mathcal{V}, \mathcal{E})$, where

$\mathcal{V} = \{1, 2, \cdots, n\}$ is the index set of vertices. A nonempty index subset of $\mathcal{V}$, denoted by $\mathcal{C}$, is called a *cluster* of graph $\mathcal{G}$. Then, *graph clustering* is to partition $\mathcal{V}$ into r disjoint clusters which cover all the elements in $\mathcal{V}$.

Definition 2.3. *Consider a graph clustering $\{\mathcal{C}_1, \mathcal{C}_2, \cdots, \mathcal{C}_r\}$ of a vertex set $\mathcal{V}$ with $|\mathcal{V}| = n$. The **characteristic vector** of the cluster $\mathcal{C}_i$ is defined by binary vector $\pi(\mathcal{C}_i) \in \mathbb{R}^n$ where $\mathbb{1}_n^T \pi(\mathcal{C}_i) = |\mathcal{C}_i|$, and the k-th element of $\pi(\mathcal{C}_i)$ is 1 when $k \in \mathcal{C}_i$ and 0 otherwise. Then, the **characteristic matrix** of the clustering is a binary matrix defined by*

$$\Pi := [\pi(\mathcal{C}_1), \pi(\mathcal{C}_2), \cdots, \pi(\mathcal{C}_r)] \in \mathbb{R}^{n \times r}. \tag{2.5}$$

Example 2.3. *Consider a graph $\mathcal{G} = (\mathcal{V}, \mathcal{E})$, with a vertex set $\mathcal{V} = \{1, 2, \cdots, 10\}$. Then,*

$$\mathcal{C}_1 = \{1, 2, 5\},\ \mathcal{C}_2 = \{3, 6, 9\},\ \text{ and } \mathcal{C}_3 = \{4, 7, 8, 10\}$$

are clusters of the graph $\mathcal{G}$, which correspond to the characteristic vectors

$$\begin{aligned}
\pi(\mathcal{C}_1) &= \begin{bmatrix} 1 & 1 & 0 & 0 & 1 & 0 & 0 & 0 & 0 & 0 \end{bmatrix}^T, \\
\pi(\mathcal{C}_2) &= \begin{bmatrix} 0 & 0 & 1 & 0 & 0 & 1 & 0 & 0 & 1 & 0 \end{bmatrix}^T, \\
\pi(\mathcal{C}_3) &= \begin{bmatrix} 0 & 0 & 0 & 1 & 0 & 0 & 1 & 1 & 0 & 1 \end{bmatrix}^T.
\end{aligned}$$

Thus, the characteristic matrix of the graph clustering $\{\mathcal{C}_1, \mathcal{C}_2, \mathcal{C}_3\}$ is given by

$$\Pi = [\pi(\mathcal{C}_1), \pi(\mathcal{C}_2), \pi(\mathcal{C}_3)] = \begin{bmatrix} 1 & 1 & 0 & 0 & 1 & 0 & 0 & 0 & 0 & 0 \\ 0 & 0 & 1 & 0 & 0 & 1 & 0 & 0 & 1 & 0 \\ 0 & 0 & 0 & 1 & 0 & 0 & 1 & 1 & 0 & 1 \end{bmatrix}^T.$$

2.2 Matrices, Systems and Norms

Matrices

The following definitions are important for studying networks.

Definition 2.4. *A square matrix A is said to be **semistable** if all eigenvalues of A are in the closed left-half plane, and all eigenvalues with zero real value are simple roots.*

Definition 2.5. *[18] A square matrix A is said to be **reducible** if it can be placed into block upper-triangular form by simultaneous row and column permutations. Conversely, A is said to be irreducible if it is not reducible.*

Definition 2.6. *[59] A square matrix A is said to be **Metzler** if the off-diagonal entries of A are all nonnegative.*

Definition 2.7. *[138] Consider a square real matrix $A \in \mathbb{R}^{n\times n}$. If $A_{ij} \leq 0$ for all $i \neq j$ and all the eigenvalues of A have positive real parts, then A is called an **M-matrix**.*

Lemma 2.3. *[138] If A is a nonsingular M-matrix, then A^{-1} is real nonnegative, i.e., all the entries of A^{-1} are real nonnegative (i.e., all the entries of A^{-1} are equal to or greater than zero).*

Note that the Laplacian matrix L, a matrix representation of a (directed or undirected) graph, is a singular M-matrix, and $-L$ is Metzler. In addition, the Laplacian matrix of a directed graph is irreducible if and only if its associated directed graph is strongly connected.

Systems and Norms

The norms for signals and systems appearing in this thesis are introduced. For more details, we refer to e.g. [7]. The $\mathcal{L}_2$-space is defined as the set of square integrable signals, i.e.,

$$\mathcal{L}_2 := \left\{ u(t) \in \mathbb{R} : \int_0^\infty u(t)^2 dt < \infty \right\}. \tag{2.6}$$

The $\mathcal{L}_2$-norm of a signal $x(t) \in \mathcal{L}_2^n$ is defined as

$$\|x(t)\|_2 = \left(\int_0^\infty x(t)^T x(t) \right)^{\frac{1}{2}}. \tag{2.7}$$

The square of this norm represents the total energy contained in the signal $x(t)$. Consider a stable, linear time-invariant (LTI) system in a state space representation

$$\mathbf{\Sigma} : \begin{cases} \dot{x}(t) = Ax(t) + Bu(t), \\ y(t) = Cx(t) + Du(t), \end{cases} \tag{2.8}$$

with $A \in \mathbb{R}^{n\times n}$, $B \in \mathbb{R}^{n\times m}$, and $C \in \mathbb{R}^{l\times n}$. The definition of a semistable system is defined in the following.

Definition 2.8. *[19] The system $\mathbf{\Sigma}_s$ is **semistable** if $\lim_{t\to\infty} x(t)$ exists for all initial conditions $x(0)$ when $u(t) = 0$.*

Now, the definition of a system is recalled from e.g. [113, 169, 174].

Definition 2.9. *The system $\mathbf{\Sigma}$ in (2.8) is **passive** if there exists a differentiable storage function $H(x) : \mathbb{R}^n \to \mathbb{R}_+$ with $H(0) = 0$ and $H(x) \geq 0$ for every x, such that*

$$H(x(t_2)) - H(x(t_1)) \leq \int_{t_1}^{t_2} u(t)^T y(t), \tag{2.9}$$

for all solution trajectories $(u_i(\cdot), x(\cdot), y(\cdot))$ *of the system (2.8). The system* $\mathbf{\Sigma}$ *is* ***lossless*** *if*

$$H(x(t_2)) - H(x(t_1)) = \int_{t_1}^{t_2} u(t)^T y(t), \tag{2.10}$$

and the system $\mathbf{\Sigma}$ *is* ***strictly passive*** *if* H *is positive definite such that*

$$H(x(t_2)) - H(x(t_1)) = \int_{t_1}^{t_2} u(t)^T y(t) - \int_{t_1}^{t_2} H(x)dt, \tag{2.11}$$

for all solution trajectories $(u_i(\cdot), x(\cdot), y(\cdot))$ *of the system (2.8).*

Furthermore, for minimal linear system, there exists a quadratic storage function $H(x) = x^T P x$ (with $P > 0$), leading to the following version of the Kalman-Yakubovich-Popov (KYP) condition [174]:

Lemma 2.4. *A linear system* $\mathbf{\Sigma}$ *in (2.8) is passive if and only if there exists a positive definite matrix* P *such that*

$$A^T P + PA \preccurlyeq 0,\ C = B^T P. \tag{2.12}$$

Equality holds if $\mathbf{\Sigma}$ *is lossless. If* $\mathbf{\Sigma}$ *is strictly passive, we have* $A^T P + PA \prec 0$ *and* $C = B^T P$.

The norm of a linear the system $\mathbf{\Sigma}$ is the gain that quantifies the amplification provided by the system between the inputs and the outputs. Let $G(s)$ be the transfer function of an LTI system $\mathbf{\Sigma}$ of input $u(t)$ and output $y(t)$. If $\mathbf{\Sigma}$ is stable, the $\mathcal{H}_\infty$-norm of $\mathbf{\Sigma}$ is the largest possible $\mathcal{L}_2$-gain over the set of square integrable input signals $u(t)$, i.e.,

$$\|\mathbf{\Sigma}\|_{\mathcal{H}_\infty} = \|G(s)\|_{\mathcal{H}_\infty} = \sup_{u(t)\in\mathcal{L}_2, \|u(t)\|_2 \neq 0} \frac{\|y(t)\|_2}{\|u(t)\|_2} = \sup_{\omega\in\mathbb{R}} \bar{\sigma}\left[G(j\omega)\right], \tag{2.13}$$

where $\bar{\sigma}$ denotes the largest singular value, and j is the imaginary unit. Furthermore, note that $G(s)$ is the Laplace transform of the impulse response $g(t)$ of the system $\mathbf{\Sigma}$, we then define the $\mathcal{H}_2$-norm of $\mathbf{\Sigma}$ as the $\mathcal{L}_2$-norm of its impulse response:

$$\|\mathbf{\Sigma}\|_{\mathcal{H}_2} = \|G(s)\|_{\mathcal{H}_2} = \sqrt{\int_0^\infty \mathsf{tr}\left[g(t)^T g(t)\right] dt}. \tag{2.14}$$

In frequency domain, the above definition becomes

$$\|\mathbf{\Sigma}\|_{\mathcal{H}_2} = \|G(s)\|_{\mathcal{H}_2} = \sqrt{\frac{1}{2\pi}\int_{-\infty}^{+\infty} \mathsf{tr}\left[G(j\omega)^H G(j\omega)\right] d\omega}, \tag{2.15}$$

The concepts of norms are of great importance in the thesis because it is the basis of error evaluation in model reduction.

Consider a stable, LTI system in a state space representation (2.8). Suppose A is Hurwitz, i.e., all eigenvalues are with negative real part. Then, the bounded real lemma can characterize the $\mathcal{H}_\infty$-norm of the system $\mathbf{\Sigma}$.

Lemma 2.5. *[28,162] A stable LTI system (A, B, C, D) has an H_∞-norm less than γ if and only if there exists a matrix $S \succ 0$ satisfying*

$$\begin{bmatrix} A^T S + SA & SB & C^T \\ B^T S & -\gamma I & D^T \\ C & D & -\gamma I \end{bmatrix} \prec 0 \tag{2.16}$$

Particularly, in the following two cases, the $\mathcal{H}_\infty$-norm of $\mathbf{\Sigma}$ can be simply obtained. The first case is a internally positive system, which is defined as follows.

Definition 2.10. *[97,140] A linear system (A, B, C, D) is called **internally positive** if for every initial state $x_0 = x(0) \in \mathbb{R}_+^n$ and all input such that $u(t) \in \mathbb{R}_+^p$ for all $t \geq 0$, the state vector $x(t)$ belongs to $\mathbb{R}_+^m$ and the output vector $y(t)$ belongs to $\mathbb{R}_+^l$ for all $t \geq 0$.*

As shown in [97], internal positivity can be written as a simple condition using the system matrices.

Lemma 2.6. *A linear system (A, B, C, D) is **internally positive** if and only if (i) the off-diagonal entries of A are all negative i.e., it is a Metzler matrix; (ii) B, C and D are all nonnegative (i.e., all the entries of these matrices are equal to or greater than zero).*

The input-output performance of a SISO positive system can be characterized as follows.

Lemma 2.7. *[140] Consider a linear system (A, B, C, D) with A Hurwitz and Metzler, while $B \in \mathbb{R}_+^{n\times 1}$, $C \in \mathbb{R}_+^{1\times n}$, and $D \in \mathbb{R}_+$. Then,*

$$\|G(s)\|_{\mathcal{H}_\infty} = \|C(sI - A)^{-1}B + D\|_{\mathcal{H}_\infty} = D - CA^{-1}B. \tag{2.17}$$

Next, the $\mathcal{H}_\infty$ characterization of a descriptor system is discussed. Consider a LTI descriptor system

$$\mathbf{\Sigma}_d : \begin{cases} E\dot{x}(t) = Ax(t) + Bu(t), \\ y(t) = Cx(t) + Du(t). \end{cases} \tag{2.18}$$

Definition 2.11. *[60] The descriptor system (2.18) is **regular** if $\mathsf{det}(sE - A)$ is not identically null; The system (2.18) is **impulse-free** if the degree of $\mathsf{det}(sE - A)$ is equal to $\mathsf{rank}(E)$; The system (2.18) is **stable** if all the roots of $\mathsf{det}(sE - A) = 0$ have negative real parts; The system (2.18) is said to be **admissible** if it is regular, impulse-free, and stable.*

Definition 2.12. *[74] A descriptor system (E, A, B, C, D) is called **internally symmetric** if $E^T = E$, $A^T = A$, $B^T = B$ and $D^T = D$.*

Particularly, if a admissible descriptor system is internally symmetric, then the $\mathcal{H}_\infty$-norm of $\mathbf{\Sigma}$ can be determined by the following manner.

Lemma 2.8. *[74] Consider a state-space symmetric descriptor system (E, A, B, C, D) with an admissible pair (E, A). If $E \preceq 0$ or $E \succeq 0$, then the $\mathcal{H}_\infty$-norm of the system transfer function $G(s) = C(sE + A)^{-1}B + D$ is given by*

$$\|G(s)\|_{\mathcal{H}_\infty} = \max\left\{|\lambda_m(D)|, |\lambda_m(G(0))|\right\},$$

where $\lambda_m(\cdot)$ denotes the largest eigenvalue.

For $\mathcal{H}_2$ norm of the LTI system $\mathbf{\Sigma}$ in (2.8), Gramians can be employed to provide an efficient computation. From [7], the *controllability* and *observability Gramians* of $\mathbf{\Sigma}$ are defined as

$$P = \int_0^\infty e^A t B B^T e^{A^T t} dt,\ Q = \int_0^\infty e^{A^T t} C^T C e^A t dt, \tag{2.19}$$

respectively. The system $\mathbf{\Sigma}$ is controllable if and only if $P \succ 0$ and observable if and only if $Q \succ 0$ [7]. Furthermore, the $\mathcal{H}_2$-norm of the system $\mathbf{\Sigma}$ can be characterized by the Gramians:

$$\|\mathbf{\Sigma}\|_{\mathcal{H}_2} = \sqrt{\mathsf{tr}(CPC^T)} = \sqrt{\mathsf{tr}(B^T Q B)}. \tag{2.20}$$

2.3 Model Reduction

We recap some basic facts on model reduction by balanced truncation from [7]. Assume a LTI system $\mathbf{\Sigma}$ as in (2.8) is asymptotically stable (i.e., A is Hurwitz) and minimal, i.e., controllable and observable, the controllability and observability Gramians, $P \succ 0$ and $Q \succ 0$, are the unique solutions of the following linear Lyapunov equations:

$$\begin{aligned} AP + PA^T + BB^T &= 0, \\ A^T Q + QA + C^T C &= 0. \end{aligned} \tag{2.21}$$

Balancing the system in (2.8) amounts to find a nonsingular state space transformation T such that

$$TPT^T = T^{-T} Q T^{-1} = \Theta, \tag{2.22}$$

with $\Theta := \mathsf{diag}\,(\theta_1, \theta_2, \cdots, \theta_n)$. The diagonal entries $\theta_1 \geq \theta_2 \geq \cdots \geq \theta_n > 0$ are called the *Hankel singular values* (HSVs) of the system.

The transformation T can be obtained by the Singular Value Decomposition (SVD) of the Gramians P and Q. More precisely, from the following SVDs

$$P = U_c \Theta_c U_c^T,\ Q = U_o \Theta_o U_o^T, \tag{2.23}$$

we define matrices

$$S := \left(U_c \Theta_c^{\frac{1}{2}}\right)^T, \text{ and } R := \left(U_o \Theta_o^{\frac{1}{2}}\right)^T. \tag{2.24}$$

such that $P = S^T S$ and $Q = R^T R$. Then, the Hankel singular values of $\mathbf{\Sigma}$ are computed as

$$SR^T = U \Theta V^T, \tag{2.25}$$

with the diagonal matrix Θ in (2.22). Moreover,

$$T^{-1} = S^T U \Theta^{-\frac{1}{2}}, \text{ and } T = \Theta^{-\frac{1}{2}} V^T R. \tag{2.26}$$

The transformation matrix T leads to the *balanced realization* of the system in (2.8), denoted by $(\tilde{A}, \tilde{B}, \tilde{C}, \tilde{D})$ with

$$\tilde{A} = TAT^{-1},\ \tilde{B} = TB,\ \tilde{C} = CT^{-1}, \text{ and } \tilde{D} = D. \tag{2.27}$$

In this realization, the state components corresponding to the smaller HSVs are less controllable and observable, and thus have less influences on the input-output behavior. It then allows the following partition of the matrices:

$$(\tilde{A}, \tilde{B}, \tilde{C}) := \left(\begin{bmatrix} \tilde{A}_{11} & \tilde{A}_{12} \\ \tilde{A}_{21} & \tilde{A}_{22} \end{bmatrix}, \begin{bmatrix} \tilde{B}_1 \\ \tilde{B}_2 \end{bmatrix}, \begin{bmatrix} \tilde{C}_1 & \tilde{C}_2 \end{bmatrix} \right), \tag{2.28}$$

where $\tilde{A}_{11} \in \mathbb{R}^{r \times r}$, $\tilde{B}_1 \in \mathbb{R}^{r \times p}$, and $\tilde{C}_1 \in \mathbb{R}^{q \times r}$, such that a reduced-order model of r dimension is obtained.

$$\hat{\mathbf{\Sigma}} : \begin{cases} \dot{z}(t) = \hat{A} z(t) + \hat{B} u(t), \\ \hat{y}(t) = \hat{C} z(t) + D u(t), \end{cases} \tag{2.29}$$

with $\hat{A} = \tilde{A}_{11}$, $\hat{B} = \tilde{B}_1$, and $\hat{C} = \tilde{C}_1$. $z(t) \in \mathbb{R}^n$ is the state of the reduced-order system, which is stable with HSVs given by $\theta_1, \ldots, \theta_r$, where r is the desired order of the reduced system. It is possible to choose r via the computable error bound:

$$\|y(t) - \hat{y}(t)\|_2 \leq 2\|u\|_2 \sum_{i=r+1}^{n} \theta_i, \text{ or equivalently, } \|\mathbf{\Sigma} - \hat{\mathbf{\Sigma}}\|_{\mathcal{H}_\infty} \leq 2 \sum_{i=r+1}^{n} \theta_i. \tag{2.30}$$

Instead of using the Lyapunov equations in (2.21), we can also work with solutions of Lyapunov inequalities to obtain a reduced-order model based on the so-called

generalized Gramians [58]. When the system in (2.8) is minimal and A is Hurwitz, a pair of positive definite matrices, $\mathcal{P} \succ 0$ and $\mathcal{Q} \succ 0$, are the *generalized controllability and observability Gramians* of the system in (2.8), respectively, if they satisfy the following linear matrix inequalities (LMIs)

$$\begin{aligned} A\mathcal{P} + \mathcal{P}A^T + BB^T &\preccurlyeq 0, \\ A^T\mathcal{Q} + \mathcal{Q}A + C^TC &\preccurlyeq 0. \end{aligned} \tag{2.31}$$

Then, similar to ordinary Lyapunov balancing, a reduced-order model can be obtained by balancing the pair of positive definite matrices $(\mathcal{P}, \mathcal{Q})$ and truncation based on the so-called *generalized Hankel singular values* (GHSVs) . Then, similar to the standard balanced truncation, the corresponding model reduction error bound is twice the sum of the neglected GHSVs.

2.4 Conclusions

In this chapter, we have presented the necessary background materials for later chapters. In particular, graph theory is used to model the interconnection topologies of network systems. The proposed method in Part I is established on the concept of graph clustering. The balancing theory is applied to develop the methods in Part II. The norms are used to characterize the approximation error between the original and reduced-order models.

Part I

CLUSTERING-BASED MODEL REDUCTION

CHAPTER 3

Clustering-Based Model Reduction of Second-Order Networks

This chapter defines a pair of pseudo controllability and observability Gramians for general semistable systems, which can be viewed as the generalization of standard Gramians for asymptotically stable systems. The pseudo Gramians are useful throughout this thesis and turn out to be particularly useful in our proposed method for clustering-based model reduction of second-order network systems, i.e., dynamical networks composed of interacting double integrators. In this chapter, we propose a general framework for structure-preserving model reduction of a second-order network system based on graph clustering. In this approach, vertex dynamics are captured by the transfer functions mapping from inputs to individual states, and the dissimilarities of vertices are quantified by the $\mathcal{H}_2$-norms of the transfer function discrepancies. The dissimilarities can be evaluated using the proposed pseudo Gramians effectively. Then, a greedy hierarchical clustering algorithm is proposed to place vertices with similar dynamics into clusters. Then, the reduced-order model is generated by the Petrov-Galerkin method, where the projection is formed by the characteristic matrix of the resulting network clustering. It is shown that the simplified system preserves an interconnection structure, i.e., it can be again interpreted as a second-order system evolving over a reduced graph. Furthermore, based on the pseudo controllability Gramian, we derive the approximation error between the full-order and reduced-order models. Finally, the approach is illustrated by an example of a small-world network.

3.1 Introduction

A network system describes the behavior of a collection of agents whose states are dynamical quantities, following some dynamical rule, and that dynamical rule includes a certain interaction protocol with neighboring agents. A variety of network systems, such as distributed power grids or mass-damper-spring networks, are given as differential equations in second-order form, see [54, 90]. For large-scale networks, the second-order form dynamic models can be so complex and high-dimensional that system analysis and controller design become considerably difficult because of the impractical amounts of storage space and computation. Therefore, this chapter aims at a method to derive a lower-dimensional model which has an input-output behavior similar to the original one as well as inherits a second-order network structure.

However, deriving reduced models for second-order network systems is not necessarily straightforward. Indeed, we are able to convert a second-order system to its equivalent first-order representation and then apply the reduction techniques used for first-order systems. However, the resulting models are not of second-order form in general. In [11, 31, 118, 151] etc., the existing model reduction methods, including balanced truncation and moment matching, have been extended to the second-order case. Although the resulting reduced model is presented in a second-order form, it may fail to preserve the interconnection topology among subsystems, i.e., such reduced models cannot be interpreted as network systems anymore.

There is another attempt to simplify the complexity of second-order networks based on time-scale separation and singular perturbation analysis, see e.g., [148] and references therein. The approach in [148] identifies the sparsely and densely connected areas of power grids, and then aggregates the state variables of the coherent areas. Through singular perturbation approximation, the algebraic structure of Laplacian matrix is maintained. Therefore, this approach indeed preserves the network structure. Nevertheless, it does not explicitly consider the influence of the external inputs into the networks, and there is no analytical expression for the approximation error between the original and aggregated model.

Recently, clustering-based model reduction methods for first-order network systems have been investigated in [21, 84, 85, 87, 126]. An extension to the second-order case can be found in [83]. In the method, graph clustering is performed based on *cluster reducibility*, which is generalized as the uncontrollability of clusters and computed through a tridiagonal realization of their first-order representation. Then, the reducible clusters are merged to construct a reduced model with preservation of a second-order network topology. Nevertheless, this approach does not take the algebraic structure of the Laplacian matrix into account, and the approximation procedure and error analysis are reliant on the asymptotic stability of the system.

This can be a limitation for some applications, e.g., the coupled swing dynamics in power networks as in [54, 148].

In this chapter, we propose a novel model reduction approach for second-order network systems based on graph clustering. In contrast to the existing techniques, this method can be applied to more general network models, which do not restrict to a special class of partitions as in [126] or to a tree topology as in [21], or to asymptotically stable models as in [83]. Besides, unlike [148], we consider the system dynamics are influenced by external input signals. In [45], preliminary results are presented, which are generalized in this chapter by extending the definition of controllability Gramian and proposing a new cluster algorithm.

This chapter starts with the introduction of the pseudo Gramians, which are novel concepts for semistable systems. We show that the new Gramians are characterized by a set of Lyapunov equations, and their ranks are strongly related to the controllability and the observability of a semistable system. Using the pseudo Gramians, the $\mathcal{H}_2$-norm of a semistable system can be easily evaluated. Therefore, this chapter employs them to facilitate the computation of dissimilarities and thus provides a crucial step in the clustering-based model reduction.

The proposed clustering-based model reduction is in the framework of Galerkin projection. The characteristic matrix of a graph clustering is used as the projection so that the interconnection topology can be preserved in the reduced-order model. More importantly, the algebraic structure of Laplacian matrix is also retained, and consequently, the reduced graph can be reconstructed. A greedy hierarchical clustering algorithm is designed to generate an appropriate network partition. Specifically, we characterize the behaviors of vertices by the transfer functions from inputs to their individual states and denote the dissimilarities by the $\mathcal{H}_2$-norms of the transfer function deviations. Then, a systematic process places those vertices with almost similar behaviors into same clusters. The feasibility and efficiency of this method are demonstrated by a numerical example.

The remainder of this chapter is organized as follows. Section 3.2 presents the mathematical model of second-order network systems and formulates the problem of structure-preserving model reduction. The pseudo Gramians are proposed in Section 3.3. In Section 3.4, we provide the framework of clustering-based model reduction. Then, in Section 3.5, we design the cluster selection algorithm. Finally, Section 3.6 illustrates the feasibility of our method by means of a numerical example, and Section 3.7 concludes the whole chapter.

3.2 Problem Formulation

Consider a network system evolving over graph $\mathcal{G}$, which has a linear time-invariant description in second-order form as

$$\mathbf{\Sigma} : M\ddot{x} + D\dot{x} + Lx = Fu, \tag{3.1}$$

where $x \in \mathbb{R}^n$ and $u \in \mathbb{R}^m$ denote the vertex states and external inputs, respectively. In this model, M, D, $L \in \mathbb{R}^{n\times n}$ are referred to inertia, damping and stiffness matrices, respectively. Note that L is also a Laplacian matrix, which represents an undirected weighted graph, see its properties in Lemma 2.1. Based on practical applications, the following *structural conditions* are assumed.

Assumption 3.1. *① $M \succ 0$ is diagonal; ② $D = D^T \succ 0$; ③ $L = L^T \succcurlyeq 0$ is a weighted Laplacian matrix of a connected undirected graph. (For the properties of L, we refer to [34]).*

A variety of physical network systems are modeled in the form of (3.1) satisfying Assumption 3.1, including the linearized swing equation in power grids [54] and mass-damper-spring networks [90]. Take the latter one, for instance, M represents the distribution of masses, and D presents the dampers on edges and vertices, while L indicates the strength of diffusive coupling among the vertices connected by springs.

Note that the system in (3.1) is not asymptotically stable since L is a singular matrix. In fact, Assumption 3.1 implies that the system $\mathbf{\Sigma}$ is *semistable* and *passive* with respect to input u and output $y = F^T\dot{x}$. We show our statement as follows.

First, the total energy of $\mathbf{\Sigma}$ is given by

$$H(x,\dot{x}) = \frac{1}{2}\dot{x}^T M\dot{x} + \frac{1}{2}x^T Lx. \tag{3.2}$$

With $y = F^T\dot{x}$ as output, we have

$$\begin{aligned} u^T y - \dot{H} &= u^T F^T\dot{x} - \dot{x}^T M\ddot{x} - x^T L\dot{x} \\ &= u^T F^T\dot{x} - \dot{x}^T(-D\dot{x} - Lx + Fu) - x^T L\dot{x} \\ &= \dot{x}^T D\dot{x} > 0. \end{aligned}$$

It follows from [99] that the system $\mathbf{\Sigma}$ is passive. Moreover, $\mathbf{\Sigma}$ can be presented in the form of a port-Hamiltonian system as in [89].

Second, the stability of the system $\mathbf{\Sigma}$ can be seen from the first-order form realization

$$\dot{\mathcal{X}} = \mathcal{A}\mathcal{X} + \mathcal{B}u \tag{3.3}$$

with $\mathcal{X}^T = \left[x^T, \dot{x}^T\right]$ as the $2n$-dimensional state and

$$\mathcal{A} = \begin{bmatrix} \mathbf{0}_{n\times n} & I \\ -M^{-1}L & -M^{-1}D \end{bmatrix},\ \mathcal{B} = \begin{bmatrix} \mathbf{0}_{n\times m} \\ M^{-1}F \end{bmatrix}. \tag{3.4}$$

From Assumption 3.1, it is easy to check that all the eigenvalues of $\mathcal{A}$ are in the closed left-half plane, and only one of them is at the origin. Therefore, the second-order network system $\mathbf{\Sigma}$ is semistable.

Remark 3.1. *The major differences with set-ups from familiar second-order systems as in [11,31,118] are that D and L in (3.1) contain the information of network spatial structures, and the system $\mathbf{\Sigma}$ is not asymptotically stable.*

Now we formulate the problem of model reduction for second-order network systems as follows.

Problem 3.1. *Given a second-order network system $\mathbf{\Sigma}$ as in (3.1), find a pair of projection matrices $W, V \in \mathbb{R}^{n\times r}$ with $r \ll n$ to construct a reduced model in the second-order form as*

$$\hat{\mathbf{\Sigma}} : \begin{cases} \hat{M}\ddot{z} + \hat{D}\dot{z} + \hat{L}z = W^T F u, \\ \hat{x} = Vz, \end{cases} \tag{3.5}$$

*where $\hat{M} = W^T M V$, $\hat{D} = W^T D V$ and $\hat{L} = W^T L V \in \mathbb{R}^{r\times r}$. We require the matrices $\hat{M}$, $\hat{D}$ and $\hat{L}$ to fulfill the **structural conditions** in Assumption 3.1 and the trajectories of $\hat{x}(t)$ to approximate those of $x(t)$ in the original system $\mathbf{\Sigma}$ with a small error.*

We call Problem 3.1 a *position-based model reduction* for second-order network systems, since the variable $\hat{x}(t)$ in (3.5) is used to approximate $x(t)$ rather than $\dot{x}(t)$. However, Problem 3.1 can be easily modified to solve *velocity-based model reduction* problems, where the second equation in (3.5) is replaced by $v = V\dot{z}$, and it requires v and $\dot{x}(t)$ to have close behaviors respect to the external input fluxes $u(t)$.

In this chapter, we mainly consider the position-based model reduction as a standard problem setting for network systems and discuss the solution of Problem 3.1 in Section 3.4 and Section 3.5. Besides, we briefly state the extension of our proposed method to velocity-based model reduction. The proposed method in this chapter is based on a new concept of Gramian matrices. We introduce them in the following section.

3.3 Gramians of Semistable System

We make the result of this section self-contained and independent of the model reduction of directed network systems. This section extends the concepts of *controllability and observability Gramians* for asymptotically stable systems to semistable ones. In our preliminary results in [39], novel Gramians are deliberately introduced for first-order network systems. Here, we present a generalization of the results to general semistable systems, whose controllability and observability can be also characterized by the newly proposed Gramians.

Consider the state-space model of a linear time-invariant system

$$\mathbf{\Sigma}_s : \begin{cases} \dot{x}(t) = Ax(t) + Bu(t), \\ y(t) = Cx(t), \end{cases} \tag{3.6}$$

with states $x \in \mathbb{R}^n$, inputs $u \in \mathbb{R}^p$ and outputs $y \in \mathbb{R}^q$. The following lemma provides a necessary and sufficient condition for the semistability of $\mathbf{\Sigma}_s$.

Lemma 3.1. *[19] The system $\mathbf{\Sigma}_s$ is semistable if and only if the zero eigenvalues of A in (3.6) are **semisimple** (i.e., the geometric multiplicity of the zero eigenvalue coincides with the algebraic multiplicity), and all the other eigenvalues have negative real parts.*

Note that asymptotically stable systems are only special cases of semistable systems so that the standard definitions of controllability and observability Gramians in (2.21) may not applicable for $\mathbf{\Sigma}_s$ that is not asymptotically stable. Instead, we can define a pair of pseudo Gramians for semistable systems.

Definition 3.1. *Consider the semistable system $\mathbf{\Sigma}_s$ as in (3.6). The **pseudo controllability and observability Gramians** are given by*

$$\mathcal{P} = \int_0^\infty (e^{A\tau} - \mathcal{J})BB^T(e^{A^T\tau} - \mathcal{J}^T)d\tau \in \mathbb{R}^{n\times n}, \tag{3.7a}$$

$$\mathcal{Q} = \int_0^\infty (e^{A^T\tau} - \mathcal{J}^T)C^TC(e^{A\tau} - \mathcal{J})d\tau \in \mathbb{R}^{n\times n}, \tag{3.7b}$$

where $\mathcal{J} := \lim_{\tau\to\infty} e^{A\tau}$ is a constant matrix.

Since the integrands in (3.7a) and (3.7b) are *absolutely integrable functions* and converge to zero as $\tau \to \infty$, the pseudo Gramians in (3.7a) and (3.7b) are well-defined. Furthermore, using the matrix $\mathcal{J}$, the Lyapunov characteristics of $\mathcal{P}$ and $\mathcal{Q}$ in Definition 3.1 are stated in the following theorem.

Theorem 3.1. *Consider the semistable system $\mathbf{\Sigma_s}$ in (3.6). The pseudo controllability and observability Gramians of $\mathbf{\Sigma_s}$, $\mathcal{P}$ and $\mathcal{Q}$ defined in (3.7), are the unique symmetric solutions of the following sets of linear matrix equations*

$$\begin{cases} 0 = A\mathcal{P} + \mathcal{P}A^T + (I - \mathcal{J})BB^T(I - \mathcal{J}^T), & \text{(3.8a)} \\ 0 = \mathcal{J}\mathcal{P}\mathcal{J}^T. & \text{(3.8b)} \end{cases}$$

$$\begin{cases} 0 = A^T\mathcal{Q} + \mathcal{Q}A + (I - \mathcal{J}^T)C^TC(I - \mathcal{J}), & \text{(3.9a)} \\ 0 = \mathcal{J}^T\mathcal{Q}\mathcal{J}. & \text{(3.9b)} \end{cases}$$

Proof. Assume that A in (3.6) has zero eigenvalues with the algebraic (or geometric) multiplicity m. Then, there exists a similarity transformation such that

$$A = \mathcal{U}D\mathcal{U}^{-1} = \begin{bmatrix} U, \bar{U} \end{bmatrix} \begin{bmatrix} \mathbf{0}_{m\times m} & \\ & \bar{D} \end{bmatrix} \begin{bmatrix} V^T \\ \bar{V}^T \end{bmatrix}, \tag{3.10}$$

where $\bar{D} \in \mathbb{R}^{(n-m)\times(n-m)}$ is Hurwitz, and the matrices $U \in \mathbb{R}^{n\times m}$ and $V \in \mathbb{R}^{n\times m}$ fulfill

$$\mathsf{im}(U) = \mathsf{ker}(A),\ \mathsf{im}(V) = \mathsf{ker}(A^T),\ \text{and}\ V^TU = I_m. \tag{3.11}$$

Moreover, $\bar{U}$ is a matrix such that $\mathcal{U} = \begin{bmatrix} U, \bar{U} \end{bmatrix}$ is nonsingular. Note that the product UV^T is invariant to the choices for U and V, and it coincides with the matrix $\mathcal{J}$ in (3.7), i.e.,

$$\mathcal{J} = \lim_{\tau\to\infty} e^{A\tau} = UV^T. \tag{3.12}$$

Therefore, the following equations hold:

$$\mathcal{J}^2 = \mathcal{J},\ A\mathcal{J} = 0,\ \text{and}\ \mathcal{J}A = 0. \tag{3.13}$$

Furthermore, for any $\tau \in \mathbb{R}$,

$$\mathcal{J}e^{A\tau} = \mathcal{J}\left(I + \sum_{k=1}^{\infty} \frac{A^k\tau^k}{k!}\right) = \mathcal{J},\ \text{and}\ e^{A\tau}\mathcal{J} = \mathcal{J}. \tag{3.14}$$

The equations in (3.13) and (3.14) are used through the following proof.

First, we show that $\mathcal{P}$ in (3.7a) satisfies the two equations in (3.8). Notice that

$$\begin{aligned} &\frac{d}{d\tau}\left[(e^{A\tau} - \mathcal{J})BB^T(e^{A^T\tau} - \mathcal{J}^T)\right] \\ &= Ae^{A\tau}BB^T(e^{A^T\tau} - \mathcal{J}^T) + (e^{A\tau} - \mathcal{J})BB^Te^{A^T\tau}A^T. \end{aligned} \tag{3.15}$$

Integrating the two terms separately leads to

$$\begin{aligned} \int_0^\infty Ae^{A\tau}BB^T(e^{A^T\tau} - \mathcal{J})d\tau &= \int_0^\infty A(e^{A\tau} - \mathcal{J} + \mathcal{J})BB^T(e^{A^T\tau} - \mathcal{J})d\tau \\ &= A\mathcal{P} + A\mathcal{J}BB^T\int_0^\infty (e^{A^T\tau} - \mathcal{J})d\tau = A\mathcal{P}, \end{aligned} \tag{3.16}$$

and similarly,

$$\int_0^\infty (e^{A\tau} - \mathcal{J})BB^Te^{A^T\tau}A^Td\tau = \mathcal{P}A^T. \tag{3.17}$$

Observe that

$$\begin{aligned}\int_0^\infty \frac{d}{d\tau}\left[(e^{A\tau}-\mathcal{J})BB^T(e^{A^T\tau}-\mathcal{J}^T)\right]d\tau &= (e^{A\tau}-\mathcal{J})BB^T(e^{A^T\tau}-\mathcal{J}^T)\Big|_0^\infty \\ &=(I-\mathcal{J})BB^T(I-\mathcal{J}^T).\end{aligned} \tag{3.18}$$

Then, the Lyapunov equation in (3.8a) is obtained by integrating both sides of (3.15). The second equation in (3.8b) can be seen from the fact that

$$\mathcal{J}\left(e^{A\tau}-\mathcal{J}\right)=\mathcal{J}-\mathcal{J}=0. \tag{3.19}$$

Next, we prove the uniqueness of the solution of (3.8) by contradiction. Assume that two symmetric matrices $\mathcal{P}_1$ and $\mathcal{P}_2$ satisfy (3.8) and $\mathcal{P}_1 \neq \mathcal{P}_2$. From (3.8a), we have

$$A(\mathcal{P}_1-\mathcal{P}_2)+(\mathcal{P}_1-\mathcal{P}_2)A^T=0, \tag{3.20}$$

which leads to

$$e^{A\tau}\left[A(\mathcal{P}_1-\mathcal{P}_2)+(\mathcal{P}_1-\mathcal{P}_2)A^T\right]e^{A^T\tau}=\frac{d}{d\tau}\left[e^{A\tau}(\mathcal{P}_1-\mathcal{P}_2)e^{A^Tt}\right]=0. \tag{3.21}$$

Therefore,

$$\int_0^\infty \frac{d}{d\tau}\left[e^{A\tau}(\mathcal{P}_1-\mathcal{P}_2)e^{A^T\tau}\right]d\tau=0, \tag{3.22}$$

which implies that

$$\mathcal{P}_1-\mathcal{P}_2=\mathcal{J}(\mathcal{P}_1-\mathcal{P}_2)\mathcal{J}^T. \tag{3.23}$$

As both $\mathcal{P}_1$ and $\mathcal{P}_2$ satisfy (3.8b), the equation (3.23) becomes zero, which, however, contradicts the assumption that $\mathcal{P}_1 \neq \mathcal{P}_2$. Therefore, the solution of (3.8a) and (3.8b) is unique.

The proof of the pseudo observability Gramian in (3.9) is similar to the proof of the controllability Gramian part, and thus the details are omitted here. Note that the equation (3.9b) is a result of

$$\left(e^{A\tau}-\mathcal{J}\right)\mathcal{J}=\mathcal{J}-\mathcal{J}=0. \tag{3.24}$$

That completes the proof. □

Remark 3.2. *It is implied by (3.8b) and (3.9b) that the pseudo Gramians $\mathcal{P}$ and $\mathcal{Q}$ are positive semidefinite. However, when A is Hurwitz, i.e., $\mathbf{\Sigma}_s$ is asymptotically stable, it follows that $\mathcal{J}=0$ such that $\mathcal{P}$ and $\mathcal{Q}$ in (3.7) become the standard Gramians in (2.21). Thus, the pseudo Gramians are generalizations of the standard ones.*

Observe that, due to the singularity of the A matrix, there may exist multiple solutions of the Lyapunov equations in (3.8a) and (3.9a). For instance, suppose a symmetric matrix $\mathcal{P}$ is a solution of (3.8a), then any matrix $\mathcal{P} + \Delta_{\mathcal{P}}$, with $\Delta_{\mathcal{P}} = \Delta_{\mathcal{P}}^T$ and $A\Delta_{\mathcal{P}} = 0$, is also a solution of (3.8a). However, combining the Lyapunov equations in (3.8a) and (3.9a) with the algebraic constraints in (3.8b) and (3.9b), we can determine the pseudo Gramians $\mathcal{P}$ and $\mathcal{Q}$ uniquely. The following corollary then indicates that the pseudo Gramians can be obtained without calculating the integrals in (3.7).

Corollary 3.1. *Let $\mathcal{P}_a$ and $\mathcal{Q}_a$ be arbitrary solutions of the Lyapunov equations in (3.8a) and (3.9a), respectively. Then, the pseudo controllability and observability Gramians, $\mathcal{P}$ and $\mathcal{Q}$ are computed as*

$$\mathcal{P} = \mathcal{P}_a - \mathcal{J}\mathcal{P}_a\mathcal{J}^T. \tag{3.25a}$$

$$\mathcal{Q} = \mathcal{Q}_a - \mathcal{J}^T\mathcal{Q}_a\mathcal{J}. \tag{3.25b}$$

with $\mathcal{J}$ a constant matrix defined in (3.7).

Proof. Since both $\mathcal{P}_a$ and $\mathcal{P}$ are solutions of (3.8a), it follows from (3.23) that

$$\mathcal{P}_a - \mathcal{P} = \mathcal{J}(\mathcal{P}_a - \mathcal{P})\mathcal{J}^T = \mathcal{J}\mathcal{P}_a\mathcal{J}^T, \tag{3.26}$$

where the second equality holds due to (3.8b). Thus, (3.25a) is verified, and (3.25b) can be proven analogously. □

In general, the $\mathcal{H}_2$-norm of a system is unbounded if the system is semistable, see the network systems in [39] for instance. Nevertheless, the following lemma provides a sufficient and necessary condition for $\mathbf{\Sigma}_s \in \mathcal{H}_2$, which can be characterized by the pseudo Gramians.

Lemma 3.2. *Consider a semistable system $\mathbf{\Sigma}_s$ in (3.6). Then, $\mathbf{\Sigma}_s \in \mathcal{H}_2$ if and only if $C\mathcal{J}B = 0$. Furthermore, if the $\mathcal{H}_2$-norm of $\mathbf{\Sigma}_s$ exists, then*

$$\|\mathbf{\Sigma}_s\|_{\mathcal{H}_2}^2 = \mathsf{tr}(C\mathcal{P}C^T) = \mathsf{tr}(B^T\mathcal{Q}B), \tag{3.27}$$

where $\mathcal{P}$ and $\mathcal{Q}$ are the pseudo controllability and observability Gramians of $\mathbf{\Sigma}_s$.

Proof. Let $g(\tau) := Ce^{A\tau}B$ be the impulse response of $\mathbf{\Sigma}_s$. It follows from [7] that

$$\|\mathbf{\Sigma}_s\|_{\mathcal{H}_2}^2 = \mathsf{tr}\left(\int_0^\infty g(\tau)^T g(\tau) d\tau\right). \tag{3.28}$$

The $\mathcal{H}_2$-norm of $\mathbf{\Sigma}_s$ is bounded if and only if $g(\tau)$ is absolutely integrable. Since $g(\tau)$ is a smooth function on $\mathbb{R}$, it is absolutely integrable if and only if

$$\lim_{\tau\to\infty} g(\tau) = C\left(\lim_{\tau\to\infty} e^{A\tau}\right)B = C\mathcal{J}B = 0. \tag{3.29}$$

Next, using the condition that $C\mathcal{J}B = 0$, we can show that

$$\mathsf{tr}(C\mathcal{P}C^T) = \mathsf{tr}\left(\int_0^\infty g(\tau)^T g(\tau) d\tau\right), \text{ and } \mathsf{tr}(B^T\mathcal{Q}B) = \mathsf{tr}\left(\int_0^\infty g(\tau) g(\tau)^T d\tau\right).$$

That completes the proof. □

Hereafter, we discuss the relationship between the controllability and the observability of the semistable system $\mathbf{\Sigma}_s$ and the pseudo Gramians. Before proceeding, the definitions of *finite-time Gramians* are introduced.

$$\mathcal{P}_s(0, t_f) = \int_0^{t_f} e^{A\tau} B B^T e^{A^T\tau} d\tau. \tag{3.30a}$$

$$\mathcal{Q}_s(0, t_f) = \int_0^{t_f} e^{A^T\tau} C^T C e^{A\tau} d\tau. \tag{3.30b}$$

Clearly, $\mathcal{P}(0, t_f)$ and $\mathcal{Q}(0, t_f)$ are bounded and positive semidefinite when t_f is finite, whose ranks characterize the controllability and observability of the system.

Lemma 3.3. *[7] Consider the system $\mathbf{\Sigma}_s$ in (3.6).*

- *$\mathbf{\Sigma}_s$ is controllable on $[0, t_f]$ if and only if the finite controllability Gramian $\mathcal{P}_s(0, t_f)$ in (3.30a) is full rank;*
- *$\mathbf{\Sigma}_s$ is observable on $[0, t_f]$ if and only if the finite observability Gramian $\mathcal{Q}_s(0, t_f)$ in (3.30b) is full rank.*

Based on the above lemma, we show that pseudo Gramians characterize the controllability and the observability of a semistable system.

Theorem 3.2. *Consider a semistable system $\mathbf{\Sigma}_s$ whose pseudo controllability and observability Gramians are denoted by $\mathcal{P}$ and $\mathcal{Q}$, respectively. Let m be the algebraic (or geometric) multiplicity of the zero eigenvalues of A. Then,*

- *$\mathbf{\Sigma}_s$ is controllable if and only if $\mathsf{rank}(\mathcal{P}) = n - m$ and $\xi^T B \neq 0$, for any nonzero vector $\xi \in \mathsf{ker}(A^T)$;*
- *$\mathbf{\Sigma}_s$ is observable if and only if $\mathsf{rank}(\mathcal{Q}) = n - m$ and $C\xi \neq 0$, for any nonzero vector $\xi \in \mathsf{ker}(A)$.*

Proof. Define the *finite-time pseudo controllability Gramian* of the system $\mathbf{\Sigma}_s$ as

$$\mathcal{P}(0, t_f) = \int_0^{t_f} (e^{A\tau} - \mathcal{J}) B B^T (e^{A^T\tau} - \mathcal{J}^T) d\tau \succcurlyeq 0. \tag{3.31}$$

First, we assume $\mathbf{\Sigma}_s$ is controllable. To determine the rank of $\mathcal{P}(0,t_f)$, we find the nullspace of $\mathcal{P}(0,t_f)$, denoted by $\mathsf{ker}(\mathcal{P}(0,t_f))$, and prove that

$$\mathsf{dim}(\mathsf{ker}(\mathcal{P}(0,t_f))) = m.$$

To this end, a nonzero vector $\xi \in \mathsf{ker}(\mathcal{P}(0,t_f))$ is characterized by

$$\xi^T(e^{A\tau} - \mathcal{J})B = 0,\ \forall \tau \in [0,t_f]\,. \tag{3.32}$$

Consider the decomposition of A in (3.10), where $A^TV = 0$ and $V^T\bar{U} = 0$, i.e., $\mathsf{im}(V) = \mathsf{ker}(A^T) = \mathsf{im}(\bar{U})^\perp$. Since the matrix $[U,\bar{U}]$ is nonsingular, we have

$$\mathsf{im}(U) \cup \mathsf{im}(\bar{U}) = \mathsf{im}(U) \cup \mathsf{im}(V)^\perp = \mathbb{R}^n. \tag{3.33}$$

Thereby, an arbitrary nonzero vector $\xi \in \mathbb{R}^n$ can be decomposed as

$$\xi = \alpha\xi_1 + \beta\xi_2, \tag{3.34}$$

where α, β are scalars, and $\xi_1 \in \mathsf{im}(V)$, $\xi_2 \in \mathsf{im}(U)^\perp$, which satisfy

$$\xi_1^T(e^{A\tau} - \mathcal{J})B = 0, \text{ and } \xi_2^T\mathcal{J} = \xi_2^TUV^T = 0. \tag{3.35}$$

The first equation in (3.35) holds due to

$$V^T\left(e^{A\tau} - \mathcal{J}\right)B = V^T\left(I + \sum_{k=1}^{\infty}\frac{A^k\tau^k}{k!} - \mathcal{J}\right) = 0. \tag{3.36}$$

With the decomposition of the vector ξ in (3.34), we rewrite (3.32) as

$$\xi^T(e^{A\tau} - \mathcal{J})B = \alpha\xi_1^T(e^{A\tau} - \mathcal{J})B + \beta\xi_2^T(e^{A\tau} - \mathcal{J})B = \beta\xi_2^Te^{A\tau}B. \tag{3.37}$$

From Lemma 3.3, $\mathbf{\Sigma}_s$ being controllable is equivalent to the positive definiteness of the standard finite-time Gramian $\mathcal{P}_s(0,t_f)$, i.e., for all nonzero vector ξ,

$$\xi^T\mathcal{P}_s(0,t_f)\xi = \int_0^{t_f}\xi^Te^{A\tau}BB^Te^{A^T\tau}\xi d\tau \tag{3.38}$$

is strictly positive, which means that there is no vector $\xi \neq 0$ such that $\xi^Te^{A\tau}B = 0$, $\forall \tau \in [0,t_f]$. Therefore, a nonzero vector $\xi \in \mathsf{ker}(\mathcal{P}(0,t_f))$ if and only if $\beta = 0$ and $\alpha \neq 0$ in (3.37), namely, $\xi \in \mathsf{im}(V)$, which yields

$$\mathsf{rank}(\mathcal{P}(0,t_f)) = n - \mathsf{dim}(\mathsf{im}(V)) = n - m. \tag{3.39}$$

Furthermore, when $\mathbf{\Sigma_s}$ is controllable, we also obtain $\xi^TB \neq 0, \forall \xi \in \mathsf{ker}(A^T)$. Otherwise, there will exist a nonzero vector $\xi \in \mathsf{im}(V)$ such that $\xi^T\mathcal{J} = 0$, which implies that $\xi^Te^{A\tau}B = \xi^T(e^{A\tau} - \mathcal{J})B = 0$. This contradicts that (3.38) is strictly positive.

Next, we prove that $\xi^T B \neq 0$, $\forall \xi \in \ker(A)$ and $\mathrm{rank}(\mathcal{P}(0,t_f)) = n - m$ are sufficient for the controllability of $\mathbf{\Sigma}_s$. Notice that any nonzero vector $\xi \in \mathbb{R}^n$ can be decomposed as a linear combination of $\xi_1 \in \mathrm{im}(V)$ and $\xi_2 \in \mathrm{im}(U)^\perp$ as in (3.34). Since $\mathrm{im}(V)$ is in the nullspace of $\mathcal{P}(0,t_f)$, and $\dim(\mathrm{im}(V)) = m$, the rank of $\mathcal{P}(0,t_f)$ then implies that

$$\xi_2^T(e^{A\tau} - \mathcal{J})B \neq 0, \ \forall \xi_2 \in \mathrm{im}(U)^\perp. \tag{3.40}$$

It follows from (3.35) that $\xi_2^T e^{A\tau} B \neq \xi_2^T \mathcal{J} B = 0$. Moreover,

$$\xi_1^T e^{A\tau} B = \xi_1^T (e^{A\tau} - \mathcal{J} + \mathcal{J}) B = \xi_1^T \mathcal{J} B. \tag{3.41}$$

Observe that $\xi^T B \neq 0$, $\forall \xi \in \ker(A)$ implies that $V^T B \neq 0$. Thus, (3.41) is nonzero for all $\xi_1 \in \mathrm{im}(V)$ since $V^T \mathcal{J} B = V^T U V^T B = V^T B \neq 0$. Consequently, we obtain $\xi^T e^{A\tau} B \neq 0$, for any nonzero vector ξ, i.e., $\mathcal{P}_s(0,t_f)$ is positive definite. It means that $\mathbf{\Sigma}_s$ is fully controllable.

Finally, the first statement in the theorem is obtained as $t_f \to \infty$. The proof of the observability part is a dual problem, whose proof follows a similar procedure. Hence, the details are omitted here. □

The dynamics of second-order networks are described by semistable systems. Therefore, in the next section, we will apply the results developed in this section to the model reduction problem of second-order network systems.

3.4 Clustering-Based Model Reduction

This section will first give a class of Galerkin projections that can deliver reduced second-order network models with interconnection structures. Then, some important properties of the resulting systems are discussed. Consider a network system $\mathbf{\Sigma}$ on graph $\mathcal{G}$ with n vertices. To approximate $\mathbf{\Sigma}$ by an r-th dimensional reduced model, we need to find a network clustering which partitions n vertices into r clusters. To preserve the structural conditions, we then characterize the projection in Problem 3.1 by the characteristic matrix of a graph clustering. More precisely, the following unnormalized Galerkin projection is applied

$$W = V = P, \tag{3.42}$$

where P is the characteristic matrix of a graph clustering, see Definition 2.5. It then leads to the r-dimensional reduced second-order network system as

$$\hat{\mathbf{\Sigma}} : \begin{cases} \hat{M}\ddot{z} + \hat{D}\dot{z} + \hat{L}z = P^T F u, \\ \hat{x} = Pz, \end{cases} \tag{3.43}$$

where $\hat{M} = P^T M P$, $\hat{D} = P^T D P$ and $\hat{L} = P^T L P \in \mathbb{R}^{r\times r}$.

This projection also can be found in [33,34,87,124]. In this chapter, we will further discuss this idea and develop our model reduction method based on it. The following proposition holds for the simplified model in (3.43).

Proposition 3.1. *The reduced network system $\hat{\mathbf{\Sigma}}$ resulting from a clustering-based projection as in (3.42) preserves the interconnection structures of the original system $\mathbf{\Sigma}$, i.e., $\hat{M}$, $\hat{D}$ and $\hat{L}$ satisfy the **structural conditions** in Assumption 3.1.*

Proof. Observe that P is a binary matrix with full column rank. It is not hard to verify that $\hat{M} \succ 0$, $\hat{D} \succ 0$ and $\hat{L} \succcurlyeq 0$.

Furthermore, since there always exists a permutation matrix T such that

$$\tilde{P} := TP = \text{diag}(\mathbb{1}_{|\mathcal{C}_1|}, \mathbb{1}_{|\mathcal{C}_2|}, \cdots, \mathbb{1}_{|\mathcal{C}_r|}), \tag{3.44}$$

we have $P = T^T \tilde{P}$ and $\hat{M} = \tilde{P}^T T M T^T \tilde{P}$. Clearly, matrix TMT^T is diagonal, and therefore, $\hat{M}$ is also. Moreover, the i-th diagonal entry of $\hat{M}$ presents the sum of all the masses with the i-th cluster.

From Definition (2.2), we have $\hat{L} = P^T R W R^T P$. Suppose the edge (i, j) of the original graph is represented by R_k, the k-th column of the incidence matrix R. Then, the entries of R_k satisfy that $R_{i,k} = -R_{j,k}$, and the other entries are zero. If vertices i and j are within the same cluster, from the definition of characteristic matrix of clustering, we have $P_i = P_j$, where P_i is the i-th row of P. Hence, we obtain $P^T R_k = 0$. Furthermore, we can define a new incidence matrix $\hat{R}$ by removing all the zero columns of $P^T R$ and a new edge weight matrix $\hat{W}$ by eliminating the rows and columns which are corresponding to the edges linking vertices in the same cluster. Consequently, it follows that $\hat{L} = P^T R W R^T P = \hat{R}\hat{W}\hat{R}^T$, where $\hat{L}$ is also a Laplacian matrix of an undirected connected graph. □

From the algebraic structures of matrices $\hat{M}$, $\hat{D}$ and $\hat{L}$, we are able to reconstruct the topology of the reduced network. The following example then illustrates the intuitive interpretation of clustering-based model reduction.

Example 3.1. *The left inset of Fig. 3.1 depicts a mass-damper-spring network system of 4*

vertices. The coefficient matrices are given by

$$M = \begin{bmatrix} 1 & 0 & 0 & 0 \\ 0 & 2 & 0 & 0 \\ 0 & 0 & 1 & 0 \\ 0 & 0 & 0 & 2 \end{bmatrix}, D = \begin{bmatrix} 4 & -2 & 0 & -1 \\ -2 & 2 & 0 & 0 \\ 0 & 0 & 3.5 & -3 \\ -1 & 0 & -3 & 4 \end{bmatrix},$$
$$L = \begin{bmatrix} 4 & -1 & -2 & -1 \\ -1 & 3 & -1 & -1 \\ -2 & -1 & 5 & -2 \\ -1 & -1 & -2 & 4 \end{bmatrix}, F = \begin{bmatrix} 1 & 0 \\ 0 & 0 \\ 0 & 0 \\ 0 & 1 \end{bmatrix}.$$

If vertex 3 and 4 are clustered, i.e., the network clustering is $\{\{1\},\{2\},\{3,4\}\}$*, the characteristic matrix* P *is then generated as*

$$P = \begin{bmatrix} 1 & 0 & 0 \\ 0 & 1 & 0 \\ 0 & 0 & 1 \\ 0 & 0 & 1 \end{bmatrix}, \tag{3.45}$$

which leads to the reduced-order model as

$$\hat{M} = \begin{bmatrix} 1 & 0 & 0 \\ 0 & 2 & 0 \\ 0 & 0 & 3 \end{bmatrix}, \hat{D} = \begin{bmatrix} 4 & -2 & -1 \\ -2 & 2 & 0 \\ -1 & 0 & 1.5 \end{bmatrix},$$
$$\hat{L} = \begin{bmatrix} 4 & -1 & -3 \\ -1 & 3 & -2 \\ -3 & -2 & 5 \end{bmatrix}, P^T F = \begin{bmatrix} 1 & 0 \\ 0 & 0 \\ 0 & 1 \end{bmatrix}.$$

Clearly, the algebraic structures of the inertia, damper, and stiffness matrices are preserved in the new system. An interpretation of the reduced model is presented in the right inset of Fig. 3.1.

Next, we discuss some important properties of the reduced second-order network system (3.43). First, the following proposition can be easily obtained.

Proposition 3.2. *The reduced second-order network system* $\hat{\mathbf{\Sigma}}$ *in (3.43) preserves the semistability and passivity of the original system* $\mathbf{\Sigma}$*.*

Proof. Proposition 3.1 states that the reduced matrices $\hat{M}$, $\hat{D}$ and $\hat{L}$ also fulfill the structural conditions list in Assumption 3.1. Therefore, we can also show the passivity and semistability of the reduced model $\hat{\mathbf{\Sigma}}$ by converting it to a first-order realization. □

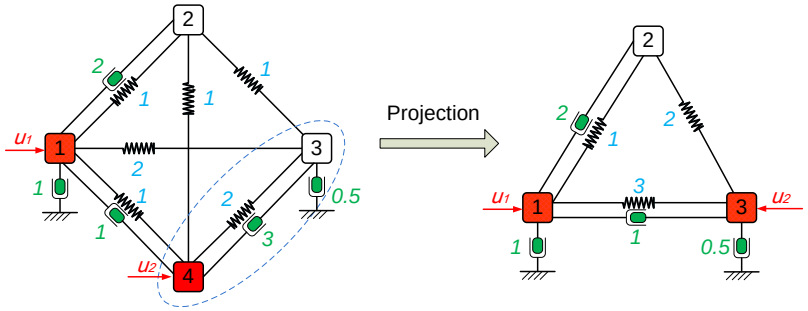

Figure 3.1: An illustrative example of clustering-based model reduction for a mass-damper-spring network system, where red blocks represent the controlled vertices.

Second, the synchronization properties of the original network system $\mathbf{\Sigma}$ is also retained in the reduced model $\hat{\mathbf{\Sigma}}$. The following theorem is extended from [34] and [33], where first-order network systems are studied.

Theorem 3.3. *Consider the second-order network system $\mathbf{\Sigma}$ and its reduced model $\hat{\mathbf{\Sigma}}$ resulting from an clustering-based projection. If their initial conditions satisfy $x(0) = Pz(0) = \hat{x}(0)$ and $\dot{x}(0) = P\dot{z}(0) = \dot{\hat{x}}(0)$, then the trajectories of both systems with $u = 0$ converge to a common value. More precisely,*

$$\lim_{t\to\infty} x(t) = \lim_{t\to\infty} \hat{x}(t) = \sigma_D^{-1} \begin{bmatrix} \mathbb{1}\mathbb{1}^T \left(Dx(0) + M\dot{x}(0)\right) \\ \mathbf{0}_{n\times 1} \end{bmatrix},$$
$$\lim_{t\to\infty} \dot{x}(t) = \lim_{t\to\infty} \dot{\hat{x}}(t) = 0,$$

where $\sigma_D = \mathbb{1}^T D \mathbb{1}$.

Proof. First, the synchronization of $\mathbf{\Sigma}$ is proved as follows.

Since $\mathcal{A}$ in (3.3) has one zero eigenvalue, we consider the Jordan matrix decomposition $\mathcal{A} = \mathsf{U}\Lambda\mathsf{U}^{-1}$, where

$$\Lambda = \begin{bmatrix} 0 & \\ & \bar{\Lambda} \end{bmatrix}, \tag{3.46}$$

with $\bar{\Lambda}$ Hurwitz. The first row of U^{-1} and the first column of U, denoted by $\mathsf{v}_1 \in \mathbb{R}^{1\times 2n}$ and $\mathsf{u}_1 \in \mathbb{R}^{2n\times 1}$, are the left and right eigenvectors of $\mathcal{A}$ corresponding to the only zero eigenvalue, respectively. Here, u_1 is an unit vector, and we have

$$\mathcal{A}^T \mathsf{v}_1^T = 0, \;\; \mathcal{A}\mathsf{u}_1 = 0 \text{ and } \mathsf{v}_1\mathsf{u}_1 = 1. \tag{3.47}$$

The above equations then lead to

$$\mathsf{v}_1 = \frac{\sqrt{n}}{\mathbb{1}^T D \mathbb{1}} \begin{bmatrix} \mathbb{1}^T D & \mathbb{1}^T M \end{bmatrix}, \text{ and } \mathsf{u}_1 = \begin{bmatrix} \frac{1}{\sqrt{n}} \mathbb{1} \\ \mathbf{0}_{n\times 1} \end{bmatrix}, \tag{3.48}$$

where the property $L\mathbb{1} = 0$ is used. Furthermore, we partition U and U^{-1} as

$$\mathsf{U} = \begin{bmatrix} \mathsf{u}_1 & \mathsf{U}_2 \end{bmatrix}, \ \mathsf{U}^{-1} = \begin{bmatrix} \mathsf{v}_1 \\ \mathsf{V}_2 \end{bmatrix}, \tag{3.49}$$

and it follows that

$$e^{\mathcal{A}t} = \mathsf{U} e^{\Lambda t} \mathsf{U}^{-1} = \begin{bmatrix} \mathsf{u}_1 & \mathsf{U}_2 \end{bmatrix} \begin{bmatrix} 1 & \\ & e^{\bar{\Lambda} t} \end{bmatrix} \begin{bmatrix} \mathsf{v}_1 \\ \mathsf{V}_2 \end{bmatrix} = \mathsf{u}_1 \mathsf{v}_1 + \mathsf{U}_2 e^{\bar{\Lambda} t} \mathsf{V}_2. \tag{3.50}$$

Observe that $\lim_{t\to\infty} \mathsf{U}_2 e^{\bar{\Lambda} t} \mathsf{V}_2 = 0$, which yields that

$$\lim_{t\to\infty} e^{\mathcal{A}t} = \mathsf{u}_1 \mathsf{v}_1 = \sigma_D^{-1} \begin{bmatrix} \mathbb{1}_n \mathbb{1}_n^T D & \mathbb{1}_n \mathbb{1}_n^T M \\ \mathbf{0}_{n\times n} & \mathbf{0}_{n\times n} \end{bmatrix}. \tag{3.51}$$

Consequently, we obtain

$$\lim_{t\to\infty} \begin{bmatrix} x(t) \\ \dot{x}(t) \end{bmatrix} = \lim_{t\to\infty} e^{\mathcal{A}t} \begin{bmatrix} x(0) \\ \dot{x}(0) \end{bmatrix} = \sigma_D^{-1} \begin{bmatrix} \mathbb{1}_n \mathbb{1}_n^T \left(D x(0) + M \dot{x}(0) \right) \\ \mathbf{0}_{n\times 1} \end{bmatrix}.$$

Proposition 3.1 indicates that the reduced-order model $\hat{\mathbf{\Sigma}}$ has the same form as the original model $\mathbf{\Sigma}$. Therefore, a similar reasoning line yields

$$\lim_{t\to\infty} \begin{bmatrix} z(t) \\ \dot{z}(t) \end{bmatrix} = \frac{1}{\mathbb{1}_r^T \hat{D} \mathbb{1}_r} \begin{bmatrix} \mathbb{1}_r \mathbb{1}_r^T \left(\hat{D} z(0) + \hat{M} \dot{z}(0) \right) \\ \mathbf{0}_{r\times 1} \end{bmatrix},$$

Then, we have the following equations for $\hat{\mathbf{\Sigma}}$:

$$\begin{aligned} \lim_{t\to\infty} \dot{\hat{x}}(t) &= \lim_{t\to\infty} P \dot{z}(t) = \mathbf{0}_{n\times 1}, \\ \lim_{t\to\infty} \hat{x}(t) &= \lim_{t\to\infty} P z(t) = P \frac{\mathbb{1}_r \mathbb{1}_r^T \left(\hat{D} z(0) + \hat{M} \dot{z}(0) \right)}{\mathbb{1}_r^T \hat{D} \mathbb{1}_r}, \end{aligned}$$

where $\hat{M} = P^T M P$, $\hat{D} = P^T D P$. The result immediately follows from $\hat{x}(0) = P z(0) = x(0)$ and $P \mathbb{1}_r = \mathbb{1}_n$. □

Remark 3.3. *Theorem 3.3 also indicates that with any initial conditions and $u = 0$, the trajectories of $\dot{x}(t)$ and $\dot{z}(t)$ always converge to zero, while those of $x(t)$ and $z(t)$ converge to a common value which is nonzero in general. Furthermore, if we denote $\xi(t)$ and $\hat{\xi}(t) \in \mathbb{R}^{n\times p}$ as the **impulse responses** of $\mathbf{\Sigma}$ and $\hat{\mathbf{\Sigma}}$, then we can obtain*

$$\begin{aligned} \lim_{t\to\infty} \xi(t) &= \lim_{t\to\infty} \hat{\xi}(t) = \sigma_D^{-1} \mathbb{1}\mathbb{1}^T F, \\ \lim_{t\to\infty} \dot{\xi}(t) &= \lim_{t\to\infty} \dot{\hat{\xi}}(t) = 0, \end{aligned} \tag{3.52}$$

which follows from the computation of $\lim_{t\to\infty} e^{\mathcal{A}t}\mathcal{B}$ with $\mathcal{A}$ and $\mathcal{B}$ defined in (3.4).

3.5 Selection of Network Clustering

The cluster selection is a crucial problem in clustering-based model reduction, since different choices of clustering yield different reduced models with different approximation qualities. In Section 3.5.1, we first specify the concept of the *pseudo controllability Gramian* to second-order network systems and then discuss a method to compute such Gramian from the state-space model (3.3). The purpose of defining such a Gramian is explained in Section 3.5.2, where a hierarchical clustering algorithm is designed for cluster selection. Finally, the approximation error is analyzed in Section 3.5.3.

3.5.1 Second-Order Pseudo Controllability Gramian

For asymptotically stable systems, we can define controllability Gramian as in (2.21). However, the standard definition is not well-defined for the network system $\mathbf{\Sigma}$. In this chapter, we adopt the notion of pseudo controllability Gramian of Section 3.3. For the second-order network system $\mathbf{\Sigma}$, we obtain a concise expression of $\mathcal{J}$ in (3.7) as

$$\mathcal{J} = \sigma_D^{-1} \begin{bmatrix} \mathbb{1}\mathbb{1}^T D & \mathbb{1}\mathbb{1}^T M \\ \mathbf{0}_{n\times n} & \mathbf{0}_{n\times n} \end{bmatrix}. \tag{3.53}$$

Then, the second-order pseudo controllability Gramian, denoted by $\mathcal{P} \in \mathbb{R}^{2n\times 2n}$, is given in (3.7a) and satisfies the Lyapunov equation in (3.8). This section provides specific results for second-order Gramians, which can be obtained from Section 3.3.

Lemma 3.4. *Suppose a symmetric matrix $\mathcal{P}_1 \in \mathbb{R}^{2n\times 2n}$ is a solution of the Lyapunov equation in (3.8a), then the following three conditions are equivalent*

1. *A symmetric matrix $\mathcal{P}_2 \in \mathbb{R}^{2n\times 2n}$ is a solution of (3.8a).*

2. *$\mathcal{P}_2$ satisfies the equation*

$$\mathcal{J}(\mathcal{P}_1 - \mathcal{P}_2)\mathcal{J}^T = \mathcal{P}_1 - \mathcal{P}_2. \tag{3.54}$$

3. *$\mathcal{P}_2$ can be expressed by*

$$\mathcal{P}_2 = \mathcal{P}_1 + \beta\Pi \tag{3.55}$$

with $\Pi := \begin{bmatrix} \mathbb{1}\mathbb{1}^T & \mathbf{0}_{n\times n} \\ \mathbf{0}_{n\times n} & \mathbf{0}_{n\times n} \end{bmatrix}$ *and β a scalar constant.*

Proof. 1) $\Rightarrow$ 2): Assume that $\mathcal{P}_2$ is also a solution of (3.8a), and denote $\Delta := \mathcal{P}_1 - \mathcal{P}_2$. We have

$$\mathcal{A}\Delta + \Delta\mathcal{A}^T = 0, \tag{3.56}$$

which leads to

$$e^{\mathcal{A}t}\left[\mathcal{A}\Delta + \Delta\mathcal{A}^T\right]e^{\mathcal{A}^T t} = \frac{d}{dt}\left[e^{\mathcal{A}t}\Delta e^{\mathcal{A}^T t}\right] = 0. \tag{3.57}$$

Therefore, we obtain

$$\int_0^\infty \frac{d}{dt}\left[e^{\mathcal{A}t}\Delta e^{\mathcal{A}^T t}\right]dt = 0, \tag{3.58}$$

which is equivalent to

$$\mathcal{J}\Delta\mathcal{J}^T = \Delta. \tag{3.59}$$

2) $\Rightarrow$ 3): Assume that $\mathcal{P}_2$ satisfies (3.54), i.e., equation (3.59) holds. Then, the entry in the i-th row and j-th column of Δ is given by $\Delta_{ij} = \mathcal{J}_i\Delta\mathcal{J}_j^T$, where $\mathcal{J}_i \in \mathbb{R}^{1\times 2n}$ presents the i-th row of $\mathcal{J}$. Note that

$$\mathcal{J}_i = \begin{cases} \sigma_D^{-1}\cdot\left[\mathbb{1}^T D, \mathbb{1}^T M\right], & 1 \le i \le n \\ \mathbf{0}_{1\times 2n}, & n+1 \le i \le 2n \end{cases} \tag{3.60}$$

with scalar $\sigma_D = \mathbb{1}^T D\mathbb{1}$. Therefore,

$$\Delta_{ij} = \sigma_D^{-2}\cdot\left(\mathbb{1}^T D\Delta D\mathbb{1} + \mathbb{1}^T M\Delta M\mathbb{1}\right) := \beta, \tag{3.61}$$

if $1 \le i, j \le n$, $\Delta_{ij} = 0$, otherwise, which implies that $\mathcal{P}_2$ is presented as equation (3.55).

3) $\Rightarrow$ 1): Observe that

$$\mathcal{A}\Pi = \begin{bmatrix} \mathbf{0} & I \\ -M^{-1}L & -M^{-1}D \end{bmatrix}\begin{bmatrix} \beta\mathbb{1}\mathbb{1}^T & \mathbf{0}_{n\times n} \\ \mathbf{0}_{n\times n} & \mathbf{0}_{n\times n} \end{bmatrix} = 0.$$

Suppose a symmetric matrix $\mathcal{P}_2$ is in the form of (3.55), we then obtain

$$\begin{aligned} &\mathcal{A}\mathcal{P}_2 + \mathcal{P}_2\mathcal{A}^T + (I-\mathcal{J})\mathcal{B}\mathcal{B}^T(I-\mathcal{J}^T) \\ =&\mathcal{A}(\mathcal{P}_1 + \beta\Pi) + (\mathcal{P}_1 + \beta\Pi)\mathcal{A}^T + (I-\mathcal{J})\mathcal{B}\mathcal{B}^T(I-\mathcal{J}^T) \\ =&\mathcal{A}\mathcal{P}_1 + \mathcal{P}_1\mathcal{A}^T + (I-\mathcal{J})\mathcal{B}\mathcal{B}^T(I-\mathcal{J}^T) = 0, \end{aligned}$$

which indicates that $\mathcal{P}_2$ is also a solution of (3.8a).

That completes the proof. □

We then can obtain the pseudo controllability Gramian in the following theorem, despite that the solutions of the Lyapunov equation in (3.8a) are not unique.

Theorem 3.4. *Consider the network system $\mathbf{\Sigma}$ as in (3.1) and let $\mathcal{P}_a$ be an arbitrary solution of the Lyapunov equation in (3.8a). Then, the pseudo controllability Gramian $\mathcal{P}$ is given by*

$$\mathcal{P} = \mathcal{P}_a + \beta_a \Pi, \tag{3.62}$$

where Π is defined in (3.55) and

$$\beta_a = -\sigma_D^{-2} \cdot \left(\left[\mathbb{1}^T D, \mathbb{1}^T M \right] \mathcal{P}_a \begin{bmatrix} D\mathbb{1} \\ M\mathbb{1} \end{bmatrix} \right). \tag{3.63}$$

Proof. Consider $\mathcal{P}_a$ as an arbitrary solution of (3.8a). Since the pseudo controllability Gramian $\mathcal{P}$ is also a solution of (3.8a), Lemma 3.4 then implies that there exists a scalar β_a such that

$$\mathcal{P} = \mathcal{P}_a + \beta_a \Pi. \tag{3.64}$$

Next, we prove that β_a satisfies (3.63) based on the definition of pseudo controllability Gramian. Denote a vector $\nu^T := \left[\mathbb{1}^T D, \mathbb{1}^T M \right] \in \mathbb{R}^{1 \times 2n}$. Then, we have

$$\nu^T \mathcal{A} = \left[\mathbb{1}^T D, \mathbb{1}^T M \right] \begin{bmatrix} \mathbf{0} & I \\ -M^{-1}L & -M^{-1}D \end{bmatrix} = 0, \tag{3.65}$$

where $\mathbb{1}^T L = 0$ is used. Since the power series expansion of $e^{\mathcal{A}t}$ is

$$e^{\mathcal{A}t} = I + \sum_{k=1}^{\infty} \frac{\mathcal{A}^k t^k}{k!}, \tag{3.66}$$

we have

$$\nu^T e^{\mathcal{A}t} = \nu^T. \tag{3.67}$$

For the matrix $\mathcal{J}$, from its definition (3.53), we have

$$\nu^T \mathcal{J} = \left[\mathbb{1}^T D, \mathbb{1}^T M \right] \cdot \sigma_D^{-1} \begin{bmatrix} \mathbb{1}\mathbb{1}^T D & \mathbb{1}\mathbb{1}^T M \\ \mathbf{0}_{n \times n} & \mathbf{0}_{n \times n} \end{bmatrix} = \nu^T, \tag{3.68}$$

where $\sigma_D = \mathbb{1}^T D \mathbb{1}$ is used. In summary, from (3.67) and (3.68), we have

$$\nu^T (e^{\mathcal{A}t} - \mathcal{J}) = \nu^T I - \nu^T \mathcal{J} = 0. \tag{3.69}$$

This implies from the definition of pseudo controllability Gramian in (3.7a), $\nu^T\mathcal{P} = 0$, and consequenly

$$\nu^T\mathcal{P}\nu = 0. \tag{3.70}$$

By substituting (3.64) into (3.70), we obtain

$$\nu^T(\mathcal{P}_a + \beta_a\Pi)\nu = 0. \tag{3.71}$$

Observe that $\nu^T\Pi\nu = (\mathbb{1}^T D\mathbb{1})^2 = \sigma_D^2$, therefore,

$$\beta_a = -\sigma_D^{-2}\nu^T\mathcal{P}_a\nu, \tag{3.72}$$

which is equivalent to (3.63). □

Remark 3.4. *The proof of Theorem 3.4 implies that $\mathcal{P}$ satisfying (3.8a) and (3.70) uniquely exists. Let both $\mathcal{P}_a$ and $\mathcal{P}_b$ satisfy (3.8a) and (3.70). Condition (3.8a) implies that for the pseudo controllability Gramian $\mathcal{P}$, there exist scalar β_a and β_b such that*

$$\mathcal{P}_a + \beta_a\Pi = \mathcal{P} = \mathcal{P}_b + \beta_b\Pi. \tag{3.73}$$

Moreover, (3.70) yields

$$\beta_a\nu^{\mathrm{T}}\Pi\nu = 0 = \beta_b\nu^{\mathrm{T}}\Pi\nu. \tag{3.74}$$

Since $\nu^{\mathrm{T}}\Pi\nu = \sigma_D^2$ is nonzero, we have $\beta_a = \beta_b = 0$. Therefore, we have $\mathcal{P}_a = \mathcal{P} = \mathcal{P}_b$.

Theorem 3.4 provides an approach to obtain the second-order pseudo controllability Gramian $\mathcal{P}$ without computing an integral. First, we solve the Lyapunov equation in (3.8a) and obtain an arbitrary solution. Then, applying (3.62) leads to the $\mathcal{P}$ matrix. In [14, 16], the algorithms to solve the Sylvester equation are proposed for nonsingular A and B matrices. Based on them, it is not difficult to generalize the methods to the singular case, e.g., the Lyapunov equation in (3.8a), just to acquire an arbitrary solution. In this chapter, we will not further discuss the computation of the matrix equation (3.8a) due to the limited space. In the following subsection, we adopt the second-order pseudo controllability Gramian to design an efficient cluster selection algorithm.

3.5.2 Hierarchical Clustering

Which method is used for cluster selection generally determines the approximation quality of the reduced-order system. Therefore, it plays a crucial role in the model reduction of a network system. Contrary to the existing algorithms in the literature, we propose a novel one that uses the $\mathcal{H}_2$-norms of transfer function discrepancy as the criterion to measure the *dissimilarities* of vertices and clusters those vertices with similar behaviors.

We first consider the transfer matrix of system $\mathbf{\Sigma}$ in (3.1)

$$\eta(s) := (s^2M + sD + L)^{-1}F \in \mathbb{R}(s)^{n\times m}, \tag{3.75}$$

and characterize the vertex behavior by the transfer function from external inputs to individual states, i.e., the behavior of the i-th vertex is captured by the transfer function

$$\eta_i(s) := \mathbf{e}_i^T\eta(s). \tag{3.76}$$

Then, the *dissimilarity* of vertices i and j is defined.

Definition 3.2. *Consider the network system $\mathbf{\Sigma}$, the **dissimilarity** of nodes i and j is defined by*

$$\mathcal{D}_{ij} := \|\eta_i(s) - \eta_j(s)\|_{\mathcal{H}_2}. \tag{3.77}$$

The boundedness of $\mathcal{D}_{ij}$ is implied by the following lemma.

Lemma 3.5. *Consider the second-order network system $\mathbf{\Sigma}$ and add an external output: $y = H_s x + H_v\dot{x}$ with $H_s, H_v \in \mathbb{R}^{p\times n}$, then the input-output transfer function*

$$G(s) := (H_s + sH_v)(s^2M + sD + L)^{-1}F \in \mathbb{R}(s)^{p\times m} \tag{3.78}$$

is $\mathcal{H}_2$ norm-bounded if and only if $H_s\mathbb{1} = 0$ or $\mathbb{1}^TF = 0$.

Proof. Denote $g(t)$ as the impulse response of $G(s)$, which is given by

$$g(t) = \begin{bmatrix} H_s & H_v \end{bmatrix} e^{\mathcal{A}t}\mathcal{B} \in \mathbb{R}^{2p\times m} \tag{3.79}$$

with $\mathcal{A}$ and $\mathcal{B}$ defined in (3.4). Theorem 3.3 implies that $e^{\mathcal{A}t}$ is a bounded smooth function of t and exponentially converges to a constant matrix $\mathcal{J}$ as $t \to \infty$. Therefore, the function $g(t)$ is *integrable* if and only if $\lim_{t\to\infty} g(t) = 0$.

From (3.52), the function $g(t)$ has an exponential convergence as follows.

$$\lim_{t\to\infty} g(t) = \begin{bmatrix} H_s & H_v \end{bmatrix} \mathcal{J}\mathcal{B} = \sigma_D^{-1}H_s\mathbb{1}\mathbb{1}^TF. \tag{3.80}$$

Observe that $H_s\mathbb{1} \in \mathbb{R}^{p\times 1}$ and $\mathbb{1}^TF \in \mathbb{R}^{1\times m}$. Therefore, we have $\lim_{t\to\infty} g(t) = 0$ if and only if $H_s\mathbb{1} = 0$ or $\mathbb{1}^TF = 0$. Notice that the function $g(t)$ being integrable equivalently implies $\mathsf{tr}\left[g(t)^Tg(t)\right]$ is also integrable, and the $\mathcal{H}_2$-norm of $G(s)$ is presented as

$$\|G(s)\|_{\mathcal{H}_2} = \left(\int_0^\infty \mathsf{tr}\left[g(t)^Tg(t)\right] dt\right)^{1/2}, \tag{3.81}$$

Thus, the $\mathcal{H}_2$-norm of $G(s)$ is bounded if and only if $\mathsf{tr}\left[g(t)^Tg(t)\right]$ is integrable that is $g(t)$ is integrable, or equivalently, $H_s\mathbb{1} = 0$ or $\mathbb{1}^TF = 0$. □

Notice that $\eta_i(s) - \eta_j(s)$ is in form of $G(s)$ with $H_s = \mathbf{e}_i^T - \mathbf{e}_j^T$ and $H_v = 0$. Since $(\mathbf{e}_i^T - \mathbf{e}_j^T)\mathbb{1} = 0$ for all $i, j \in \{1, 2, \cdots, n\}$, the above lemma then implies that $\mathcal{D}_{ij}$ in (3.77) is always bounded for the network system $\mathbf{\Sigma}$.

Now we define a *dissimilarity matrix* $\mathcal{D}$ whose entries are $\mathcal{D}_{ij}$. Clearly, $\mathcal{D}$ is nonnegative symmetric matrix with zero diagonal elements.

Computing matrix $\mathcal{D}$ poses a major challenge, especially for large-scale systems, while there are several methods, such as using the Riemann sum or linear matrix inequalities as in e.g., [155]. However, the proposed pseudo controllability Gramian provides a more efficient computational method due to the following theorem.

Theorem 3.5. *Consider the input-output transfer function $G(s) := (H_s + sH_v)\eta(s)$ as in (3.78). If $H_s\mathbb{1} = 0$ or $\mathbb{1}^T F = 0$, then the $\mathcal{H}_2$-norm of $G(s)$ is computed by*

$$\|G(s)\|_{\mathcal{H}_2}^2 = \mathsf{tr}\left(H\mathcal{P}H^T\right). \tag{3.82}$$

where $H := \begin{bmatrix} H_s & H_v \end{bmatrix}$ and $\mathcal{P}$ is the second-order pseudo controllability Gramian defined in (3.7a). Specifically, the relation between the dissimilarity measure $\mathcal{D}_{ij}$ and the pseudo controllability Gramian $\mathcal{P}$ is given by

$$\mathcal{D}_{ij} = \sqrt{\mathsf{tr}\left(\begin{bmatrix}\mathbf{e}_{ij}^T, \mathbf{0}_{1\times n}\end{bmatrix}\mathcal{P}\begin{bmatrix}\mathbf{e}_{ij} \\ \mathbf{0}_{n\times 1}\end{bmatrix}\right)}. \tag{3.83}$$

The proof follows directly from Lemma 3.2. To compute the dissimilarity matrix $\mathcal{D}$, we first calculate $\mathcal{P}$ by Theorem 3.4 and then just apply vector-matrix multiplication to obtain all the entries of $\mathcal{D}$.

The entries of $\mathcal{D}$ indicate the similarities of vertices. Based on the $\mathcal{D}$ matrix, we propose a hierarchical clustering algorithm to generate an appropriate network clustering for the system $\mathbf{\Sigma}$. This approach links the pairs of vertices that are in close proximity and place them into binary clusters. Then, the newly formed clusters can be merged into larger clusters according to the *cluster dissimilarity*. The dissimilarity of clusters $\mathcal{C}_\mu$ and $\mathcal{C}_\nu$ is defined by

$$\delta(\mathcal{C}_\mu, \mathcal{C}_\nu) = \frac{1}{|\mathcal{C}_\mu| \cdot |\mathcal{C}_\nu|} \sum_{i\in\mathcal{C}_\mu} \sum_{j\in\mathcal{C}_\nu} \mathcal{D}_{ij}. \tag{3.84}$$

The notation $\delta(\mathcal{C}_\mu, \mathcal{C}_\nu)$ is characterized by the average dissimilarity between all pairs of vertices in the clusters $\mathcal{C}_\mu$ and $\mathcal{C}_\nu$.

The idea of hierarchical clustering has been extensively used in many fields, including pattern recognition, data compression, computer graphics, and process networks, see [77,78,94]. This chapter is the first one that introduces this clustering algorithm to model reduction of network systems and defines the distance by the

norm of transfer functions. In hierarchical clustering, we first assign each vertex into an individual cluster and then merge two clusters into a single one if they have the least dissimilarity. Finally, we can cluster the vertices into a binary, hierarchical tree, which is called *dendrogram*. The pseudocode of hierarchical clustering is described in Algorithm 1. Notice that Algorithm 1 is a greedy method.

Algorithm 1 Hierarchical Clustering

Input: M, D, L and F, model order n, desired order r
Output: P, $\hat{M}$, $\hat{D}$, $\hat{L}$

Compute the Gramian $\mathcal{P}$ by Theorem 3.4
Compute the dissimilarity matrix $\mathcal{D}$ by Theorem 3.5
Place each vertex into its own singleton cluster, that is $\mathcal{C}_i \leftarrow \{i\}$ for all $1 \leq i \leq n$
$k \leftarrow n$
while $k > r$ **do**
    Set δ_{m} to be an arbitrary large number
    for $i = 1 : k-1$ and $j = 2 : i-1$ **do**
        Compute $\delta(\mathcal{C}_i, \mathcal{C}_j)$ by (3.84)
        if $\delta_{\mathrm{m}} > \delta(\mathcal{C}_i, \mathcal{C}_j)$ **then**
            $\mu \leftarrow i$, $\nu \leftarrow j$, $\delta_{\mathrm{m}} \leftarrow \delta(\mathcal{C}_i, \mathcal{C}_j)$
        end if
    end for
    Merge cluster μ and ν into a single cluster
    $k \leftarrow k - 1$
end while
Compute $P \in \mathbb{R}^{n \times r}$
$\hat{M} \leftarrow P^T M P$, $\hat{D} \leftarrow P^T D P$, $\hat{L} \leftarrow P^T L P$

Remark 3.5. *The pseudo controllability Gramian analysis leads to a pair-wise distance notion of vertices, and the clustering algorithm is a simple consequence of it. We can also adopt other clustering algorithms, such as iterative clustering, K-means clustering, or other greedy clustering strategies, to our problem. We choose hierarchical clustering because it can obtain a reduced network with small approximation error and low computational cost.*

Remark 3.6. *The clustering algorithm does not focus on manipulating any individual edges, since the dissimilarity matrix $\mathcal{D}$ contains the dissimilarity of every pair of vertices. Even if two vertices are not adjacent, their dissimilarity can also be measured based on their responses to the external inputs. If the two vertices have very similar behaviors, they are then aggregated, because the obtained reduced network generally has a smaller approximation error.*

3.5.3 Error Analysis

Now, we analyze the approximation error between the full-order and reduced-order system. First, we denote

$$\hat{\eta}(s) := P(s^2\hat{M} + s\hat{D} + \hat{L})^{-1}P^T F \in \mathbb{R}(s)^{n\times m} \tag{3.85}$$

as the transfer function of the reduced-order system (3.43) and $\hat{\eta}_i(s) := \mathbf{e}_i^T\hat{\eta}(s)$. Then the following lemma indicates the boundedness of the approximation error.

Lemma 3.6. *Consider the second-order network system $\boldsymbol{\Sigma}$ in (3.1) and the reduced model $\hat{\boldsymbol{\Sigma}}$ in (3.43) resulting from graph clustering. $\eta(s)$ and $\hat{\eta}(s)$ are the transfer functions defined in (3.75) and (3.85), respectively. Then, the following statements holds:*

1. *$\|\eta_i(s) - \hat{\eta}_j(s)\|_{\mathcal{H}_2}$ is bounded for any $i, j = \{1, 2, \cdots, n\}$.*
2. *$\|\eta(s) - \hat{\eta}(s)\|_{\mathcal{H}_2}$ is bounded.*

Proof. Note that the $\mathcal{H}_2$-norm of $\eta_i(s) - \hat{\eta}_j(s)$ is given by

$$\|\eta_i(s) - \hat{\eta}_j(s)\|_{\mathcal{H}_2}^2 = \int_0^\infty \|\mathbf{e}_i^T\xi(t) - \mathbf{e}_j^T\hat{\xi}(t)\|_2^2 dt, \tag{3.86}$$

where $\xi(t)$ and $\hat{\xi}(t)$ are the impulse responses of $\boldsymbol{\Sigma}$ and $\hat{\boldsymbol{\Sigma}}$, respectively. Furthermore, both $\xi(t)$ and $\hat{\xi}(t)$ are bounded smooth functions of t, which exponentially converge to the same value. From Remark 3.3, we have $\lim_{t\to\infty}\xi(t) = \lim_{t\to\infty}\hat{\xi}(t) = \sigma_D^{-1}\mathbb{1}\mathbb{1}^T F$. Therefore,

$$\lim_{t\to\infty}\left[\mathbf{e}_i^T\xi(t) - \mathbf{e}_j^T\hat{\xi}(t)\right] = 0. \tag{3.87}$$

For bounded initial conditions $\xi_i(0)$ and $\hat{\xi}_j(0)$, the integral in (3.86) is bounded, i.e., $\|\eta_i(s) - \hat{\eta}_j(s)\|_{\mathcal{H}_2}^2 < \infty$. It means that the norm of each row of $\eta(s) - \hat{\eta}(s)$ is finite, therefore, $\|\eta(s) - \hat{\eta}(s)\|_{\mathcal{H}_2}$ is also bounded. □

Now, we explore the method to compute the approximation error in terms of the $\mathcal{H}_2$-norm. For simplicity, we denote

$$\hat{\mathcal{A}} = \begin{bmatrix} \mathbf{0}_{r\times r} & I_r \\ -\hat{M}^{-1}\hat{L} & -\hat{M}^{-1}\hat{D} \end{bmatrix},\ \hat{\mathcal{B}} = \begin{bmatrix} \mathbf{0}_{r\times m} \\ \hat{M}^{-1}P^T F \end{bmatrix}. \tag{3.88}$$

for the reduced system $\hat{\boldsymbol{\Sigma}}$ in (3.43). Since $P\mathbb{1}_r = \mathbb{1}_n$, $\mathbb{1}_r^T\hat{D}\mathbb{1}_r = \mathbb{1}_r^T P^T D P\mathbb{1}_r = \mathbb{1}_n^T D\mathbb{1}_n$, the convergence matrix of $\hat{\boldsymbol{\Sigma}}$ is given by

$$\hat{\mathcal{J}} = \sigma_D^{-1}\cdot\begin{bmatrix} \mathbb{1}_r\mathbb{1}_r^T\hat{D} & \mathbb{1}_r\mathbb{1}_r^T\hat{M} \\ \mathbf{0}_{r\times r} & \mathbf{0}_{r\times r} \end{bmatrix} \tag{3.89}$$

with $\sigma_D = \mathbb{1}_n^T D \mathbb{1}_n$.

Next, we consider the following error system:

$$\mathbf{\Sigma}_{\boldsymbol{e}} : \begin{cases} \dot{\omega} = \mathcal{A}_{\mathsf{e}}\omega + \mathcal{B}_{\mathsf{e}}u, \\ \delta = \mathcal{C}_{\mathsf{e}}\omega, \end{cases} \tag{3.90}$$

where

$$\mathcal{A}_{\mathsf{e}} = \begin{bmatrix} \mathcal{A} & 0 \\ 0 & \hat{\mathcal{A}} \end{bmatrix} \in \mathbb{R}^{(2n+2r)\times(2n+2r)}, \ \mathcal{B}_{\mathsf{e}} = \begin{bmatrix} \mathcal{B} \\ \hat{\mathcal{B}} \end{bmatrix} \in \mathbb{R}^{(2n+2r)\times m},$$
$$\mathcal{C}_{\mathsf{e}} = \begin{bmatrix} I_n & \mathbf{0}_{n\times n} - P & \mathbf{0}_{n\times r} \end{bmatrix} \in \mathbb{R}^{n\times(2n+2r)}.$$

Then, the approximation error between the full-order and reduced-order system is equivalent to computing $\|\mathbf{\Sigma_e}\|_{\mathcal{H}_2}$.

Lemma 3.6 guarantees that, by clustering-based projection, the approximation error between the full-order and reduced-order models is bounded. Now, we exploit the method to compute the errors $\|\mathbf{\Sigma} - \hat{\mathbf{\Sigma}}\|_{\mathcal{H}_2}$.

To this end, we define the *coupling pseudo controllability Gramian* of system $\mathbf{\Sigma_e}$, which is formulated as

$$\mathcal{P}_{\mathsf{x}} = \int_0^\infty (e^{\mathcal{A}t} - \mathcal{J})\mathcal{B}\hat{\mathcal{B}}^T(e^{\hat{\mathcal{A}}^T t} - \hat{\mathcal{J}}^T)dt \in \mathbb{R}^{2n\times 2r}. \tag{3.91}$$

The following lemma provides a method to obtain $\mathcal{P}_{\mathsf{x}}$ without integration.

Lemma 3.7. *Consider the error system $\mathbf{\Sigma_e}$ in (3.90) and its coupling pseudo controllability Gramian is computed by*

$$\mathcal{P}_{\mathsf{x}} = \tilde{\mathcal{P}}_{\mathsf{x}} + \beta_{\mathsf{x}}\Pi_{\mathsf{x}}, \tag{3.92}$$

where $\tilde{\mathcal{P}}_{\mathsf{x}}$ is an arbitrary solution of the following Sylvester equation

$$\mathcal{A}\tilde{\mathcal{P}}_{\mathsf{x}} + \tilde{\mathcal{P}}_{\mathsf{x}}\hat{\mathcal{A}} + \mathcal{B}\hat{\mathcal{B}}^T = 0, \tag{3.93}$$

and β_{x} is a scalar constant given by

$$\beta_{\mathsf{x}} = -\sigma_D^{-2} \cdot \left[\mathbb{1}_n^T D, \mathbb{1}_n^T M\right] \tilde{\mathcal{P}}_{\mathsf{x}} \begin{bmatrix} \hat{D}\mathbb{1}_r \\ \hat{M}\mathbb{1}_r \end{bmatrix} \tag{3.94}$$

with $\sigma_D = \mathbb{1}_n^T D \mathbb{1}_n$.

Proof. By similar reasoning as in the proofs of Lemma 3.4 and Theorem 3.4, the following results can be obtained:

First, $\mathcal{P}_{\mathsf{x}}$ is the solution of the matrix equation in (3.93).

Second, both $\tilde{\mathcal{P}}_{\mathsf{x}}$ and $\mathcal{P}_{\mathsf{x}}$ are the solutions of equation (3.93) if only if they satisfy

$$\mathcal{J}(\tilde{\mathcal{P}}_{\mathsf{x}} - \mathcal{P}_{\mathsf{x}})\hat{\mathcal{J}}^T = \tilde{\mathcal{P}}_{\mathsf{x}} - \mathcal{P}_{\mathsf{x}}, \tag{3.95}$$

or equivalently, $\mathcal{P}_{\mathsf{x}}$ can be expressed as

$$\mathcal{P}_{\mathsf{x}} = \tilde{\mathcal{P}}_{\mathsf{x}} + \beta_{\mathsf{x}}\Pi_{\mathsf{x}}, \tag{3.96}$$

with $\Pi_{\mathsf{x}} := \begin{bmatrix} \mathbb{1}_n\mathbb{1}_r^T & \mathbf{0}_{n\times r} \\ \mathbf{0}_{n\times r} & \mathbf{0}_{n\times r} \end{bmatrix}$ and β_{x} a scalar constant.

Third, $\mathcal{P}_{\mathsf{x}}$ satisfies

$$\begin{bmatrix}\mathbb{1}_n^T D, \mathbb{1}_n^T M\end{bmatrix} \mathcal{P}_{\mathsf{x}} \begin{bmatrix} \hat{D}\mathbb{1}_r \\ \hat{M}\mathbb{1}_r \end{bmatrix} = 0. \tag{3.97}$$

Note that

$$\begin{bmatrix}\mathbb{1}_n^T D, \mathbb{1}_n^T M\end{bmatrix} \Pi_{\mathsf{x}} \begin{bmatrix} \hat{D}\mathbb{1}_r \\ \hat{M}\mathbb{1}_r \end{bmatrix} = \mathbb{1}_n^T D\mathbb{1}_n\mathbb{1}_r^T\hat{D}\mathbb{1}_r = \sigma_D^2. \tag{3.98}$$

Therefore, from (3.96) and (3.97), we obtain the expression of β_{x} as in (3.94). □

Based on the coupling pseudo controllability Gramian, the approximation error between the full-order and reduced-order system, i.e., $\|\mathbf{\Sigma_e}\|_{\mathcal{H}_2}$ is obtained as follows.

Theorem 3.6. *Consider the second-order network system $\mathbf{\Sigma}$ in (3.1) and the reduced model $\hat{\mathbf{\Sigma}}$ in (3.43) resulting from graph clustering. Then the error between $\mathbf{\Sigma}$ and $\hat{\mathbf{\Sigma}}$ in terms of the $\mathcal{H}_2$-norm is computed by*

$$\|\mathbf{\Sigma} - \hat{\mathbf{\Sigma}}\|_{\mathcal{H}_2} = \sqrt{\mathsf{tr}\left(\mathcal{C}_{\mathbf{e}} \begin{bmatrix} \mathcal{P}_n & \mathcal{P}_{\mathsf{x}} \\ \mathcal{P}_{\mathsf{x}}^T & \mathcal{P}_r \end{bmatrix} \mathcal{C}_{\mathbf{e}}^T\right)}, \tag{3.99}$$

where $\mathcal{C}_{\mathbf{e}}$ is defined in (3.90), and $\mathcal{P}_n \in \mathbb{R}^{2n\times 2n}$ and $\mathcal{P}_r \in \mathbb{R}^{2r\times 2r}$ are the second-order pseudo controllability Gramians of the full-order system $\mathbf{\Sigma}$ and reduced-order system $\hat{\mathbf{\Sigma}}$, respectively. $\mathcal{P}_{\mathsf{x}}$ is the coupling pseudo controllability Gramian of the error system (3.90).

Proof. We extend the concept of pseudo controllability Gramian to the error system $\mathbf{\Sigma_e}$:

First, the convergence matrix of system $\mathbf{\Sigma_e}$ is given by

$$\mathcal{J}_{\mathsf{e}} = \lim_{t\to\infty} e^{\mathcal{A}_{\mathsf{e}}t} = \begin{bmatrix} \mathcal{J} & 0 \\ 0 & \hat{\mathcal{J}} \end{bmatrix}. \tag{3.100}$$

Second, the pseudo controllability Gramian of system $\mathbf{\Sigma_e}$ is defined by

$$\mathcal{P}_{\mathsf{e}} = \int_0^\infty (e^{\mathcal{A}_{\mathsf{e}}t} - \mathcal{J}_{\mathsf{e}})\mathcal{B}_{\mathsf{e}}\mathcal{B}_{\mathsf{e}}^T(e^{\mathcal{A}_{\mathsf{e}}^T t} - \mathcal{J}_{\mathsf{e}}^T)dt, \tag{3.101}$$

which can partitioned as

$$\mathcal{P}_{\mathsf{e}} = \begin{bmatrix} \mathcal{P}_n & \mathcal{P}_{\mathsf{x}} \\ \mathcal{P}_{\mathsf{x}}^T & \mathcal{P}_r \end{bmatrix}. \tag{3.102}$$

Note that $\mathcal{C}_{\mathbf{e}}\mathcal{J}_{\mathbf{e}}\mathcal{B}_{\mathbf{e}} = 0$, since

$$\begin{aligned}
\mathcal{C}_{\mathbf{e}}\mathcal{J}_{\mathbf{e}}\mathcal{B}_{\mathbf{e}} =& \begin{bmatrix} [I_n, \mathbf{0}_n]\mathcal{J} & [-P, \mathbf{0}_r]\hat{\mathcal{J}} \end{bmatrix} \mathcal{B}_{\mathbf{e}} \\
=& \sigma_D^{-1} \begin{bmatrix} \mathbb{1}_n\mathbb{1}_n^T D & \mathbb{1}_n\mathbb{1}_n^T M & -P\mathbb{1}_r\mathbb{1}_r^T\hat{D} & -P\mathbb{1}_r\mathbb{1}_r^T\hat{M} \\ \mathbf{0}_{n\times n} & \mathbf{0}_{n\times n} & \mathbf{0}_{n\times r} & \mathbf{0}_{n\times r} \end{bmatrix} \cdot \begin{bmatrix} \mathbf{0}_{n\times m} \\ M^{-1}F \\ \mathbf{0}_{r\times m} \\ \hat{M}^{-1}P^TF \end{bmatrix} \\
=& \begin{bmatrix} \mathbb{1}_n\mathbb{1}_n^T F - P\mathbb{1}_r\mathbb{1}_r^T P^T F \\ \mathbf{0}_{n\times m} \end{bmatrix} = \mathbf{0}_{2n\times m}.
\end{aligned}$$

Therefore,

$$\begin{aligned}
\mathcal{C}_{\mathbf{e}}\mathcal{P}_{\mathbf{e}}\mathcal{C}_{\mathbf{e}}^T &= \int_0^\infty \mathcal{C}_{\mathbf{e}}(e^{\mathcal{A}_{\mathsf{e}}t} - \mathcal{J}_{\mathsf{e}})\mathcal{B}_{\mathsf{e}}\mathcal{B}_{\mathsf{e}}^T(e^{\mathcal{A}_{\mathsf{e}}^T t} - \mathcal{J}_{\mathsf{e}}^T)\mathcal{C}_{\mathbf{e}}^T dt \\
&= \int_0^\infty \mathcal{C}_{\mathbf{e}}e^{\mathcal{A}_{\mathsf{e}}t}\mathcal{B}_{\mathsf{e}}\mathcal{B}_{\mathsf{e}}^T e^{\mathcal{A}_{\mathsf{e}}^T t}\mathcal{C}_{\mathbf{e}}^T dt.
\end{aligned} \tag{3.103}$$

Finally, we have $\|\mathbf{\Sigma} - \hat{\mathbf{\Sigma}}\|_{\mathcal{H}_2} = \|\mathbf{\Sigma}_{\mathbf{e}}\|_{\mathcal{H}_2} = \sqrt{\mathsf{tr}\,(\mathcal{C}_{\mathbf{e}}\mathcal{P}_{\mathbf{e}}\mathcal{C}_{\mathbf{e}}^T)}$. □

We apply the above theorem to evaluate the exact approximation error between the original and reduced-order network systems. To this end, three Gramians are computed: the pseudo controllability Gramians of the original and reduced-order systems and the coupling pseudo controllability Gramian.

Now, an extension of the clustering-based method to *velocity-based model reduction* for second-order network system is discussed, where the closeness of $\dot{x}_i$ and $\dot{x}_j$ with different i, j is considered. For a given system $\mathbf{\Sigma}$ as in (3.1), we intend to find a system

$$\hat{\mathbf{\Sigma}}_v : \begin{cases} \hat{M}\ddot{z} + \hat{D}\dot{z} + \hat{L}z = P^T F u, \\ v = P\dot{z}, \end{cases} \tag{3.104}$$

such that the state $\dot{x}(t)$ in (3.1) is approximated by $v(t)$ in $\hat{\mathbf{\Sigma}}_v$. To this end, the pseudo controllability Gramian $\mathcal{P}$ is used. Denote

$$\zeta(s) := s(s^2M + sD + L)^{-1}F \;\text{ and }\; \zeta_i(s) := \mathbf{e}_i^T\zeta(s). \tag{3.105}$$

The behavior of the i-th vertex is captured by the transfer function from external inputs to the velocity of the i-th vertex $\dot{x}(t)$. Then, we consider a velocity dissimilarity matrix $\mathcal{D}^v$ with the (i, j)-th entry as

$$\mathcal{D}_{ij}^v = \|\zeta_i(s) - \zeta_j(s)\|_{\mathcal{H}_2} \tag{3.106}$$

Here, the dissimilarity between two vertices is measured by the velocity difference over time. Similar to (3.83), $\mathcal{D}_{ij}^v$ is computed by

$$\|\mathcal{D}_{ij}^v\|_{\mathcal{H}_2} = \sqrt{\mathsf{tr}\left(\begin{bmatrix}\mathbf{0}_{1\times n}, \mathbf{e}_{ij}^T\end{bmatrix} \mathcal{P} \begin{bmatrix}\mathbf{0}_{n\times 1} \\ \mathbf{e}_{ij}\end{bmatrix}\right)}. \tag{3.107}$$

Using the matrix $\mathcal{D}^v$, the hierarchical clustering algorithm is also applicable for *velocity-based model reduction*. To estimate the approximation error, we just replace $\mathcal{C}_\mathsf{e}$ in Theorem 3.6 by

$$\mathcal{C}_e^v = \begin{bmatrix}\mathbf{0}_{n\times n} & I_n & \mathbf{0}_{n\times r} & -P\end{bmatrix}. \tag{3.108}$$

3.6 Small-World Network Example

In this section, we demonstrate the feasibility of our model reduction method by a simulation. We generate a mass-damper-spring system evolving on an undirected connected network with 70 vertices, see Fig. 3.2. The blue, red and yellow segments present the edges connecting by springs, dampers and both of them, respectively.

The masses are set by

$$M_{ii} = (i \bmod 10) + 1, \tag{3.109}$$

where **mod** presents a modulo operation. In Fig. 3.2, the bigger size of a vertex means it has a larger mass. The topologies of spring and damper couplings are generated by Watts-Strogatz model [173], which is a random graph generator producing graphs with small-world properties. Furthermore, the damper on each vertex is set to be proportional to its mass. we add 5 inputs to the network, and the input matrix F is randomized as a 70-by-5 matrix, whose entries are in the range of $[-1, 1]$.

We apply the hierarchical clustering algorithm to reduce the full-order second-order network system. The two clusters with the nearest distance are merged into a single one and finally, Algorithm 1 will group the vertices into a binary, hierarchical tree, called *dendrogram*, see Fig. 3.3. The dendrogram is fairly straightforward to interpret the result of graph clustering: The bottom vertical lines are called leaves, which represent the vertices on the graph. Besides, each fusion of two clusters is indicated by the splitting of a vertical line into two branches, and the horizontal position of the split, shown by the short horizontal bar, reads the similarities between the two clusters. In Fig. 3.3, we use five different colors to show the result of graph clustering with five clusters.

The resulting reduced network systems are shown in Fig. 3.4, where simplified networks with the different number of vertices are presented. We find that the simplified network system with lower dimension trends to have more edges simultaneously connected by springs and dampers.

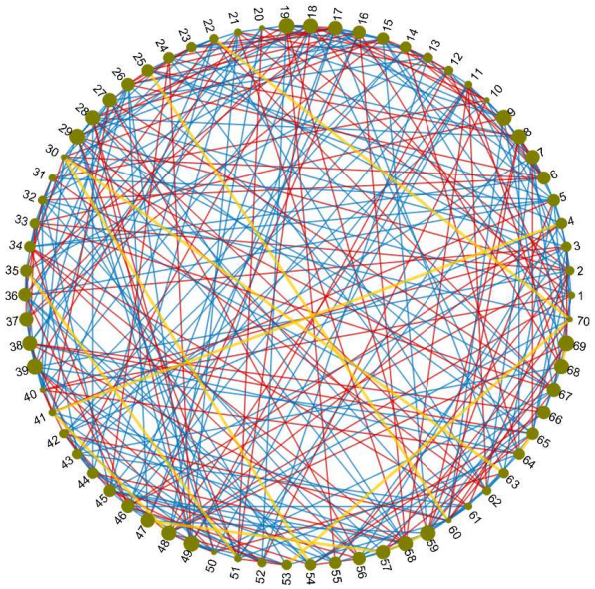

Figure 3.2: Original second-order networks with 70 vertices

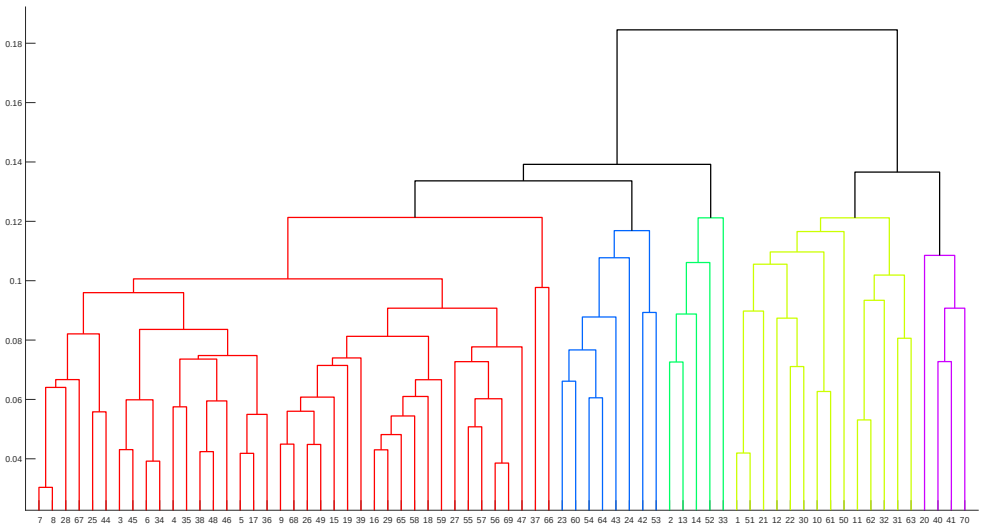

Figure 3.3: Dendrogram depicting the graph clustering, where the horizontal axis is labeled by vertex numberings, while the vertical axis represents the dissimilarity between clusters.

Next, we compare our hierarchical clustering algorithm with other clustering strategies to illustrate that hierarchical clustering is effective in obtaining a reduced-order network system with smaller errors. The two additional strategies we use for the comparison are described as follows.

- Random clustering randomly assigns n vertices in $\mathcal{V}$ into r nonempty subsets.
- Simple greedy clustering aggregates the vertices if they have smaller pair-wise dissimilarities. More specifically, it first clusters the most similar two vertices and then the pairs of vertices with the second smallest dissimilarity. In the following steps, it recursively aggregates the vertices with bigger and bigger dissimilarity until r clusters are obtained. At each step, two clusters are unified if they have intersections.

Fig. 3.5 depicts the comparison of three strategies in their approximation errors. The random clustering is performed for 50 times, and the average of the approximation errors is plotted in Fig. 3.5. Generally, the errors obtained by the different clustering strategies decrease as the reduced order r increases. However, it is clear that the hierarchical clustering algorithm has better performance than the other two strategies. When $r = 5$, the approximation error obtained by hierarchical clustering is $\|\mathbf{\Sigma} - \hat{\mathbf{\Sigma}}\|_{\mathcal{H}_2} = 0.5967$, which implies that behaviors of the full-order model can be well-approximated.

We implement this numerical experiment by Matlab 2016a in the environment of the 64-bit operating system with Intel Core i5-3470 CPU @ 3.20GHz, RAM 8.00 GB. To find the fifth-dimensional simplified model, it costs 1.1656s, while the time of computing the Gramian is 1.1167s. Therefore, the time consumption is mainly taken by the first step of Algorithm 1, and once the pseudo controllability Gramian is obtained, the hierarchical clustering can be processed rapidly.

Remark 3.7. *Note that numerical methods for solving Lyapunov equations generally have at least a computational complexity $\mathcal{O}(n^3)$, while the clustering procedure in Algorithm 1 requires a computational complexity $\mathcal{O}(n^2)$. When the dimension of the network n is large, solving the Lyapunov equation in (3.8a) contributes heavily to the computing time. In contrast, the computing time of the hierarchical clustering algorithm is much lower. Although we take a 70-dimensional network system for this example, the proposed method is also applicable for much larger networks.*

3.7 Conclusions

Based on graph clustering, we have developed a model reduction method for interconnected second-order systems. A hierarchical clustering algorithm is proposed

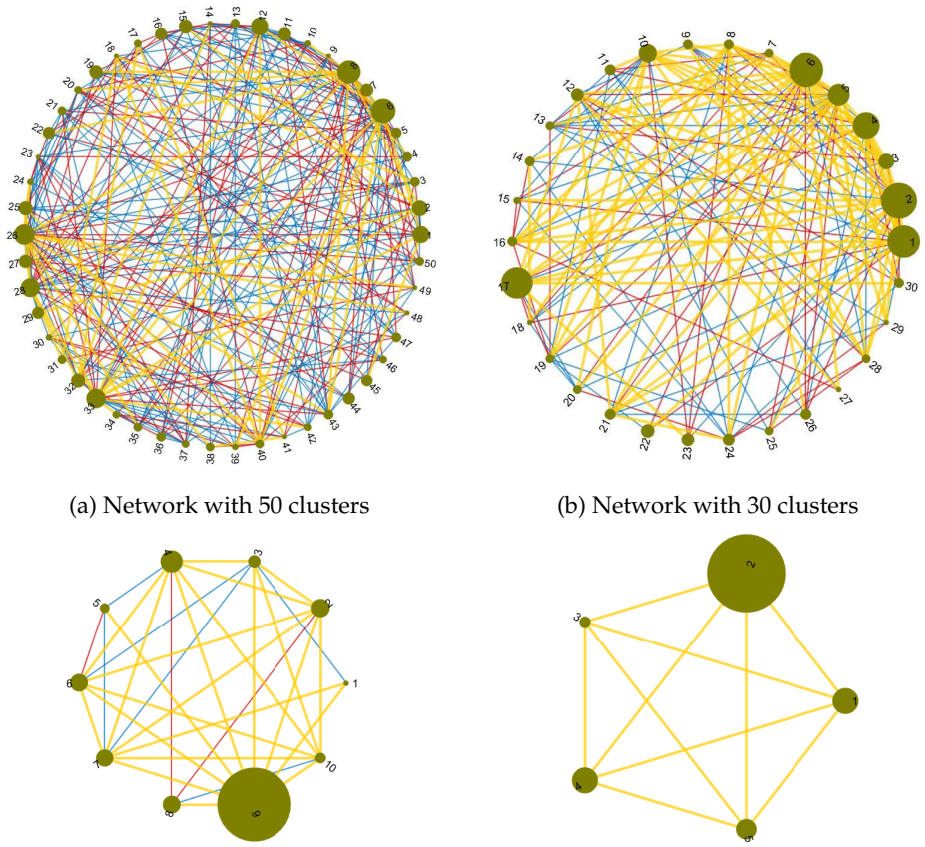

(a) Network with 50 clusters

(b) Network with 30 clusters

(c) Network with 10 clusters

(d) Network with 5 clusters

Figure 3.4: Reduced network with different numbers of clusters

to find an appropriate clustering such that the vertices with similar responses with respect to external inputs are merged. Then, a projection using cluster matrix is applied to yield lower-dimensional network model. It is verified that such reduced system preserves network structures. Besides, we introduce the pseudo controllability Gramian for the computation of $\mathcal{H}_2$-norms, which improve the feasibility of our algorithm. Finally, the efficiency of the proposed method has been illustrated by an experiment. It is worth mentioning that although we consider a linear second-order network system as in (3.1), the proposed method can be extended to more general network systems, such as networks consisting of higher-order linear dynamics and directed networks, which will be discussed in Chapter 5 and Chapter 6, respectively.

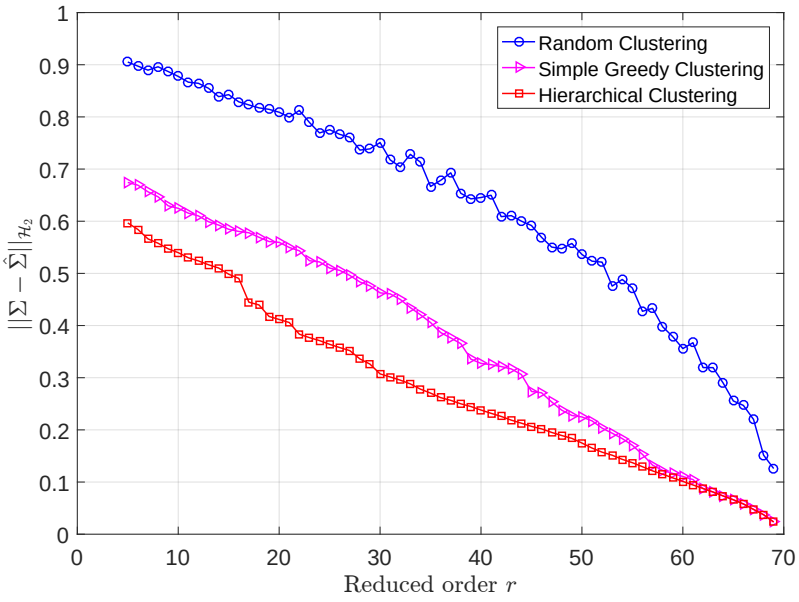

Figure 3.5: Approximation error comparisons of hierarchical clustering algorithm with random and simple greedy clustering strategies, where the curve of random clustering is plotted based on the mean of 50 times experiments.

In the next chapter, we extend the method proposed for second-order networks to power networks with distributed controllers.

CHAPTER 4

Clustering-Based Model Reduction of Power Networks

This chapter considers structure preserving model reduction of power networks with distributed controllers. The studied system and controller are modeled as second-order and first-order ordinary differential equations, which are coupled to a closed-loop system. This chapter uses the idea developed in Chapter 3 and considers an application to controlled power networks. By transfer functions, we characterize the behavior of each node (generator or load) in the power network and define a novel notion of dissimilarity between two nodes by the $\mathcal{H}_2$-norm of the transfer function deviation. Then, the reduction methodology is developed based on separately clustering the generators and loads according to their behavior dissimilarities. The characteristic matrix of the resulting clustering is adopted for the Galerkin projection to derive explicit reduced-order power models and controllers. Finally, we illustrate the proposed method by the IEEE 30-bus system example.

4.1 Introduction

This chapter further extends the proposed clustering-based reduction method in Chapter 3 and studies its application in power networks that are controlled by distributed controllers. Power networks, nowadays, are experiencing the penetration and integration of a wide array of new electronic devices and renewable energy sources, see [15, 46] for an overview. In the foreseeable future, power networks will

become more and more complex with more variation in the generators, uncertain loads, and denser transmission lines. Centralized power generation is being replaced by a more distributed generation.

The immense size of power grids yields mathematical models with high dimensions complicating the further analysis. In most cases, a complete model of the power network is neither practical nor necessary for e.g. transient analysis, failure detection, distributed controller design, or system simulation. Therefore, we need to construct a reduced-order model that can approximate the behavior of the original complex power system with an acceptable accuracy. More importantly, we desire to preserve the network structure in the reduced-order model such that it can be interpreted as a reduced network with a less complex topology. Specifically, the reduced power system is evolving over a simpler network that consists of fewer generator and load buses and sparser transmission lines. The network structure is necessary for the application of sensor allocation, and the management of distributed power generation. The main interest of This chapter is to investigate the problem of model order reduction for power networks with distributed controllers while the preservation of network structures.

Conventional model reduction techniques, including balanced truncation and Krylov subspace methods, have been extended to the dynamic reduction of power systems. In these papers, the power network systems are modeled in first-order state space representations, and the reduced-order models are constructed within the framework of Petrov-Galerkin projection. Although these methods provide systematic procedures to produce lower-dimensional models, which benefits the computation and simulation of power systems, the network structure is not retained through the reductions, and the projected states in the reduced-order model often lack a physical interpretation. A structure-preserving approach is proposed in [40], where the network model is firstly reduced by the balanced truncation, which still preserves the semistability such that the reduced-order model can be reformed as a network system. In spite of fewer nodes, the obtained reduced network has a complete interconnection. This restricts the use of the reduced-order models in the further applications, especially the implementation of distributed control laws. In a distributed control network, control laws are implemented locally by each generator, and these controllers send and receive data through a communication network, which is only connecting generators and in general, has a different topology from the power network, see [6, 56, 103, 119, 123, 165–168] for more details. In this case, each generator can only receive information from its adjacent generators through the communication network, which means that the control signals have to be generated by using only part of the system states. However, in the reduced-order model resulting from the conventional approaches, each state is composed of a linear combination of all the

original states. As a result, the controllers designed based on such models are not able to be realized in a distributed fashion.

Another network simplification method is the Kron reduction, which has been widely used in e.g. classic circuit theory, smart grid monitoring, and transient stability assessment. The extension of this approach for model order reduction of electric networks can be found in [30, 52, 123] and references therein. The network structure of a power system is preserved as the Schur complement of the Laplacian matrix of the original network is again a Laplacian matrix, which represents a smaller network. Despite the simplicity of implementation, the Kron reduction modeling only eliminates the load buses in the power network [52]. To reduce the complexity of a network of synchronous generators, which is modeled by a second-order swing equation [55], [148] proposes a method based on time-scale separation and singular perturbation analysis. This approach identifies the sparsely and densely connected areas of power grids and then aggregates the state variables of the coherent areas. Similar to Kron reduction, the algebraic structure of the Laplacian matrix is maintained through the singular perturbation approximation. However, the method in [148] ignores the fluctuation of power demands from the loads.

Clustering analysis of power networks, derived from the concept of *diakoptics*, has been intensively explored in the study of coherency recognition, area aggregation, and behavior approximation in the power grid. A large and complex power network could be more easily analyzed and managed when it is decomposed into several smaller components. The coherency-based approach is most popular for the clustering analysis of electric networks. Many related results have been reported in the literature, see [9, 46, 47, 80, 116, 139, 177] and the references therein. The generator coherency is introduced to describe the tendency of generators when the disturbances are affecting the system. The reduced model of the power network then results from aggregating those coherent generators. However, the coherency identification is a data-driven process, which heavily relies on the accuracy of the sampling data generated from the time-domain voltage angle responses of the generator buses.

The presented work provides a novel model order reduction scheme for power networks with the associated distributed controllers. The reduction procedure is developed based on Chapter 3, where the reduction of second-order network systems is studied. This chapter explores the application of power networks that contain many generator and load buses, and the proposed method aims to *simultaneously* simplify the structures of the transmission network and its distributed controller.

By linearizing the nonlinear *structure preserving model* of the power network [17], we obtain the network model in a second-order representation. Together with the distributed controller, the closed-loop system is derived, which is semistable and contains the Laplacian matrices of the power transmission network and the commu-

nication graph of the controllers. The clustering analysis of the networks is based on the closed-loop system. Similar to the idea in Chapter 3, that a reduced-order model is generated by clustering the nodes behaving similarly. More specifically, the behaviors of network nodes are characterized by transfer functions, and an $\mathcal{H}_2$ norm characterization of the dissimilarity of nodal behaviors are adapted such that the hierarchical clustering algorithm in Chapter 3 can find suitable clusterings for generator and load nodes, respectively. This notion of dissimilarity is data-independent, which means that we do not need the time-domain sample data to evaluate the differences among the nodes. Compared with Chapter 3, the current chapter mainly focuses on the application of power networks whose models couple the generator and load dynamics with the distributed controllers. The proposed method need to reduce the power network and communication network simultaneously, instead of only simplifying the network system as in Chapter 3. The definition of nodal behaviors cannot be directly applied, since the influence of communication networks of the distributed controllers has to be concerned, and the behaviors of generator and load nodes are supposed to be treated differently.

As the dissimilarity is defined in terms of the $\mathcal{H}_2$-norm, we use the controllability Gramian of the closed-loop system to evaluate the dissimilarities between all pairs of generator and load buses. The result of Section 3.3 in Chapter 3 is used. Besides, the hierarchical clustering algorithm in Chapter 3 is also employed to generate appropriate network clusterings for both generators and loads, so that the nodes with similar behaviors are grouped into the same clusters. Then, the Galerkin method is applied to yield a reduced-order power network with a simplified distributed controller. The characteristic matrices of the resulting clusterings are used as the projection matrices. It is shown that the algebraic structures of Laplacian matrices are retained in the reduced-order model. Consequently, the interconnection topologies of the power transmission network and communication network of the controller are simplified.

4.2 Power Network and Distributed Controller

Consider a connected power network consisting of n synchronous generators and m loads. Denote $\mathcal{V}_g = \{1, \cdots, n\}$ and $\mathcal{V}_l = \{n+1, \cdots, n+m\}$ as the index sets of generator and load buses, respectively. Then, the interconnection structure of the power grid can be represented by a connected undirected graph

$$\mathcal{G} = (\mathcal{V}_g \cup \mathcal{V}_l, \mathcal{E}), \text{ with } \mathcal{E} \subset (\mathcal{V}_g \cup \mathcal{V}_l) \times (\mathcal{V}_g \cup \mathcal{V}_l).$$

$\mathcal{E}$ is the set of unordered pairs (i, j) representing transmission lines between nodes i and j, which are assumed to be inductive. Notice that $|\mathcal{V}_g| = n$ and $|\mathcal{V}_l| = m$,

therefore, $\mathcal{G}$ contains $n+m$ nodes.

The dynamics of generators and loads in a power network are characterized by nonlinear structure-preserving models [17,51] as follows.

(1) Generator bus $i \in \mathcal{V}_g$:

$$\begin{aligned} \dot{\theta}_i &= \omega_i, \\ M_i\dot{\omega}_i &= -D_i\omega_i - \sum_{j=1}^{n+m} V_iV_jX_{ij}^{-1}\sin(\theta_i-\theta_j) + P_i^m; \end{aligned} \tag{4.1}$$

(2) Load bus $i \in \mathcal{V}_l$:

$$\begin{aligned} \dot{\theta}_i &= \omega_i \\ 0 &= -D_i\omega_i - \sum_{j=1}^{n+m} V_iV_jX_{ij}^{-1}\sin(\theta_i-\theta_j) - P_i^l. \end{aligned} \tag{4.2}$$

All the symbols in the models are described as follows.

- θ_i: voltage phase angle;
- ω_i: voltage frequency w.r.t the nominal reference ω^* (typically 50 Hz or 60 Hz);
- $M_i > 0$: angular momentum of generator i;
- $D_i > 0$: damping coefficient;
- $V_i > 0$: the voltage magnitude at node i;
- $X_{ij} \geq 0$: the inductance of the transmission line connecting nodes i and j;
- P_i^m: controllable power generation;
- P_i^l: unknown power demand.

The above structure-preserving power network models are commonly used in the stability analysis and controller design of power networks, including the analysis of network synchronization and frequency regulation, see [17,51,165]. For example, [61] studies the full-order description of synchronous generators in a grid setting. However, controlling such model turns out to be rather complicated. Furthermore, it should be remarked that the models in (4.1) and (4.2) are simplifications for the real power systems based on the assumption that the influence of the windings of the generators is negligible and the power lines are assumed to be lossless. Therefore, only very slow electromechanical transients will be affected by the type of feedback

that is proposed for using in this chapter. For example, transients as described in [102] would not be applicable.

To obtain a linear model based on (4.1) and (4.2), we follow [123, 158] and assume that the differences of the phase angles are relatively small, i.e., $\theta_i - \theta_j \approx 0$ for any $i, j \in \mathcal{V}_g \cup \mathcal{V}_l$, which is satisfied in a vicinity of the nominal condition. This assumption then leads to a linearizion of the power network model in the following compact second-order form

$$\mathbf{\Sigma}_p : \begin{bmatrix} M_g & 0 \\ 0 & 0 \end{bmatrix} \begin{bmatrix} \ddot{\theta}_g \\ \ddot{\theta}_l \end{bmatrix} + \begin{bmatrix} D_g & 0 \\ 0 & D_l \end{bmatrix} \begin{bmatrix} \dot{\theta}_g \\ \dot{\theta}_l \end{bmatrix} + \begin{bmatrix} L_1 & L_{12} \\ L_{12}^T & L_2 \end{bmatrix} \begin{bmatrix} \theta_g \\ \theta_l \end{bmatrix} = \begin{bmatrix} P_m \\ -P_l \end{bmatrix}, \tag{4.3}$$

where $\theta_g \in \mathbb{R}^n$, $\theta_l \in \mathbb{R}^m$ are the state vectors collecting θ_i with $i \in \mathcal{V}_g$ and $i \in \mathcal{V}_l$, respectively. Matrices M_g, D_g, and D_l are diagonal and positive definite, which are defined as $M_g := \text{diag}(M_1, M_2, \cdots, M_n) \in \mathbb{R}^{n\times n}$, $D_g := \text{diag}(D_1, D_2, \cdots, D_n) \in \mathbb{R}^{n\times n}$, and $D_l := \text{diag}(D_{n+1}, D_{n+1}, \cdots, D_{n+m}) \in \mathbb{R}^{m\times m}$. Moreover, P_m and P_l are collections of P_i^m with $i \in \mathcal{V}_g$ and P_i^l with $i \in \mathcal{V}_l$, respectively. The weighted Laplacian matrix $\mathcal{L} \in \mathbb{R}^{(n+m)\times(n+m)}$ of the network topology $\mathcal{G}$ is partitioned as

$$\mathcal{L} = \begin{bmatrix} L_1 & L_{12} \\ L_{12}^T & L_2 \end{bmatrix}. \tag{4.4}$$

The (i, j)-th entry of $\mathcal{L}$ is given by

$$W_{ij} = W_{ji} := V_i V_j X_{ij}^{-1}, \tag{4.5}$$

which is interpreted as the maximum real power transfer between any two nodes i and j with constant voltage levels. The value of W_{ij} is positive if there is a physical cable directly connecting nodes i and j and zero otherwise. $\mathcal{L}$ has a very special structure as stated in Lemma 2.1.

It is a crucial task to maintain the frequencies of generators and loads in the power network close to the nominal value. However, with the growth of the network size, centralized controllers become increasingly expensive due to the need for the information of all generators. Recently, distributed averaging PI controllers have been proposed for the frequency control of power networks, see [6, 56, 123] for the details. The distributed controllers exchange information over a communication network

$$\mathcal{G}_c := (\mathcal{V}_g, \mathcal{E}_c), \text{ with } \mathcal{E}_c \subset \mathcal{V}_g \times \mathcal{V}_g,$$

which is assumed to be undirected and connected. It should be emphasized that the topology of the communication network $\mathcal{V}_g$ is generally different from the topology

of the power network $\mathcal{G}$. For each generator $i \in \mathcal{V}_g$, the controller takes the form

$$\begin{aligned} Q_i\dot{\xi}_i &= -\omega_i - \sum_{j\in\mathcal{N}_i} c_{ij}(\xi_i - \xi_j), \\ P_i^m &= \xi_i. \end{aligned} \tag{4.6}$$

Here, $\mathcal{N}_i$ represents the set of neighboring generators of node i in $\mathcal{G}_c$, i.e., the collection of generators that generator i communicates with. The coefficients $c_{ij} = c_{ji} > 0$ reflect the strengths of the connection between generators i and j. Q_i is a positive gain. The controller (4.6) is designed to regulate the frequency deviation to zero and enforce the controller states ξ_i to reach a consensus, i.e., the generated power deviation of all generators becomes equal at steady state.

Notice that the controller (4.6) only needs the information from the neighbors of generator i, therefore can be implemented in a distributed fashion. We now write the controller in the vector form

$$\mathbf{\Sigma}_c : \begin{cases} Q\dot{\xi} = -\mathcal{L}_c\xi - \omega_g, \\ P_m = \xi, \end{cases} \tag{4.7}$$

where $\mathcal{L}_c$ is the Laplacian matrix of the communication network whose (i, j) entry is given by c_{ij}. The vector $\xi \in \mathbb{R}^n$ is the collection of ξ_i, $i \in \mathcal{V}_g$, and $Q := \text{diag}(Q_1, Q_2, \cdots, Q_n)$. $\omega_g := \dot{\theta}_g \in \mathbb{R}^n$ represent the frequencies of all the generators.

By substituting the distributed controller (4.7) for P_m in (4.3), we obtain the closed-loop system

$$\mathbf{\Sigma}_{cl} : \; E\dot{x} = Ax + Bd \tag{4.8}$$

where the state variable $x^T := \begin{bmatrix} \theta_g^T & \theta_l^T & \omega_g^T & \xi^T \end{bmatrix} \in \mathbb{R}^{3n+m}$ and

$$E = \begin{bmatrix} D_g & 0 & M_g & 0 \\ 0 & D_l & 0 & 0 \\ M_g & 0 & 0 & 0 \\ 0 & 0 & 0 & Q \end{bmatrix}, \; A = \begin{bmatrix} -L_1 & -L_{12} & 0 & I_n \\ -L_{12}^T & -L_2 & 0 & 0 \\ 0 & 0 & M_g & 0 \\ 0 & 0 & -I_n & -\mathcal{L}_c \end{bmatrix}, \text{ and } B = \begin{bmatrix} 0 \\ -I_m \\ 0 \\ 0 \end{bmatrix}. \tag{4.9}$$

Here $d := P_l$ is the power consumption of the m loads, which is uncontrollable and regarded as the stochastic disturbance of the closed-loop system (4.8). We analyze the stability of $\mathbf{\Sigma}_{cl}$ in the following theorem.

Theorem 4.1. *The closed-loop power system $\mathbf{\Sigma}_{cl}$ is semistable, and its impulse response converge to zero.*

Proof. Observe that $\det(E) = \det(D_g)\det(D_l)\det(D_g^{-1}M_g) \neq 0$. Therefore, E is non-singular, and its inverse reads as

$$E^{-1} = \begin{bmatrix} 0 & 0 & M_g^{-1} & 0 \\ 0 & D_l^{-1} & 0 & 0 \\ M_g^{-1} & 0 & -M_g^{-1}D_gM_g^{-1} & 0 \\ 0 & 0 & 0 & Q^{-1} \end{bmatrix}. \tag{4.10}$$

which gives

$$E^{-1}A = \begin{bmatrix} 0 & 0 & I_n & 0 \\ -D_l^{-1}L_{12}^T & -D_l^{-1}L_2 & 0 & 0 \\ -M_g^{-1}L_1 & -M_g^{-1}L_{12} & -M_g^{-1}D_g & M_g^{-1} \\ 0 & 0 & -Q^{-1} & -Q^{-1}\mathcal{L}_c \end{bmatrix}. \tag{4.11}$$

By [123], interconnecting the controller $\mathbf{\Sigma}_c$ and the power network system $\mathbf{\Sigma}_p$ results in a zero frequency deviation and consensus of the controller states. It then implies that, with impulse signals as disturbances of the closed-loop system $\mathbf{\Sigma}_{cl}$, all the state trajectories converge to constant values, i.e., $\lim_{t\to\infty} e^{E^{-1}At}$ exists. Thus, $\mathbf{\Sigma}_{cl}$ is semistable by the definition in [19].

Furthermore,using the third property of Laplacian matrices in Lemma 2.1, it is easy to check that

$$\ker(E^{-1}A) = \ker(A) = \text{span}\left(\begin{bmatrix} \mathbb{1}_n^T & \mathbb{1}_m^T & 0_n^T & 0_n^T \end{bmatrix}^T\right). \tag{4.12}$$

Together with semistability, we conclude that $E^{-1}A$ only has one zero eigenvalue at the origin, and all the other eigenvalues have strict negative real parts. Notice that the vectors

$$v_R \in \text{span}\left(\begin{bmatrix} \mathbb{1}_n \\ \mathbb{1}_m \\ 0_n \\ 0_n \end{bmatrix}\right) \text{ and } v_L \in \text{span}\left(\begin{bmatrix} \mathbb{1}_n \\ 0_m \\ 0_n \\ Q\mathbb{1}_n \end{bmatrix}\right) \tag{4.13}$$

are the right and left eigenvector of $E^{-1}A$ corresponding to the zero eigenvalue, respectively, i.e., $E^{-1}Av_R = 0$ and $v_L^TE^{-1}A = 0$. Based on this, we can obtain the following decomposition

$$E^{-1}A = \mathcal{U}D\mathcal{U}^{-1} = [v_R, V_R]\begin{bmatrix} 0 & \\ & \bar{D} \end{bmatrix}\begin{bmatrix} v_L^T \\ V_L^T \end{bmatrix}, \tag{4.14}$$

where $\mathcal{U}$ is unitary, and $\bar{D} \in \mathbb{R}^{3n+m-1}$ is Hurwitz. Hence, $\|v_R\|_2 = 1$ and $v_L^Tv_R = 1$,

which yields

$$v_R = \frac{1}{\sqrt{n+m}} \begin{bmatrix} \mathbb{1}_n \\ \mathbb{1}_m \\ 0_m \\ 0_n \end{bmatrix} \text{ and } v_L = \frac{\sqrt{n+m}}{n} \begin{bmatrix} \mathbb{1}_n \\ 0_m \\ 0_n \\ Q\mathbb{1}_n \end{bmatrix}, \tag{4.15}$$

Then, the convergence value of the impulse response is computed as

$$\begin{aligned} \lim_{t\to\infty} \left(e^{E^{-1}At}\right) E^{-1}B &= v_R v_L^T E^{-1} B \\ &= \frac{1}{n} \begin{bmatrix} \mathbb{1}_n\mathbb{1}_n^T & 0_{n\times m} & 0_{n\times n} & \mathbb{1}_n\mathbb{1}_n^T Q \\ \mathbb{1}_m\mathbb{1}_n^T & 0_{m\times m} & 0_{m\times n} & \mathbb{1}_m\mathbb{1}_n^T Q \\ 0_{n\times n} & 0_{n\times m} & 0_{n\times n} & 0_{n\times n} \\ 0_{n\times n} & 0_{n\times m} & 0_{n\times n} & 0_{n\times n} \end{bmatrix} \begin{bmatrix} 0_n \\ D_l^{-1} \\ 0_n \\ 0_n \end{bmatrix} = 0. \end{aligned} \tag{4.16}$$

That completes the proof.

□

Remark 4.1. *Due to the singularity of matrix $E^{-1}A$, the closed-loop system $\mathbf{\Sigma}_{cl}$ is not asymptotically stable. However, Theorem 4.1 indicates that, for any initial condition, the unforced system responses can reach the steady states at zero. Theorem 4.1 also offers a physical interpretation for the power network. The distributed controller in (4.7) eliminates the effects of disturbances, namely a sudden impulse change in the power demand, and steers the frequencies of all the nodes (i.e., the generator and load buses) to the nominal value ω^*. Note that the frequency at the steady state is independent from the disturbances.*

4.3 Model Reduction of Power Networks

To uncover the community structure of generators and loads, a novel clustering method is proposed and applied in this section, where the clusters are constructed based on the differences of nodes behaviors.

We propose a new method for cluster selection in power networks. The choices of clustering will determine the accuracy of network approximation. i.e., how close the behaviors of the reduced and original networks are. Hence, the cluster selection algorithm is the most crucial part of the clustering-based model reduction. This chapter provides a new way of cluster selection, which involves a particular notion of dissimilarity and an adaption of the hierarchical clustering algorithm. The details of our method are described hereafter.

4.3.1 Characterization and Computation of Dissimilarity

In the context of clustering, node dissimilarities intuitively describe how different the nodes are from each other. In contrast with the existing results in the literature, such as [46, 94, 139], the clusters of a power network in this chapter are identified without sampling data from a real system. We calculate the *dissimilarities* of network nodes by the $\mathcal{H}_2$-norms of transfer function discrepancies, rather than the Euclidean distances of the relative positions. Then, potentially, we can place the nodes with similar behaviors into the same clusters.

More precisely, by considering the state variables of the closed-loop power system $\mathbf{\Sigma}_{cl}$ in (4.8), the behavior of generator i ($i \in \mathcal{V}_g$) is characterized by its responses of the voltage angles θ_i, the frequencies ω_i and the controller states ξ_i. We include ξ_i into behavior characterization of generators since we also approximate the controller $\mathbf{\Sigma}_c$. When the generators are clustered, the communication network of the distributed controllers is automatically simplified. Hence, the effects of the controller states ξ_i are also needed to be included. As for the behavior of load i ($i \in \mathcal{V}_l$), it can be simply represented by its voltage angle responses θ_i with respect to the stochastic disturbances d.

The behaviors of generators and loads can be expressed in the complex frequency domain by the transfer functions from d to the indicative state variables. Denote two new binary vectors

$$\boldsymbol{\alpha}_i = \mathbf{e}_i + \mathbf{e}_{i+n+m} + \mathbf{e}_{i+2n+m},\ \boldsymbol{\beta}_i = \mathbf{e}_{i+n}, \tag{4.17}$$

where $\mathbf{e}_i$ is the i-th unit base vector. Then the behavior of generator i is given by

$$\Psi_i^g(s) = \frac{\begin{bmatrix}\theta_i(s) & \omega_i(s) & \xi_i(s)\end{bmatrix}^T}{d(s)} = \boldsymbol{\alpha}_i^T(sI - \mathcal{A})\mathcal{B},\ \ i = \{1, 2, \cdots, n\}, \tag{4.18}$$

where $\theta_i(s)$, $\omega_i(s)$, $\xi_i(s)$, and $d(s)$ are the Laplace transforms of the states θ_i, ω_i, ξ_i, and the input d, respectively, in the closed-loop system. Furthermore, the behavior of load $i \in \mathcal{V}_l$ is represented by

$$\Psi_i^l(s) = \frac{\theta_{i+n}(s)}{d(s)} = \boldsymbol{\beta}_i^T(sI - \mathcal{A})\mathcal{B},\ \ i = \{1, 2, \cdots, m\}. \tag{4.19}$$

It is worth to mention that the definitions of behaviors here are different from the one in Chapter 3. As we aim to reduce the communication network as well, we include the state of the distributed controller in the definition of generator behavior.

Thereupon, a pairwise *dissimilarity* of nodes i and j is defined for generators and loads respectively.

$$\mathcal{D}_{ij}^g = \|\Psi_i^g(s) - \Psi_j^g(s)\|_{\mathcal{H}_2},\ \ \mathcal{D}_{ij}^l = \|\Psi_i^l(s) - \Psi_j^l(s)\|_{\mathcal{H}_2}. \tag{4.20}$$

Moreover, the *dissimilarity matrices* for the generators and loads are denoted by $\mathcal{D}^g \in \mathbb{R}^{n\times n}$ and $\mathcal{D}^l \in \mathbb{R}^{m\times m}$, which are constructed by collecting $\mathcal{D}^g_{ij}$ and $\mathcal{D}^l_{ij}$. Clearly, $\mathcal{D}^g$ and $\mathcal{D}^l$ are symmetric matrices with nonnegative entries and zero diagonal elements. Besides, the boundedness of $\mathcal{D}^g$ and $\mathcal{D}^l$ are also guaranteed by Theorem 4.1. The reason of the boundedness are explained as follows.

For simplicity, let

$$\mathcal{A} = E^{-1}A,\ \mathcal{B} = E^{-1}B, \tag{4.21}$$

where E, A, B are system coefficients of the closed-loop system $\mathbf{\Sigma}_{cl}$ in (4.8). Note that impulse response of node i in $\mathbf{\Sigma}_{cl}$ is expressed by $e^{\mathcal{A}t}\mathcal{B}$, which is a bounded smooth function of t and exponentially converges to zero. Thus, the boundedness of $\mathcal{D}^g_{ij}$ and $\mathcal{D}^l_{ij}$ can be seen from the the definition of $\mathcal{H}_2$-norm [7].

$$\begin{aligned}\|\Psi^g_i(s) - \Psi^g_j(s)\|^2_{\mathcal{H}_2} &= \int_0^\infty (\boldsymbol{\alpha}_i - \boldsymbol{\alpha}_j)^T e^{\mathcal{A}t}\mathcal{B}\mathcal{B}^T e^{\mathcal{A}^T t}(\boldsymbol{\alpha}_i - \boldsymbol{\alpha}_j)dt \\ &= (\boldsymbol{\alpha}_i - \boldsymbol{\alpha}_j)^T \mathcal{P}(\boldsymbol{\alpha}_i - \boldsymbol{\alpha}_j),\end{aligned} \tag{4.22}$$

and similarly,

$$\|\Psi^l_i(s) - \Psi^l_j(s)\|^2_{\mathcal{H}_2} = (\boldsymbol{\beta}_i - \boldsymbol{\beta}_j)^T \mathcal{P}(\boldsymbol{\beta}_i - \boldsymbol{\beta}_j). \tag{4.23}$$

In both equations, $\mathcal{P}$ is the pseudo controllability Gramian of the closed-loop system $\mathbf{\Sigma}_{cl}$, see (3.7a) for the definition of pseudo controllability Gramian. For large-scale networks, (4.22) and (4.23) provide an efficient method to compute matrix $\mathcal{D}$, since we first calculate $\mathcal{P}$ and then just apply vector-matrix multiplication to obtain all the entries of $\mathcal{D}$. However, the semistability of $\mathbf{\Sigma}_{cl}$ poses a challenge to implement this idea. For asymptotically stable systems, their controllability Gramians can be uniquely determined by solving the associated continuous-time algebraic Lyapunov equation in (2.21).

In the semistable case, $\mathcal{A}$ is not Hurwitz, which results in multiple solutions of the below Lyapunov equation [14].

$$\mathcal{A}\mathcal{P} + \mathcal{P}\mathcal{A}^T + \mathcal{B}\mathcal{B}^T = 0. \tag{4.24}$$

To characterize the pseudo controllability Gramian from the solutions of (4.24), the following lemma is proven.

Lemma 4.1. *The pseudo controllability Gramian $\mathcal{P}$ of the semistable power system $\mathbf{\Sigma}_{cl}$ is positive semidefinite, and it is uniquely determined by the combination of (4.24) and*

$$v_L^T \mathcal{P} v_L = 0, \tag{4.25}$$

where v_L is the left eigenvector of $\mathcal{A}$ given in (4.15).

Proof. Since $v_L^T \mathcal{A} = 0$, for any t, we have

$$\begin{aligned} v_L^T e^{\mathcal{A}t}\mathcal{B} &= v_L^T \left(I + \mathcal{A}t + \frac{\mathcal{A}^2}{2}t^2 + \cdots \right) \mathcal{B} \\ &= v_L^T \mathcal{B} = \frac{\sqrt{n+m}}{n} \begin{bmatrix} \mathbb{1}_n^T & 0_m^T & 0_n^T & \mathbb{1}_n^T Q \end{bmatrix} \begin{bmatrix} 0_n \\ D_l^{-1} \\ 0_n \\ 0_n \end{bmatrix} = 0. \end{aligned} \tag{4.26}$$

Thus, (4.25) holds. It then yields $v_L^T \mathcal{P} v_L = 0$, which means $\mathcal{P}$ is positive semidefinite.

Next, we show that solving the Lyapunov equation (4.24) together with (4.25) will yield a unique solution. Assume that two symmetric matrices $\mathcal{P}_1$ and $\mathcal{P}_2$ are both the solutions of (4.24) and (4.25). From (4.24), we have

$$\mathcal{A}(\mathcal{P}_1 - \mathcal{P}_2) + (\mathcal{P}_1 - \mathcal{P}_2)\mathcal{A}^T = 0, \tag{4.27}$$

which leads to

$$e^{\mathcal{A}t} \left[\mathcal{A}(\mathcal{P}_1 - \mathcal{P}_2) + (\mathcal{P}_1 - \mathcal{P}_2)\mathcal{A}^T \right] e^{\mathcal{A}^T t} = \frac{d}{dt} \left[e^{\mathcal{A}t}(\mathcal{P}_1 - \mathcal{P}_2) e^{\mathcal{A}^T t} \right] = 0. \tag{4.28}$$

Therefore,

$$\int_0^\infty \frac{d}{dt} \left[e^{\mathcal{A}t}(\mathcal{P}_1 - \mathcal{P}_2) e^{\mathcal{A}^T t} \right] dt = 0. \tag{4.29}$$

Note that $\lim_{t\to\infty} e^{\mathcal{A}t} = v_R v_L^T$. Then, we obtain from (4.29) that

$$\mathcal{P}_1 - \mathcal{P}_2 = v_R v_L^T (\mathcal{P}_1 - \mathcal{P}_2) v_L v_R^T, \tag{4.30}$$

which is equal to zero due to (4.25). Thus, we obtain $\mathcal{P}_1 \neq \mathcal{P}_2$. As a result, the common solution of (4.24) and (4.25) is unique. □

In the following theorem, we then provide a method to determine the controllability Gramian of the semistable system $\mathbf{\Sigma}_{cl}$ by solving linear matrix equations.

Theorem 4.2. *Let $\mathcal{P}_a$ be an arbitrary solution that fulfills (4.24). Then, the pseudo controllability Gramian $\mathcal{P}$ of the closed-loop power system $\mathbf{\Sigma}_{cl}$ in (4.8) is computed as*

$$\mathcal{P} = \mathcal{P}_a - \mathcal{J}\mathcal{P}_a\mathcal{J}^T, \tag{4.31}$$

where $\mathcal{J}$ is a constant matrix defined by

$$\mathcal{J} := \lim_{t\to\infty} e^{\mathcal{A}t} = \frac{1}{n} \begin{bmatrix} \mathbb{1}_n\mathbb{1}_n^T & 0_{n\times m} & 0_{n\times n} & \mathbb{1}_n\mathbb{1}_n^T Q \\ \mathbb{1}_m\mathbb{1}_n^T & 0_{m\times m} & 0_{m\times n} & \mathbb{1}_m\mathbb{1}_n^T Q \\ 0_{n\times n} & 0_{n\times m} & 0_{n\times n} & 0_{n\times n} \\ 0_{n\times n} & 0_{n\times m} & 0_{n\times n} & 0_{n\times n} \end{bmatrix} \in \mathbb{R}^{(3n+m)\times(3n+m)}. \tag{4.32}$$

Proof. Equation (4.26) implies that $\mathcal{J}\mathcal{P}\mathcal{J}^T = 0$. From (4.30) in the proof of Lemma 4.1, we have

$$\mathcal{P}_a - \mathcal{P} = \mathcal{J}(\mathcal{P}_a - \mathcal{P})\mathcal{J}^T = \mathcal{J}\mathcal{P}_a\mathcal{J}^T, \tag{4.33}$$

which leads to (4.31). □

It should be remarked that $\mathcal{P}$ in (4.31) does not depend on the choice of $\mathcal{P}_a$, which can be any symmetric real solution of (4.24). Besides, we can modify the Hessenberg-Schur method (SB04MD (SLICOT)) in [68] to solve the Lyapunov equation with a nonsingular $\mathcal{A}$ matrix. The output of the adapted Hessenberg-Schur algorithm will give one solution of (4.24), and we then use the relation in (4.31) to obtain the real value of $\mathcal{P}$. Hereafter, we apply (4.22) and (4.23) to determine all the dissimilarities of different pairs of generators or loads in the power grid.

4.3.2 Reduced Model of Power Network

In Section 4.3.1, the dissimilarities are calculated in the closed-loop systems. Now we apply the idea of hierarchical clustering to group the generator and load buses separately. The idea of hierarchical clustering has been extensively explored in many fields, including pattern recognition, data compression, and network science, see [13, 94]. Hierarchical clustering, in principle, is a greedy algorithm, whose running time grows polynomially with the size of the studied networks. Compared to the K-means algorithm, another popular clustering method, the result of hierarchical clustering is not affected by the initializations of the graph partitions. Due to the above qualities, we choose and adapt the hierarchical algorithm to cluster the generator and load buses for the purpose of model order reduction. The details of the hierarchical clustering can be found in Section 3.5.2.

In this chapter, the generators and loads are grouped separately on account of different evaluation criteria of dissimilarities, see Section 4.3.1, yet the same hierarchical clustering procedures can be applied for both. It is because the hierarchical clustering only needs the dissimilarity matrices $\mathcal{D}^g$ and $\mathcal{D}^l$, whose entries already contain the dissimilarities of all pairs of generator and load nodes. Hereby, we only analyze the clustering of generators and the clustering of loads in parallel. Both procedures go in the same way, hence we only present it for any $\mathcal{D} \in \{\mathcal{D}^g, \mathcal{D}^l\}$.

Suppose that we acquire r clusters of generator buses and q clusters of load buses. Correspondingly, the characteristic matrices are denoted by $\Pi_g \in \mathbb{R}^{n\times r}$ and $\Pi_l \in \mathbb{R}^{m\times q}$, respectively. Let

$$\Pi_p = \begin{bmatrix} \Pi_g & 0 \\ 0 & \Pi_l \end{bmatrix}. \tag{4.34}$$

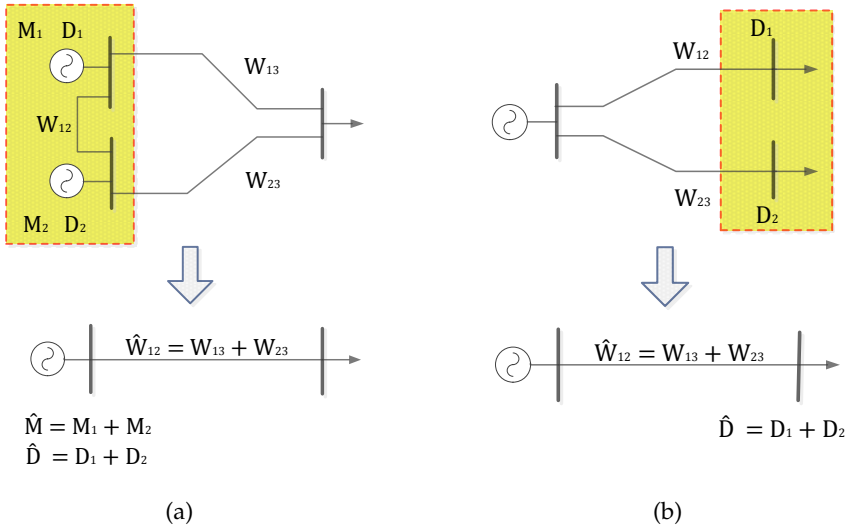

Figure 4.1: Illustration of Aggregation of generator buses (a) and load buses (b). The nodes in the same cluster are included in the dashed boxes.

Then, a simplified weighted power network $\hat{\mathcal{G}}$ can be obtained by aggregating all the nodes with the same clusters in the original complex network. Mathematically, the reduced Laplacian matrix of $\hat{\mathcal{G}}$ is generated by the following projection.

$$\hat{\mathcal{L}} = \Pi_p^T \mathcal{L} \Pi_p = \begin{bmatrix} \Pi_g^T L_1 \Pi_g & \Pi_g^T L_{12} \Pi_g \\ \Pi_l^T L_{12}^T \Pi_l & \Pi_l^T L_2 \Pi_l \end{bmatrix} := \begin{bmatrix} \hat{L}_{11} & \hat{L}_{12} \\ \hat{L}_{12}^T & \hat{L}_{22} \end{bmatrix} \in \mathbb{R}^{(r+q)\times(r+q)}, \tag{4.35}$$

where $\mathcal{L}$ is the weighted Laplacian matrix representing the original network. Similarly, the inertia and damping coefficients in the reduced network are given by

$$\hat{M}_g = \Pi_g^T M_g \Pi_g, \ \hat{D}_g = \Pi_g^T D_g \Pi_g \in \mathbb{R}^{r\times r}, \text{ and } \hat{D}_l = \Pi_l^T D_l \Pi_l \in \mathbb{R}^{q\times q}. \tag{4.36}$$

This clustering-based projection also has a physical interpretation, as shown in Fig. 4.1, which shows the aggregation of generator and load buses respectively. Notice that the nodes in the same cluster can be aggregated even if they do not have a direct connection with each other.

The transmission lines contained in a cluster are neglected, while those connecting two clusters are aggregated. Moreover, the maximum real power transfer on the new branch between the clusters $\mathcal{C}_\mu$ and $\mathcal{C}_\nu$ is given by

$$\hat{W}_{\mu,\nu} = \sum_{i\in\mathcal{C}_\mu} \sum_{j\in\mathcal{C}_\nu} W_{ij}, \tag{4.37}$$

where W_{ij} is the maximum real power transfer between nodes i and j. In the reduced network, a node represents a cluster of nodes in the original network, and its angular momentum and damping coefficient are the sum of these parameters of generators and loads in the original power network. Specifically, the inertia and damping coefficients of the cluster $\mathcal{C}_i$ are computed as

$$\hat{M}_\mu = \sum_{i \in \mathcal{C}_\mu} M_i \text{ and } \hat{D}_\mu = \sum_{i \in \mathcal{C}_\mu} D_i. \tag{4.38}$$

Now, we are ready to present the reduced-order power system of $\mathbf{\Sigma}_p$ in (4.3), which is obtained by Galerkin projection.

$$\hat{\mathbf{\Sigma}}_p : \begin{bmatrix} \hat{M}_g & 0 \\ 0 & 0 \end{bmatrix} \begin{bmatrix} \ddot{\hat{\theta}}_g \\ \ddot{\hat{\theta}}_l \end{bmatrix} + \begin{bmatrix} \hat{D}_g & 0 \\ 0 & \hat{D}_l \end{bmatrix} \begin{bmatrix} \dot{\hat{\theta}}_g \\ \dot{\hat{\theta}}_l \end{bmatrix} + \begin{bmatrix} \hat{L}_1 & \hat{L}_{12} \\ \hat{L}_{12}^T & \hat{L}_2 \end{bmatrix} \begin{bmatrix} \hat{\theta}_g \\ \hat{\theta}_l \end{bmatrix} = \begin{bmatrix} \Pi_g^T P_m \\ -\Pi_l^T P_l \end{bmatrix}, \tag{4.39}$$

where the Laplacian matrix and $\hat{M}_g$, $\hat{D}_g$, $\hat{D}_l$ are defined in (4.35) and (4.36), respectively. $\hat{\theta}_g \in \mathbb{R}^r$ and $\hat{\theta}_l \in \mathbb{R}^q$ are the voltage phase angles of the aggregated generators and loads in the reduced-order power network, which are used to approximate the states in the original system:

$$\theta_g \approx \Pi_g \hat{\theta}_g,\ \omega_g \approx \Pi_g \hat{\omega}_g = \Pi_g \dot{\hat{\theta}}_g, \text{ and } \theta_l \approx \Pi_l \hat{\theta}_l. \tag{4.40}$$

In this model reduction method, we essentially do clustering for generators and loads respectively. Note that the distributed controllers in this chapter are mounted to the generators. Thus, when the generators are clustered, the network of distributed controllers are clustered automatically. As a result, both the plants and the controllers are reduced. Based on (4.39), the reduced-order nonlinear power system can be also constructed, which follows the same form as (4.1) or (4.2). Here, the reduced-order nonlinear model is omitted.

As the generators are clustered, the size of the communication network $\mathcal{G}_c$ for the distributed controller in (4.7) is also simplified. As a result, the dimension of the controller is reduced simultaneously. Analogously, the representation of the lower-dimensional controller is written as

$$\hat{\mathbf{\Sigma}}_c : \begin{cases} \hat{Q}\dot{\hat{\xi}} = -\hat{\mathcal{L}}_c \hat{\xi} - \Pi_g^T \Pi_g \hat{\omega}_g, \\ P_m = \Pi_g \hat{\xi}, \end{cases} \tag{4.41}$$

where $\hat{Q} := \Pi_g^T Q \Pi_g$, and $\hat{\xi} \in \mathbb{R}^r$ is states of the reduced-order controller. $\hat{\mathcal{L}}_c := \Pi_g^T \mathcal{L}_c \Pi_g$ represents the simplified communication network.

Combining the reduced versions of the power network $\hat{\mathbf{\Sigma}}_p$ and the distributed controller $\hat{\mathbf{\Sigma}}_c$, we derive the reduced-order closed-loop system as follows.

$$\mathbf{\Sigma}_{cl} :\ \hat{E}\dot{\hat{x}} = \hat{A}\hat{x} + \hat{B}d, \tag{4.42}$$

where $\hat{x}^T := \begin{bmatrix} \hat{\theta}_g^T & \hat{\theta}_l^T & \hat{\omega}_g^T & \hat{\xi} \end{bmatrix} \in \mathbb{R}^{3r+q}$ and

$$\hat{E} = \begin{bmatrix} \hat{D}_g & 0 & \hat{M}_g & 0 \\ 0 & \hat{D}_l & 0 & 0 \\ \hat{M}_g & 0 & 0 & 0 \\ 0 & 0 & 0 & \hat{Q} \end{bmatrix}, \hat{A} = \begin{bmatrix} -\hat{L}_1 & -\hat{L}_{12} & 0 & \Pi_g^T \Pi_g \\ -\hat{L}_{12}^T & -\hat{L}_2 & 0 & 0 \\ 0 & 0 & \hat{M}_g & 0 \\ 0 & 0 & -\Pi_g^T \Pi_g & -\hat{\mathcal{L}}_c \end{bmatrix}, \text{ and } \hat{B} = \begin{bmatrix} 0 \\ -\Pi_l^T \\ 0 \\ 0 \end{bmatrix}. \tag{4.43}$$

Here $d := P_l$ is the uncontrollable power demand in (4.8). The Galerkin projection matrix for the closed-loop system $\mathbf{\Sigma}_{cl}$ is

$$\Pi = \begin{bmatrix} \Pi_g & 0 & 0 & 0 \\ 0 & \Pi_l & 0 & 0 \\ 0 & 0 & \Pi_g & 0 \\ 0 & 0 & 0 & \Pi_g \end{bmatrix}, \tag{4.44}$$

which satisfies

$$\hat{E} = \Pi^T E \Pi, \ \hat{A} = \Pi^T A \Pi, \text{ and } \hat{B} = \Pi^T B. \tag{4.45}$$

Next, the properties of the reduced-order models are discussed in the following theorem.

Theorem 4.3. *The reduced power network $\mathbf{\Sigma}_p$ in (4.39) and the distributed controller $\mathbf{\Sigma}_c$ in (4.41) preserve the network structures, namely, $\hat{\mathcal{L}}$ in (4.35) and $\hat{\mathcal{L}}_c$ in (4.41) are still Laplacian matrices representing a simplified power network and a communication network. The closed-loop system $\mathbf{\Sigma}_{cl}$ in (4.42) is also semistable, and its impulse response converges to zero.*

Proof. In Chapter 3, we have proven that the Galerkin projection based on the characteristic matrix of network clustering can preserve the algebraic structure of a Laplacian matrix, which means $\hat{\mathcal{L}}$ in (4.35) and $\hat{\mathcal{L}}_c$ in (4.41) are the reduced Laplacian matrices representing the simplified power network and communication links. Besides, (4.38) shows that $\hat{M}_g$, $\hat{D}_g$, and $\hat{D}_l$ are diagonal and positive definite. Therefore, the reduced models in (4.39) and (4.41) have the same structures as (4.8) and (4.7), respectively.

Follow the same reasoning line of Theorem 4.1, the closed-loop system $\mathbf{\Sigma}_{cl}$ is semistable. It has only one pole at the origin, and all the other poles are located in the open-left half plane. The vectors

$$\hat{v}_L = \frac{\sqrt{r+q}}{n} \begin{bmatrix} \Pi_g^T \Pi_g \mathbb{1}_r \\ 0_q \\ 0_r \\ \hat{Q} \mathbb{1}_r \end{bmatrix} \text{ and } \hat{v}_R = \frac{1}{\sqrt{r+q}} \begin{bmatrix} \mathbb{1}_r \\ \mathbb{1}_q \\ 0_r \\ 0_r \end{bmatrix} \tag{4.46}$$

are the left and right eigenvectors of $\hat{E}^{-1}\hat{A}$ corresponding to the only zero eigenvalue, which can be verified by $\hat{v}_L^T\hat{E}^{-1}\hat{A} = 0$, and $\hat{E}^{-1}\hat{A}\hat{v}_R = 0$. Note that the characteristic matrix of the graph clustering has the property $\Pi_g \mathbb{1}_r = \mathbb{1}_n$. Hence, $\|\hat{v}_R\|_2 = 1$, and $\hat{v}_L^T\hat{v}_R = 1$. We further obtain

$$\begin{aligned}\lim_{t\to\infty}\left(e^{\hat{E}^{-1}\hat{A}t}\right)\hat{E}^{-1}\hat{B} &= \hat{v}_R\hat{v}_L^T\hat{E}^{-1}\hat{B} \\ &= \frac{1}{n}\begin{bmatrix} \mathbb{1}_r\mathbb{1}_r^T\Pi_g^T\Pi_g & 0_{r\times q} & 0_{r\times r} & \mathbb{1}_r\mathbb{1}_r^T\hat{Q} \\ \mathbb{1}_q\mathbb{1}_r^T\Pi_g^T\Pi_g & 0_{q\times q} & 0_{q\times r} & \mathbb{1}_q\mathbb{1}_r^T\hat{Q} \\ 0_{r\times r} & 0_{r\times q} & 0_{r\times r} & 0_{r\times r} \\ 0_{r\times r} & 0_{r\times q} & 0_{r\times r} & 0_{r\times r} \end{bmatrix}\begin{bmatrix} 0_r \\ \hat{D}_l^{-1}\Pi_l^T \\ 0_r \\ 0_r \end{bmatrix} = 0.\end{aligned} \tag{4.47}$$

That completes the proof. □

4.4 Case Study

We illustrate the proposed method on the IEEE 30-bus test system [164], which contains 6 generator buses and 41 transmission lines. The graph representation of this power system is depicted in Fig. 4.2a. In order to fit the network data into the index setting of the states in our model (4.3), we use the bus numberings that are different from the original system date. Now, the generator buses are with the indices from 1 to 6. Assume that the distributed controllers of the generators are identical and connected based on the communication network in Fig. 4.2b. The control parameters in (4.6) are given by $Q_i = 0.1$ for all generators and $c_{ij} = 1$. Thereby the closed-loop power system in (4.42) is established, which include 42 states, namely the voltage phase angles of generators and loads, $\theta_g \in \mathbb{R}^6$ and $\theta_l \in \mathbb{R}^{24}$, the generator voltage frequencies $\omega_g \in \mathbb{R}^6$, and the controller states $\xi \in \mathbb{R}^6$. The positive semidefinite controllability Gramian is then obtained by Theorem 4.2. Consequently, the dissimilarity matrices of generator and load behaviors are computed using (4.22) and (4.23). Due to space reasons, we only give the results for generators as follows.

$$\mathcal{D}^g = \begin{bmatrix} 0 & 0.0737 & 0.0824 & 0.3147 & 0.1401 & 0.2319 \\ 0.0737 & 0 & 0.0854 & 0.2899 & 0.1071 & 0.2121 \\ 0.0824 & 0.0854 & 0 & 0.3124 & 0.1445 & 0.2418 \\ 0.3147 & 0.2899 & 0.3124 & 0 & 0.2472 & 0.3374 \\ 0.1401 & 0.1071 & 0.1445 & 0.2472 & 0 & 0.2041 \\ 0.2319 & 0.2121 & 0.2418 & 0.3374 & 0.2041 & 0 \end{bmatrix}. \tag{4.48}$$

We then group the generator and load nodes by Algorithm 1, which divides the node sets in the original network into several subsets that contain nodes with small

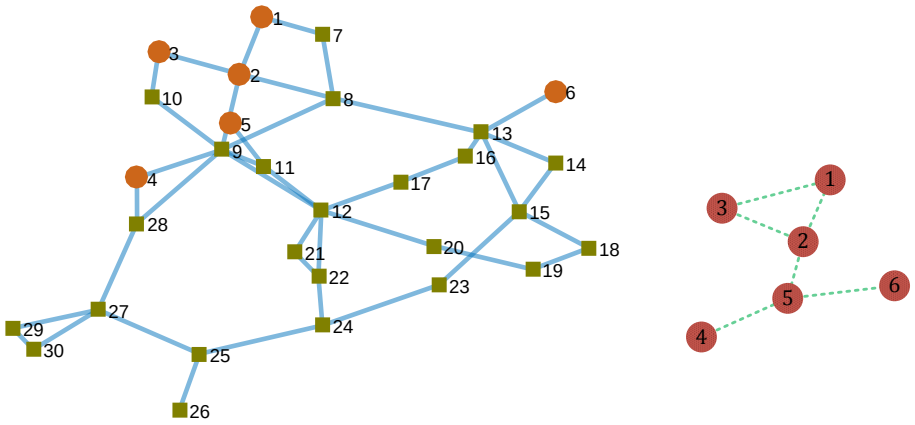

(a) (b)

Figure 4.2: (a) The topology of IEEE 30-bus test system. The generators and load buses are represented by circles and squares, respectively. (b) The communication network that links the distributed controllers on 6 generators.

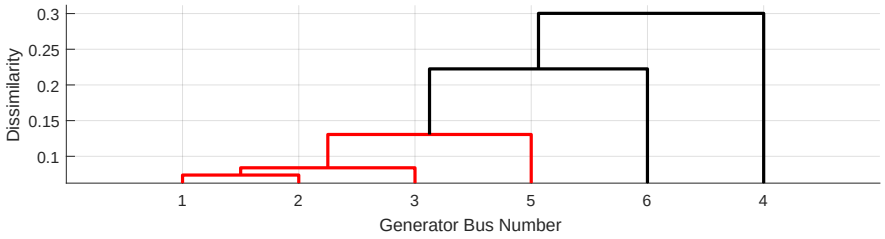

(a)

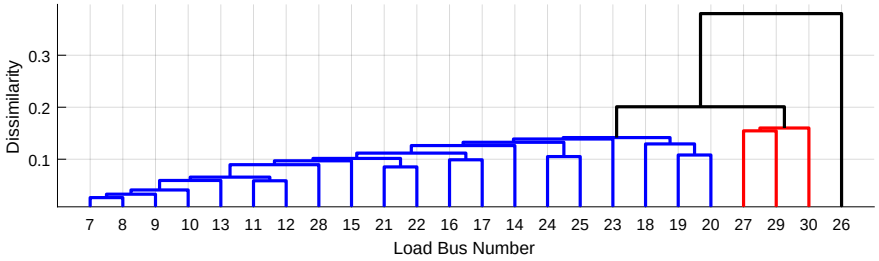

(b)

Figure 4.3: Dendrograms showing the clusterings of 6 generator buses (a) and 24 load buses. The horizontal axis are labeled by bus numberings, and the dissimilarity data are read from vertical axis.

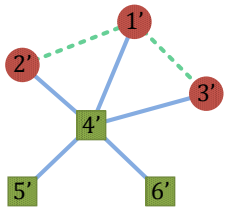

Figure 4.4: The reduced topology of the power transmission lines and communication links, which are represented by solid and dashed edges, respectively.

dissimilarities to each other. The clustering results of the generator and load nodes are straightforwardly interpreted by the dendrograms in Fig. 4.3. The leaves are the bottom vertical lines representing the buses, and the clustering of two nodes is indicated by merging two leaves into a single branch. The dissimilarity can be read from the horizontal position of each fusion. In this example, we cluster node sets of the generators and loads as in Table 4.1, where we obtain 3 clusters of generators and 3 clusters of loads. The clustering results are reasonable owing to the hierarchical structures of the dendrograms.

Using the characteristic matrices of the resulting clusterings for Galerkin projection, we obtain the reduced-order models of the power networks and distributed controller in forms of (4.39) and (4.41). The simplified networks are depicted in Fig. 4.4. Therefore, the network structures are preserved through the reduction process, which means that we can use the power network with much smaller size to approximate the behavior of the original one.

Next, the quality of the approximation is evaluated. We consider the outputs of the closed-loop system $\mathbf{\Sigma}_{cl}$ as θ_g, θ_l, ω_g, and ξ, respectively. Correspondingly, they are approximated by $\Pi_g\hat{\theta}_g$, $\Pi_l\hat{\theta}_l$, $\Pi_g\hat{\omega}_g$, and $\Pi_g\hat{\xi}$, which are assumed to be the outputs of reduced-order model and controller. Based on this, we compute the approximation errors of those variables in terms of $\mathcal{H}_2$-norms, see Table 4.2. The errors are not significant if we think of the values of the node dissimilarities in (4.48) and the dimension of the reduced closed-loop model which is considerably lower compared to the original system.

Next, the performance of the reduced-order model is further demonstrated in the time domain. The states of both the original and simplified networks are initialized at zero. From 0 to 20 seconds, the power demands of the 24 loads, P_l, are assumed by a random vector with all entries in the range $[0, 3]$. After 20 seconds, the demands are set to be a new random constant vector, which is generated from $[0, 1]$. The unit of P_l is 100 MVA. In Fig. 4.5, we compare the state trajectories of both systems,

Table 4.1: Clustering results of generator and load buses

Clusters	$\mathcal{C}_1$	$\mathcal{C}_2$	$\mathcal{C}_3$
Generator Buses	1, 2, 3, 5	4	6

Clusters	$\mathcal{C}_4$	$\mathcal{C}_5$	$\mathcal{C}_6$
Load Buses	7, 8, 9, 10, 11, 12, 13, 14, 15, 16, 17, 18, 19, 20, 21, 22, 23, 24, 25, 28	27, 29, 30	26

Table 4.2: The approximation errors evaluated by $\mathcal{H}_2$-norms

Variables	θ_g	θ_l	ω_g	ξ
Errors	0.0791	0.2088	0.2379	0.1187

i.e., the phase angles of the generators and loads, the frequencies of the generators and the states of the controllers. Evolving over time, each state trajectory of the reduced network show a similar directional tendency to the trajectories representing a cluster of nodes in the original network. Furthermore, the most of the response curves of the full-order system are approximated by those of the reduced model with acceptable errors. Besides, in Fig. 4.5c, we can see how the full-order and reduced-order distributed controllers regulate the generator frequency deviations back to zero in both systems. Moreover, Fig. 4.5d illustrates that the states of both controllers are synchronized to the same trajectories.

We implement this numerical test by Matlab 2016a in the environment of a 64-bit operating system with Intel Core i5-3470 CPU @ 3.20GHz, RAM 8.00 GB. We observe that the evaluation of dissimilarities takes 0.0564 seconds, while the clustering algorithm only uses 0.0033 seconds to find three clusters for both generator and load buses. Therefore, the total computation time is mainly consumed by the calculation of the controllability Gramian for dissimilarity evaluation.

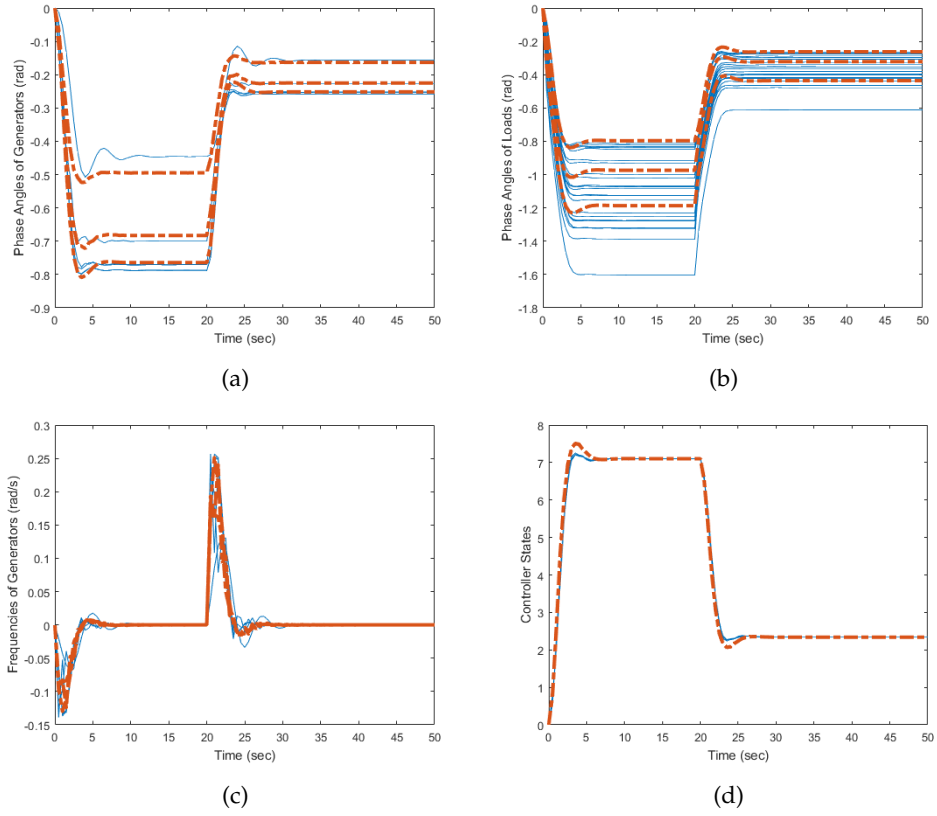

Figure 4.5: The comparisons of the state responses of the full-order and reduced-order power systems, where the solid and dashed lines are representing the trajectories of the original and simplified networks, respectively

4.5 Conclusions

We have considered the reduced-order modeling of power networks and distributed controllers, which are expressed as semistable second-order and first-order differential algebraic equations, respectively. By exploiting the controllability Gramian of the semistable closed-loop system, we have proposed a novel notion of node dissimilarity and apply a hierarchical clustering approach to divide the generator and load buses into several subsets. Towards the preservation of network structures in the reduced-order models, the characteristic matrices of the resulting clusters are adopted for the Galerkin projections of both power system and its controller.

The explicit reduced-order models are established in the same forms of the original models, which inherit a network interpretation for the interconnections of the power units. A numerical example, at last, has shown the performance of the reduced-order model and controller. This chapter provides an idea to explore clusterings of controlled power networks based on dynamical models. Compared to Chapter 3, this chapter provides a generalization for the definition of nodal behaviors. This result can be further extended in the next chapter to linear multi-agent systems, which are composed of multiple interacting higher-order subsystems.

CHAPTER 5

Clustering-Based Model Reduction of Multi-Agent Systems

This chapter investigates a model reduction scheme for large-scale multi-agent systems. The system consists of identical linear time-invariant subsystems interconnected via a large-scale network. To reduce the network complexity, we introduce a notion of nodal dissimilarity based on the $\mathcal{H}_2$-norms of the transfer function deviations, which is similar to the one introduced in Chapter 3 for the second-order networks. Here we study the general multi-agent systems and propose a new graph clustering approach to aggregate the pairs of subsystems with smaller dissimilarities. The simplified network system is verified to preserve an interconnection structure and synchronization properties of a network. Moreover, a computable bound of the approximation error between the full-order and reduced-order models is provided, and the feasibility of the proposed approach is demonstrated by network examples.

5.1 Introduction

We focus on the clustering-based reduction of multi-agent systems, which roughly refer to network systems that are composed of multiple interacting first-order linear subsystems. Multi-agent systems represent a broader class of network systems. A second-order network discussed in Chapter 3 can be also written in the form of a multi-agent system with double integrators as the agent dynamics. Although, the second-order structure is not considered, the interconnection among the ver-

tices are supposed to be preserved. In recent decades, multi-agent systems (or network systems) have received increasing attention from the system and control field, see [117, 145] for an overview. However, multi-agent systems with complex interconnection structures are often modeled by high-dimensional differential equations, which complicates system analysis, online simulation, controller design, etc. Thus, it is of clear importance to find a less complex network model to approximate the input-output characteristics of a full-order model. This chapter aims to lower the complexity of networks by reducing the number of vertices.

In this chapter, reducing the complexity of underlying networks is of particular interest. Related to this work, our preliminary results on networked single-integrators and double-integrators can be found in [34, 35, 39, 45]. To characterize a broader class of networks, we consider, in this chapter, systems that are composed of identical higher-order linear subsystems interconnecting through a general undirected graph. The notion of *dissimilarity* from Chapter 3 is extended to characterize pairwise distances among agents. Specifically, this chapter interprets the behaviors of agents as the transfer matrices from external control inputs to the outputs of individual agents, and the generalize dissimilarity between two agents to the $\mathcal{H}_2$-norm of the transfer matrix deviations. In contrast to [84, 86], where the clustering selection requires a prescribed error bound that relies on the positivity of the network system, the proposed framework utilizes a pairwise notion, the vertex dissimilarity, such that a dissimilarity matrix is established. It is an extension and generalization of the concept in conventional clustering problems in data mining, see e.g. [2, 94], where static data objects are classified. Owing to the consistency, many existing clustering algorithms in computer graphics can be adapted to efficiently reduce the complexity of dynamical network systems. Furthermore, the pairwise dissimilarities allow for an easy modification to only aggregate adjacent nodes as in [21]. Finally, the proposed method shows that the simplified model retains the network structure and preserves the synchronization property of the network.

The remainder of this chapter is organized as follows. The models of multi-agent systems and the form of reduced-order models are presented in Section 5.2. In Section 5.3, the cluster selection algorithm is provided based on the concept of dissimilarity, and the $\mathcal{H}_2$ error bound is given. Section 5.4 presents specific results for networked integrators. Section 5.5 illustrates the proposed method by a simulation example, and Section 5.6 summarizes this chapter.

5.2 Problem Formulation

In this section, we introduce the mathematical model of a multi-agent system and then address the model reduction problem in the framework of graph clustering.

5.2.1 Multi-Agent Systems

Consider a multi-agent system defined on a connected undirected graph $\mathcal{G} = (\mathcal{V}, \mathcal{E})$, with $\mathcal{V} = \{1, 2, \cdots, n\}$. The dynamics of each node is described as

$$\begin{cases} \dot{x}_i = Ax_i + Bv_i, \\ y_i = Cx_i, \end{cases} \tag{5.1}$$

where $x_i \in \mathbb{R}^{\bar{n}}$, $v_i, y_i \in \mathbb{R}^{\bar{m}}$ are the state, control input and measured output of agent i, respectively. We assume all the agents are identical in the network, and a diffusive coupling rule is applied as

$$m_i v_i = -\sum_{j=1, j\neq i}^{n} w_{ij} (y_i - y_j) + \sum_{j=1}^{p} f_{ij} u_j, \tag{5.2}$$

where $m_i \in \mathbb{R} > 0$ is the inertia of node i, and $u_j \in \mathbb{R}$ with $j = \{1, 2, \cdots, p\}$ are external control signals. Furthermore, $f_{ij} \in \mathbb{R}$ represents the amplification of u_j acting on node i, and w_{ij} stands for the intensity of the coupling between nodes i and j. As an undirected graph is assumed in this chapter, we have $w_{ij} = w_{ji}$. By (5.1) and (5.2), we establish a compact model describing the dynamics of the overall network. Let $F \in \mathbb{R}^{n\times p}$ be the collection of f_{ij} and denote inertia matrix $M := \text{diag}\,(m_1, m_2, \cdots, m_n) \in \mathbb{R}^{n\times n}$. We then obtain

$$\mathbf{\Sigma} : \begin{cases} (M \otimes I_{\bar{n}})\dot{x} = (M \otimes A - L \otimes BC)\, x + (F \otimes B)u, \\ y = (I \otimes C)x. \end{cases} \tag{5.3}$$

with a combined state vector $x^T := \left[x_1^T, x_2^T, \cdots, x_n^T\right] \in \mathbb{R}^{n\bar{n}}$, external control inputs $u^T := \left[u_1^T, u_2^T, \cdots, u_p^T\right] \in \mathbb{R}^{p\bar{m}}$, and external measurements $y^T := \left[y_1^T, y_2^T, \cdots, y_n^T\right] \in \mathbb{R}^{n\bar{m}}$. In the model, $L \in \mathbb{R}^{n\times n}$ is the *Laplacian matrix* of the interconnection graph, whose (i, j) entry is given by

$$L_{ij} = \begin{cases} \sum_{j=1, j\neq i}^{n} w_{ij}, & i = j \\ -w_{ij}, & \text{otherwise.} \end{cases} \tag{5.4}$$

For more details of Laplacian matrices, we refer to Section 2.1. The Laplacian matrix L indicates the interconnection topology and the edge weights of $\mathcal{G}$. Assume the multi-agent system is evolving over a connected, weighted undirected graph, then L fulfills the structural conditions in Remark 2.1, namely, $L^T = L \succcurlyeq 0$ and $\texttt{ker}(L) = \texttt{span}(\mathbb{1}_n)$.

A special case of system (5.3) is networked single-integrators. Consider $x_i \in \mathbb{R}$, $A = 0$, and $B = C = 1$ in the subsystem (5.1), the networked single-integrator system is then reformulated as

$$\mathbf{\Sigma_s} : M\dot{x} = -Lx + Fu. \tag{5.5}$$

A variety of physical systems are of this form, such as *mass-damper systems* and *single-species reaction networks*, see e.g., [87,124] and the references therein. System (5.5) is in the form of a *gradient system*, and also convertible into a *port-Hamiltonian system* [87]. System $\mathbf{\Sigma}_\mathsf{s}$ is called *semistable* (see Definition 2.8), since it has a simple pole at the origin. In this chapter, we discuss this class of network systems as a special result.

Synchronization is an important property in the context of multi-agent systems. With $u = 0$, the system $\mathbf{\Sigma}$ in (5.3) *synchronizes* if

$$\lim_{t\to\infty} [x_i(t) - x_j(t)] = 0, \ \forall\, i, j = \{1, 2, \cdots, n\}. \tag{5.6}$$

Note that $M^{-1}L$ has only real eigenvalues, which are denoted by $\lambda_1 \geq \cdots \geq \lambda_{n-1} > \lambda_n = 0$. Based on the eigenvalues, the following lemma then provides a sufficient condition for the synchronization of $\mathbf{\Sigma}$.

Corollary 5.1. *The multi-agent system $\mathbf{\Sigma}$ synchronizes if $A - \lambda_1 BC$ and $A - \lambda_{n-1}BC$ are **generalized negative definite**, i.e., their symmetric parts are strictly negative definite.*

Proof. Denote $\Phi_i := A - \lambda_i BC$. For any $\lambda_1 \geq \lambda_i \geq \lambda_{n-1}$, there exists a pair of constants $c_1, c_2 \geq 0$ with $c_1 + c_2 = 1$ such that $\Phi_i = c_1\Phi_1 + c_2\Phi_{n-1}$. Observe that

$$\frac{1}{2}\left(\Phi_i + \Phi_i^T\right) = \frac{c_1}{2}\left(\Phi_1 + \Phi_1^T\right) + \frac{c_2}{2}\left(\Phi_{n-1} + \Phi_{n-1}^T\right) \prec 0.$$

The synchronization of $\mathbf{\Sigma}$ then follows from e.g. [107, 125], which state that the multi-agent system $\mathbf{\Sigma}$ in (5.3) **synchronizes** if and only if $A - \lambda_k BC$ is Hurwitz for all $k = \{1, 2, \cdots, n-1\}$. By definition, Φ_i is generalized negative definite and consequently, is Hurwitz for all $i = 1, 2, \cdots, n-1$. That leads the conclusion. □

Note that the agent system (5.1) is allowed to be unstable as the synchronization condition in Corollary 5.1 does not require A to be Hurwitz. However, to avoid the trajectories of agents converging to infinity, we assume that the agent system (5.1) is Lyapunov stable, which excludes it from having poles in the open right-half plane.

5.2.2 Clustering-Based Reduction Framework

In graph theory, clustering is an important tool to simplify the topology of a complex graph and capture its essential structure. This idea is applied to dynamical networks in this section. Recall the concepts of graph clustering in Chapter 2. If n nodes are partitioned into r clusters, we form reduced-order model as

$$\hat{\mathbf{\Sigma}} : \begin{cases} (\hat{M} \otimes I_{\bar{n}})\dot{z} = \left(\hat{M} \otimes A - \hat{L} \otimes B\right) z + (\hat{F} \otimes B)u, \\ \hat{y} = (P \otimes C)z, \end{cases} \tag{5.7}$$

where $\hat{M} := P^T M P$, $\hat{L} := P^T L P$ and $\hat{F} = P^T F$ with P corresponding the characteristic matrix of a graph clustering. The reduced state z presents the dynamics of clusters, and $\hat{y} = (P \otimes I)z$ provides an approximation of the original outputs y.

For system (5.5) with networked single-integrators, clustering-based projection yields the reduced model as

$$\hat{\mathbf{\Sigma}}_{\mathsf{s}} : \begin{cases} \hat{M}\dot{z} = -\hat{L}z + \hat{F}u, \\ \hat{x} = Pz. \end{cases} \tag{5.8}$$

Remark 5.1. *From Definition 2.3, P is a binary matrix, which satisfies $P\mathbb{1}_r = \mathbb{1}_n$ and $\mathbb{1}_n^T P = [|\mathcal{C}_1|, |\mathcal{C}_2|, \cdots, |\mathcal{C}_r|]$. The specific structure of P guarantees that $\hat{M}$ is diagonal positive definite and $\hat{L}$ is a Laplacian matrix [34, 87, 124]. Hence, the reduced model $\hat{\mathbf{\Sigma}}$ is again in the form of system (5.3) and can be interpreted as a multi-agent system with less agents. Thus, the network structure is guaranteed to be preserved by the clustering-based projection. Furthermore, because of $\mathtt{ker}(\hat{L}) = \mathtt{span}(\mathbb{1}_r)$, $\hat{L}$ characterizes a connected reduced graph with r nodes.*

To formulate the problem to be investigated in this chapter, the following assumption is made for the agent dynamics in (5.1).

Assumption 5.1. *The multi-agent system $\mathbf{\Sigma}$ synchronizes, i.e., satisfies the condition in Corollary 5.1, and the A matrix of the agent dynamics (5.1) has no eigenvalues with positive real parts.*

Based on the above assumption, we formulate the model reduction problem of system $\mathbf{\Sigma}$ in the framework of Petrov-Galerkin projection.

Problem 5.1. *Given a multi-agent system $\mathbf{\Sigma}$ as in (5.3) and a desired reduced order r. Find a suitable clustering P such that reduced-order model $\hat{\mathbf{\Sigma}}$ in (5.7) achieves a small approximation error, i.e., $\|\mathbf{\Sigma} - \hat{\mathbf{\Sigma}}\|_{\mathcal{H}_\infty}$ or $\|\mathbf{\Sigma} - \hat{\mathbf{\Sigma}}\|_{\mathcal{H}_2}$ is as small as possible.*

Example 5.1. *Consider a 5-dimensional mass-damper system in Fig. 5.1, left inset and take the velocities of masses as state variables. The network system is modeled in the form of (5.5) with*

$$M = I_5,\ L = \begin{bmatrix} 6 & -3 & 0 & -2 & -1 \\ -3 & 4 & -1 & 0 & 0 \\ 0 & -1 & 6 & -2 & -3 \\ -2 & 0 & -2 & 5 & -1 \\ -1 & 0 & -3 & -1 & 5 \end{bmatrix},\ F = \begin{bmatrix} 1 & 0 \\ 0 & 0 \\ 0 & 0 \\ 0 & 1 \\ 0 & 1 \end{bmatrix}.$$

The diagonal entries of M matrix and $-L_{ij}$ $(i \neq j)$ represent mass parameters and the damping coefficient of the edge (i, j), respectively. u_1 and u_2 indicate the external forces acting on the 1st and 4th mass blocks. We choose a graph clustering as shown in Fig.

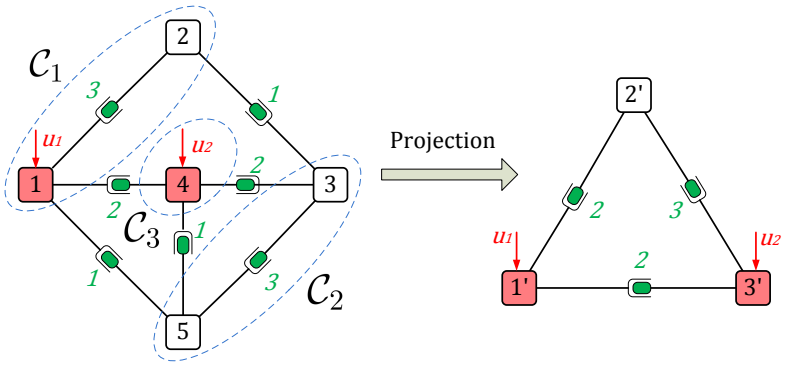

Figure 5.1: An illustrative example of clustering-based model reduction for a mass-damper network system, where red blocks represent the controlled nodes

5.1 that partitions the nodes set of the original network into 3 clusters: $\{\mathcal{C}_1, \mathcal{C}_2, \mathcal{C}_3\} = \{\{1,2\},\{3,5\},\{4\}\}$. *By Definition 2.3, the characteristic matrix is*

$$P = \begin{bmatrix} 1 & 1 & 0 & 0 & 0 \\ 0 & 0 & 1 & 0 & 1 \\ 0 & 0 & 0 & 1 & 0 \end{bmatrix}^T,$$

which leads to a reduced-order model with

$$\hat{M} = \begin{bmatrix} 2 & 0 & 0 \\ 0 & 2 & 0 \\ 0 & 0 & 1 \end{bmatrix}, \hat{L} = \begin{bmatrix} 4 & -2 & -2 \\ -2 & 5 & -3 \\ -2 & -3 & 5 \end{bmatrix}, \hat{F} = \begin{bmatrix} 1 & 0 \\ 0 & 1 \\ 0 & 1 \end{bmatrix}.$$

Clearly, it maintains the algebraic structures of the inertia and Laplacian matrices. Therefore, the network structure is preserved, which allows for a physical interpretation of the reduced model, as shown in Fig. 5.1, right inset.

5.2.3 Synchronization Preservation

The definition of *interlacing* is first introduced.

Definition 5.1. *[67] Suppose* $X \in \mathbb{R}^{n\times n}$ *and* $Y \in \mathbb{R}^{r\times r}$ *are symmetric matrices, where* $r \leq n$. *Let sequences* $\lambda_1(X) \geq \lambda_2(X) \geq \cdots \geq \lambda_n(X)$ *and* $\lambda_1(Y) \geq \lambda_2(Y) \geq \cdots \geq \lambda_r(Y)$ *be the eigenvalues of* X *and* Y, *respectively. Then, the eigenvalues of* Y ***interlace*** *those of* X *if for* $i = 1, 2, \cdots, r$,

$$\lambda_{n-r+i}(X) \leq \lambda_i(Y) \leq \lambda_i(X), \tag{5.9}$$

Lemma 5.1. *[67] Consider symmetric matrices $X \in \mathbb{R}^{n\times n}$ and $Y \in \mathbb{R}^{r\times r}$, where $r \leq n$. If there exists a matrix $S \in \mathbb{R}^{n\times r}$ such that $S^TS = I_r$ and $Y = S^TXS$, then the eigenvalues of Y **interlace** those of X.*

Based on Lemma 5.1 and Corollary 5.1, the following theorem shows that the cluster-based model reduction method preserves the synchronization property in the reduced-order multi-agent system.

Theorem 5.1. *Consider the original system $\mathbf{\Sigma}$ and the corresponding reduced-order model $\hat{\mathbf{\Sigma}}$ resulting from graph clustering. The eigenvalues of $M^{-1}L$ **interlace** those of $\hat{M}^{-1}\hat{L}$. Moreover, if $\mathbf{\Sigma}$ satisfies the synchronization condition in Corollary 5.1, then $\hat{\mathbf{\Sigma}}$ also **synchronizes**, and their impulse responses, denoted by $\xi(t)$ and $\hat{\xi}(t)$, satisfy*

$$\lim_{t\to\infty}\xi(t) = \lim_{t\to\infty}\hat{\xi}(t) = \sigma_M^{-1}\mathbb{1}\mathbb{1}^TF \otimes \lim_{t\to\infty} Ce^{At}B, \tag{5.10}$$

where $\sigma_M = \mathbb{1}^TM\mathbb{1}$.

Proof. It follows from [67] that the eigenvalues of matrix $\hat{M}^{-1/2}\hat{L}\hat{M}^{-1/2}$ *interlace* those of $M^{-1/2}LM^{-1/2}$, since there exists a matrix $S := M^{1/2}P\hat{M}^{-1/2} \in \mathbb{R}^{n\times r}$ with $S^TS = I$ such that

$$S^T\left(M^{-1/2}LM^{-1/2}\right)S = \hat{M}^{-1/2}\hat{L}\hat{M}^{-1/2}. \tag{5.11}$$

As $M^{-1}L$ and $\hat{M}^{-1}\hat{L}$ are similar to $M^{-1/2}LM^{-1/2}$ and $\hat{M}^{-1/2}\hat{L}\hat{M}^{-1/2}$, respectively, we obtain that the eigenvalues of $\hat{M}^{-1}\hat{L}$ also interlace those of $M^{-1}L$, i.e.,

$$\lambda_1 \geq \hat{\lambda}_i \geq \lambda_{n-1}, \forall\, i = 1, 2, \cdots, r-1, \tag{5.12}$$

where $\hat{\lambda}_i$ are the i-th largest eigenvalue of $\hat{M}^{-1}\hat{L}$. Moreover, $\mathbf{\Sigma}$ satisfies the synchronization condition in Corollary 5.1, i.e., $A - \lambda_1 BC$ and $A - \lambda_{n-1}BC$ are generalized negative definite, which then leads to the generalized negative definiteness of $A - \hat{\lambda}_i BC, \forall\, i = 1, 2, \cdots, r-1$ due to (5.12). Thus, system $\hat{\mathbf{\Sigma}}$ also synchronizes by Corollary 5.1.

Next, we prove that the impulse responses of $\mathbf{\Sigma}$ and $\hat{\mathbf{\Sigma}}$ converge to the same value. The proof of the synchronization of $\mathbf{\Sigma}$ follows from e.g., [107]. Consider the eigenvalue decomposition $M^{-1}L = \mathcal{U}\Lambda_o\mathcal{U}^{-1}$, where $\mathcal{U} \in \mathbb{R}^{n\times n}$ is nonsingular, and

$$\Lambda_o = \begin{bmatrix} 0 & \\ & \bar{\Lambda}_o \end{bmatrix} \text{ with } \bar{\Lambda}_o = \operatorname{diag}(\lambda_1, \cdots, \lambda_{n-1}). \tag{5.13}$$

The matrices $\mathcal{U}$ and $\mathcal{U}^{-1}$ are partitioned as

$$\mathcal{U} = \begin{bmatrix}\mathcal{U}_1 & \mathcal{U}_2\end{bmatrix}, \mathcal{U}^{-1} = \begin{bmatrix}\mathcal{V}_1^T & \mathcal{V}_2^T\end{bmatrix}^T, \tag{5.14}$$

where $\mathcal{V}_1^T, \mathcal{U}_1 \in \mathbb{R}^{n\times 1}$ are the left and right eigenvectors corresponding to the zero eigenvalue, respectively. Here, $\mathcal{U}_1$ is a unit vector, and we have

$$(M^{-1}L)^T\mathcal{V}_1^T = 0,\ (M^{-1}L)\mathcal{U}_1 = 0 \text{ and } \mathcal{V}_1\mathcal{U}_1 = 1, \tag{5.15}$$

which yields

$$\mathcal{V}_1 = \sqrt{n}\sigma_M^{-1}\mathbb{1}^T M, \text{ and } \mathcal{U}_1 = \frac{\mathbb{1}}{\sqrt{n}}. \tag{5.16}$$

Note that

$$\begin{aligned} e^{\left[I\otimes A-(M^{-1}L)\otimes BC\right]t} &= (\mathcal{U}\otimes I)e^{(I\otimes A-\Lambda_o\otimes BC)t}(\mathcal{U}^{-1}\otimes I) \\ &= \mathcal{U}_1\mathcal{V}_1\otimes e^{At} + \mathcal{U}_2\mathcal{V}_2\otimes e^{\left(I_{n-1}\otimes A-\bar{\Lambda}_o\otimes BC\right)t}, \end{aligned}$$

where $I_{n-1}\otimes A-\bar{\Lambda}\otimes BC$ is Hurwitz by Corollary 5.1. Therefore, the impulse response of the original system $\mathbf{\Sigma}$ converges as

$$\begin{aligned} \xi(t) =& (I\otimes C)\left[e^{\left(I\otimes A-M^{-1}L\otimes BC\right)t}\right](M^{-1}F\otimes B) \\ \to& \mathcal{U}_1\mathcal{V}_1M^{-1}F\otimes\lim_{t\to\infty}Ce^{At}B, \text{ as } t\to\infty, \\ =& \sigma_M^{-1}\mathbb{1}\mathbb{1}^TF\otimes\lim_{t\to\infty}Ce^{At}B. \end{aligned} \tag{5.17}$$

Similarly, the impulse response of the reduced-order system $\hat{\mathbf{\Sigma}}$ is given by

$$\begin{aligned} \hat{\xi}(t) \to& (P\otimes C)\left(\sigma_M^{-1}\mathbb{1}_r\mathbb{1}_r^T\hat{F}\otimes e^{At}B\right), \text{ as } t\to\infty, \\ =& \sigma_M^{-1}P\mathbb{1}_r\mathbb{1}_r^TP^TF\otimes\lim_{t\to\infty}Ce^{At}B \\ =& \sigma_M^{-1}\mathbb{1}_n\mathbb{1}_n^TF\otimes\lim_{t\to\infty}Ce^{At}B. \end{aligned}$$

To obtain the above result, the equations $P\mathbb{1}_r = \mathbb{1}_n$ and $\mathbb{1}_r^TP^TMP\mathbb{1}_r = \mathbb{1}_n^TM\mathbb{1}_n = \sigma_M^{-1}$ are used. That completes the proof. □

The following proposition specifies $\mathbf{\Sigma}$ as a networked port-Hamiltonian system. In this case, system $\mathbf{\Sigma}$ and its reduced-order model $\hat{\mathbf{\Sigma}}$ are synchronized.

Proposition 5.1. *Consider the agent dynamics in (5.1) which is a **port-Hamiltonian system**, i.e.,*

$$A = (J-R)Q,\ \ C = B^TQ$$

with $J = -J^T$, $R = R^T$ and $R, Q \succ 0$. Then, both $\mathbf{\Sigma}$ and $\hat{\mathbf{\Sigma}}$ are synchronized.

Proof. Denote $\Phi_i := J - R - \lambda_i BB^T$. From [107], the synchronization of $\mathbf{\Sigma}$ is equivalently characterized by the Hurwitz stability of matrix $\Phi_i Q$ for any $i = 1, 2, \cdots, n-1$. Observe that $\Phi_i + \Phi_i^T = -2(R + \lambda_i BB^T) \prec 0$. Therefore,

$$\frac{1}{2}\left(Q^{1/2}\Phi_i Q^{1/2} + Q^{1/2}\Phi_i^T Q^{1/2}\right) \prec 0, \tag{5.18}$$

which implies $Q^{1/2}\Phi_i Q^{1/2}$ to be generalized negative definite and consequently, is Hurwitz stable. Since $\Phi_i Q \sim Q^{1/2}\Phi_i Q^{1/2}$, $\Phi_i Q$ is also Hurwitz. Then the synchronization of system $\mathbf{\Sigma}$ can be proved by Corollary 5.1.

Since the eigenvalues of $\hat{M}^{-1}\hat{L}$ also interlace those of $M^{-1}L$, the synchronization of its reduced-order model can be obtained similarly. □

5.3 Approximation of Multi-Agent Systems

Denote the transfer matrices of system $\mathbf{\Sigma}$ and $\hat{\mathbf{\Sigma}}$ by

$$\eta(s) = (I \otimes C)\left[M \otimes (sI - A) + L \otimes BC\right]^{-1}(F \otimes B), \tag{5.19a}$$

$$\hat{\eta}(s) = (P \otimes C)\left[\hat{M} \otimes (sI - A) + \hat{L} \otimes BC\right]^{-1}(\hat{F} \otimes B). \tag{5.19b}$$

Then the transfer matrices from the external inputs to the outputs of individual subsystem are expressed as

$$\eta_i(s) := (\mathbf{e}_i^T \otimes I)\eta(s),\ \hat{\eta}_i(s) := (\mathbf{e}_i^T \otimes I)\hat{\eta}(s). \tag{5.20}$$

As a natural outcome of Theorem 5.1, the following corollary implies that the approximation error between $\mathbf{\Sigma}$ and $\hat{\mathbf{\Sigma}}$ is always bounded, even if $\mathbf{\Sigma}$ is not asymptotically stable.

Corollary 5.2. *Consider the multi-agent system $\mathbf{\Sigma}$ and the reduced model $\hat{\mathbf{\Sigma}}$ resulting from an arbitrary clustering. Then, $\|\eta(s) - \hat{\eta}(s)\|_{\mathcal{H}_2}$ is always bounded.*

Proof. Denote $\Xi_{ij}(t) := (\mathbf{e}_i^T \otimes I)\xi(t) - (\mathbf{e}_j^T \otimes I)\hat{\xi}(t)$, where $\xi(t)$ and $\hat{\xi}(t)$ are the impulse responses of system $\mathbf{\Sigma}$ and $\hat{\mathbf{\Sigma}}$, respectively. Then, by the definition of $\mathcal{H}_2$-norm, we have

$$\|\eta_i(s) - \hat{\eta}_j(s)\|_{\mathcal{H}_2}^2 = \int_0^\infty \mathtt{tr}\left[\Xi_{ij}^T(t)\Xi_{ij}(t)\right] dt, \tag{5.21}$$

Note that $\xi(t)$ and $\hat{\xi}(t)$ are bounded smooth functions of t. It follows from $\mathbf{e}_{ij}^T\mathbb{1} = 0$ and the Lyapunov stability of (A, B, C) that

$$\lim_{t\to\infty} \Xi_{ij}^T(t) = \sigma_M^{-1}\mathbf{e}_{ij}^T\mathbb{1}\mathbb{1}^T F \otimes \left(\lim_{t\to\infty} Ce^{At}B\right) = 0. \tag{5.22}$$

Thus, for bounded initial conditions $\xi_i(0)$ and $\hat{\xi}_j(0)$, the integral in (5.21) is bounded, i.e., $\|\eta_i(s) - \hat{\eta}_j(s)\|_{\mathcal{H}_2}^2 < \infty$. Consequently, $\|\eta(s) - \hat{\eta}(s)\|_{\mathcal{H}_2}^2$ is finite. □

5.3.1 Vertex Dissimilarity

The transfer matrix $\eta_i(s)$ defined in (5.20) represents the mapping from the external control signals u to the outputs x_i, which can be interpreted as the behavior of the i-th agent. Then, we recall the dissimilarity of two nodes in Definition 3.2. Particularly, if $\mathcal{D}_{ij} = 0$, nodes i and j are 0-dissimilar.

The dissimilarity matrix (or distance matrix), defined by $\mathcal{D} := [\mathcal{D}_{ij}]$, is nonnegative, symmetric, and with zero diagonal elements. The concept of dissimilarity matrix is commonly used in signal processing, as it describes a pairwise distance between two observations. Conventionally, the dissimilarity is characterized by the Euclidean distance, see e.g., [4, 178]. However, Definition 3.2 extends the domain of this notation to the norm of the difference between nodal dynamics. The idea to measure the similarity of transfer functions for clustering of dynamical networks can be also seen in [84, 85]. When each cluster only has two nodes, the notion of the dissimilarity in (3.77) coincides with that of the cluster reducibility in [84, 85].

An efficient computation of the $\mathcal{H}_2$-norm in (3.77) requires the controllability Gramian of $\mathbf{\Sigma}$, which however may not exist when $\mathbf{\Sigma}$ is not asymptotically stable, see Chapter 3. Inspired by [84], we extract out the asymptotically stable parts from $\mathbf{\Sigma}$ by a specific transformation and employ the controllability Gramian of the asymptotically stable system, we develop an efficient way for the computation of the pairwise dissimilarities.

Theorem 5.2. *Consider the multi-agent system $\mathbf{\Sigma}$ in (5.3) that synchronizes. Denote*

$$\mathcal{S}_n := \frac{1}{n}\left[\mathbb{1}_{n-1}\mathbb{1}_{n-1}^T - nI_{n-1}, \mathbb{1}_{n-1}\right] \in \mathbb{R}^{(n-1)\times n}. \tag{5.23}$$

Then, $\bar{\mathcal{P}} \in \mathbb{R}^{\bar{n}(n-1)\times\bar{n}(n-1)}$ is the unique solution of the Lyapunov equation

$$\bar{A}\bar{\mathcal{P}} + \bar{\mathcal{P}}\bar{A} + \bar{\mathcal{B}}\bar{\mathcal{B}}^T = 0, \tag{5.24}$$

where

$$\begin{aligned} \bar{\mathcal{A}} :&= I_{n-1}\otimes A - (\mathcal{S}_n\mathcal{S}_n^T)^{-1}\mathcal{S}_n M^{-1} L\mathcal{S}_n^T \otimes BC, \\ \bar{\mathcal{B}} :&= (\mathcal{S}_n\mathcal{S}_n^T)^{-1}\mathcal{S}_n M^{-1} F \otimes B. \end{aligned} \tag{5.25}$$

*Furthermore, the (i,j) entry of the **dissimilarity matrix** is computed as follows:*

- $\mathcal{D}_{ii} = 0$, *if* $i \in \{1, 2, \cdots, n\}$;
- $\mathcal{D}_{ni}^2 = \mathcal{D}_{in}^2 = \mathsf{tr}\left[(\mathbf{e}_i^T \otimes C)\bar{\mathcal{P}}(\mathbf{e}_i \otimes C)\right]$, *if* $i \in \{1, 2, \cdots, n-1\}$;
- $\mathcal{D}_{ij}^2 = \mathcal{D}_{ji}^2 = \mathsf{tr}\left[(\mathbf{e}_{ij}^T \otimes C)\bar{\mathcal{P}}(\mathbf{e}_{ij} \otimes C)\right]$, *if* $i, j \in \{1, 2, \cdots, n-1\}$.

where $\mathbf{e}_i$, $\mathbf{e}_{ij} \in \mathbb{R}^{n-1}$.

Proof. Consider the following transformation matrices

$$\mathcal{T}_n := \begin{bmatrix} \mathcal{S}_n^T & \frac{1}{n}\mathbb{1}_n \end{bmatrix}, \mathcal{T}_n^{-1} = \begin{bmatrix} (\mathcal{S}_n\mathcal{S}_n^T)^{-1}\mathcal{S}_n \\ \mathbb{1}_n^T \end{bmatrix}, \tag{5.26}$$

and define new state variables

$$\delta := (\mathcal{T}_n^{-1} \otimes I_{\bar{n}})x = \left(\begin{bmatrix} -I_{n-1} & \mathbb{1}_{n-1} \\ \mathbb{1}_{n-1}^T & 1 \end{bmatrix} \otimes I_{\bar{n}} \right) x := \begin{bmatrix} \delta_d \\ \delta_a \end{bmatrix},$$

where

$$\begin{aligned} \delta_d &= ([-I_{n-1}, \mathbb{1}_{n-1}] \otimes I_{\bar{n}})\, x \in \mathbb{R}^{m(n-1)}, \\ \delta_a &= (\mathbb{1}_n^T \otimes I_{\bar{n}})x \in \mathbb{R}^m. \end{aligned} \tag{5.27}$$

Note that $(\mathbf{e}_i^T \otimes I_{\bar{n}})\delta_d \in \mathbb{R}^{\bar{n}}$ represents the error between the states of the i-th and the n-th agents, while $\delta_a \in \mathbb{R}^{\bar{n}}$ indicates the average of all the agent states.

We then substitute $x = (\mathcal{T}_n \otimes I_{\bar{n}}) \cdot \delta$ to the network model $\mathbf{\Sigma}$ in (5.3) and multiply $\mathcal{T}_n^{-1}M^{-1} \otimes I_{\bar{n}}$ from the left side. It then leads to an equivalent representation of $\mathbf{\Sigma}$ as

$$\dot{\delta} = (I_n \otimes A - \tilde{L} \otimes BC)\delta + (\tilde{F} \otimes B)u. \tag{5.28}$$

where

$$\begin{aligned} \tilde{L} &= \begin{bmatrix} (\mathcal{S}_n\mathcal{S}_n^T)^{-1}\mathcal{S}_n M^{-1} L \mathcal{S}_n^T & 0 \\ \mathbb{1}^T M^{-1} L \mathcal{S}_n^T & 0 \end{bmatrix}, \\ \tilde{F} &= \begin{bmatrix} (\mathcal{S}_n\mathcal{S}_n^T)^{-1}\mathcal{S}_n M^{-1} F \\ \mathbb{1}^T M^{-1} F \end{bmatrix}. \end{aligned} \tag{5.29}$$

It is not hard to see that $\bar{L}$ and $M^{-1}L$ share all the nonzero eigenvalues, and the synchronization of $\mathbf{\Sigma}$ implies that matrix $\bar{\mathcal{A}}$ in (5.25) is Hurwitz [107]. Now, consider an output $y = H\delta$, and denote $\eta_d(s)$ as the transfer function of the system $(\bar{A}, \bar{B}, H)$. Since $\bar{\mathcal{A}}$ is Hurwitz, the controllability Gramian $\bar{\mathcal{P}}$ is the unique solution of the Lyapunov equation in (5.24). Thus, it follows from [7] that

$$\|\eta_d(s)\|_{\mathcal{H}_2} = \sqrt{\mathtt{tr}(H\bar{\mathcal{P}}H^T)}, \tag{5.30}$$

We obtain the pairwise dissimilarities $\mathcal{D}_{ii}$, $\mathcal{D}_{ni}$ and D_{ij}, if H in (5.30) is replaced by $\mathbf{e}_j^T \otimes C$, $\mathbf{e}_i^T \otimes C$ or $H = \mathbf{e}_{ij}^T \otimes C$, respectively. □

Example 5.2. *We again use Example 5.1 to illustrate the flows of the two graph clustering algorithms. From Theorem 5.2, we have*

$$\bar{\mathcal{A}} = \begin{bmatrix} -7 & 3 & -3 & 1 \\ 2 & -4 & -2 & -1 \\ -1 & 1 & -9 & 1 \\ 1 & 0 & -1 & -6 \end{bmatrix}, \ \bar{\mathcal{B}} = \begin{bmatrix} -1 & 1 \\ 0 & 1 \\ 0 & 1 \\ 0 & 0 \end{bmatrix}.$$

Solving the Lyapunov equation in (5.24) yields

$$\bar{\mathcal{P}} = \begin{bmatrix} 0.1716 & 0.1285 & 0.0647 & 0.0098 \\ 0.1285 & 0.1476 & 0.0800 & 0.0066 \\ 0.0647 & 0.0800 & 0.0573 & 0.0004 \\ 0.0098 & 0.0066 & 0.0004 & 0.0016 \end{bmatrix} \tag{5.31}$$

Then, the dissimilarity matrix is given by

$$\mathcal{D} = \begin{bmatrix} 0 & 0.2494 & 0.3154 & 0.3919 & 0.4142 \\ 0.2494 & 0 & 0.2119 & 0.3688 & 0.3842 \\ 0.3154 & 0.2119 & 0 & 0.2410 & 0.2394 \\ 0.3919 & 0.3688 & 0.2410 & 0 & 0.0396 \\ 0.4142 & 0.3842 & 0.2394 & 0.0396 & 0 \end{bmatrix}.$$

The minimal value in $\mathcal{D}$, 0.0396, indicates that vertices 4 and 5 are of strongest similarity compared to the other pairs of vertices.

5.3.2 Cluster Selection and Error Analysis

The appropriate selection of clusters is crucial for the approximation precision of network reduction. The main contribution of this chapter comes from a novel clustering procedure. Compared to the existing results in e.g. [21, 84, 126]. our idea is a generalization of the conventional clustering in signal processing [94]. Instead of classifying a large number of static data and measuring their differences by the Euclidean norms, we generalize the method for dynamical systems, where the domain of dissimilarity is extended to Definition 3.2. With the new notation of dissimilarity, the model reduction problem of networks is connected to the conventional data clustering problems.

Note that the value of $\mathcal{D}_{ij}$ indicates the dissimilarity of agent i and j in terms of transfer functions. Intuitively, clustering the agents with higher similarity can potentially deliver a reduced-order model with smaller approximation error. Based on this, standard clustering schemes in signal processing can be adapted to generate a suitable partition of the network, e.g., the iterative clustering in [34] and the

hierarchical clustering in Chapter 3. In this chapter, a more efficient algorithm is proposed in Algorithm 2.

Algorithm 2 Network Clustering Algorithm

1: Compute matrix $\mathcal{D}$ using Theorem 5.2.
2: Place each node into its own singleton cluster, i.e.,

$$\mathcal{C}_k \leftarrow \{k\},\ \forall\, 1 \leq k \leq n.$$

3: Find two clusters $\mathcal{C}_\mu$ and $\mathcal{C}_\nu$ such that

$$(\mu, \nu) := \arg\min \left(\max_{i,j \in \mathcal{C}_\mu \cup \mathcal{C}_\nu} \mathcal{D}_{ij} \right). \tag{5.32}$$

4: Merge clusters $\mathcal{C}_\mu$ and $\mathcal{C}_\nu$ into a single cluster.
5: If there are more than r clusters, repeat the steps 3 and 4. Otherwise, compute $P \in \mathbb{R}^{n \times r}$ and generate

$$\hat{M} \leftarrow P^T M P, \hat{L} \leftarrow P^T L P, \hat{F} \leftarrow P^T F.$$

The proposed algorithm is implicitly based on pairwise dissimilarities of the agents and minimizes within-cluster variances. The variance within a cluster is evaluated by the maximal dissimilarity between all pairs of nodes in the cluster. Note that the formation of clusters in Algorithm 2 does not focus on manipulating any individual edges. Even if two nodes are not adjacent, they can be placed into the same cluster when they have very similar behaviors.

Remark 5.2. *It should be emphasized that Algorithm 2 can be easily adapted to aggregate adjacent nodes only. To this end, we first introduce the definition of adjacent clusters as follows: Two clusters $\mathcal{C}_\mu$ and $\mathcal{C}_\nu$ are adjacent if there exist $i \in \mathcal{C}_\mu$ and $j \in \mathcal{C}_\nu$ such that nodes i and j are connected by an edge. Then, we modify step 3 in Algorithm 2 where we find two adjacent clusters such that (5.32) holds.*

Now the approximation error between the original and reduced multi-agent systems is analyzed using the dissimilarities in (3.77). For simplicity, we denote

$$\mathcal{S}_r := \frac{1}{r} \left[\mathbb{1}_{r-1} \mathbb{1}_{r-1}^T - r I_{r-1}, \mathbb{1}_{r-1} \right] \in \mathbb{R}^{(r-1) \times r}, \tag{5.33}$$

and

$$\bar{P} := P \hat{M}^{-1} \mathcal{S}_r^T, \bar{M} := \bar{P}^T M \bar{P}, \bar{L} := \bar{P}^T L \bar{P}. \tag{5.34}$$

Theorem 5.3. *Consider the multi-agent system $\mathbf{\Sigma}$ in (5.3). Suppose $\mathbf{\Sigma}$ synchronizes (i.e., it satisfies the conditions of Corollary (5.1). If the graph clustering is given by $\{\mathcal{C}_1, \mathcal{C}_2, \cdots, \mathcal{C}_r\}$, then the approximation error between $\mathbf{\Sigma}$ and the clustered system $\hat{\mathbf{\Sigma}}$ is bounded by*

$$\|\eta(s) - \hat{\eta}(s)\|_{\mathcal{H}_2} < \gamma_s \cdot \sum_{k=1}^{r} |\mathcal{C}_k| \cdot \max_{i,j \in \mathcal{C}_k} \mathcal{D}_{ij}, \tag{5.35}$$

where γ_s is a positive scalar satisfying

$$\begin{bmatrix} \bar{\mathcal{X}} & \bar{P}^T L \otimes BC & -\bar{P}^T \otimes C^T \\ L\bar{P} \otimes C^T B^T & -\gamma_s I & I \\ -\bar{P} \otimes C & I & -\gamma_s I \end{bmatrix} \prec 0, \tag{5.36}$$

with $\bar{\mathcal{X}} := \bar{M} \otimes (A^T + A) - \bar{L} \otimes (C^T B^T + BC)$. Particularly, if A in (5.1) is generalized negative definite, i.e., $A + A^T \prec 0$, then γ_s is characterized by

$$\begin{bmatrix} \mathcal{X} & L \otimes BC & -I \otimes C^T \\ L \otimes C^T B^T & -\gamma_s I & I \\ -I \otimes C & I & -\gamma_s I \end{bmatrix} \prec 0, \tag{5.37}$$

with $\mathcal{X} := M \otimes (A^T + A) - L \otimes (C^T B^T + BC)$.

Proof. The approximation error can be evaluated by the following transfer function.

$$\eta_{\mathsf{e}}(s) := \eta(s) - \hat{\eta}(s) = \mathcal{C}_{\mathsf{e}}(sI - \mathcal{A}_{\mathsf{e}})^{-1}\mathcal{B}_{\mathsf{e}}, \tag{5.38}$$

with

$$\begin{aligned} \mathcal{A}_{\mathsf{e}} &= I_{n+r} \otimes A - \begin{bmatrix} M^{-1}L & \\ & \hat{M}^{-1}\hat{L} \end{bmatrix} \otimes BC, \\ \mathcal{B}_{\mathsf{e}} &= \begin{bmatrix} M^{-1}F \\ \hat{M}^{-1}\hat{F} \end{bmatrix} \otimes B,\ \mathcal{C}_{\mathsf{e}} = \begin{bmatrix} I_n & -P \end{bmatrix} \otimes I_{\bar{n}}. \end{aligned} \tag{5.39}$$

Inspired by [84,85], we rewrite the error system into a cascade form. Consider the following nonsingular matrices

$$\mathcal{T} = \begin{bmatrix} 0 & I_n \\ I_r & P \end{bmatrix} \otimes I_{\bar{n}},\ \mathcal{T}^{-1} = \begin{bmatrix} -P & I_r \\ I_n & 0 \end{bmatrix} \otimes I_{\bar{n}}. \tag{5.40}$$

with $P = \hat{M}^{-1}P^T M \in \mathbb{R}^{r \times n}$. It then follows that

$$\begin{aligned} sI - \mathcal{T}^{-1}\mathcal{A}_{\mathsf{e}}\mathcal{T} &= \begin{bmatrix} \hat{\Omega}(s) & -PM^{-1}L(I - PP) \otimes BC \\ 0 & \Omega(s) \end{bmatrix}, \\ \mathcal{T}^{-1}\mathcal{B}_{\mathsf{e}} &= \begin{bmatrix} 0 \\ M^{-1}F \end{bmatrix} \otimes B, \mathcal{C}_{\mathsf{e}}\mathcal{T} = \begin{bmatrix} -P & I - PP \end{bmatrix} \otimes I, \end{aligned}$$

where $\Omega(s)$ and $\hat{\Omega}(s)$ are transfer functions defined by

$$\begin{aligned}\Omega(s) &:= sI_n - I_n \otimes A + M^{-1}L \otimes BC,\\ \hat{\Omega}(s) &:= sI_r - I_r \otimes A + \hat{M}^{-1}\hat{L} \otimes BC.\end{aligned} \tag{5.41}$$

Thus, applying a transformation using (5.40) to (5.38) leads to

$$\begin{aligned}\eta_{\mathsf{e}}(s) &= \mathcal{C}_{\mathsf{e}}\mathcal{T}(sI - \mathcal{T}^{-1}\mathcal{A}_{\mathsf{e}}\mathcal{T})^{-1}\mathcal{T}^{-1}\mathcal{B}_{\mathsf{e}}\\ &= -(P \otimes C)\hat{\Omega}^{-1}(s)\left[PM^{-1}L(I-PP) \otimes BC\right]\eta(s)\\ &\qquad + \left[(I-PP) \otimes C\right]\eta(s)\\ &= \Big[I \otimes C - (P \otimes C)\hat{\Omega}^{-1}(s)(PM^{-1}L \otimes BC)\Big]\\ &\qquad \cdot \left[(I-PP) \otimes I\right]\eta(s),\end{aligned} \tag{5.42}$$

where $\eta(s) = \Omega^{-1}(s)(M^{-1}F \otimes B)$ and

$$\begin{aligned}&PM^{-1}L(I-PP) \otimes BC\\ &\qquad = (PM^{-1}L \otimes BC)\left[(I-PP) \otimes I\right],\end{aligned}$$

are used for derivation of the last expression in (5.42).

Denote the following two transfer functions

$$\eta_{\mathsf{e}}^a(s) := I \otimes C - (P \otimes C)\hat{\Omega}^{-1}(s)(\hat{M}^{-1}P^TL \otimes BC), \tag{5.43a}$$

$$\eta_{\mathsf{e}}^b(s) := \left[(I-PP) \otimes I\right]\eta(s). \tag{5.43b}$$

such that $\eta_{\mathsf{e}}(s) := \eta_{\mathsf{e}}^a(s) \cdot \eta_{\mathsf{e}}^b(s)$. Thus, the approximation error between the original and reduced-order multi-agent systems, $\mathbf{\Sigma}$ and $\hat{\mathbf{\Sigma}}$, is bounded as

$$\|\eta_{\mathsf{e}}(s)\|_{\mathcal{H}_2} \le \|\eta_{\mathsf{e}}^a(s)\|_{\mathcal{H}_\infty}\|\eta_{\mathsf{e}}^b(s)\|_{\mathcal{H}_2}. \tag{5.44}$$

In the rest of the proof, we will show the boundedness of $\|\eta_{\mathsf{e}}^a(s)\|_{\mathcal{H}_\infty}$ and $\|\eta_{\mathsf{e}}^b(s)\|_{\mathcal{H}_2}$ and analyze their upper bounds respectively.

First, we discuss the transfer function $\eta_{\mathsf{e}}^a(s)$ in (5.43a), which is associated with a linear system with coefficient matrices

$$\begin{aligned}A_a &:= I_r \otimes A - \hat{M}^{-1}\hat{L} \otimes BC,\\ B_a &:= \hat{M}^{-1}P^TL \otimes BC,\\ C_a &:= -P \otimes C, \text{and } D_a := I_r \otimes C.\end{aligned} \tag{5.45}$$

Using the matrix $\mathcal{S}_r$ in (5.33), which satisfies $\mathcal{S}_r\mathbb{1}_r = 0$, we define transformation matrices

$$\mathcal{T}_r := \begin{bmatrix}\hat{M}^{-1}\mathcal{S}_r^T & \frac{1}{r}\mathbb{1}_r\end{bmatrix}, \mathcal{T}_r^{-1} = \begin{bmatrix}(\mathcal{S}_r\hat{M}^{-1}\mathcal{S}_r^T)^{-1}\mathcal{S}_r\\ \sigma_M^{-1}\mathbb{1}_r^T\hat{M}\end{bmatrix},$$

where $\sigma_M = \mathbb{1}_r^T \hat{M} \mathbb{1}_r = \mathbb{1}_n^T M \mathbb{1}_n$. It then leads to

$$\mathcal{T}_r^{-1} A_a \mathcal{T}_r = \begin{bmatrix} A_s & 0 \\ 0 & A \end{bmatrix}, \mathcal{T}_r^{-1} B_a = \begin{bmatrix} B_s \\ 0 \end{bmatrix}, C_a \mathcal{T}_r = \begin{bmatrix} C_s & * \end{bmatrix}$$

with

$$\begin{aligned} A_s &:= I_{r-1} \otimes A - \bar{M}^{-1} \bar{L} \otimes BC, \\ B_s &:= \bar{M}^{-1} \bar{P}^T L \otimes BC, \\ C_s &:= -\bar{P} \otimes C. \end{aligned} \tag{5.46}$$

The matrices $\bar{M}$, $\bar{L}$ and $\bar{P}$ are defined in (5.34).

Clearly, the above transformation splits $\eta_{\mathsf{e}}^a(s)$ as $\eta_{\mathsf{e}}^a(s) = \text{blkdiag}(C, g_s(s))$ with a static gain C and the system

$$g_s(s) := C_s(sI - A_s)^{-1} B_s + I_{r-1} \otimes C. \tag{5.47}$$

Observe that

$$\begin{aligned} &\bar{M}^{-1} \bar{L} = (\bar{P}^T M \bar{P})^{-1} \bar{P}^T L \bar{P} \\ &= (\mathcal{S}_r^T \hat{M}^{-1} P^T M P \hat{M}^{-1} \mathcal{S}_r^T)^{-1} \mathcal{S}_r^T \hat{M}^{-1} P^T L P \hat{M}^{-1} \mathcal{S}_r^T \\ &= (\mathcal{S}_r \hat{M}^{-1} \mathcal{S}_r^T)^{-1} \mathcal{S}_r (\hat{M}^{-1} \hat{L}) \mathcal{S}_r^T. \end{aligned}$$

Thus, $\bar{M}^{-1} \bar{L}$ shares all the nonzero eigenvalues with $\hat{M}^{-1} \hat{L}$. Moreover, Theorem 5.1 implies that $\hat{\boldsymbol{\Sigma}}$ also synchronizes as the original multi-agent system $\hat{\boldsymbol{\Sigma}}$ synchronizes. Then, it follows from [107] that A_s is Hurwitz. Consequently, the transfer function $g_s(s)$ is shown to be asymptotically stable, and hence,

$$\|\eta_{\mathsf{e}}^a(s)\|_{\mathcal{H}_\infty} \leq \max\{\|C\|_2, \|g_s(s)\|_{\mathcal{H}_\infty}\} \leq \|g_s(s)\|_{\mathcal{H}_\infty}. \tag{5.48}$$

We use the bounded real lemma (see e.g. [28]) to characterize the $\mathcal{H}_\infty$-norm of $g_s(s)$ in (5.47). There exists a positive scalar γ_s such that $\|g_s(s)\|_{\mathcal{H}_\infty} < \gamma_s$, if the following inequality holds for a matrix $K \succ 0$.

$$\begin{bmatrix} A_s^T K + K A_s & K B_s & C_s^T \\ B_s^T K & -\gamma_s I & I \\ C_s & I & -\gamma_s I \end{bmatrix} \prec 0. \tag{5.49}$$

Let $K = \bar{M} \otimes I$ in (5.49), it then yields the LMI in (5.36), which is feasible as $\bar{\mathcal{X}}$ is negative definite.

In the special case that $A + A^T \prec 0$, $\mathcal{X}$ is also negative definite so that the LMI in (5.37) is feasible. Observe that (5.36) can be obtained from (5.37) by pre-multiplying

and post-multiplying the matrix blkdiag$(\bar{P}^T, I, I)$ and its transpose, respectively. Thus, γ_s is a solution of (5.36) if it satisfies (5.37).

Next, the $\mathcal{H}_2$-norm of transfer function (5.43b) is discussed. Without loss of generality, let

$$\begin{aligned} P &= \mathsf{blkdiag}\left(\mathbb{1}_{|\mathcal{C}_1|}, \mathbb{1}_{|\mathcal{C}_2|}, \cdots, \mathbb{1}_{|\mathcal{C}_r|}\right), \\ M &= \mathsf{blkdiag}\left(M_1, M_2, \cdots, M_r\right), \end{aligned}$$

with $M_i \in \mathbb{R}^{|\mathcal{C}_i|\times|\mathcal{C}_i|}$. Denote $\hat{m}_i = \mathbb{1}^T M_i \mathbb{1}$, then $\hat{M} = \mathrm{diag}(\hat{m}_1, \hat{m}_2, \cdots, \hat{m}_r)$. Define a vector of transfer functions

$$\left(\eta^{\mathcal{C}_i}\right)^T := \left[\left(\eta_1^{\mathcal{C}_i}\right)^T, \left(\eta_2^{\mathcal{C}_i}\right)^T, \cdots, \left(\eta_{|\mathcal{C}_i|}^{\mathcal{C}_i}\right)^T\right], \tag{5.50}$$

where $\eta_k^{\mathcal{C}_i}$ represents the behavior of the k-th node in the cluster $\mathcal{C}_i$. We can also write the expression $[(I - PP) \otimes I]\,\eta(s)$ into a block diagonal form whose i-th block diagonal entry is given by

$$\begin{aligned} &\left(\left[I_{|\mathcal{C}_i|} - \mathbb{1}_{|\mathcal{C}_i|}\mathbb{1}_{|\mathcal{C}_i|}^T \hat{m}^{-1} M_i\right] \otimes I\right)\eta^{\mathcal{C}_i} \\ &\qquad = \begin{bmatrix} \sum\limits_{k\in\mathcal{C}_i, k\neq 1} \hat{m}_i^{-1} m_k \left(\eta_1^{\mathcal{C}_i} - \eta_k^{\mathcal{C}_i}\right) \\ \vdots \\ \sum\limits_{k\in\mathcal{C}_i, k\neq|\mathcal{C}_i|} \hat{m}_i^{-1} m_k \left(\eta_{|\mathcal{C}_i|}^{\mathcal{C}_i} - \eta_k^{\mathcal{C}_i}\right) \end{bmatrix}. \end{aligned} \tag{5.51}$$

It is noted that $\|\eta_j^{\mathcal{C}_i} - \eta_k^{\mathcal{C}_i}\|_{\mathcal{H}_2} \leq \|\eta_{\max}^{\mathcal{C}_i}\|_{\mathcal{H}_2}$, where $\eta_{\max}^{\mathcal{C}_i}$ refers to the biggest divergence of node behaviors within the cluster $\mathcal{C}_i$. It then leads to

$$\left\| \sum_{k\in\mathcal{C}_i, k\neq 1} \hat{m}_i^{-1} m_k \left(\eta_1^{\mathcal{C}_i} - \eta_k^{\mathcal{C}_i}\right) \right\|_{\mathcal{H}_2} \leq \|\eta_{\max}^{\mathcal{C}_i}\|_{\mathcal{H}_2}. \tag{5.52}$$

Therefore, we obtain

$$\begin{aligned} \|\eta_{\mathsf{e}}^b(s)\|_{\mathcal{H}_2} &\leq \sum_{k=1}^{r} \left\| \left(I_{|\mathcal{C}_k|} - \hat{m}^{-1}\mathbb{1}_{|\mathcal{C}_k|}\mathbb{1}_{|\mathcal{C}_k|}^T M_k\right)\eta^{\mathcal{C}_k} \right\|_{\mathcal{H}_2} \\ &\leq \sum_{k=1}^{r} |\mathcal{C}_k| \cdot \|\eta_{\max}^{\mathcal{C}_k}\|_{\mathcal{H}_2} = \sum_{k=1}^{r} |\mathcal{C}_k| \cdot \max_{i,j\in\mathcal{C}_k} \mathcal{D}_{ij}. \end{aligned}$$

That completes the proof. □

Specifically, when A is generalized negative definite, γ_s is obtained by an *a priori* calculation, i.e., its value is only determined by the original system $\mathbf{\Sigma}$. Besides, from (5.35), we can see that the proposed clustering algorithm is effective, as Algorithm 2 aims to minimize the maximal within-cluster dissimilarity of each cluster such that the sum term in (5.35) would be smaller. Consequently, the error bound of $\|\eta(s) - \hat{\eta}(s)\|_{\mathcal{H}_2}$ will potentially be lower.

5.4 Approximation of Networked Single-Integrators

In this section, we zoom in on the system of interconnected single-integrators as in (5.5). The approximation error between systems $\mathbf{\Sigma_s}$ and $\hat{\mathbf{\Sigma}}_\mathbf{s}$ is analyzed, and an error bound is established. Here, we denote the transfer functions of the network system $\mathbf{\Sigma}_\mathbf{s}$ in (5.5) and the reduced-order model $\hat{\mathbf{\Sigma}}_\mathbf{s}$ with the states as outputs by

$$\eta(s) = (sM + L)^{-1}F, \tag{5.53}$$

$$\hat{\eta}(s) = P(s\hat{M} + \hat{L})^{-1}\hat{F}, \tag{5.54}$$

respectively, and let $\eta_i(s) = \mathbf{e}_i^T\eta(s)$ and $\hat{\eta}_i(s) = \mathbf{e}_i^T\hat{\eta}(s)$.

Since the network system $\mathbf{\Sigma_s}$ is the special case of system $\mathbf{\Sigma}$ in (5.3) with $A = 0$ and $B = 1$, the following two results directly follows from Theorem 5.1 and Corollary 5.2, respectively.

Corollary 5.3. *Consider network system $\mathbf{\Sigma}_\mathbf{s}$ and its reduced-order model $\hat{\mathbf{\Sigma}}_\mathbf{s}$ resulting from a clustering-based projection. Let $\xi(t) \in \mathbb{R}^{n\times p}$ and $\hat{\xi}(t) \in \mathbb{R}^{n\times p}$ be the impulse responses of x in (5.5) and $\hat{x}$ in (5.8), respectively. We have*

$$\lim_{t\to\infty} \xi(t) = \lim_{t\to\infty} \hat{\xi}(t) = \sigma_M^{-1}\mathbb{1}\mathbb{1}^T F. \tag{5.55}$$

Corollary 5.4. *Consider the transfer functions in (5.53) and (5.54), the following statements holds:*

- *$\|\eta_i(s) - \hat{\eta}_j(s)\|_{\mathcal{H}_2}$ is bounded for any $i, j \in \{1, 2, \cdots, n\}$.*
- *$\|\mathbf{\Sigma_s} - \hat{\mathbf{\Sigma}}_\mathbf{s}\|_{\mathcal{H}_2}$ is bounded.*

Corollary 5.4 guarantees that, by the clustering-based projection, the approximation error between the full-order and reduced-order models is bounded. Specifically, the error bound is given by the following theorem.

Theorem 5.4. *Denote*

$$L_s = M^{-1/2}LM^{-1/2},\ \hat{L}_s = \hat{M}^{-1/2}\hat{L}\hat{M}^{-1/2}. \tag{5.56}$$

Let $\mathcal{L}$ and $\hat{\mathcal{L}}$ be the Moore-Penrose inverses of L_s and $\hat{L}_s$, respectively. Then, the $\mathcal{H}_\infty$ error between $\mathbf{\Sigma_s}$ and $\hat{\mathbf{\Sigma}}_\mathbf{s}$ is bounded as

$$\|\eta(s) - \hat{\eta}(s)\|_{\mathcal{H}_\infty} < \frac{1}{2}\|\mathcal{F}^T \Psi \mathcal{F}\|_2, \tag{5.57}$$

where

$$\Psi = \begin{bmatrix} \mathcal{L} + P\hat{\mathcal{L}}P^T & \mathcal{L} - P\hat{\mathcal{L}}P^T \\ \mathcal{L} - P\hat{\mathcal{L}}P^T & \mathcal{L} + P\hat{\mathcal{L}}P^T \end{bmatrix}, \ \mathcal{F} = \begin{bmatrix} F & \\ & I_n \end{bmatrix}. \tag{5.58}$$

Proof. Since L_s and $\hat{L}_s$ are similar to $M^{-1}L$ and $\hat{M}^{-1}\hat{L}$, respectively, the following spectral decompositions are obtained:

$$L_s = \mathsf{U}\Lambda_o\mathsf{U}^T, \ \ \hat{L}_s = \hat{\mathsf{U}}\Lambda_r\hat{\mathsf{U}}^T, \tag{5.59}$$

where the diagonal entries in Λ_o and Λ_r are also the eigenvalues of $M^{-1}L$ and $\hat{M}^{-1}\hat{L}$, respectively. We the use the following partitioned matrices:

$$\Lambda_o = \begin{bmatrix} 0 & \\ & \bar{\Lambda}_o \end{bmatrix}, \ \ \Lambda_r = \begin{bmatrix} 0 & \\ & \bar{\Lambda}_r \end{bmatrix} \tag{5.60}$$

where $\bar{\Lambda}_o \in \mathbb{R}^{(n-1)\times(n-1)}$ and $\bar{\Lambda}_r \in \mathbb{R}^{(r-1)\times(r-1)}$ are diagonal and positive definite.

$$\mathsf{U} = \begin{bmatrix} \mathsf{u}_1 & \mathsf{U}_2 \end{bmatrix}, \ \ \hat{\mathsf{U}} = \begin{bmatrix} \hat{\mathsf{u}}_1 & \hat{\mathsf{U}}_2 \end{bmatrix}, \tag{5.61}$$

where u_1 and $\hat{\mathsf{u}}_1$ are the eigenvectors corresponding to the zero eigenvalues of L_s and $\hat{L}_s$, respectively. It follows that

$$\mathsf{u}_1 = \frac{M^{1/2}\mathbb{1}_n}{\sqrt{\sigma_M}}, \ \ \hat{\mathsf{u}}_1 = \frac{\hat{M}^{1/2}\mathbb{1}_r}{\sqrt{\sigma_M}} \tag{5.62}$$

and

$$\mathcal{L} = M^{-1/2}\mathsf{U}_2\bar{\Lambda}_o^{-1}\mathsf{U}_2^T M^{-1/2}, \hat{\mathcal{L}} = \hat{M}^{-1/2}\hat{\mathsf{U}}_2\bar{\Lambda}_r^{-1}\hat{\mathsf{U}}_2^T\hat{M}^{-1/2}. \tag{5.63}$$

To study the approximation error, we consider the error system $\mathbf{\Sigma_e} := \mathbf{\Sigma_s} - \hat{\mathbf{\Sigma}}_\mathbf{s}$ whose state is given by $\omega^T = \begin{bmatrix} x^T, z^T \end{bmatrix} \in \mathbb{R}^{n+r}$, where x and z are the states of $\mathbf{\Sigma_s}$ and $\hat{\mathbf{\Sigma}}_\mathbf{s}$, respectively. Then, the state-space representation of $\mathbf{\Sigma_e}$ is formalized as

$$\mathbf{\Sigma_e} : \begin{cases} \dot{\omega} = \mathcal{A}_\mathsf{e}\omega + \mathcal{B}_\mathsf{e}u, \\ \psi = \mathcal{C}_\mathsf{e}\omega, \end{cases} \tag{5.64}$$

with

$$\mathcal{A}_\mathsf{e} = -\begin{bmatrix} M^{-1}L & 0 \\ 0 & \hat{M}^{-1}\hat{L} \end{bmatrix}, \mathcal{B}_\mathsf{e} = \begin{bmatrix} M^{-1}F \\ \hat{M}^{-1}\hat{F} \end{bmatrix}, \mathcal{C}_\mathsf{e} = \begin{bmatrix} I_n & -P \end{bmatrix}.$$

Applying the transform

$$\omega = \text{diag}\left(M^{-1/2}\mathsf{U}, \hat{M}^{-1/2}\hat{\mathsf{U}}\right) \cdot \tilde{\omega} \tag{5.65}$$

to the error system $\mathbf{\Sigma}_\mathsf{e}$ leads to

$$\mathbf{\Sigma}_\mathsf{e}: \begin{cases} \dot{\tilde{\omega}} = -\begin{bmatrix} 0 & & \\ & \bar{\Lambda}_o & \\ & & 0 \\ & & & \bar{\Lambda}_r \end{bmatrix} \tilde{\omega} + \begin{bmatrix} \mathsf{u}_1^T M^{-1/2} F \\ \mathsf{U}_2^T M^{-1/2} F \\ \hat{\mathsf{u}}_1^T \hat{M}^{-1/2} \hat{F} \\ \hat{\mathsf{U}}_2 \hat{M}^{-1/2} \hat{F} \end{bmatrix} u, \\ \psi = \begin{bmatrix} M^{-1/2}\mathsf{u}_1 & M^{-1/2}\mathsf{U}_2 \\ & -P\hat{M}^{-1/2}\hat{\mathsf{u}}_1 & -P\hat{M}^{-1/2}\hat{\mathsf{U}}_2 \end{bmatrix} \tilde{\omega}. \end{cases}$$

From Corollary 5.3, we have

$$\begin{aligned} &M^{-1/2}\mathsf{u}_1\mathsf{u}_1^T M^{-1/2} F - P\hat{M}^{-1/2}\hat{\mathsf{u}}_1\hat{\mathsf{u}}_1^T \hat{M}^{-1/2}\hat{F} \\ &= \sigma_M^{-1}\mathbb{1}_n\mathbb{1}_n^T F - \sigma_M^{-1} P\mathbb{1}_r\mathbb{1}_r^T P^T F = 0. \end{aligned} \tag{5.66}$$

Therefore, it is not hard to obtain that the following stable system

$$\bar{\mathbf{\Sigma}}_\mathsf{e}: \begin{cases} \dot{\bar{\omega}} = -\begin{bmatrix} \bar{\Lambda}_o & \\ & \bar{\Lambda}_r \end{bmatrix} \bar{\omega} + \begin{bmatrix} \mathsf{U}_2^T M^{-1/2} F \\ \hat{\mathsf{U}}_2^T \hat{M}^{-1/2} \hat{F} \end{bmatrix} u, \\ \psi = \begin{bmatrix} M^{-1/2}\mathsf{U}_2 & -P\hat{M}^{-1/2}\hat{\mathsf{U}}_2 \end{bmatrix} \bar{\omega}. \end{cases} \tag{5.67}$$

has the identical input-output relation as the system $\mathbf{\Sigma}_\mathsf{e}$, since they share the same transfer function. Consequently, we have

$$\|\eta(s) - \hat{\eta}(s)\|_{\mathcal{H}_\infty}^2 = \|\bar{\mathbf{\Sigma}}_\mathsf{e}\|_{\mathcal{H}_\infty}. \tag{5.68}$$

Denote

$$\tilde{\Lambda} = \begin{bmatrix} \bar{\Lambda}_o & \\ & \bar{\Lambda}_r \end{bmatrix}, \tilde{B} = \begin{bmatrix} \mathsf{U}_2^T M^{-1/2} F \\ \hat{\mathsf{U}}_2^T \hat{M}^{-1/2} \hat{F} \end{bmatrix}, \tilde{C} = \begin{bmatrix} M^{-1/2}\mathsf{U}_2 & -P\hat{M}^{-1/2}\hat{\mathsf{U}}_2 \end{bmatrix}. \tag{5.69}$$

We then apply Lemma 2.5 to $\bar{\mathbf{\Sigma}}_\mathsf{e}$. If the inequality in (2.16) is satisfied with $S = I$, i.e.,

$$\begin{bmatrix} -2\tilde{\Lambda} & \tilde{B} & \tilde{C}^T \\ \tilde{B}^T & -\gamma_0 I & 0 \\ \tilde{C} & 0 & -\gamma_0 I \end{bmatrix} \prec 0, \tag{5.70}$$

the system $\bar{\mathbf{\Sigma}}_{\mathsf{e}}$ has $\mathcal{H}_\infty$-norm less than γ_0. The above inequality is equivalent to

$$\begin{aligned}\gamma_0 I \succ & \frac{1}{2}\begin{bmatrix}\tilde{B}^T\\ \tilde{C}\end{bmatrix}\tilde{\Lambda}^{-1}\begin{bmatrix}\tilde{B} & \tilde{C}^T\end{bmatrix}\\ &= \frac{1}{2}\begin{bmatrix}F^T(\mathcal{L}+P\hat{\mathcal{L}}P^T)F & F^T(\mathcal{L}-P\hat{\mathcal{L}}P^T)\\ (\mathcal{L}-P\hat{\mathcal{L}}P^T)F & \mathcal{L}+P\hat{\mathcal{L}}P^T\end{bmatrix} := \frac{1}{2}\mathcal{F}^T\Psi\mathcal{F}.\end{aligned} \tag{5.71}$$

This then leads to equation (5.57). □

Moreover, when only two nodes are clustered and aggregated, the $\mathcal{H}_\infty$-norm bounds of the approximation error for the individual nodes are characterized by the following theorem.

Theorem 5.5. *Consider an n-th dimensional network system $\mathbf{\Sigma}_{\mathsf{s}}$ and its $(n-1)$-th dimensional simplified model $\hat{\mathbf{\Sigma}}_{\mathsf{s}}$ resulting from clustering vertices μ and ν. Denote $\delta_\eta := \eta_\mu(s) - \eta_\nu(s)$. Then, the approximation error of each vertex is bounded as*

$$\|\eta_i(s) - \hat{\eta}_i(s)\|_{\mathcal{H}_\infty} \le \frac{\rho\sqrt{n-2}}{m_i}\|\delta_\eta\|_{\mathcal{H}_\infty}, \text{ for all } i \ne \mu,\nu, \tag{5.72a}$$

$$\|\eta_\mu(s) - \hat{\eta}_\mu(s)\|_{\mathcal{H}_\infty} \le \frac{m_\nu + \sum_{i=1,i\ne\mu,\nu}^{n} m_i}{m_\mu + m_\nu}\|\delta_\eta\|_{\mathcal{H}_\infty}, \tag{5.72b}$$

$$\|\eta_\nu(s) - \hat{\eta}_\nu(s)\|_{\mathcal{H}_\infty} \le \frac{m_\mu + \sum_{i=1,i\ne\mu,\nu}^{n} m_i}{m_\mu + m_\nu}\|\delta_\eta\|_{\mathcal{H}_\infty}. \tag{5.72c}$$

In the first inequality,

$$\rho := \left\| \left[\bar{M} + (m_\mu + m_\nu)^{-1}\mathbb{1}\mathbb{1}^T\right]^{-1}\right\|_2,$$

where $\bar{M}$ is a square submatrix obtained by removing the μ and ν rows and columns of M .

Proof. Without loss of generality, we suppose the vertex $n-1$ and n of the original system $\mathbf{\Sigma}_{\mathsf{s}}$ are aggregated. Besides, we denote $\delta\eta := \eta_{n-1}(s) - \eta_n(s) \in \mathbb{R}(s)^{1\times p}$ and

$$\begin{aligned}\Delta\eta_a &= \begin{bmatrix}\eta_1(s) - \hat{\eta}_1(s)\\ \eta_2(s) - \hat{\eta}_2(s)\\ \vdots\\ \eta_{n-2}(s) - \hat{\eta}_{n-2}(s)\end{bmatrix},\\ \Delta\eta_b &= \eta_{n-1}(s) - \hat{\eta}_{n-1}(s),\\ \Delta\eta_c &= \eta_n(s) - \hat{\eta}_n(s).\end{aligned} \tag{5.73}$$

In this case, the cluster matrix $P \in \mathbb{R}^{n\times(n-1)}$ is given by

$$P = \begin{bmatrix} I_{n-2} & 0 \\ 0 & \mathbb{1}_2 \end{bmatrix}. \tag{5.74}$$

Furthermore, we partition L and M as

$$L = \begin{bmatrix} L_{11} & L_{12} \\ L_{12}^T & L_{22} \end{bmatrix}, M = \begin{bmatrix} M_{11} & 0 \\ 0 & M_{22} \end{bmatrix}, \tag{5.75}$$

where $L_{11}, M_{11} \in \mathbb{R}^{(n-2)\times(n-2)}$, $M_{22} = \mathsf{diag}[m_{n-1}, m_n]$. $L_{12} \in \mathbb{R}^{(n-2)\times 2}$ can be presented by $L_{12} = [-\ell_1, -\ell_2]$ with ℓ_1 and ℓ_2 being nonnegative vectors. For simplicity, we denote $\tilde{m} = m_{n-1} + m_n$.

Recall the expressions of transfer functions in (5.53), we have

$$(sM + L)\begin{bmatrix} \eta_1(s) \\ \vdots \\ \eta_n(s) \end{bmatrix} = B, \tag{5.76}$$

$$(s\hat{M} + \hat{L})\begin{bmatrix} \hat{\eta}_1(s) \\ \vdots \\ \hat{\eta}_{n-1}(s) \end{bmatrix} = \hat{B}. \tag{5.77}$$

Reshuffling (5.76), we obtain

$$(sM + L)P\begin{bmatrix} \eta_1(s) \\ \vdots \\ \eta_{n-1}(s) \end{bmatrix} = B + \begin{bmatrix} -\ell_2 \\ sm_n + \mathbb{1}^T\ell_2 \end{bmatrix}\delta\eta, \tag{5.78}$$

Multiplying P^T from left to (5.78) yields

$$(s\hat{M} + \hat{L})\begin{bmatrix} \eta_1(s) \\ \vdots \\ \eta_{n-1}(s) \end{bmatrix} = \hat{B} + \begin{bmatrix} -\ell_2 \\ sm_n + \mathbb{1}^T\ell_2 \end{bmatrix}\delta\eta. \tag{5.79}$$

Then, we subtract (5.79) from (5.77) and obtain

$$(s\hat{M} + \hat{L})\begin{bmatrix} \Delta\eta_a \\ \Delta\eta_b \end{bmatrix} = \begin{bmatrix} -\ell_2 \\ sm_n + \mathbb{1}^T\ell_2 \end{bmatrix}\delta\eta. \tag{5.80}$$

Furthermore, with $L\mathbb{1} = 0$, we have

$$s\hat{M} + \hat{L} = \begin{bmatrix} sM_{11} + L_{11} & -L_{11}\mathbb{1} \\ -\mathbb{1}^T L_{11} & s\tilde{m} + \mathbb{1}^T L_{11}\mathbb{1} \end{bmatrix}. \tag{5.81}$$

Pre-multiplying (5.80) by

$$T = \begin{bmatrix} I_{n-2} & 0 \\ \mathbb{1}^T & 1 \end{bmatrix}. \tag{5.82}$$

further gives the following equation

$$\begin{bmatrix} sM_{11} + L_{11} & -L_{11}\mathbb{1} \\ \mathbb{1}^T M_{11} & \tilde{m} \end{bmatrix} \begin{bmatrix} \Delta\eta_a \\ \Delta\eta_b \end{bmatrix} = \begin{bmatrix} -\ell_2 \\ m_n \end{bmatrix} \delta\eta \tag{5.83}$$

By solving the above equation, the error expressions of $\Delta\eta_a$ and $\Delta\eta_b$ are respectively given by

$$\Delta\eta_a = K_a(s)\delta\eta, \text{ and } \Delta\eta_b = K_b(s)\delta\eta \tag{5.84}$$

with

$$K_a(s) = M_{11}^{-1}\left[sL_{11}^{-1} + \tilde{M}\right]^{-1}\left(\frac{m_n}{\tilde{m}}\mathbb{1} - L_{11}^{-1}\ell_2\right), \tag{5.85}$$

$$K_b(s) = \frac{m_n + \mathbb{1}^T M_{11}(sM_{11} + L_{11})^{-1}\ell_2}{\tilde{m} + \mathbb{1}^T M_{11}(sM_{11} + L_{11})^{-1}L_{11}\mathbb{1}}. \tag{5.86}$$

Here, $\tilde{M} = M_{11}^{-1} + \tilde{m}^{-1}\mathbb{1}\mathbb{1}^T$.

Moreover, since $\hat{\eta}_n = \hat{\eta}_{n-1}$, we have

$$\Delta\eta_b - \Delta\eta_c = \delta\eta. \tag{5.87}$$

Also note that $L_{11}\mathbb{1} = \ell_1 + \ell_2$. As result, we can obtain $\Delta\eta_c = K_c(s)\delta\eta$ with

$$K_c(s) = -\frac{m_{n-1} + \mathbb{1}^T M_{11}(sM_{11} + L_{11})^{-1}\ell_1}{\tilde{m} + \mathbb{1}^T M_{11}(sM_{11} + L_{11})^{-1}L_{11}\mathbb{1}}. \tag{5.88}$$

Next, based on the derived error formulas, we further investigate the error bounds.

Denote $\Omega(s) = \left[sL_{11}^{-1} + \tilde{M}\right]^{-1}$, then we have for $1 \le i \le n-2$,

$$\Delta\eta_i = \mathbf{e}_i^T K_a(s)\delta_\eta = \mathbf{e}_i^T M_{11}^{-1}\Omega(s)\left(\frac{m_n}{\tilde{m}}\mathbb{1} - L_{11}^{-1}\ell_2\right)\delta_\eta. \tag{5.89}$$

Consequently,

$$\begin{aligned} \|\Delta\eta_i\| &\le \|\mathbf{e}_i^T M_{11}^{-1}\| \cdot \|\Omega(s)\| \cdot \|\frac{m_n}{\tilde{m}}\mathbb{1} - L_{11}^{-1}\ell_2\| \cdot \|\delta_\eta\| \\ &= m_i^{-1} \cdot \|\Omega(s)\| \cdot \|\frac{m_n}{\tilde{m}}\mathbb{1} - L_{11}^{-1}\ell_2\| \cdot \|\delta_\eta\|. \end{aligned} \tag{5.90}$$

First, as $\Omega(s)$ can be regarded as a state-space symmetric descriptor system with identity input and output matrices, by Lemma 2.8, its $\mathcal{H}_\infty$ norm is

$$\|\Omega(s)\| = \lambda_m(\tilde{M})^{-1} := \rho. \tag{5.91}$$

Then, equation $L_{11}\mathbb{1} = \ell_1 + \ell_2$ leads to

$$\frac{m_n}{\tilde{m}}\mathbb{1} - L_{11}^{-1}\ell_2 = \frac{m_n}{\tilde{m}}(L_{11}^{-1}\ell_1 + L_{11}^{-1}\ell_2) - L_{11}^{-1}\ell_2 = L_{11}^{-1}(\frac{m_n}{\tilde{m}}\ell_1 - \frac{m_{n-1}}{\tilde{m}}\ell_2). \quad (5.92)$$

Note that L_{11} is a M-matrix, therefore, L_{11}^{-1} is a nonnegative matrix by Lemma 2.3. Besides, since $L_{11}\mathbb{1} = \ell_1 + \ell_2$ and ℓ_1, ℓ_2 are vectors with real nonnegative elements, we can guarantee that both $L_{11}^{-1}\ell_1$ and $L_{11}^{-1}\ell_2$ not greater than $L_{11}^{-1}L_{11}\mathbb{1} = \mathbb{1}$ entry-wise. Then, from (5.92),

$$\|\frac{m_n}{\tilde{m}}\mathbb{1} - L_{11}^{-1}\ell_2\| \leq \frac{m_n}{\tilde{m}}\|L_{11}^{-1}\ell_1\| + \frac{m_{n-1}}{\tilde{m}}\|L_{11}^{-1}\ell_2\| \leq \|\mathbb{1}\| = \sqrt{n-2}. \quad (5.93)$$

Finally, by (5.90), (5.91) and (5.93), we have the bound for $\Delta\eta_i$. After replacing $n-1$ and n by μ and ν respectively, it is equivalent to (5.72a) .

Next, we find the $\mathcal{H}_\infty$ bound for $K_b(s)$ in (5.86). Note that $K_b(s)$ is in the form of a quotient of two SISO transfer functions, i.e.,

$$K_b(s) := \frac{G_n(s)}{G_d(s)}, \quad (5.94)$$

where

$$G_d(s) = \mathbb{1}^T(sI + L_{11}M_{11}^{-1})^{-1}L_{11}\mathbb{1} + \tilde{m}, \quad (5.95a)$$
$$G_n(s) = \mathbb{1}^T(sI + L_{11}M_{11}^{-1})^{-1}(-\ell_2) + m_n. \quad (5.95b)$$

The state-space representation of $G_d(s)$ is

$$\begin{aligned}\dot{x} &= -(L_{11}M_{11}^{-1})x + (L_{11}\mathbb{1})u,\\ y &= \mathbb{1}^T x + \tilde{m}u.\end{aligned}$$

With $\tilde{m} \neq 0$, we have

$$\begin{aligned}\dot{x} &= -(L_{11}M_{11}^{-1})x + (L_{11}\mathbb{1})\left(-\tilde{m}^{-1}\mathbb{1}^T x + \tilde{m}^{-1}y\right),\\ u &= -\tilde{m}^{-1}\mathbb{1}^T x + \tilde{m}^{-1}y,\end{aligned}$$

which leads to the inverse transfer function as

$$G_d(s)^{-1} = -\tilde{m}^{-2}\mathbb{1}^T\left[sL_{11}^{-1} + \tilde{M}\right]^{-1}\mathbb{1} + \tilde{m}^{-1}. \quad (5.96)$$

Observe that $G_0(s)^{-1}$ is a state-space symmetric descriptor system and Note that

$$|G_d(0)^{-1}| = |G_d(0)|^{-1} = \frac{1}{\mathbb{1}^T M_{11}\mathbb{1} + \tilde{m}} < \tilde{m}^{-1}. \quad (5.97)$$

Thus, by Lemma 2.8,

$$\|G_d^{-1}(s)\| = \tilde{m}^{-1}. \tag{5.98}$$

On the other hand, $G_n(s)$ is a internally positive system by Definition 2.10, then Lemma 2.7 yields $\|G_n(s)\| = m_n + \mathbb{1}^T M_{11}(-L_{11}^{-1}\ell_2) \leq m_n + \mathbb{1}^T M_{11}\mathbb{1}$. Therefore,

$$\|K_b(s)\| \leq \|G_n(s)\| \cdot \|G_d^{-1}(s)\| = \frac{m_n + \sum_{i=1}^{n-2} m_i}{\tilde{m}}, \tag{5.99}$$

which leads to the error bound in (5.72b).

Similarly, we can obtain the bound for $\Delta\eta_c$ as in (5.72c). □

The dynamics of a cluster is captured by $\hat{\eta}_i(s)$, which is used to approximate the dynamics of all the vertices in this cluster. Theorem 5.5 indicates that this approximation error is bounded by the dissimilarity of the aggregated vertices. Based on Theorem 5.5, we have the following corollary directly.

Corollary 5.5. *If the reduced-order model $\hat{\mathbf{\Sigma}}_\mathbf{s}$ is derived from aggregating two 0-dissimilar vertices in the full-order system $\mathbf{\Sigma}_\mathbf{s}$, then $\|\mathbf{\Sigma}_\mathbf{s} - \hat{\mathbf{\Sigma}}_\mathbf{s}\|_{\mathcal{H}_2} = 0$.*

5.5 Numerical Examples

5.5.1 Path Network

To illustrate the feasibility of our method proposed in Section 5.3, we use the example in [21] for comparison. The thermal model of interconnected rooms in a building is considered, where the network is described by a path graph with 6 nodes, see Fig. 5.2a, and each room is an agent as in (5.1) with

$$\begin{aligned} A &= R_i^{-1}\begin{bmatrix} C_1^{-1} & C_1^{-1} \\ C_2^{-1} & C_2^{-1} \end{bmatrix} + R_o^{-1}\begin{bmatrix} C_1^{-1} & 0 \\ 0 & 0 \end{bmatrix} \in \mathbb{R}^{2\times 2}, \\ B &= \begin{bmatrix} C_1^{-1} & 0 \end{bmatrix}^T,\ C = \begin{bmatrix} 1 & 0 \end{bmatrix}. \end{aligned} \tag{5.100}$$

The meaning of the parameters can be found in [21], which provides their values as $C_1 = 4.35 \cdot 10^4$, $C_2 = 9.24 \cdot 10^6$, $R_i = 2.0 \cdot 10^{-3}$, and $R_o = 2.3 \cdot 10^{-2}$. Moreover, the inertia and Laplacian matrices are given by

$$M = I_6, L = R_w^{-1}\begin{bmatrix} 1 & -1 & 0 & 0 & 0 & 0 \\ -1 & 2 & -1 & 0 & 0 & 0 \\ 0 & -1 & 2 & -1 & 0 & 0 \\ 0 & 0 & -1 & 2 & -1 & 0 \\ 0 & 0 & 0 & -1 & 2 & -1 \\ 0 & 0 & 0 & 0 & -1 & 1 \end{bmatrix}, \tag{5.101}$$

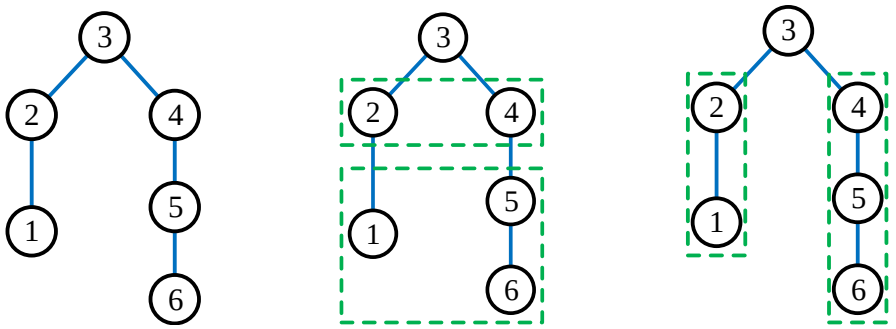

Figure 5.2: The clustering of a network that is composed of 6 interconnected rooms. (a) The cluster selection generated by Algorithm 2. (b) The clustering result in [21] and modified Algorithm 2 in Remark 5.2.

where $R_w = 1.6 \cdot 10^{-2}$ represents the nominal thermal resistance between two adjacent rooms. The input matrix $F = \begin{bmatrix} \mathbf{e}_3 & R_o^{-1}\mathbb{1}_6 \end{bmatrix}$ indicates the distribution of external inputs.

By Theorem 5.2, the dissimilarity matrix is computed as $\mathcal{D} =$

$$\begin{bmatrix} 0 & 0.0095 & 0.1332 & 0.0094 & 0.0011 & 0.0028 \\ 0.0095 & 0 & 0.1268 & 0.0004 & 0.0099 & 0.0114 \\ 0.1332 & 0.1268 & 0 & 0.1268 & 0.1332 & 0.1337 \\ 0.0094 & 0.0004 & 0.1268 & 0 & 0.0098 & 0.0112 \\ 0.0011 & 0.0099 & 0.1332 & 0.0098 & 0 & 0.0019 \\ 0.0028 & 0.0114 & 0.1337 & 0.0112 & 0.0019 & 0 \end{bmatrix} \cdot 10^{-3}$$

Then, Algorithm 2 generate a graph clustering: $\{\{1,5,6\},\{2,4\},\{3\}\}$, see Fig. 5.2b, which is different from the result in [21], see Fig. 5.2c. Taking the output of the third agent as the external output of the whole system, we calculate the approximation error as $\|\boldsymbol{\Sigma} - \hat{\boldsymbol{\Sigma}}\|_{\mathcal{H}_\infty} = 9.4171 \cdot 10^{-5}$, while it is $8.4663 \cdot 10^{-4}$ in [21]. Thus, our method produces a more accurate approximation of the network system. Next, using Remark 5.2, we adapt Algorithm 2 to only cluster adjacent agents. It then yields an identical clustering result as in [21].

5.5.2 Small-World Network

Next, the efficiency of the proposed approach is verified by a large-scale small-world network example. This simulation is implemented with Matlab 2016a in the

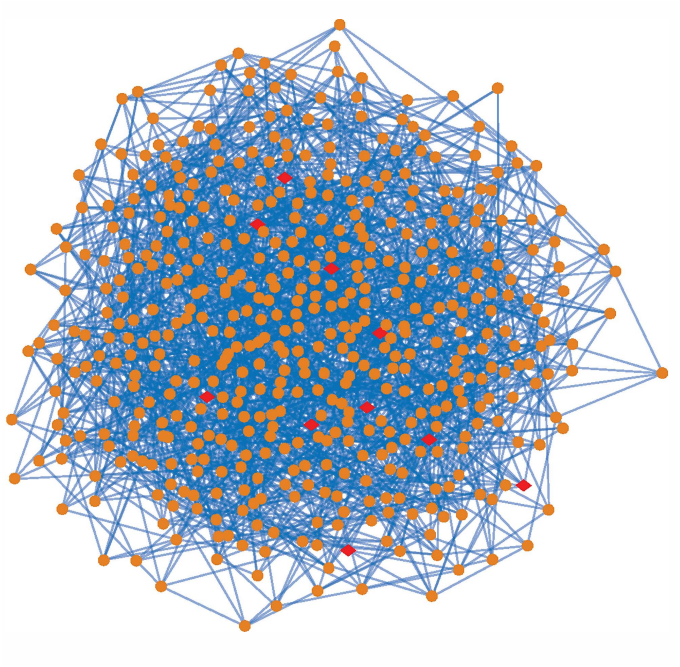

Figure 5.3: Watts-Strogatz network with 500 nodes and 2000 edges

environment of 64-bit operating system, which is equipped with Intel Core i5-3470 CPU @ 3.20GHz, RAM 8.00 GB.

The agents are oscillators with coefficients

$$A = \begin{bmatrix} 0 & 1 \\ -1 & 1 \end{bmatrix}, B = C = I_2. \tag{5.102}$$

The Laplacian matrix L representing the underlying network is created by the Watts-Strogatz model [173], which is a random graph generator producing graphs with small-world properties. In this example, the original network contains 500 nodes and 2000 edges, as shown in Fig. 5.3. In (5.3), the diagonal entries of the inertia matrix M are chosen randomly from the range 1 to 10, and $F \in \mathbb{R}^{500\times 10}$ is a binary matrix, whose (i, j) entry is 1 if the the j-th input affects the i-th node, and 0 otherwise. Here, we randomly assign 10 nodes to be controlled. In Fig. 5.3, the controlled nodes are labeled by diamond markers.

In the simulation, the original multi-agent system has a dimension of 1000, and we use Algorithm 2 to reduce the number of agents to 5. The approximation errors of the reduced models with different dimensions are shown in Fig. 5.5, which compares the

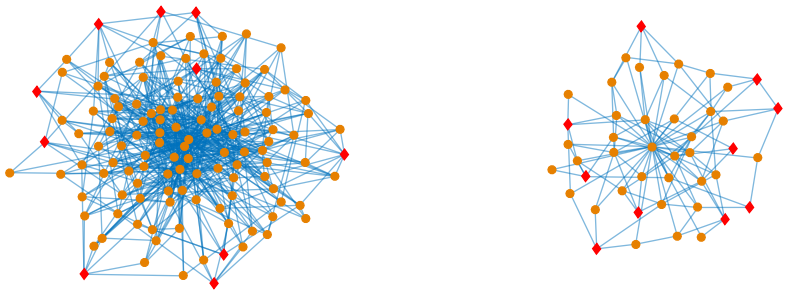

Figure 5.4: Reduced Watts-Strogatz networks with 125 clusters (left) and 45 clusters (right)

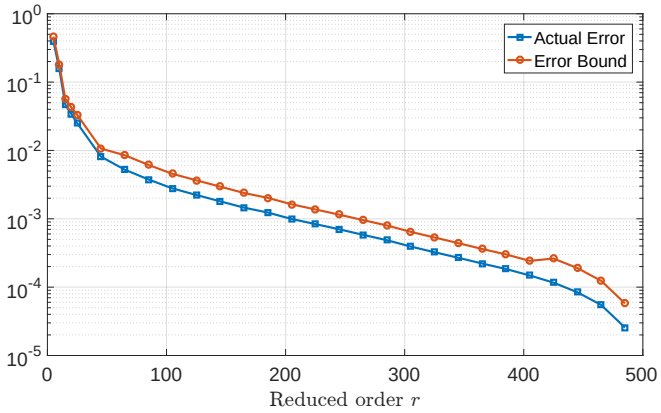

Figure 5.5: Approximation error versus reduced order r

actual approximation errors and the associated bounds in terms of $\mathcal{H}_2$-norms. From Fig. 5.5, the exact errors and the error bounds of $\|\mathbf{\Sigma} - \hat{\mathbf{\Sigma}}\|_{\mathcal{H}_2}$ show negative relations with the reduced dimension r. In particular, when $r < 40$, the approximation errors rapidly decrease as r increases. Table 5.1 list the actual approximation errors and the error bounds at different reduced order r. The reduced networks with 125 nodes and 45 nodes are shown in Fig. 5.4. The time for computation of the dissimilarity matrix is approximately 85 seconds, while it only takes 0.004s, on average, for Algorithm 2 to find a suitable clustering.

In conclusion, this simulation example demonstrates that hierarchical clustering algorithm is feasible and effective in model reduction of large-scale multi-agent systems.

Table 5.1: The exact approximation errors and the error bounds

Clusters	Actual Error	Error Bound	γ_s
$r = 45$	0.0081	0.107	1.3223
$r = 125$	0.0022	0.0037	1.6348
$r = 225$	$8.4 \cdot 10^{-4}$	$13.7 \cdot 10^{-4}$	1.6348
$r = 425$	$1.2 \cdot 10^{-4}$	$2.6 \cdot 10^{-4}$	2.2598

5.6 Conclusions

In this chapter, we propose a general framework of structure preserving model reduction for multi-agent systems. The proposed method builds a connection to the conventional data clustering. The pairwise Euclidean distance in statistical clustering is generalized to the behavior dissimilarity in our framework, which is measured by the norm of transfer function variance. Based on the dissimilarity matrix, which is known as distance matrix in statistical analysis, we are able to adapt the well-developed algorithms for the statistical clustering to solve the model reduction problem. Therefore, the proposed method is a novel extension and generalization of the conventional clustering analysis. Moreover, to generate an appropriate graph clustering, an efficient clustering algorithm is proposed, which can be also easily adapted to only aggregate adjacent agents.

Note that the results presented in Chapter 3, Chapter 4, and Chapter 5 are considering systems evolving over undirected networks. In the next chapter, we discuss the clustering-based model reduction of directed networks.

CHAPTER 6

Clustering-Based Model Reduction of Directed Dynamical Networks

This chapter investigates a model reduction problem for linear directed network systems, in which the interconnections among the vertices are described by general weakly connected digraphs. We introduce a concept of vertex clusterability to guarantee the boundedness of the approximation error and use the newly proposed Gramians to facilitate the evaluation of the dissimilarity of each pair of vertices. A clustering algorithm is thereto provided to generate an appropriate graph clustering, whose characteristic matrix is employed as the projections in the Petrov-Galerkin reduction framework. The obtained reduced-order system preserves the weakly connected directed network structure, and the approximation error is computed by the pseudo Gramians. Finally, the efficiency of the proposed approach is illustrated by numerical examples.

6.1 Introduction

We extend the results in the above chapters to a more general case that the vertices in a network are connected by directed edges. The extension is not straightforward since the clustering of directed networks and projection matrices have to be carefully chosen in order to guarantee the boundedness of the approximation error. For undirected networks, any graph clustering can result in a bounded approximation error, however, this conclusion does not hold in the directed case. Moreover, directed

networks have more applications, which appear in e.g., social and ecological interactions, chemical reactions and physical networks, see e.g. [12, 27, 79, 88, 130, 163] for an overview.

A pioneering model reduction approach dealing with semistable directed networks is proposed in [84]. The graph clustering is formed based on a notion of cluster reducibility, characterized by the uncontrollability of local states. Merging the vertices in the reducible clusters then yields a reduced-order model that preserves the structural information of a directed network. In this method, the studied network essentially has a strongly connected topology, since a positive *Frobenius eigenvector* of the system matrix is needed for the projection. An alternative approach in [41] focuses on the behavior of individual vertices described by transfer functions and pairwise dissimilarities evaluated by function norms. The vertices behaving similarly are sequentially assimilated to a single vertex. This approach is preferable for a consensus network and applicable to a strongly connected topology. In broader applications of dynamical networks, for instance, biochemical systems, sensor coordination, gene regulation, weakly connected spatial structures commonly appear in the networks, see e.g., [3, 120, 159, 163].

This motivates us to consider weakly connected directed networks. As undirected networks and strongly connected networks are only subcategories of weakly connected ones, the systems studied in this chapter describe more general scenarios, and the proposed method can be also applied to the former two cases. It is worth noting that a model reduction problem of weakly connected directed networks has been absent from the literature so far. The major difficulty for such networks is an appropriate clustering selection scheme. The approximation accuracy heavily relies on the resulting graph clustering, whereas finding an optimal clustered network is roughly an NP-hard problem even for static networks [2, 94]. More importantly, in [41, 84], projections are generated using the positive Frobenius eigenvectors of the system matrix. However, such vectors may not exist in the weakly connected case. Furthermore, a weakly connected network may not reach a global consensus as strongly connected ones do. Instead, a local consensus is achievable among the vertices that are able to influence each other. Consequently, the clustering for a weakly connected graph has to be prudently selected to avoid an unbounded approximation error.

To tackle the above difficulties, this chapter introduces a definition of vertex clusterability for weakly connected networks and shows that the boundedness of the approximation error is guaranteed if and only if clusterable vertices are aggregated. Thereby, the concept of dissimilarity is defined only for clusterable vertices. In contrast to [34, 41], the input and output dissimilarities are considered based on the responses of the vertex states to the external inputs and the measurement of the state

discrepancy from the output channels, respectively. Thus, the pairwise dissimilarities are evaluated by combining the input and output efforts. Then, according to the vertex clusterability and dissimilarity, a graph cut algorithm is designed to partition the underlying network into a desired number of clusters. Then, a clustering-based projection is employed to reduce the dimension of the original network system, where the projection matrix is generated from the left kernel space of the system matrix. The proposed method yields a reduced-order model that preserves not only the structure and connectedness of directed network but several fundamental properties, including consensus, semistability, and asymptotic behaviors of the vertex.

The rest of this chapter is organized as follows: Section 6.2 presents the model of directed networks, and the Petrov-Galerkin reduction framework is established based on graph clustering. Then, in Section 6.3 we define the vertex clusterability and dissimilarity, and propose a scheme for model reduction of directed networks. The proposed method is illustrated through an example in Section 6.4, and finally, concluding remarks are made in Section 6.5.

6.2 Directed Network Systems and Graph Clustering

In this chapter, the interactions among the vertices are described by a directed graph. The network model is first introduced in the form of Laplacian dynamics. Based on graph clustering, a projection framework for network structure-preserving model reduction is presented.

6.2.1 Directed Network Systems

A directed network system describes the dynamics evolving over a digraph $\mathcal{G}$. Let $x_i(t) \in \mathbb{R}$ be the state of a vertex i, which is diffusively coupled with the other vertices as

$$\dot{x}_i(t) = -\sum_{j=1, j\neq i}^{n} w_{ij}\left[x_i(t) - x_j(t)\right] + \sum_{k=1}^{p} f_{ik}u_k(t), \tag{6.1}$$

where $w_{ij} \in \mathbb{R}_+$ and $f_{ij} \in \mathbb{R}$ represent the weight of the edge a_{ij} and the amplification of the input $u_k \in \mathbb{R}$ acting on the vertex i, respectively. Then, we describe the dynamics of all the vertices on a directed consensus network by the following linear time-invariant system

$$\mathbf{\Sigma}: \begin{cases} \dot{x}(t) = -\mathcal{L}x(t) + Fu(t), \\ y(t) = Hx(t), \end{cases} \tag{6.2}$$

where $x(t) \in \mathbb{R}^n$ is the collection of the vertex states. The vectors $u \in \mathbb{R}^p$ and $y \in \mathbb{R}^q$ are the external control flows and measurements. The input and output matrices F and H then represent the distributions of the external inflows and outflows, respectively. The Laplacian matrix $\mathcal{L}$ is associated with a *weakly connected weighted* digraph $\mathcal{G}$, which reflects the diffusive coupling among the vertices of $\mathcal{G}$. We refer to Lemma 2.2 for the structural property of $\mathcal{L}$. Throughout the chapter, we suppose the digraph $\mathcal{G}$ contains n_d SCCs, $\{\mathcal{S}_1, \ldots, \mathcal{S}_{n_d}\}$, such that $\mathcal{S}_i \cap \mathcal{S}_j = \varnothing$, for any i, j, and $\cup_{j=1,\cdots,n_d} \mathcal{S}_i = \mathbb{V}$. Moreover, the set $\mathbb{S}_L \subseteq \mathbb{V}$ collects all the vertices in the LSCCs of $\mathcal{G}$, and $\mathcal{S}_i \subseteq \mathbb{S}_L$ if $\mathcal{S}_i$ is a LSCC of $\mathcal{G}$.

A typical example of (6.2) is a chemical reaction network, (see e.g., [3, 73, 120]), where chemical species are the vertex states $x_i(t)$. The directed edges represent a series of chemical reactions converting source species to target species, and the edge weights are the rate constants of the corresponding reactions.

Remark 6.1. *The network system $\mathbf{\Sigma}$ is semistable due to the Laplacian matrix $\mathcal{L}$, which is singular and reducible (i.e., $\mathcal{L}$ is similar via a permutation to a block upper triangular matrix). Furthermore, by Geršgorin's circle theorem (see, e.g., [95]), the real part of each nonzero eigenvalue of $\mathcal{L}$ is strictly positive.*

A strongly connected digraph is called *balanced* if the indegree and outdegree of each node are equal [67, 176]. In e.g. the mass action kinetics chemical reaction networks [81, 91], the balancing of a directed network is necessary to preclude sustained oscillations, multi-stability or other types of exotic dynamic behavior. This chapter extends the definition of balanced digraphs to the weakly connected case.

Definition 6.1. *A weakly connected digraph $\mathcal{G}$ is **generalized balanced** if each LSCC is balanced, i.e., $\sum_{j\in\mathcal{S}_k} w_{ij} = \sum_{j\in\mathcal{S}_k} w_{ji}$, $\forall i \in \mathcal{S}_k \subseteq \mathbb{S}_L$.*

The following lemma then shows that any directed network system in (6.2) can be converted to its generalized balanced form.

Lemma 6.1. *Consider a directed graph Laplacian matrix $\mathcal{L}$. There always exists positive diagonal matrix $M \in \mathbb{R}^{n\times n}$ such that $L := M\mathcal{L}$ is a Laplacian matrix associating with a generalized balanced digraph.*

Proof. A reducible Laplacian matrix $\mathcal{L}$ is permutation-similar to a block upper triangular matrix. Thus, there exists a permutation matrix $\mathcal{T}_\mu$ such that

$$\mathcal{L} = \mathcal{T}_\mu \cdot \begin{bmatrix} \mathcal{L}_{l1} & \cdots & 0 & 0 \\ \vdots & \ddots & \vdots & \vdots \\ 0 & \cdots & \mathcal{L}_{lm} & 0 \\ * & \cdots & * & \mathcal{L}_r \end{bmatrix} \mathcal{T}_\mu^T, \tag{6.3}$$

where the first m diagonal blocks, $\mathcal{L}_{li}$ ($i = 1, \cdots, m$), are the Laplacian matrices associated with the m LSCCs of $\mathcal{G}$, while $\mathcal{L}_r$ relates to the remaining vertices in $\mathcal{G}$. It is well-known that the Laplacian associated to a strongly connected digraph has a simple zero eigenvalue, whose associated left eigenvector has all positive entries, see this statement in e.g., [41, 176]. Therefore, there exists a positive vector ν_i such that $\mathcal{L}_{li}^T \nu_i = 0$ for each $i = 1, \cdots, m$. Then, it is verified that $\mathsf{diag}(\nu_i)\mathcal{L}_{li}$ represents a balanced directed subgraph, since

$$\mathbb{1}^T \mathsf{diag}(\nu_i)\mathcal{L}_{li} = 0 \text{ and } \mathsf{diag}(\nu_i)\mathcal{L}_{li}\mathbb{1} = 0. \tag{6.4}$$

Let

$$M := \mathsf{diag}\left([\nu_1^T, \cdots, \nu_m^T, \nu_r^T]\right) \cdot \mathcal{T}_\mu^T \tag{6.5}$$

with ν_r an arbitrary positive vector. Then, $L := M\mathcal{L}$ represents a generalized balanced digraph by Definition 6.1. □

Example 6.1. *Consider the weakly connected graph in Fig. 2.2, where the weights the edges are labeled. The weighted Laplacian matrix is written as*

$$\mathcal{L} = \left[\begin{array}{ccc:c:cc} 1 & 0 & -1 & 0 & 0 & 0 \\ -2 & 2 & 0 & 0 & 0 & 0 \\ 0 & -2 & 2 & 0 & 0 & 0 \\ \hdashline 0 & -1 & 0 & 2 & 0 & -1 \\ \hdashline 0 & 0 & 0 & 0 & 3 & -3 \\ 0 & 0 & 0 & 0 & -1 & 1 \end{array}\right]. \tag{6.6}$$

By (6.5), we choose $M = \mathsf{diag}\left([2, 1, 1, \alpha, 1, 3]^T\right)$ with α an arbitrary positive scalar such that

$$L = M\mathcal{L} = \left[\begin{array}{ccc:c:cc} 2 & 0 & -2 & 0 & 0 & 0 \\ -2 & 2 & 0 & 0 & 0 & 0 \\ 0 & -2 & 2 & 0 & 0 & 0 \\ \hdashline 0 & -\alpha & 0 & 2\alpha & 0 & -\alpha \\ \hdashline 0 & 0 & 0 & 0 & 3 & -3 \\ 0 & 0 & 0 & 0 & -3 & 3 \end{array}\right] \tag{6.7}$$

is a Laplacian matrix associating with a generalized balanced digraph.

Consider the directed network system $\mathbf{\Sigma}$ in (6.2). Then, Lemma 6.1 implies that there exists an equivalent representation:

$$\mathbf{\Sigma} : \begin{cases} M\dot{x}(t) = -Lx(t) + MFu(t), \\ y(t) = Hx(t), \end{cases} \tag{6.8}$$

where $M \in \mathbb{R}^{n\times n}$ is positive diagonal such that $L := M\mathcal{L}$ is a Laplacian matrix associating with a generalized balanced digraph. The introduction of the generalized balanced form (6.8) of directed networks is meaningful, as in the following sections, it will be employed to define the vertex clusterability and dissimilarity. Moreover, it can be seen as an extension of undirected networks in [34], where M is the vertex weights and L corresponds to an undirected graph.

6.2.2 Projection by Graph Clustering

This subsection constructs the reduced network system in the Petrov-Galerkin framework in which the projection matrix is chosen as the characteristic matrix of graph clustering. Before proceeding, we provide some notions regarding graph clustering [34, 126].

Consider a weakly connected digraph $\mathcal{G} = (\mathbb{V}, \mathbb{E})$. Then, a *graph clustering* is to divide the vertex set $\mathbb{V}$ into r nonempty and disjoint subsets, i.e., $\{\mathcal{C}_1, \mathcal{C}_2, \cdots, \mathcal{C}_r\}$, where $\mathcal{C}_i$ is called a *cell* (or a *cluster*) of $\mathcal{G}$.

Definition 6.2. *The **characteristic matrix** of the clustering $\mathcal{S}$ is denoted by a binary matrix $\Pi \in \mathbb{R}^{n\times r}$, whose (i,j)-entry is defined by*

$$\Pi_{ij} := \begin{cases} 1, & \text{vertex } i \in \mathcal{C}_j, \\ 0, & \text{otherwise.} \end{cases} \tag{6.9}$$

Clearly, the entries in each row of Π has a single 1 entry while all the others are 0, which means that each vertex is included in a unique cell. Moreover, Π satisfies

$$\Pi \mathbb{1}_n = \mathbb{1}_r. \tag{6.10}$$

Now, we consider the system $\mathbf{\Sigma}$ on digraph $\mathcal{G}$ of n vertices. To formulate a reduced model of dimension r, we first find a graph clustering that partitions the vertices of $\mathcal{G}$ into r cells. Then, we use the characteristic matrix of the clustering to construct the projection in the Petrov-Galerkin framework, which yields a reduced network system. Specifically, the following left and right projection matrices are utilized:

$$\Pi^\dagger := (\Pi^T N \Pi)^{-1} \Pi^T N, \text{and } \Pi, \tag{6.11}$$

where N is a diagonal matrix such that $\Pi^T N \Pi$ is invertible, and $\Pi^\dagger \in \mathbb{R}^{r\times n}$ is the *reflexive generalized inverse* of Π (see [141] for the definition). Both Π and N are to be determined in the latter sections. Wherein, Π is formed as the clustering of $\mathcal{G}$ is selected.

The reason that we select the pair of projection matrices in (6.11) is due to its potential to preserve a network structure. With this projection, the r-dimensional

projected model is given as

$$\hat{\mathbf{\Sigma}}: \begin{cases} \dot{z}(t) = -\hat{\mathcal{L}} z(t) + \hat{F} u(t), \\ \hat{y}(t) = \hat{H} z(t), \end{cases} \tag{6.12}$$

where $z(t) \in \mathbb{R}^r$, and

$$\hat{\mathcal{L}} := \Pi^\dagger \mathcal{L} \Pi, \ \hat{F} = \Pi^\dagger F \text{ and } \hat{H} = H\Pi.$$

It can be verified that $\hat{\mathcal{L}}\mathbb{1}_r = 0$, and $\hat{\mathcal{L}}$ has nonnegative diagonal entries and nonpositive off-diagonal elements. Thus, the reduced matrix $\hat{\mathcal{L}} \in \mathbb{R}^{r\times r}$ is a lower-dimensional Laplacian matrix representing a digraph with fewer vertices, and the reduced-order system $\hat{\mathbf{\Sigma}}$ models a smaller-sized weakly connected directed network. In other words, the network structure is guaranteed to be preserved.

Under the projection framework (6.11), the rest of this chapter investigates the structure-preserving model reduction problem of the system $\mathbf{\Sigma}$, formulated as follows.

Problem 6.1. *Given a directed network system $\mathbf{\Sigma}$ in (6.2), find matrices Π and N such that the obtained reduced-order model $\hat{\mathbf{\Sigma}}$ in (6.12) approximates the original system $\mathbf{\Sigma}$ in a way that $\|\mathbf{\Sigma} - \hat{\mathbf{\Sigma}}\|_{\mathcal{H}_2}$ is bounded and small.*

6.3 Model Reduction

The strategy of constructing a suitable reduced-order network system is discussed with two parts in this section. The first part shows the conditions to guarantee the boundedness of the approximation error $\|\mathbf{\Sigma} - \hat{\mathbf{\Sigma}}\|_{\mathcal{H}_2}$, and the second part develops an effective scheme to find an appropriate clustering such that the reduction error $\|\mathbf{\Sigma} - \hat{\mathbf{\Sigma}}\|_{\mathcal{H}_2}$ is small.

6.3.1 Clusterability

Denote the transfer matrices of $\mathbf{\Sigma}$ and $\hat{\mathbf{\Sigma}}$ by

$$\eta(s) = H\left(sI_n + \mathcal{L}\right)^{-1} F, \text{ and } \hat{\eta}(s) = \hat{H}(sI_r + \hat{\mathcal{L}})^{-1}\hat{F}, \tag{6.13}$$

respectively. Note that both $\mathbf{\Sigma}$ and $\hat{\mathbf{\Sigma}}$ are not asymptotically stable, which means $\|\eta(s)\|_{\mathcal{H}_2}$ or $\|\hat{\eta}(s)\|_{\mathcal{H}_\infty}$ may be unbounded potentially. The results in [41,84] shows that when $\mathcal{G} \in \mathbb{G}_s$, even a random partition of $\mathbb{V}$ can deliver an bounded reduction error $\|\eta(s) - \hat{\eta}(s)\|_{\mathcal{H}_2}$ with a properly chosen N. However, such a conclusion no longer holds for more general digraphs $\mathcal{G} \in \mathbb{G}_q$ or $\mathcal{G} \in \mathbb{G}_w$. Thereby, the following definition is introduced based on the generalized balanced representation of $\mathbf{\Sigma}$ in (6.8).

Definition 6.3. *In the network (6.2), the vertices i and j are **clusterable** if $\mathbf{e}_{ij} \in \ker(L)^{\perp}$ and $\mathbf{e}_{ij} \in \ker(L^T)^{\perp}$ simultaneously, where L is defined in (6.8). Furthermore, the graph clustering of $\mathcal{G}$ is **proper** if the vertices in each cell are clusterable.*

Furthermore, the physical meaning of the clusterability is explained in the following lemma.

Lemma 6.2. *The vertices i and j are clusterable if and only if the following conditions hold:*

- *the vertices i and j reach consensus, i.e., when $u = 0$,*

$$\lim_{t\to\infty} [x_i(t) - x_j(t)] = 0,$$

  for all initial conditions.

- *the vertices i and j are either contained in the same LSCC or $i, j \in \mathbb{V}\backslash\mathbb{S}_L$.*

Proof. Consider the decomposition of $\mathcal{L}$ as in (3.10), and we obtain

$$\mathcal{L}U = 0,\ V^T\mathcal{L} = 0,\ \text{and } V^TU = I_m, \tag{6.14}$$

where $U, V \in \mathbb{R}^{n\times m}$ with m the algebraic multiplicity of the zero eigenvalue of $\mathcal{L}$, i.e., the number of LSCCs in $\mathcal{G}$. It follows from $L = M\mathcal{L}$ that

$$\mathsf{im}(U) = \ker(L),\ \mathsf{im}(M^{-1}V) = \ker(L^T) \tag{6.15}$$

with M given in (6.5). By Definition 6.3, the clusterability of vertices i and j is thus equivalent to

$$\mathbf{e}_{ij}^T U = 0,\ \text{and } \mathbf{e}_{ij}^T M^{-1} V = 0. \tag{6.16}$$

Hereafter, we prove that (6.16) holds if and only if the two conditions in this lemma are satisfied.

Note that for any initial condition $x_0 \in \mathbb{R}^n$, the zero input response of $\mathbf{\Sigma}$ converge to

$$\lim_{t\to\infty} e^{-\mathcal{L}t}x_0 = \mathcal{J}x_0 = UV^Tx_0. \tag{6.17}$$

Thus, vertices i and j reach consensus $\forall x_0$ equivalently means that the i-th and j-th rows of U coincide, i.e., $\mathbf{e}_{ij}^T U = 0$. Furthermore, it follows from e.g., [176] that

$$\mathbf{e}_i^T V = 0,\ \forall i \in \mathbb{V}\backslash\mathbb{S}_L. \tag{6.18}$$

Thus, by the definition of generalized balanced graph, $\mathbf{e}_{ij}^T M^{-1} V = 0$ holds if and only if vertices i and j belongs to the same LSCC, or $i, j \in \mathbb{V}\backslash\mathbb{S}_L$ (in the latter case, $\mathbf{e}_i^T M^{-1} V = \mathbf{e}_j^T M^{-1} V = 0$ due to (6.18)). □

Remark 6.2. *The clusterability of different types of digraphs is discussed. If $\mathcal{G} \in \mathbb{G}_s$, we have $U = \frac{1}{\sqrt{n}}\mathbb{1}_n$ meaning that all the vertices achieve a global consensus, i.e., $\forall i, j \in \mathbb{V}$, $x_i(t) \to x_j(t)$ as $t \to \infty$. Moreover, $V \in \mathbb{R}^n$ has all positive entries [41, 84] such that $\mathbb{1}^T L = \mathbb{1}^T M\mathcal{L} = 0$. Thus, all the vertices are clusterable. When $\mathcal{G} \in \mathbb{G}_q$, i.e., $\mathcal{G}$ contains a single LSCC, the directed network can still reach a global consensus due to $\mathsf{ker}(\mathcal{L}) = \mathsf{im}(\mathbb{1}_n)$, whereas there will be two sets of clusterable vertices, which are the vertices inside $\mathbb{S}_L$ and all the other vertices outside $\mathbb{S}_L$. In a more general case that $\mathcal{G} \in \mathbb{G}_w$, the system $\mathbf{\Sigma}$ in (6.2) may not achieve a global consensus. Instead, a local consensus is achievable among the vertices that are able to influence each other. Namely, $\mathbf{\Sigma}$ forms cells of consensus with different consensus values in each cell. It is guaranteed that the vertices in the same LSCC are clusterable.*

The definition of clusterability is nontrivial as it determines the feasibility of a graph clustering. More specifically, we find that the boundedness of the approximation error between the original and reduced systems is guaranteed only if clusterable vertices are classified in the same cell.

Consider the permutation transformation in (6.3), and denote the following set of diagonal matrices:

$$\mathbb{N} := \left\{ N \in \mathbb{R}^{n\times n} : \Pi^T N \Pi \text{ is invertible, } \; N\mathbb{1} \in \mathsf{im}\left(\mathcal{T}_\mu \cdot \mathsf{blkdiag}(\nu_1, \cdots, \nu_m, I)\right) \right\}, \tag{6.19}$$

where $\mathcal{T}_\mu$ is the permutation matrix reforming $\mathcal{L}$ into a block upper triangular form, and ν_i is the left eigenvector of the diagonal block matrix $\mathcal{L}_{li}$ in (6.3), i.e., $\mathcal{L}_{li}^T \nu_i = 0$. Then, the clustering-based projection matrices in (6.11), i.e., N and Π, are selected according to the following theorem to guarantee the boundedness of the error between $\mathbf{\Sigma}$ and $\hat{\mathbf{\Sigma}}$.

Theorem 6.1. *Consider the directed network system $\mathbf{\Sigma}$ in (6.2) and its reduced-order model $\hat{\mathbf{\Sigma}}$ in (6.12). For all input and output matrices H and F, the error $\|\eta(s) - \hat{\eta}(s)\|_{\mathcal{H}_2}$ is bounded if and only if Π in (6.11) characterizes a proper clustering of $\mathcal{G}$ and $N \in \mathbb{N}$.*

Proof. The $\mathcal{H}_2$-norm of the approximation error is given by

$$\|\eta(s) - \hat{\eta}(s)\|_{\mathcal{H}_2}^2 = \int_0^\infty \|\xi(t) - \hat{\xi}(t)\|_2^2 dt, \tag{6.20}$$

where $\xi(t) := He^{-\mathcal{L}t}F$ and $\hat{\xi}(t) := H\Pi e^{-\hat{\mathcal{L}}t}\Pi^\dagger F$ are the impulse responses of $\mathbf{\Sigma}$ and $\hat{\mathbf{\Sigma}}$, respectively. Since both $\xi(t)$ and $\hat{\xi}(t)$ are smooth functions over $t \in \mathbb{R}_+$, the integral in (6.20) is finite if and only if the error $\xi(t) - \hat{\xi}(t)$ exponentially converges to zero. Hence, for general H and F matrices, the boundedness of $\|\eta(s) - \hat{\eta}(s)\|_{\mathcal{H}_2}$ is equivalent to

$$\mathcal{J} = \Pi\hat{\mathcal{J}}\Pi^\dagger. \tag{6.21}$$

with $\mathcal{J} := \lim_{\tau\to\infty} e^{-\mathcal{L}\tau}$ and $\hat{\mathcal{J}} := \lim_{\tau\to\infty} e^{-\hat{\mathcal{L}}\tau}$.

To prove the "if" part, we assume $\{\mathcal{C}_1, \mathcal{C}_2, \cdots, \mathcal{C}_r\}$ to be a proper clustering of $\mathcal{G}$. With $N \in \mathbb{N}$, we verify

$$U = \Pi\Pi^\dagger U, \text{ and } V^T = V^T\Pi\Pi^\dagger \tag{6.22}$$

as follows. Without loss of generality, assume that

$$\Pi = \mathsf{blkdiag}\left(\mathbb{1}_{|\mathcal{C}_1|}, \mathbb{1}_{|\mathcal{C}_2|}, \cdots, \mathbb{1}_{|\mathcal{C}_r|}\right). \tag{6.23}$$

Accordingly, the matrices U and V in (6.14) are partitioned as $U^T = [U_1^T, \cdots, U_r^T]$ and $V^T = [V_1^T, \cdots, V_r^T]$. Meanwhile, the projection $\Gamma = \Pi\Pi^\dagger$ is written in a block diagonal form with the i-th diagonal entry as

$$\Gamma_i = \mathbb{1}_{|\mathcal{C}_i|}(\mathbb{1}_{|\mathcal{C}_i|}^T N_i \mathbb{1}_{|\mathcal{C}_i|})^{-1}\mathbb{1}_{|\mathcal{C}_i|}^T N_i. \tag{6.24}$$

Since N_i is the corresponding principal submatrix in N, i.e., it is diagonal and nonsingular, the equations in (6.22) hold if and only if

$$U_i = \Gamma_i U_i, \text{ and } V_i^T = V_i^T\Gamma_i. \tag{6.25}$$

It follows from Lemma 6.2 that $U_i = \mathbb{1}_{|\mathcal{C}_i|}$, which verifies the first equation in (6.25). Moreover, as the vertices in $\mathcal{C}_i$ are clusterable, Lemma 6.2 implies that these vertices are either contained in the same LSCC or in the set $\mathbb{V}\backslash\mathbb{S}_L$. In the first case, $V_i = N_i\mathbb{1}_{|\mathcal{C}_i|}$ owing to $\delta(N) \in \mathbb{N}$, and the second case indicates that $V_i = 0$ from (6.18). It is verified that the second equation in (6.25) are satisfied in both cases. Thus, the equations in (6.22) hold. Based on this, we compute $\hat{\mathcal{J}}$ in (6.21) for the reduced-order system $\hat{\mathbf{\Sigma}}$. Let $\hat{U} := \Pi^\dagger U$ and $\hat{V}^T := V^T\Pi$, which leads to

$$\hat{\mathcal{L}}\hat{U} = \Pi^\dagger\mathcal{L}\Pi\Pi^\dagger U = \Pi^\dagger\mathcal{L}U = 0, \hat{V}^T\hat{\mathcal{L}} = V^T\Pi\Pi^\dagger\mathcal{L}\Pi = V^T\mathcal{L}\Pi = 0. \tag{6.26}$$

Furthermore, due to

$$\hat{V}^T\hat{U} = V^T\Pi\Pi^\dagger U = V^T U = I_m, \tag{6.27}$$

we obtain

$$\hat{\mathcal{J}} := \hat{U}\hat{V}^T = \Pi^\dagger U V^T\Pi, \tag{6.28}$$

and thus,

$$\Pi\hat{\mathcal{J}}\Pi^\dagger = \Pi\Pi^\dagger U V^T\Pi\Pi^\dagger = UV^T = \mathcal{J}. \tag{6.29}$$

Consequently, the error $\|\eta(s) - \hat{\eta}(s)\|_{\mathcal{H}_2}$ is bounded.

For the "only if" part, $\|\eta(s) - \hat{\eta}(s)\|_{\mathcal{H}_2}$ is assumed to be bounded for all H and F matrices, equivalently, (6.21) holds. Similarly, the block diagonal structure of Π in (6.23) is assumed without loss of generality such that (6.21) is presented as

$$\begin{bmatrix} U_1 \\ \vdots \\ U_r \end{bmatrix} \left[V_1^T, \cdots, V_r^T\right] = \begin{bmatrix} \mathbb{1}_{|\mathcal{C}_1|}\tilde{U}_1 \\ \vdots \\ \mathbb{1}_{|\mathcal{C}_r|}\tilde{U}_r \end{bmatrix} \left[\tilde{V}_1^T\Pi_1^\dagger, \cdots, \tilde{V}_r^T\Pi_r^\dagger\right], \tag{6.30}$$

where $\Pi_i^\dagger := (\mathbb{1}_{|\mathcal{C}_i|}^T N_i \mathbb{1}_{|\mathcal{C}_i|})^{-1}\mathbb{1}_{|\mathcal{C}_i|}^T N_i$, $\tilde{U}_i := \mathbf{e}_i^T\tilde{U}$ and $\tilde{V}_i := \mathbf{e}_i^T\tilde{V}$, with $\tilde{U}$ and $\tilde{V}$ fulfilling

$$\mathsf{im}(\tilde{U}) = \mathsf{ker}(\hat{\mathcal{L}}),\ \mathsf{im}(\tilde{V}) = \mathsf{ker}(\hat{\mathcal{L}}^T),\ \text{and}\ \tilde{V}^T\tilde{U} = I. \tag{6.31}$$

The matrices $U_i, V_i \in \mathbb{R}^{|\mathcal{C}_i|\times m}$ are the corresponding submatrices of U and V, respectively. Then, (6.30) yields

$$U_i V_j^T = \mathbb{1}_{|\mathcal{C}_i|}\tilde{U}_i\tilde{V}_j^T\Pi_j^\dagger = \alpha_{ij}\cdot\mathbb{1}_{|\mathcal{C}_i|}\mathbb{1}_{|\mathcal{C}_j|}^T N_j,\ \ \forall i,j = 1,2,\cdots,r. \tag{6.32}$$

with a scalar $\alpha_{ij} := \tilde{U}_i\tilde{V}_j^T\cdot(\mathbb{1}_{|\mathcal{C}_j|}^T N_j \mathbb{1}_{|\mathcal{C}_j|})^{-1}$. It follows that

$$\mathbf{e}_{ij}^T U_k = 0,\ \text{and}\ V_k^T N_k^{-1}\mathbf{e}_{ij} = 0,\ \forall i,j \in \mathcal{C}_k. \tag{6.33}$$

Note that $LU = 0$ and $V^T N^{-1} L = 0$ with L defined in (6.8). Thus, we obtain $\forall i,j \in \mathcal{C}_k$, $\mathbf{e}_{ij} \in \mathsf{ker}(L)^\perp$ and $\mathbf{e}_{ij} \in \mathsf{ker}(L^T)^\perp$. As the result holds for all cells $\mathcal{C}_1, \mathcal{C}_2, \cdots, \mathcal{C}_r$, the graph clustering is proper by Definition 6.3.

Next, we prove that $N \in \mathbb{N}$ is also necessary for a bounded approximation error. Clearly, $\Pi^T N \Pi$ has to be invertible in (6.11). A proper clustering $\{\mathcal{C}_1, \mathcal{C}_2, \cdots, \mathcal{C}_r\}$ means that each cell $\mathcal{C}_k$ ($k = 1, \cdots, r$) is included in either $\mathbb{V}\backslash\mathbb{S}_L$ or a LSCC, denoted by $\mathcal{S}_\mu$. If $\mathcal{C}_k \subseteq \mathbb{V}\backslash\mathbb{S}_L$, we have $V_k = 0$ owing to (6.18) such that (6.32) is equal to zero, and thus N_k can be an arbitrary nonsingular diagonal matrix, that is $N_k \in \mathsf{im}(I)$.

For the second case that $\mathcal{C}_k \subseteq \mathcal{S}_\mu$, we can assume, without loss of generality, that the set $\mathcal{S}_\mu$ is the union of μ disjoint cells $\mathcal{C}_1, \cdots, \mathcal{C}_k, \cdots, \mathcal{C}_\mu$. Let $\mathcal{L}_\mu$ be the Laplacian matrix associated with $\mathcal{S}_\mu$ and $U_s, V_s \in \mathbb{R}^{|\mathcal{S}_\mu|\times m}$ be the rows of U, V that correspond to $\mathcal{S}_\mu$. Thus, we obtain from [176] that

$$\mathsf{im}(U_s) = \mathsf{ker}(\mathcal{L}_\mu) = \mathsf{im}(\mathbb{1}_{|\mathcal{S}_\mu|}), \mathsf{im}(V_s) = \mathsf{ker}(\mathcal{L}_\mu^T) = \mathsf{im}(\nu_s), \tag{6.34}$$

where ν_s has strictly positive entries, and $\nu_s \in \{\nu_1, \cdots, \nu_m\}$. Then, from (6.32), we can find a permutation matrix $\mathcal{T}_s$ such that

$$\mathcal{T}_s U_s V_s^T = \beta\mathbb{1}_{|\mathcal{S}_\mu|}\nu_s = \begin{bmatrix} \alpha_{11}\mathbb{1}_{|\mathcal{C}_1|}\mathbb{1}_{|\mathcal{C}_1|}^T N_1 & \cdots & \alpha_{1\mu}\mathbb{1}_{|\mathcal{C}_1|}\mathbb{1}_{|\mathcal{C}_\mu|}^T N_\mu \\ \vdots & \ddots & \vdots \\ \alpha_{\mu 1}\mathbb{1}_{|\mathcal{C}_\mu|}\mathbb{1}_{|\mathcal{C}_1|}^T N_1 & \cdots & \alpha_{\mu\mu}\mathbb{1}_{|\mathcal{C}_\mu|}\mathbb{1}_{|\mathcal{C}_\mu|}^T N_\mu^T \end{bmatrix},$$

with β and α_{ij} scalars. It follows that $\alpha_{1i} = \alpha_{2i} = \cdots = \alpha_{\mu i}$, $\forall i = 1, \cdots, \mu$, and

$$\mathsf{blkdiag}(N_1, \cdots, N_\mu)\mathbb{1}_{|\mathcal{S}_\mu|} \in \mathsf{im}(\nu_s). \tag{6.35}$$

The above reasoning can be applied to all the LSCCs such that $N \in \mathbb{N}$ is obtained.

That completes the proof. □

Let n_c be the number of the maximal clusterable cells, then Theorem 6.1 implies that the reduction order r should not be less than n_c. Otherwise, the approximation error will be unbounded. Besides, we use $\Pi^\dagger = (\Pi^T M \Pi)^{-1}\Pi^T M$ as the left projection matrix with M in (6.5), where we choose $\nu_r = \mathbb{1}$ in this chapter such that $M \in \mathbb{N}$. Thereby, the following section will focus on finding an appropriate clustering such that the approximation error $\|\mathbf{\Sigma} - \hat{\mathbf{\Sigma}}\|_{\mathcal{H}_2}$ is as small as possible.

Example 6.2. *Consider the weakly connected graph in Fig. 2.2, whose Laplacian matrix is given in (6.6). Then, the right and left nullspaces can be characterized by*

$$U^T = \begin{bmatrix} 0.25 & 0.25 & 0.25 & 0.125 & 0 & 0 \\ 0 & 0 & 0 & 0.125 & 0.25 & 0.25 \end{bmatrix}, V^T = \begin{bmatrix} 2 & 1 & 1 & 0 & 0 & 0 \\ 0 & 0 & 0 & 0 & 1 & 3 \end{bmatrix}.$$

Thus, we can choose $M = \mathsf{diag}(2, 1, 1, 1, 1, 3)$ *such that a Laplacian matrix in the generalized balanced form (6.8) is obtained. By Definition 6.3, a proper clustering of the digraph is given by* $\mathcal{C}_1 = \{1, 2, 3\}$, $\mathcal{C}_2 = \{4\}$, *and* $\mathcal{C}_3 = \{5, 6\}$, *which yields*

$$\Pi = \begin{bmatrix} 1 & 1 & 1 & 0 & 0 & 0 \\ 0 & 0 & 0 & 1 & 0 & 0 \\ 0 & 0 & 0 & 0 & 1 & 1 \end{bmatrix}. \tag{6.36}$$

As a result, a 3-dimensional network system is obtained in form of (6.12) with the reduced Laplacian matrix as

$$\hat{\mathcal{L}} = \Pi^\dagger \mathcal{L} \Pi = \begin{bmatrix} 0 & 0 & 0 \\ -1 & 2 & -1 \\ 0 & 0 & 0 \end{bmatrix}, \tag{6.37}$$

which represents a simpler weakly connected digraph as shown in Fig. 6.1a. Next, we suppose $H = F = I_6$ *in (6.2) and compute the approximation error:* $\|\mathbf{\Sigma} - \hat{\mathbf{\Sigma}}\|_{\mathcal{H}_2} = 0.7852$, *which is bounded.*

For comparison reasons, we consider an alternative clustering, namely, $\mathcal{C}_1 = \{1, 2\}$, $\mathcal{C}_2 = \{3, 4\}$, *and* $\mathcal{C}_3 = \{5, 6\}$, *while keeping the same* M *matrix. Then, a different reduced-order system* $\hat{\mathbf{\Sigma}}$ *is obtained with the Laplacian matrix*

$$\hat{\mathcal{L}} = \Pi^\dagger \mathcal{L} \Pi = \begin{bmatrix} \frac{2}{3} & -\frac{2}{3} & 0 \\ -\frac{3}{2} & 2 & -\frac{1}{2} \\ 0 & 0 & 0 \end{bmatrix}. \tag{6.38}$$

(a) (b)

Figure 6.1: (a) A reduced digraph obtained by a proper graph clustering. (b) A reduced digraph generated from an alternative graph clustering.

It represents a reduced digraph as in Fig. 6.1b, which is quasi strongly connected, and the approximation error is shown to be unbounded. Next, we use the proper clustering as before but a different M matrix, e.g., $M = I$ and $M = \mathsf{diag}(1, 2, 2, 1, 1, 2)$. We find that both yield unbounded reduction errors.

6.3.2 Vertex Dissimilarity

The concept of clusterability determines the boundedness of the approximation error and is only dependent on the topology of the underlying network, i.e., the directed Laplacian matrix, whereas this section investigates how to find a reduced-order model such that the magnitude of the approximation error is small. To this end, the structures of the inputs and outputs are considered as well to define the concept of vertex dissimilarity that will be regarded as a criteria for selecting appropriate graph clusterings.

Definition 6.4. *Consider the directed network system $\mathbf{\Sigma}$ in (6.2) and its generalized balanced form (6.8). The **dissimilarity** of a pair of clusterable vertices is defined by*

$$\mathcal{D}_{ij} = \mathcal{D}^I_{ij} \cdot \mathcal{D}^O_{ij}, \tag{6.39}$$

where $\mathcal{D}^I_{ij}$ and $\mathcal{D}^O_{ij}$ are input and output dissimilarities of vertices i, j:

$$\begin{aligned} \mathcal{D}^I_{ij} &:= \|(\mathbf{e}_i - \mathbf{e}_j)^T (sM + L)^{-1} MF\|_{\mathcal{H}_2}, \\ \mathcal{D}^O_{ij} &:= \|H(sM + L)^{-1}(\mathbf{e}_i - \mathbf{e}_j)\|_{\mathcal{H}_2}. \end{aligned} \tag{6.40}$$

Remark 6.3. *Note that when either $\mathcal{D}^I_{ij}$ or $\mathcal{D}^O_{ij}$ is zero, it is reasonable to have the dissimilarity $\mathcal{D}_{ij} = 0$. This is the reason that in (6.39), we use the product of $\mathcal{D}^I_{ij}$ and $\mathcal{D}^O_{ij}$ instead of the sum of them.*

The physical meanings of the input and output dissimilarities are explained. First, to quantify the input dissimilarity between a pair of vertices i and j, we steer the network system $\mathbf{\Sigma}$ by injecting a series of impulse signals, i.e., let $u(t)$ in (6.2) be a vector of delta functions. Then, the responses of the vertices i and j are compared, i.e.,

$$\Xi_i(t) - \Xi_j(t) = \left[\xi_{i1}(t) - \xi_{j1}(t), \cdots, \xi_{ip}(t) - \xi_{jp}(t)\right], \tag{6.41}$$

with $\xi_{ij}(t) \in \mathbb{R}$ the trajectory of the vertex i to the impulse in the j-th input channel. Thus, a proper measurement of the input dissimilarity between the vertices i and j is given by

$$\mathcal{D}_{ij}^I = \sqrt{\int_0^\infty \left[\Xi_i(t) - \Xi_j(t)\right] \left[\Xi_i(t) - \Xi_j(t)\right]^T dt}. \tag{6.42}$$

Essentially, the value of $\mathcal{D}_{ij}^I$ indicates how controllable the error between vertices i and j is. More precisely, the smaller $\mathcal{D}_{ij}^I$ means a smaller amount of input energy required to steer the vertices i and j to consensus. Similarly, the output dissimilarity of the clusterable vertices i and j is characterized by

$$\mathcal{D}_{ij}^O = \sqrt{\int_0^\infty \left[\Psi_i(t) - \Psi_j(t)\right]^T \left[\Psi_i(t) - \Psi_j(t)\right] dt}, \tag{6.43}$$

where $\Psi_i(t) - \Psi_j(t) \in \mathbb{R}^q$ is the output of $\mathbf{\Sigma}$ when only vertices i, j are perturbed by an impulse signal. Thus, $\mathcal{D}_{ij}^O$ indicates how observable the error between vertices i and j is, i.e., the larger $\mathcal{D}_{ij}^O$, the less energy generated by the natural response of the perturbation on vertices i and j, and thus more difficult the error between vertices i and j can be measured.

Remark 6.4. *For vertices that are not clusterable, their dissimilarities are not properly defined, since Theorem 6.1 implies that merging unclusterable vertices may cause an unbounded reduction error. Therefore, we can simply assign $\mathcal{D}_{ij}$ to be a sufficiently large positive value when i and j are unclusterable.*

Unlike the previous works in [34, 84] etc., the outputs of the system $\mathbf{\Sigma}$ are also taken into account when defining the dissimilarity. As we find that the output structures also have an impact on the approximation error, see the numerical examples in Section 6.4, which motivates us to combine the input and output dissimilarities in order to obtain more accurate reduced networks.

Notice that the computation of $\mathcal{D}_{ij}$ for each pair of clusterable vertices i, j using the definition of norms may be a formidable task when the scale of the directed network is large. Thereby, the notions of pseudo controllability and observability Gramians in Section 3.3 are applied to facilitate the computation of vertex dissimilarities.

Theorem 6.2. *Consider a connected directed network $\mathbf{\Sigma}$. The dissimilarity between two clusterable vertices i and j is computed as*

$$\mathcal{D}_{ij} = \sqrt{\mathbf{e}_{ij}^T \mathcal{P} \mathbf{e}_{ij} \mathbf{e}_{ij}^T M^{-1} \mathcal{Q} M^{-1} \mathbf{e}_{ij}}, \tag{6.44}$$

where $\mathbf{e}_{ij} := \mathbf{e}_i - \mathbf{e}_j$, and $\mathcal{P}$, $\mathcal{Q}$ are the pseudo controllability and observability Gramians of $\mathbf{\Sigma}$, respectively.

Proof. Using the clusterability of vertices i and j, we have

$$\mathbf{e}_{ij}^T \mathcal{J} F = 0, \text{ and } H \mathcal{J} M^{-1} \mathbf{e}_{ij} = 0 \tag{6.45}$$

Therefore, from Lemma 3.2, $\mathcal{D}_{ij}$ is bounded for any clusterable vertices i, j, and

$$\mathcal{D}_{ij}^I = \sqrt{\mathbf{e}_{ij}^T \mathcal{P} \mathbf{e}_{ij}}, \text{ and } \mathcal{D}_{ij}^O = \sqrt{\mathbf{e}_{ij}^T M^{-1} \mathcal{Q} M^{-1} \mathbf{e}_{ij}}, \tag{6.46}$$

which gives (6.44). □

6.3.3 Minimal Network Realization

We discuss a novel concept of minimal realization for network systems. Before proceeding, the following definitions are introduced.

Let $\mathbb{V}_{\mathcal{I}}$ and $\mathbb{V}_{\mathcal{O}}$ be the subsets of $\mathbb{V}$ such that $i \in \mathbb{V}_{\mathcal{I}}$ and $i \in \mathbb{V}_{\mathcal{O}}$ if the vertex i is steered directly by the input u and directly measured by the output y, respectively.

Definition 6.5. *A vertex j is **reachable** if there exists a directed path from any vertex $i \in \mathbb{V}_{\mathcal{I}} \setminus j$ to j, and **detectable** if there is a directed path from j to all vertex $i \in \mathbb{V}_{\mathcal{O}} \setminus j$. Two vertices i and j are **0-dissimilar** if $\mathcal{D}_{ij} = 0$.*

Physically, unreachable vertices cannot receive information from the inputs, and thus their states is not controllable. Similarly, vertices that are undetectable cannot pass their information to the outputs, namely, their states are unobservable. The 0-dissimilar condition relies on the specific structures of a network topology. For some networks with special topologies, e.g., complete graphs, lattices, trees, rings, star graphs, etc., we can obtain them directly from the underlying graphs. Consider a digraph graph $\mathcal{G} = (\mathbb{V}, \mathbb{E})$. An *in-neighbor* (resp. *out-neighbor*) of a vertex i of $\mathcal{G}$ is a vertex j with $a_{ji} \in \mathbb{E}$ (resp. $a_{ij} \in \mathbb{E}$). The set of all the in-neighbors and out-neighbors of i in $\mathcal{G}$, denoted by $\mathcal{N}_I(i)$ and $\mathcal{N}_O(i)$, are called the *in-neighborhood* and *out-neighborhood* of i, respectively. Generally, if two vertices $i, j \notin \mathbb{V}_{\mathcal{I}}$ has a zero input dissimilarity, i.e., $\mathcal{D}_{ij}^I = 0$ if they share the same in-neighborhood, and

$$w_{ki} = w_{kj}, \ \forall k \in \mathcal{N}_I(i) = \mathcal{N}_I(j).$$

Analogously, $\mathcal{D}^O_{ij} = 0$ for two vertices $i, j \notin \mathbb{V}_{\mathcal{O}}$, when

$$w_{ik} = w_{jk},\ \forall k \in \mathcal{N}_O(i) = \mathcal{N}_O(j).$$

More precisely, the condition for checking the 0-dissimilarity between a pair i, j is given as follows.

Proposition 6.1. *Consider the network system $\mathbf{\Sigma}$ with p inputs, clusterable vertices i and j are 0-dissimilar if there exists a scalar β such that*

$$\mathbf{e}_{ij}^T \begin{bmatrix} F & \mathcal{L} - \beta I \end{bmatrix} = 0, \text{ or } \begin{bmatrix} HM^{-1} & \mathcal{L} - \beta I \end{bmatrix} \mathbf{e}_{ij} = 0. \tag{6.47}$$

Proof. By definition, vertices i and j are 0-dissimilar if $\mathcal{D}^I_{ij} = 0$ or $\mathcal{D}^O_{ij} = 0$. Thus, we first derive the sufficient condition for $\mathcal{D}^I_{ij} = 0$, i.e.,

$$\int_0^\infty \mathbf{e}_{ij}^T (e^{-\mathcal{L}t} - \mathcal{J}) F F^T (e^{-\mathcal{L}^T t} - \mathcal{J}^T) \mathbf{e}_{ij} dt = 0, \tag{6.48}$$

which is equivalent to $\mathbf{e}_{ij}^T (e^{-\mathcal{L}t} - \mathcal{J})F = \mathbf{e}_{ij}^T e^{-\mathcal{L}t} F = 0$, $\forall t \in \mathbb{R}_+$. It follows from the first equation in (6.47) that $\forall k \geq 1$,

$$\mathbf{e}_{ij}^T \mathcal{L}^k = \mathbf{e}_{ij}^T (\mathcal{L} - \beta I + \beta I)\mathcal{L}^{k-1} = \beta \mathbf{e}_{ij}^T \mathcal{L}^{k-1} = \cdots = \beta^{k-1} \mathbf{e}_{ij}^T \mathcal{L} = \beta^k \mathbf{e}_{ij}^T. \tag{6.49}$$

As a result, the Taylor expansion of $\mathbf{e}_{ij}^T e^{-\mathcal{L}t} F$ yields

$$\mathbf{e}_{ij}^T e^{-\mathcal{L}t} F = \sum_{k=0}^{\infty} \frac{(-t)^k}{k!} \mathbf{e}_{ij}^T \mathcal{L}^k F = \mathbf{e}_{ij}^T F + \sum_{k=1}^{\infty} \frac{(-t)^k \beta^k}{k!} \mathbf{e}_{ij}^T F = 0. \tag{6.50}$$

Therefore, (6.48) holds. Analogously, the second equation in (6.47) implies that $H(e^{-\mathcal{L}t} - \mathcal{J})M^{-1}\mathbf{e}_{ij} = He^{-\mathcal{L}t}M^{-1}\mathbf{e}_{ij} = 0$, $\forall t \in \mathbb{R}_+$. Thus, $\mathcal{D}^O_{ij} = 0$. □

Thereby, the following concept is proposed.

Definition 6.6. *The network system $\mathbf{\Sigma}$ in (6.2) is called a **minimal network realization** if all the vertices are reachable and detectable, and there does not exist 0-dissimilar vertices in the underlying network.*

Parallel to the minimal realization of general linear systems obtained by Kalman decomposition, a minimal network realization is acquired by removing unreachable and undetectable vertices and aggregating 0-dissimilar vertices. The following result shows that no approximation error is generated in the realization of the network minimality.

Theorem 6.3. *If the reduced-order model $\hat{\mathbf{\Sigma}}$ is obtained by*

- *removing all unreachable or undetectable vertices*
- *or merging all 0-dissimilarity vertices (i.e., $\mathcal{D}_{ij} = 0$),*

then $\|\mathbf{\Sigma} - \hat{\mathbf{\Sigma}}\|_{\mathcal{H}_2} = 0$.

Proof. Neglecting the vertices that are not reachable or detectable is equivalent to remove uncontrollable or observable states of $\mathbf{\Sigma}$. Therefore, the reduction will not change the transfer function of the system, namely, $\|\mathbf{\Sigma} - \hat{\mathbf{\Sigma}}\|_{\mathcal{H}_2} = 0$.

Next, we show that clustering all 0-dissimilarity vertices does not generate an approximation error neither. To this end, we denote

$$\chi(s) := (sI_n + \mathcal{L})^{-1}, \hat{\chi}(s) := (sI_r + \hat{\mathcal{L}})^{-1}. \tag{6.51}$$

and let $\tilde{\Gamma} := I - \Pi\Pi^\dagger$, which satisfies

$$\tilde{\Gamma}^T = \tilde{\Gamma}, \text{ and } \tilde{\Gamma}^2 = \tilde{\Gamma}. \tag{6.52}$$

Consider the error system $\mathbf{\Sigma}_e = \mathbf{\Sigma} - \hat{\mathbf{\Sigma}}$, whose transfer function is $\eta(s) - \hat{\eta}(s) := H\eta_e F$ with

$$\eta_e = \begin{bmatrix} I & -\Pi \end{bmatrix} \begin{bmatrix} \chi(s) & 0 \\ 0 & \hat{\chi}(s) \end{bmatrix} \begin{bmatrix} I \\ \Pi^\dagger \end{bmatrix}, \tag{6.53}$$

where $\Pi^\dagger$ is the reflexive generalized inverse of Π in (6.11). Then, using the following nonsingular matrices

$$T_1 = \begin{bmatrix} I & \Pi^\dagger \\ 0 & I_r \end{bmatrix}, T_1^{-1} = \begin{bmatrix} I_n & -\Pi^\dagger \\ 0 & I_r \end{bmatrix}, T_2 = \begin{bmatrix} I_n & 0 \\ \Pi^\dagger & I_r \end{bmatrix}, T_2^{-1} = \begin{bmatrix} I_n & 0 \\ -\Pi^\dagger & I_r \end{bmatrix}, \tag{6.54}$$

we further obtain

$$\begin{aligned}
\eta_e =& \begin{bmatrix} I & -\Pi \end{bmatrix} T_1 \left(T^{-1} \begin{bmatrix} \chi(s) & 0 \\ 0 & \hat{\chi}(s) \end{bmatrix} T_1 \right) \cdot T_1^{-1} \begin{bmatrix} \chi(s)^{-1} & 0 \\ 0 & \hat{\chi}(s)^{-1} \end{bmatrix} T_2 \\
& \cdot \left(T_2^{-1} \begin{bmatrix} \chi(s) & 0 \\ 0 & \hat{\chi}(s) \end{bmatrix} T_2 \right) T_2^{-1} \begin{bmatrix} I \\ \Pi^\dagger \end{bmatrix} \\
=& \chi(s) \begin{bmatrix} I & -\tilde{\Gamma}\mathcal{L}\hat{\chi}(s) \end{bmatrix} \cdot \begin{bmatrix} \chi(s)^{-1} - \Pi\hat{\chi}(s)\Pi^\dagger & -\Pi\hat{\chi}(s) \\ \hat{\chi}(s)\Pi^\dagger & \hat{\chi}(s) \end{bmatrix} \cdot \begin{bmatrix} I & \hat{\chi}(s)\Pi^\dagger\mathcal{L}\tilde{\Gamma} \end{bmatrix} \chi(s) \\
=& \tilde{\Gamma} \left[\chi(s)^{-1} - \mathcal{L}\Pi\hat{\chi}(s)\Pi^\dagger\mathcal{L} \right] \tilde{\Gamma}.
\end{aligned}$$

where the property in (6.52) is used to obtain the above equation. Clearly, $\|\eta_e\|_{\mathcal{H}_2} = 0$ if

$$\tilde{\Gamma}\chi(s)F = 0 \text{ or } H\chi(s)\tilde{\Gamma} = 0. \tag{6.55}$$

To prove (6.55), we assume, without loss of generality, that vertices $1, 2, \cdots, k$ are 0-dissimilar, namely, $\mathbf{e}_1^T\chi(s)F = \mathbf{e}_2^T\chi(s)F = \cdots = \mathbf{e}_k^T\chi(s)F$, or $H\chi(s)M^{-1}\mathbf{e}_1 = H\chi(s)M^{-1}\mathbf{e}_2 = \cdots = H\chi(s)M^{-1}\mathbf{e}_k$, which means

$$\chi(s)F := \begin{bmatrix} \mathbb{1}_k\mathbf{e}_1^T\chi(s)F \\ * \end{bmatrix} \text{ or } H\chi(s) := \begin{bmatrix} H\chi(s)M^{-1}\mathbf{e}_1\mathbb{1}_k^T & * \end{bmatrix} M. \tag{6.56}$$

When all the 0-dissimilar vertices are assigned into a single cell, the following block matrices are obtained.

$$\Pi = \begin{bmatrix} \mathbb{1}_k & \\ & I_{n-k} \end{bmatrix},\ M = \begin{bmatrix} M_a & \\ & M_b \end{bmatrix}, M_a \in \mathbb{R}^{k\times k} \tag{6.57}$$

where Π is the characteristic matrix of the partition. When the vertices $1, 2, \cdots, k$ are 0-input-dissimilar, we obtain

$$\begin{aligned} \tilde{\Gamma}\chi(s)F &= \begin{bmatrix} I_k - \dfrac{\mathbb{1}_k\mathbb{1}_k^TM_a}{\mathbb{1}_k^TM_a\mathbb{1}_k} & \\ & 0 \end{bmatrix} \begin{bmatrix} \mathbb{1}_k\mathbf{e}_1^T\chi(s)F \\ * \end{bmatrix} \\ &= \begin{bmatrix} \left(\mathbb{1}_k - \dfrac{\mathbb{1}_k\mathbb{1}_k^TM_a\mathbb{1}_k}{\mathbb{1}_k^TM_a\mathbb{1}_k}\right)\mathbf{e}_1^T\chi(s)F & \\ & 0 \end{bmatrix} = 0. \end{aligned}$$

When the vertices $1, 2, \cdots, k$ are 0-output-dissimilar, we also have

$$\begin{aligned} H\chi(s)\tilde{\Gamma} &= \begin{bmatrix} H\chi(s)M^{-1}\mathbf{e}_1\mathbb{1}_k^TM_a & * \end{bmatrix} \begin{bmatrix} I_k - \dfrac{\mathbb{1}_k\mathbb{1}_k^TM_a}{\mathbb{1}_k^TM_a\mathbb{1}_k} & \\ & 0 \end{bmatrix} \\ &= \begin{bmatrix} H\chi(s)M^{-1}\mathbf{e}_1\left(\mathbb{1}_k^TM_a - \dfrac{\mathbb{1}_k^TM_a\mathbb{1}_k\mathbb{1}_k^TM_a}{\mathbb{1}_k^TM_a\mathbb{1}_k}\right) & \\ & 0 \end{bmatrix} = 0. \end{aligned}$$

Therefore, when clustering 0-dissimilar vertices, the equation (6.55) holds, which yields that $\|\eta_e\|_{\mathcal{H}_2} = \|\mathbf{\Sigma} - \hat{\mathbf{\Sigma}}\|_{\mathcal{H}_2} = 0$. □

Introducing the concept of the minimal network realization is to facilitate the computation of a reduced-order model. As finding the minimal network takes much less effort than solving the pseudo Gramians and calculating vertex dissimilarities, see the simulation results in Section 6.4.

Remark 6.5. *It is worth mentioning that the minimal network realization is different from the concept of minimality in the sense of the controllability and observability of a state-space model. In a minimal network realization, all the vertices should not only be reachable and*

detectable but also have a certain dissimilarity. The minimal network is defined in the viewpoint of graph topologies. It, however, does not necessarily mean that the vertex states have to be controllable and observable.

The following proposition concludes the relation between the two types of minimal realizations, namely, the classical minimality is sufficient for network minimality, but not vice versa.

Proposition 6.2. *If the network system $\mathbf{\Sigma}$ is minimal, then $\mathbf{\Sigma}$ is also a minimal network realization.*

Proof. The system $\mathbf{\Sigma}$ in (6.2) is minimal means that it is both controllable and observable. Consider the pseudo Gramians of $\mathbf{\Sigma}$, $\mathcal{P}$ and $\mathcal{Q}$, which are defined in (3.7). Thereby, we obtain from Theorem 3.2, (3.8b) and (3.9b) that

$$\mathsf{rank}(\mathcal{P}) = n - m, \text{ and } \mathsf{ker}(\mathcal{P}) = \mathsf{im}(V), \tag{6.58}$$

and

$$\mathsf{rank}(\mathcal{Q}) = n - m, \text{ and } \mathsf{ker}(\mathcal{Q}) = \mathsf{im}(U), \tag{6.59}$$

where m is the number of LSCCs in $\mathcal{G}$, and $U, V \in \mathbb{R}^{n\times m}$ are defined in (6.14).

Now, assume that (6.2) is not a minimal network realization, i.e., it contains at least a pair of vertices that are clusterable and 0-dissimilar. Thus,

$$\mathcal{D}^I_{ij} = \sqrt{\mathbf{e}_{ij}^T \mathcal{P} \mathbf{e}_{ij}} = 0 \text{ or } \mathcal{D}^O_{ij} = \sqrt{\mathbf{e}_{ij}^T M^{-1} \mathcal{Q} M^{-1} \mathbf{e}_{ij}} = 0,$$

which means that $\mathbf{e}_{ij} \in \mathsf{ker}(\mathcal{P})$ or $\mathbf{e}_{ij} M^{-1} \in \mathsf{ker}(\mathcal{Q})$. However, Lemma 6.2 implies that for clusterable vertices i, j, $\mathbf{e}_{ij}^T U = 0$ and $\mathbf{e}_{ij}^T M^{-1} V = 0$. They mean that $\mathbf{e}_{ij} \notin \mathsf{im}(U)$ and $\mathbf{e}_{ij} \notin \mathsf{im}(M^{-1}V)$, which cause contradictions to (6.58).

Therefore, 0-dissimilar vertices cannot exist in a directed network system that is controllable and observable. □

A simple counterexample for the converse statement is given by a network example with only two vertices:

$$\mathcal{L} = \begin{bmatrix} 1 & -1 \\ -1 & 1 \end{bmatrix}, \; F = H^T = \begin{bmatrix} 1 & -1 \end{bmatrix}. \tag{6.60}$$

Both vertices are reachable and detachable by Definition 6.5, and the dissimilarity of the two vertices is $\mathcal{D}_{12} = 1$. Thus, this system is a minimal network realization. However, $\mathsf{rank}\,[F, -LF] = \mathsf{rank}\,\left[H^T, -L^T H^T\right] = 1$ implies that the system is uncontrollable and unobservable.

6.3.4 Clustering Algorithm and Error Computation

This subsection provides the algorithm for selecting an appropriate clustering for the network system $\mathbf{\Sigma}$. To this end, a *distance graph* of the network system $\mathbf{\Sigma}$ is defined. Let $\mathcal{X}$ be a matrix whose (i,j)-entry is given by

$$\mathcal{X}_{ij} = \begin{cases} \mathcal{D}_{ij}^{-1}, & \text{if vertices } i,j \text{ are clusterable;} \\ 0, & \text{otherwise.} \end{cases} \tag{6.61}$$

A larger value of $\mathcal{X}_{ij} \in \mathbb{R}_+$ indicates a higher similarity between vertices i, j. Clearly, $\mathcal{X}$ is nonnegative, symmetric and has zero diagonal entries. Thus, it can be seen as a weighted adjacency matrix that characterizes an undirected disconnected graph, namely a distance graph, denoted by $\mathcal{G}_D$. Denote the Laplacian matrix of $\mathcal{G}_D$ by

$$L_D = L_D^T = \mathsf{diag}(\mathcal{X}\mathbb{1}) - \mathcal{X}. \tag{6.62}$$

Note that $\mathcal{G}_D$ shares the same vertex set $\mathbb{V}$ with the original directed network $\mathcal{G}$. From e.g., [67], the *rank* of the undirected graph $\mathcal{G}_D$ is defined by $n - c$ with $n = |\mathbb{V}|$ and c the number of connected components of $\mathcal{G}_D$ which satisfies $c = \mathsf{rank}(L_D)$.

The idea of clustering algorithm is to remove certain edges of $\mathcal{G}_D$ such that it leaves r connected components, i.e., $\mathbb{V}$ is partitioned into r cells. Then we aggregate vertices in each cell as one vertex. Denote $\Omega := \mathsf{diag}(\omega_1, \omega_1, \cdots, \omega_{n_e})$, where n_e is the number of the edges of $\mathcal{G}_D$, and $\omega_1 \geq \omega_2 \geq \cdots \geq \omega_{n_e} > 0$ are the descending sort of the edge weights $\mathcal{X}_{ij}$. Let $\mathcal{B} \in \mathbb{R}^{n \times n_e}$ be the incidence matrix of L_D, then the graph clustering problem becomes finding a matrix partition

$$L_D = \mathcal{B}\Omega\mathcal{B}^T = \begin{bmatrix} \mathcal{B}_1 & \mathcal{B}_2 \end{bmatrix} \begin{bmatrix} \Omega_1 & 0 \\ 0 & \Omega_2 \end{bmatrix} \begin{bmatrix} \mathcal{B}_1^T \\ \mathcal{B}_2^T \end{bmatrix} \tag{6.63}$$

such that $\mathsf{rank}(\mathcal{B}_1\Omega_1\mathcal{B}_1^T) = n - r$, where r is the desired reduction order. $\mathcal{B}_2$ corresponds the edges of $\mathcal{G}_D$ with lower weights, namely, the edges connecting higher dissimilar vertices, and thus these edges are supposed to be removed. Thereby, the partition of $\mathbb{V}$ is generated by assign the vertices that are connected by the edges indicated by $\mathcal{B}_1$ into the same cell. Specifically, we describe the proposed clustering-based model reduction method as follows.

By Algorithm 3, a reduced-order network system $\hat{\mathbf{\Sigma}}$ is obtained, which achieves a bounded approximation error, see Theorem 6.1. Based on the proposed pseudo Gramians in Section 3.3, the following theorem then provides an efficient method to compute the $\mathcal{H}_2$ error between the original and the reduced-order network systems.

Theorem 6.4. *Let $\mathcal{P}_o$ and $\mathcal{P}_r$ be the pseudo controllability Gramians of the full-order and reduced-order network systems, $\mathbf{\Sigma}$ and $\hat{\mathbf{\Sigma}}$, respectively. Then, the approximation error*

Algorithm 3 Clustering-Based Reduction Algorithm

Input: $\mathcal{L}$, F and H, desired order r
Output: $\hat{\mathcal{L}}$, $\hat{F}$, and $\hat{H}$

1: Remove all the unreachable and undetectable vertices.
2: Find and merge the 0-dissimilar vertices by Proposition 6.1.
3: Compute the pseudo Gramians $\mathcal{P}$ and $\mathcal{Q}$ using Theorem 3.1 and Corollary 3.1.
4: Calculate the dissimilarity between clusterable vertices by Theorem 6.2, and construct the Laplacian matrix L_D in (6.62) for the distance graph.
5: Find a matrix partition (6.63) such that

$$\mathsf{rank}(\mathcal{B}_1\Omega_1\mathcal{B}_1^T) = n - r.$$

6: Compute $\Pi \in \mathbb{R}^{n\times r}$ according to $\mathcal{B}_1$.
7: Generate $\hat{\mathcal{L}}$ and $\hat{F}$ using the projection Π as in (6.12).

between $\mathbf{\Sigma}$ and $\hat{\mathbf{\Sigma}}$ is computed as

$$\|\mathbf{\Sigma} - \hat{\mathbf{\Sigma}}\|_{\mathcal{H}_2}^2 = \mathsf{tr}\left[H(\mathcal{P}_o + \Pi\mathcal{P}_r\Pi^T - 2\Pi\mathcal{P}_x)H^T\right], \tag{6.64}$$

where $\mathcal{P}_x := \tilde{\mathcal{P}}_x - \Pi^\dagger\mathcal{J}\Pi\tilde{\mathcal{P}}_x\mathcal{J}^T \in \mathbb{R}^{r\times n}$ with $\tilde{\mathcal{P}}_x$ an arbitrary symmetric solution of the following Sylvester equation:

$$\hat{\mathcal{L}}^T\tilde{\mathcal{P}}_x + \tilde{\mathcal{P}}_x\mathcal{L}^T - \Pi^\dagger(I - \mathcal{J})FF^T(I - \mathcal{J}^T) = 0. \tag{6.65}$$

Proof. To derive the approximation error, we consider the following system.

$$\mathbf{\Sigma_e} : \begin{cases} \dot{\omega}(t) = \mathcal{A}\omega(t) + \mathcal{B}u(t), \\ \delta(t) = \mathcal{C}\omega(t), \end{cases} \tag{6.66}$$

where the state vectors $\omega(t)^T := \left[x(t)^T, \hat{x}(t)^T\right]^T$, $\delta(t) := y(t) - \hat{y}(t)$, and

$$\mathcal{A} = -\begin{bmatrix} \mathcal{L} & 0 \\ 0 & \hat{\mathcal{L}} \end{bmatrix}, \ \mathcal{F} = \begin{bmatrix} F \\ \hat{F} \end{bmatrix}, \ \mathcal{H} = \begin{bmatrix} H & -\hat{H} \end{bmatrix}.$$

Obviously, $\|\mathbf{\Sigma_e}\|_{\mathcal{H}_2} = \|\mathbf{\Sigma} - \hat{\mathbf{\Sigma}}\|_{\mathcal{H}_2}$. Observe that $\mathbf{\Sigma_e}$ is a semistable system due to $\mathcal{A}$ matrix in (6.66), and by Theorem 6.1, the $\mathcal{H}_2$ norm of $\mathbf{\Sigma_e}$ is bounded. From Lemma 3.2, we obtain

$$\|\mathbf{\Sigma_e}\|_{\mathcal{H}_2}^2 = \mathsf{tr}(\mathcal{H}\mathcal{P}_e\mathcal{H}^T), \tag{6.67}$$

where $\mathcal{P}_e$ is the pseudo controllability Gramian of the error system $\mathbf{\Sigma_e}$.

To obtain $\mathcal{P}_e$, we refer to Theorem 3.1 that $\mathcal{P}_e$ is a solution of the Lyapunov equation

$$\mathcal{A}\tilde{\mathcal{P}}_e + \tilde{\mathcal{P}}_e\mathcal{A}^T + (I - \mathcal{J}_e)\mathcal{F}\mathcal{F}^T(I - \mathcal{J}_e^T) = 0. \tag{6.68}$$

Here, $\mathcal{J}_e := \text{blkdiag}(\mathcal{J}, \hat{\mathcal{J}})$ where $\hat{\mathcal{J}} = \Pi^\dagger \mathcal{J} \Pi$ is implied by (6.21). Let

$$\tilde{\mathcal{P}}_e = \begin{bmatrix} \tilde{\mathcal{P}}_o & \tilde{\mathcal{P}}_x^T \\ \tilde{\mathcal{P}}_x & \tilde{\mathcal{P}}_r \end{bmatrix}, \tag{6.69}$$

with $\tilde{\mathcal{P}}_o \in \mathbb{R}^{n\times n}$ and $\tilde{\mathcal{P}}_r \in \mathbb{R}^{r\times r}$. Accordingly, (6.68) is partitioned into three equations:

$$\begin{cases} \mathcal{L}\tilde{\mathcal{P}}_o + \tilde{\mathcal{P}}_o \mathcal{L}^T - (I_n - \mathcal{J})FF^T(I_n - \mathcal{J}^T) = 0, & \text{(6.70a)} \\ \hat{\mathcal{L}}\tilde{\mathcal{P}}_r + \tilde{\mathcal{P}}_r \hat{\mathcal{L}}^T - (I_r - \hat{\mathcal{J}})\hat{F}\hat{F}^T(I_r - \hat{\mathcal{J}}^T) = 0, & \text{(6.70b)} \\ \hat{\mathcal{L}}\tilde{\mathcal{P}}_x + \tilde{\mathcal{P}}_x \mathcal{L}^T - (I_r - \hat{\mathcal{J}})\hat{F}F^T(I_n - \mathcal{J}^T) = 0, & \text{(6.70c)} \end{cases}$$

where (6.70c) is equivalent to (6.65) due to $\hat{F} = \Pi^\dagger F$ and $\hat{\mathcal{J}}\Pi^\dagger = \Pi^\dagger \mathcal{J} \Pi\Pi\Pi^\dagger = \Pi^\dagger \mathcal{J}$ (see (6.22)). Then, using Corollary 3.1, the pseudo controllability Gramian of $\mathbf{\Sigma_e}$ is computed.

$$\begin{aligned} \mathcal{P}_e &= \tilde{\mathcal{P}}_e - \mathcal{J}_e \tilde{\mathcal{P}}_e \mathcal{J}_e^T \\ &= \begin{bmatrix} \tilde{\mathcal{P}}_o - \mathcal{J}\tilde{\mathcal{P}}_o\mathcal{J}^T & \tilde{\mathcal{P}}_x^T - \mathcal{J}\tilde{\mathcal{P}}_x^T\hat{\mathcal{J}}^T \\ \tilde{\mathcal{P}}_x - \hat{\mathcal{J}}\tilde{\mathcal{P}}_x\mathcal{J}^T & \tilde{\mathcal{P}}_r - \hat{\mathcal{J}}\tilde{\mathcal{P}}_r\hat{\mathcal{J}}^T \end{bmatrix} := \begin{bmatrix} \mathcal{P}_o & \mathcal{P}_x^T \\ \mathcal{P}_x & \mathcal{P}_r \end{bmatrix}, \end{aligned}$$

where $\mathcal{P}_o$ and $\mathcal{P}_r$ are the pseudo controllability Gramians of the systems $\mathbf{\Sigma}$ and $\hat{\mathbf{\Sigma}}$, respectively.

Thereby, we evaluate the approximation error as follows.

$$\begin{aligned} \|\mathbf{\Sigma} - \hat{\mathbf{\Sigma}}\|_{\mathcal{H}_2}^2 &= \mathsf{tr}\left(\begin{bmatrix} H & -\hat{H} \end{bmatrix} \begin{bmatrix} \mathcal{P}_o & \mathcal{P}_x^T \\ \mathcal{P}_x & \mathcal{P}_r \end{bmatrix} \begin{bmatrix} H^T \\ -\hat{H}^T \end{bmatrix} \right) \\ &= \mathsf{tr}(H\mathcal{P}_o H^T + \hat{H}\mathcal{P}_r\hat{H}^T - 2\hat{H}\mathcal{P}_x H^T), \end{aligned} \tag{6.71}$$

which leads to (6.64). □

Notice that the error in (6.64) can be also characterized by pseudo observability Gramians. Suppose $\mathcal{Q}_o$ and $\mathcal{Q}_r$ are the pseudo observability Gramians of $\mathbf{\Sigma}$ and $\hat{\mathbf{\Sigma}}$, respectively. Then, an alternative computation for (6.64) is

$$\|\mathbf{\Sigma} - \hat{\mathbf{\Sigma}}\|_{\mathcal{H}_2}^2 = \mathsf{tr}\left[F^T(\mathcal{Q}_o + (\Pi^\dagger)^T\mathcal{Q}_r\Pi^\dagger - 2\mathcal{Q}_x\Pi^\dagger)F\right], \tag{6.72}$$

where $\mathcal{Q}_x := \tilde{\mathcal{Q}}_x - \mathcal{J}^T\tilde{\mathcal{Q}}_x\Pi^\dagger\mathcal{J}\Pi \in \mathbb{R}^{n\times r}$ with $\tilde{\mathcal{Q}}_x$ an symmetric solution of the Sylvester equation:

$$\mathcal{L}^T\tilde{\mathcal{Q}}_x + \tilde{\mathcal{Q}}_x\hat{\mathcal{L}} - (I - \mathcal{J}^T)H^T H(I - \mathcal{J})\Pi = 0. \tag{6.73}$$

The proof for the above statement is similar to Theorem 6.4 and thus is omitted.

6.4 Numerical Examples

6.4.1 Sensor Network

A sensor network in [41] is considered and adapted to illustrate the proposed method in this chapter. The topology of the studied directed network is depicted in Fig. 6.2a, which is weakly connected and contains three LSCCs: $\{1, 2, 3, 4, 5\}$, $\{15, 16\}$ and $\{20\}$. All the directional edges have identical weights that equal to 1. The sets $\mathbb{V}_{\mathcal{I}} := \{2, 7, 16\}$ and $\mathbb{V}_{\mathcal{O}} := \{5, 9, 11\}$ are collections of controlled and measured vertices, respectively. The minimal network is realized by two steps. First, the unreachable vertex 20 and undetectable vertices 17, 18 and 19. Then, three pairs of 0-dissimilar vertices, namely $\{1, 5\}$, $\{8, 9\}$, and $\{13, 14\}$ are found by Proposition 6.1 and clustered to obtain Fig. 6.2b, which is still weakly connected as there are two LSCCs.

By considering the effects of both inputs and outputs, we compute the vertex dissimilarities of the minimal network using Theorem 6.2. Then, to yield a reduced-order network system of 7 vertices, we apply Algorithm 3, that leads to the following graph clustering

$$\mathcal{C}_1 = \{1, 2, 3, 4\},\ \mathcal{C}_2 = \{5, 6\},\ \mathcal{C}_3 = \{7\},$$
$$\mathcal{C}_4 = \{8\},\ \mathcal{C}_5 = \{9\},\ \mathcal{C}_6 = \{10, 11\},\ \mathcal{C}_7 = \{12, 13\}.$$

Thus, a simplified directed network is constructed as in Fig. 6.3a, which indicates that the network structure is preserved in the new model. Also, the approximation error is computed: $\|\mathbf{\Sigma} - \hat{\mathbf{\Sigma}}\|_{\mathcal{H}_2} = 0.1969$. Next, we only use the input information for selecting clusters, namely, only the input dissimilarities are considered as the criteria for the partition of the vertices. As a result, we obtain a different clustering of the minimal network, where $\mathcal{C}_2 = \{5, 7\}$, and $\mathcal{C}_3 = \{6\}$. This produces a simplified directed network with a different topology as shown in Fig. 6.3b. In this case, the approximation error is evaluated as $\|\mathbf{\Sigma} - \hat{\mathbf{\Sigma}}\|_{\mathcal{H}_2} = 0.2514$, which is almost 30% larger than the one obtained in the former case. Thus, to better approximate the input-output behavior of a network system, the output distributions should also be considered in order to construct a more accurate reduced-order network model.

6.4.2 Large-Scale Directed Network

The efficiency of the proposed approach is verified by a large-scale directed network example, see Fig. 6.4. Note that the methods in [41, 84] are not applicable for this networks, since it is not strongly connected. The data of directed weighted graph is acquired from The Harwell-Boeing Sparse Matrix Collection, which is available

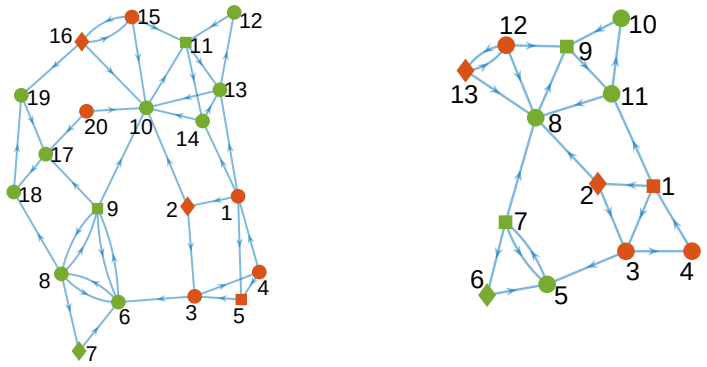

(a) (b)

Figure 6.2: (a) A directed sensor network consisting of 20 vertices. (b) A minimal network realization of this directed network, which is obtained by removing vertices 17, 18, 19, 20 and merging pairs $\{1, 5\}$, $\{8, 9\}$, $\{13, 14\}$ in Fig. 6.2a. In both figures, the controlled and measured vertices are labeled as diamonds and squares, respectively.

(a) (b)

Figure 6.3: (a) The reduced directed network generated by the proposed dissimilarity-based clustering. (b) The alternative directed network obtained by only considering the input dissimilarity. In the two figures, vertex 1 is labeled as a hexagram indicating that it is controlled and measured simultaneously.

at https://math.nist.gov/MatrixMarket/data/Harwell-Boeing. In this chapter, the simulation is implemented with Matlab 2018a in the environment of 64-bit operating system, which is equipped with Intel Core i5-3470 CPU @ 3.20GHz, RAM 8.00 GB.

We select three controlled and three measured vertices: $\mathbb{V}_{\mathcal{I}} := \{1, 152, 728\}$ and $\mathbb{V}_{\mathcal{O}} := \{246, 615, 733\}$. For comparison purposes, we reduce the original networks by

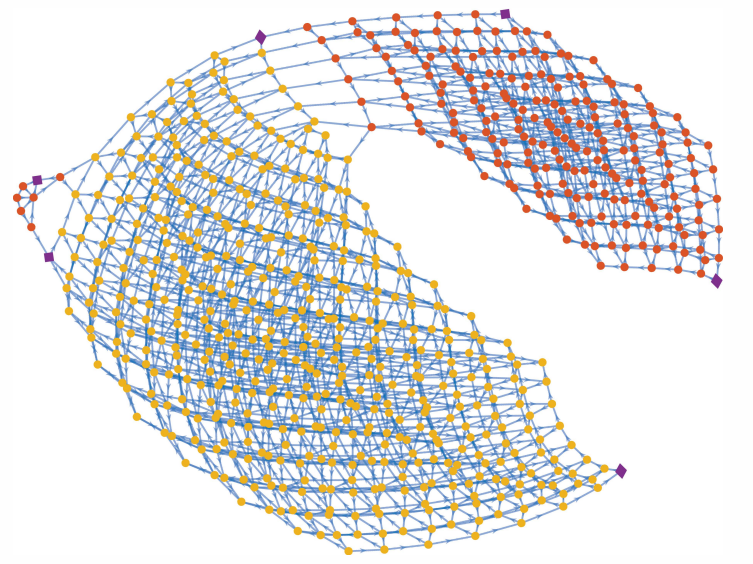

Figure 6.4: A weakly connected directed network consisting of 735 vertices, where the controlled and measured vertices are labeled as diamonds and squares, respectively.

the dissimilarity-based (proposed method in this chapter), input dissimilarity-based (the methods in e.g., [41]) and random clustering methods, respectively. The $\mathcal{H}_2$-norm approximation errors of the reduced models with different dimensions from 10 vertices to 700 are computed by Theorem 6.4, see the Fig. 6.5, which shows that the proposed method considering the output efforts as well generally has a better performance than the one only take into account the influence of inputs. The approximation errors of both methods decay rapidly when the reduced order $r < 100$, and they both have a distinct advantage over the random clustering method, where the cells are selected randomly from the largest clusterable sets. Note that when $r = 100$, the approximation errors $\|\mathbf{\Sigma} - \hat{\mathbf{\Sigma}}\|_{\mathcal{H}_2} = 0.0011$, while the maximal values of input and output dissimilarities are 0.8839 and 3.6949, respectively. Hence, the reduced-order network with 100 vertices provides a rather accurate approximation of the original 735-vertex network. To illustrate the efficiency of the proposed method, when producing the 100-dimensional reduced network, we record and list the computational cost for each step in Table 6.1. It indicates that the majority of the computation time is spent on solving the pseudo Gramians. In contrast, the time for computing the minimal network, vertex dissimilarities and for the clustering algorithm is much less. To be more efficient for even larger networks, e.g., $n > 5000$, we can consider the

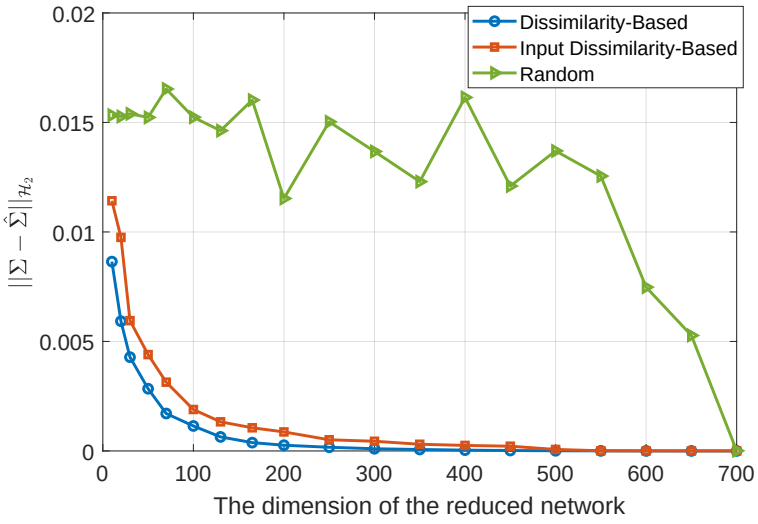

Figure 6.5: Approximation error comparisons among the proposed dissimilarity-based clustering, input dissimilarity-based clustering and random clustering algorithms.

Alternating Direction Implicit (ADI) method or Krylov subspace method to generate low rank approximations to the solutions of the Lyapunov equations in (3.8) and (3.9). As these numerical algorithms are more effective than the standard approach due to the sparsity of the Laplacian matrix $\mathcal{L}$. We refer to e.g., [93,105] for more details. However, we do not apply these here since we can still compute the Gramians using standard approach within a reasonable time. Hence, it is no need for such an approximation.

In Fig. 6.6, the topologies of reduced-order networks with different dimensions are plotted to demonstrate the preservation of directed network structures. In conclusion, this simulation example shows that the proposed clustering method is feasible and effective in model reduction of large-scale directed network systems.

6.5 Conclusions

This chapter solves a structure preserving model reduction problem for directed network systems that obey locally consensus protocols and have semistable dynamics. The notion of clusterability is proposed to classify the groups of vertices that can be aggregated to guarantee a bounded approximation error. The pairwise dissimilarity,

Table 6.1: Computation time for each step

Minimal Network	23.8949s
Pseudo Gramians	538.0895s
Dissimilarity	99.5960s
Graph Clustering	0.0035s

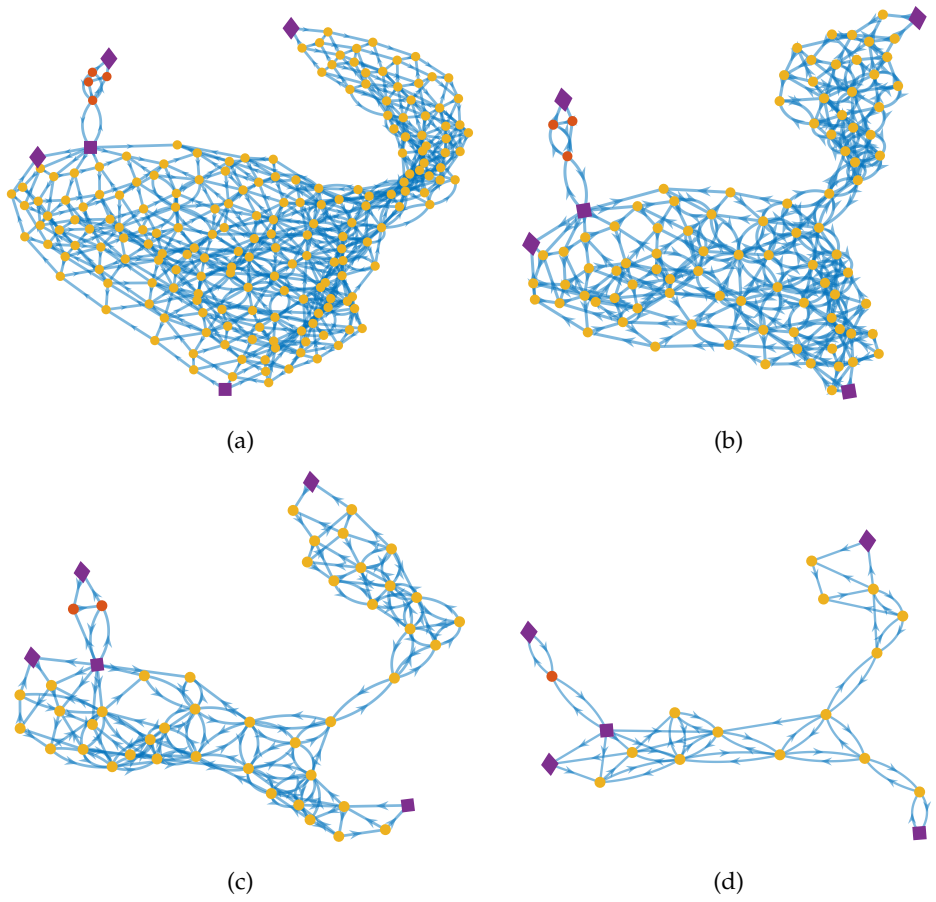

(a) (b) (c) (d)

Figure 6.6: Reduced directed networks with different dimensions. (a) $r = 200$; (b) $r = 100$; (c) $r = 50$; (d) $r = 20$.

quantifying the difference between two clusterable vertices, can be characterized for a directed network based on the pseudo controllability and observability Gramians of semistable systems in Chapter 3. A graph clustering algorithm then disassembles the vertices that behave differently. The reduced-order model is obtained in the Petrov-Galerkin framework with projections generated from the resulting clustering of the network. It is shown that the reduced-order model preserves a network structure among the clusters, as a reduced Laplacian matrix. The proposed method provides an effective way to reducing the complexity of linear network systems. However, the extension to this result to nonlinear networks is not straightforward. For networks with nonlinear coupling or nonlinear nodal dynamics, the primary problem to investigate is: how to determine and evaluate the dissimilarities between the vertices when we cannot use the $\mathcal{H}_2$ norms as in the linear case? In this thesis, we will not discuss the clustering-based approaches for nonlinear networks, and we leave it for our future research.

Part II

BALANCED TRUNCATION OF NETWORK SYSTEMS

CHAPTER 7

Balanced Truncation of Networked Linear Passive Systems

This chapter studies model order reduction of multi-agent systems consisting of identical linear passive subsystems, where the interconnection topology is characterized by an undirected weighted graph. Balanced truncation based on a pair of specifically selected generalized Gramians is implemented on the asymptotically stable part of the full-order network model, which leads to a reduced-order system preserving the passivity of each subsystem. Moreover, it is proven that there exists a coordinate transformation to convert the resulting reduced-order model to a state-space model of Laplacian dynamics. Thus, the proposed method simultaneously reduces the complexity of the network structure and individual agent dynamics, and it preserves the passivity of the subsystems and the synchronization of the network. Moreover, it allows for the *a priori* computation of a bound on the approximation error. Finally, the feasibility of the method is demonstrated by an example.

7.1 Introduction

For model order reduction with the preservation of network structure, mainstream methodologies are focusing on graph clustering, see the results in Part I. From the results of networked single integrators in Chapter 3, Chapter 5 and papers [34, 36, 86, 87, 126, 127], we have observed that the clustering-based approaches naturally maintain the spatial structure of networks and show an insightful physical inter-

pretation for the reduction process. Further extensions to directed and second-order networks can be found in [35, 84] and Chapter 3. Nevertheless, the approximation accuracy of these methods highly relies on the selection of node clusters, and finding a reduced network with the best approximation in general is an NP-hard problem, see [94]. A combination of the Krylov subspace method with graph clustering is proposed by [122], where a reduced-order model is firstly found by the Iterative Rational Krylov Algorithm (IRKA), and then the partition of network nodes is obtained by the QR decomposition with column pivoting on the projection matrix. However, no error bound is provided for the network approximation. Differently, the work [21] considers so-called edge dynamics of networks with a tree topology, and the importance of edges is characterized by generalized edge controllability and observability Gramians. Nodes linked by the less important edges are clustered, and an *a priori* bound for the approximation error is then computed based on the generalized singular values of the edge dynamics. Nonetheless, the application of this approach is still restrictive since the reduction process and error bound are heavily reliant on the tree topology of the studied network. Another attempt to simplify the complexity of network structure is developed based on singular perturbation approximation, which is mainly applied to electrical grids and chemical reaction networks (see e.g., [26, 46, 142] and references therein). The network structure is preserved as the Schur complement of the Laplacian matrix of the original network is again a Laplacian matrix, which represents a smaller-scale network. Despite the simplicity, it is challenging to implement this approach for multi-agent systems with higher-order agent dynamics as the Laplacian matrix is coupled with agent systems in this case.

In contrast to clustering-based approaches, as discussed in Part I, the generalized balanced truncation method can be applied to reduce multi-agent systems by lowering the dimension of the individual subsystem while keeping the interconnection topology untouched. Related methods can be found in [125, 152] which are developed based on the generalization of balanced truncation, and can be interpreted as structure-preserving model reduction procedures.

In this chapter, we aim to find a technique that can reduce the complexity of network structures and individual agent dynamics simultaneously, extending preliminary results in [40]. This problem setting has been only seldom studied in the literature so far, and different from [86], we aim to reduce the network structure and agent dynamics in a unified framework. Particularly, this chapter considers multi-agent systems composed of identical higher-order linear passive subsystems, where the interconnection topology is characterized by an undirected weighted graph. It is remarked that passive systems are natural candidates to model many types of real physical systems and the passivity property benefits the synchronization and

stability analysis of network systems [90,100,113,172]. The core step in the proposed reduction technique for networked passive systems is balancing the asymptotically stable part based on generalized Gramians. After truncating the balanced model, we obtain a reduced-order system that has a lower dimension and has preserved the passivity of the subsystems. Although the network structure is not necessarily preserved in this step, a novel coordinate transformation is applied to convert the resulting reduced-order model to its equivalent state-space realization of Laplacian dynamics, which represents a simplified network with fewer agents. The network structure we show that there exists a set of coordinates in which the reduced-order model can again be interpreted as a network system. Specifically, the main contributions of this chapter are summarized as follows:

First, the balancing method is used for the reduction of multi-agent systems in a structure-preserving manner. Based on two selected generalized Gramians, the balanced truncation is applied to reduce the network structure and agent dynamics via a unified framework. The obtained reduced-order model can potentially achieve a smaller approximation error than the other network reduction approaches, e.g., graph clustering. Furthermore, unlike [86,122,126], the proposed method also guarantees the *a priori* computation of a bound on the approximation error with respect to external inputs and outputs.

Second, this chapter proposes the necessary and sufficient condition of a matrix being similar to a Laplacian matrix (see Theorem 7.2). Using this result, the reduction process is designed to preserve the Laplacian structure in the reduced network. It is verified that the reduced-order model maintains the passivity of the agent dynamics and inherits a network interpretation. Consequently, the synchronization property is restored in the reduced-order multi-agent system.

Third, the studied models of the multi-agent dynamics are relatively general in terms of the network topology and the structures of the input and output matrices. Specifically, the underlying communication graph, in contrast to [21], can be formed with various topologies, which do not restricted to tree graphs. Furthermore, there are no restrictions on the input and output distributions. Unlike the clustering-based approaches in e.g. [34,35,84,86], the effort of state observability is also considered. Moreover, we do not assume special structure of the output matrix as in [122,126], which consider weighted incidence matrix as an output matrix.

The remainder of this chapter is organized as follows. Section 7.2 provides the preliminaries regarding passivity and formulates the model reduction problem of networked passive systems. Then, the approximation procedure based on the balanced truncation approach is presented in Section 7.3, which provides the main results of this chapter. Finally, the proposed method is illustrated by means of an example in Section 7.4 and some concluding remarks are summarized in Section 7.5.

7.2 Preliminaries and Problem Formulation

Consider a network of N vertices, and the dynamics on each vertex is described by the following linear time-invariant model

$$\mathbf{\Sigma_i}: \begin{cases} \dot{x}_i = Ax_i + B\nu_i, \\ \eta_i = Cx_i, \end{cases} \tag{7.1}$$

where $x_i \in \mathbb{R}^n$, $\nu_i \in \mathbb{R}^m$ and $\eta_i \in \mathbb{R}^m$ are the states, control inputs and outputs of agent i, respectively. Throughout the chapter, we assume that the system realization in (7.1) is *minimal* and *passive* (see Definition 2.9). Passivity is a natural property of many real physical systems, including mechanical systems, power networks, and thermodynamical systems (see e.g., [76, 100, 172]).

In a multi-agent system, all the agents are interacting through a weighted undirected connected graph $\mathcal{G}$ containing N vertices. For agent i, the static communication protocol is implemented as

$$\nu_i = -\sum_{j=1, j\neq i}^{N} w_{ij}\left(\eta_i - \eta_j\right) + \sum_{j=1}^{p} f_{ij}u_j, \tag{7.2}$$

where $w_{ij} \in \mathbb{R} \geq 0$ stands for the intensity of the coupling between vertices i and j. Besides, $u_j \in \mathbb{R}^m$ with $j = \{1, 2, \cdots, p\}$ are external control signals acting on the agents, and $f_{ij} \in \mathbb{R}$ represents the amplification of the j-th input acting on agent i, which is zero when u_j has no effect on vertex i. Similarly, $y_i \in \mathbb{R}^m$ is the i-th external output, which is introduced as

$$y_i = \sum_{j=1}^{N} h_{ij}\eta_j,\ i = 1, 2, \cdots, q, \tag{7.3}$$

where $h_{ij} \in \mathbb{R}$. Combining (7.1), (7.2), and (7.3), we obtain the total multi-agent system in a compact form as

$$\mathbf{\Sigma}: \begin{cases} \dot{x} = \left(I_N \otimes A - L \otimes BC\right)x + (F \otimes B)u, \\ y = (H \otimes C)x. \end{cases} \tag{7.4}$$

Here, $F \in \mathbb{R}^{N\times p}$ and $H \in \mathbb{R}^{q\times N}$ are the collections of f_{ij} and h_{ij}, respectively, and $x := \left[x_1^T, \cdots, x_n^T\right]^T \in \mathbb{R}^{Nn}, u := \left[u_1^T, \cdots, u_p^T\right]^T \in \mathbb{R}^{pm}, y := \left[y_1^T, \cdots, y_q^T\right]^T \in \mathbb{R}^{qm}$ are the combined state vector, external control inputs and measured outputs, respectively. Furthermore, $L \in \mathbb{R}^{N\times N}$ is the *Laplacian matrix* of the underlying graph $\mathcal{G}$ with the (i, j)-th entry as

$$L_{ij} = L_{ji} = \begin{cases} \sum_{j=1, j\neq i}^{N} w_{ij}, & \text{if } i = j, \\ -w_{i,j}, & \text{otherwise.} \end{cases} \tag{7.5}$$

This chapter assumes that the underlying graph $\mathcal{G}$ is *undirected* and *connected*, such that the Laplacian matrix L has the properties described in Lemma 2.1.

Here, we address the model order reduction problem for multi-agent systems of the form (7.4) as follows.

Problem 7.1. *Given a multi-agent system $\mathbf{\Sigma}$ as in (7.4), find a reduced-order model*

$$\hat{\mathbf{\Sigma}} : \begin{cases} \dot{\hat{x}} = (I_k \otimes \hat{A} - \hat{L} \otimes \hat{B}\hat{C})\hat{x} + (\hat{F} \otimes \hat{B})u, \\ \hat{y} = (\hat{H} \otimes \hat{C})\hat{x}, \end{cases} \tag{7.6}$$

such that the following objectives are achieved:

- *$\hat{L} \in \mathbb{R}^{k\times k}$, with $k \leq N$, is an undirected graph Laplacian satisfying the structural conditions in Lemma 2.1.*

- *The lower-order approximation of the agent dynamics*

$$\hat{\mathbf{\Sigma}}_\mathbf{i} : \begin{cases} \dot{\hat{x}}_i = \hat{A}\hat{x}_i + \hat{B}\hat{\nu}_i, \\ \hat{\eta}_i = \hat{C}\hat{x}_i, \end{cases} \tag{7.7}$$

  with the reduced state vector $\hat{x}_i \in \mathbb{R}^r$ ($r \leq n$), is passive, i.e., satisfies the KYP condition in Lemma 2.4.

- *The overall approximation error $\|\mathbf{\Sigma} - \hat{\mathbf{\Sigma}}\|_{\mathcal{H}_\infty}$ is small.*

It is worth emphasizing that the *simultaneous* reduction of both the agent dynamics and the interconnection structure is pursued in Problem 7.1.

Remark 7.1. *If $k = N$ and $r < n$, the above problem setting can be specialized to reduce the dimension of each subsystems as in [125, 152]. When $k < N$ and $r = n$, then the simplification of the network structure is discussed as in [21, 122], where the reduction is based on graph clustering.*

This chapter proposes to address Problem 7.1 using the following two-step procedure. First, to pursue the preservation of passivity for the subsystem and a small approximation error, we exploit a pair of generalized Gramians for the balanced truncation of $\mathbf{\Sigma}$. Second, a specific coordinate transformation is introduced that, when applied to the reduced-order system obtained in the first step, recovers a network interpretation for this model by guaranteeing the properties in Lemma 2.1.

7.3 Main Results

The minimality and passivity of the subsystems does not guarantee that the whole system $\mathbf{\Sigma}$ is asymptotically stable. Therefore, to apply Lyapunov balancing, Section 7.3.1 isolates the asymptotically stable part of $\mathbf{\Sigma}$, and Section 7.3.2 then derives the lower-order approximation of $\mathbf{\Sigma}$ using a balanced truncation method based on generalized Gramians. To preserve the network structure, a coordinate transformation is proposed in Section 7.3.3, to restore the Laplacian structure in the reduced-order model.

7.3.1 Separation of Network System

The split of $\mathbf{\Sigma}$ is based on the fact that L is a symmetric matrix with a single simple zero eigenvalue, as stated in Lemma 2.1. We therefore consider the following *spectral decomposition* of the Laplacian matrix as:

$$L = T\Lambda T^T = \begin{bmatrix} T_1 & T_2 \end{bmatrix} \begin{bmatrix} \bar{\Lambda} & \\ & 0 \end{bmatrix} \begin{bmatrix} T_1^T \\ T_2^T \end{bmatrix}, \tag{7.8}$$

where $T_2 = \mathbb{1}/\sqrt{N} \in \mathbb{R}^N$ by the first condition in Lemma 2.1, and

$$\bar{\Lambda} := \mathsf{diag}(\lambda_1, \lambda_2, \cdots, \lambda_{N-1}), \tag{7.9}$$

with $\lambda_1 \geq \lambda_2 \geq \cdots \geq \lambda_{N-1} > 0$ the nonzero eigenvalues of L. Then, applying a coordinate transformation $x = (T \otimes I)z$, to $\mathbf{\Sigma}$ yields

$$\begin{cases} \dot{z} = (I \otimes A - \Lambda \otimes BC)\, z + (T^T F \otimes B)u, \\ y = (HT \otimes C)z. \end{cases} \tag{7.10}$$

Observe that (7.8) implies the structure

$$I \otimes A - \Lambda \otimes BC = \mathsf{blkdiag}(I \otimes A - \bar{\Lambda} \otimes BC, A). \tag{7.11}$$

Since A in (7.1) is not necessarily Hurwitz, meaning that the overall system $\mathbf{\Sigma}$ may not be asymptotically stable, a direct application of the balanced truncation method to $\mathbf{\Sigma}$ is not feasible. To overcome this difficulty, we split the system $\mathbf{\Sigma}$ into two components connected in parallel as in Fig. 7.1. In Fig. 7.1, we have the *average module* as

$$\mathbf{\Sigma_a}: \begin{cases} \dot{z}_a = Az_a + \dfrac{1}{\sqrt{N}}(\mathbb{1}_N^T F \otimes B)u, \\ y_a = \dfrac{1}{\sqrt{N}}(H\mathbb{1}_N \otimes C)z_a, \end{cases} \tag{7.12}$$

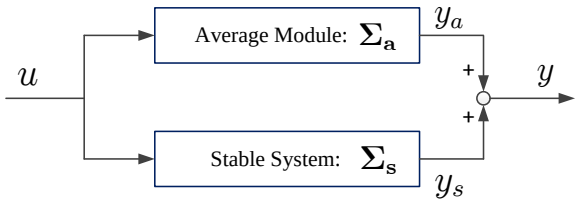

Figure 7.1: The separation of the multi-agent system.

with $z_a \in \mathbb{R}^n$, and the stable system as

$$\mathbf{\Sigma_s}: \begin{cases} \dot{z}_s = (I_{N-1} \otimes A - \bar{A} \otimes BC)z_s + (\bar{F} \otimes B)u, \\ y_s = (\bar{H} \otimes C)z_s. \end{cases} \tag{7.13}$$

where $z_s \in \mathbb{R}^{(N-1)\times n}$, $\bar{F} = T_1^T F$, and $\bar{H} = HT_1$. The synchronization property is proved using the asymptotic stability of $\mathbf{\Sigma_s}$ in the following lemma.

Lemma 7.1. *Consider the network system $\mathbf{\Sigma}$ in (7.4), where the graph $\mathcal{G}$ is connected, and each subsystem $\mathbf{\Sigma_i}$ in (7.1) is observable. Then, $\mathbf{\Sigma}$ synchronizes for $u = 0$, i.e.,*

$$\lim_{t\to\infty} [x_i(t) - x_j(t)] = 0, \ \ \forall i, j \in \{1, 2, \cdots, N\} \tag{7.14}$$

for any initial condition $x_i(0)$, $i = 1, 2, \cdots, N$.

Proof. The connectedness implies that $\bar{A}$ in (7.13) is diagonal and positive definite. If the passive system in (7.1) is observable, then any negative feedback $\nu_i(t) = -\lambda\eta_i(t) = -\lambda BCx_i$, with $\lambda > 0$, asymptotically stabilizes the origin $x_i = 0$ (see [76, Thm. 2.18]). Then, a closed-loop system of (7.1) defined by

$$\dot{x} = (A - \lambda_i BC)x \tag{7.15}$$

is asymptotically stable for any $i = 1, 2, \cdots, N-1$. Note that

$$I \otimes A - \bar{A} \otimes BC = \mathsf{blkdiag}(A - \lambda_1 BC, \cdots, A - \lambda_{N-1} BC).$$

Hence, $\mathbf{\Sigma_s}$ is asymptotically stable, which means the synchronization of $\mathbf{\Sigma}$ by e.g. [107, 125]. □

The above proof implies that $\mathbf{\Sigma_s}$ is asymptotically stable. Thus, it can be balanced and truncated to generate a lower-order approximation $\hat{\mathbf{\Sigma}}_\mathbf{s}$, which gives the reduced subsystems $(\hat{A}, \hat{B}, \hat{C})$ resulting in a reduced-order average module $\hat{\mathbf{\Sigma}}_\mathbf{a}$. Then, combining $\hat{\mathbf{\Sigma}}_\mathbf{s}$ with $\hat{\mathbf{\Sigma}}_\mathbf{a}$ formulates a reduced-order model $\tilde{\mathbf{\Sigma}}$ whose input-output behavior is

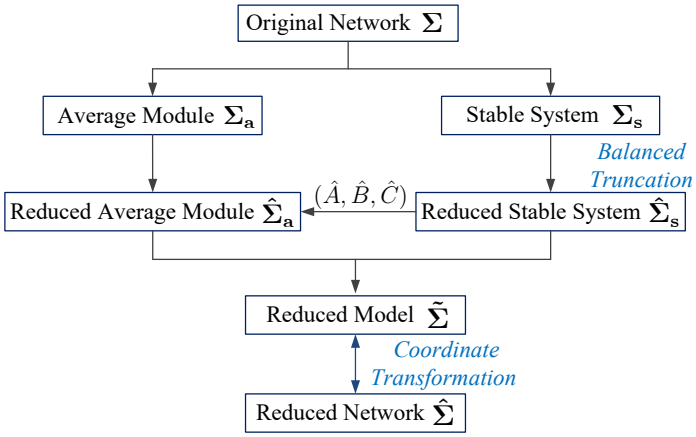

Figure 7.2: The scheme for the structure preserving model order reduction of networked passive systems

similar to that of the original system $\boldsymbol{\Sigma}$. However, at this stage, the network structure is not necessarily preserved by $\tilde{\boldsymbol{\Sigma}}$. Therefore, in the second step, by a particular coordinate transformation, we remodel $\tilde{\boldsymbol{\Sigma}}$ as $\hat{\boldsymbol{\Sigma}}$, which restores the algebraic structure of a Laplacian matrix. The whole procedure is summarized in Fig. 7.2, and the detailed implementations are discussed in the following subsections.

7.3.2 Balanced Truncation by Generalized Gramians

Following [58], the generalized Gramians of the asymptotically stable system $\boldsymbol{\Sigma}_\mathbf{s}$ are defined.

Definition 7.1. *Consider the stable system $\boldsymbol{\Sigma}_\mathbf{s}$ in (7.13), and denote $\Phi := I \otimes A - \bar{\Lambda} \otimes BC$. Two positive definite matrices $\mathcal{X}$ and $\mathcal{Y}$ are said to be the generalized controllability and observability Gramians of $\boldsymbol{\Sigma}_\mathbf{s}$, respectively, if they satisfy*

$$\Phi\mathcal{X} + \mathcal{X}\Phi^T + (\bar{F} \otimes B)(\bar{F}^T \otimes B^T) \preccurlyeq 0, \tag{7.16a}$$

$$\Phi^T\mathcal{Y} + \mathcal{Y}\Phi + (\bar{H}^T \otimes C^T)(\bar{H} \otimes C) \preccurlyeq 0. \tag{7.16b}$$

Moreover, a generalized balanced realization is achieved when $\mathcal{X} = \mathcal{Y} > 0$ are diagonal. The diagonal entries are called generalized Hankel singular values (GHSVs).

To find a pair of generalized Gramians, we first consider the following accompanying system of $\boldsymbol{\Sigma}_\mathbf{s}$, which only contains the information of the network configuration:

$$\dot{\bar{z}} = -\bar{\Lambda}\bar{z} + \bar{F}u, \;\; \bar{y} = \bar{H}\bar{z}, \tag{7.17}$$

where $\bar{\Lambda}$ is defined in (7.9). Assume $\bar{\Lambda}$ in (7.9) has s distinct diagonal entries ordered as: $\bar{\lambda}_1 > \bar{\lambda}_2 > \cdots > \bar{\lambda}_s$. We then rewrite it as

$$\bar{\Lambda} = \mathsf{blkdiag}(\bar{\lambda}_1 I_{m_1}, \bar{\lambda}_2 I_{m_2} \cdots, \bar{\lambda}_s I_{m_s}), \tag{7.18}$$

where m_i is the multiplicity of $\bar{\lambda}_i$, and $\sum_{i=1}^{s} m_i = N - 1$.

In order to guarantee that the reduced-order model will satisfy the desired properties in Problem 7.1, we define the generalized controllability and observability Gramians of (7.17) as the solutions X and Y to the following Lyapunov equation and inequality, respectively:

$$-\bar{\Lambda}X - X\bar{\Lambda} + \bar{F}\bar{F}^T = 0, \tag{7.19a}$$
$$-\bar{\Lambda}Y - Y\bar{\Lambda} + \bar{H}^T\bar{H} \preccurlyeq 0. \tag{7.19b}$$

Here, $X = X^T \succ 0$ and Y is

$$Y := \mathsf{blkdiag}(Y_1, Y_2, \cdots, Y_s), \tag{7.20}$$

with $Y_i = Y_i^T \succ 0$ and $Y_i \in \mathbb{R}^{m_i \times m_i}$, for $i = 1, 2, \cdots, s$. The block-diagonal structure of Y in (7.20) is crucial as it guarantees that the reduced-order model, obtained by performing balanced truncation on the basis of X and Y, can be interpreted as a network system again, see Lemma 7.2 and Theorem 7.2. Note that a constraint on the algebraic structure of X is not required for the preservation of network structure. Therefore, we use the standard controllability Gramian characterized by (7.19a) in order to achieve a lower error bound. Compared with our former notation in [40], the definition of the observability Gramian is more general, since it is not necessary to be strictly diagonal.

Remark 7.2. *There exist a variety of networks, especially symmetric ones such as stars, circles, chains or complete graphs, whose Laplacian matrices have repeated eigenvalues. Particularly, when L refers to a complete graph with identical weights, all the eigenvalues in (7.9) are equal. Then, Y becomes a full matrix, and (7.19b) is specialized to an equality. Besides, by the duality between controllability and observability, we can also use*

$$-\bar{\Lambda}X - X\bar{\Lambda} + \bar{F}\bar{F}^T \preccurlyeq 0, \tag{7.21a}$$
$$-\bar{\Lambda}Y - Y\bar{\Lambda} + \bar{H}^T\bar{H} = 0. \tag{7.21b}$$

to characterize the pair X and Y for the balanced truncation, where X now is constrained to have a block-diagonal structure.

The existence of the solutions X and Y in (7.19a) and (7.19b) are guaranteed, as $\bar{\Lambda} \succ 0$ is positive diagonal and has the structure as given in (7.18). Furthermore, in

practice, the generalized observability Gramian is obtained by minimizing the trace of Y, see e.g., [21, 152].

Next, based on X and Y, we further define a pair of generalized Gramians for the stable system $\mathbf{\Sigma_s}$, and therefore a balancing transformation can be applied in the following theorem.

Theorem 7.1. *Consider X, Y as the generalized Gramians of the accompanying system in (7.17), and let $K_m \succ 0$ and $K_M \succ 0$ be the minimum and maximum solutions of*

$$A^T K + KA \preccurlyeq 0,\ C = B^T K. \tag{7.22}$$

Then, the matrices

$$\mathcal{X} := X \otimes K_M^{-1} \text{ and } \mathcal{Y} := Y \otimes K_m \tag{7.23}$$

characterize generalized Gramians of the asymptotically stable system $\mathbf{\Sigma_s}$, i.e., satisfying the inequalities in (7.16a) and (7.16b), respectively.

Moreover, there exists a nonsingular matrix $\mathcal{T}$ such that $\mathbf{\Sigma_s}$ is balanced, i.e.,

$$\mathcal{T}\mathcal{X}\mathcal{T}^T = \mathcal{T}^{-T}\mathcal{Y}\mathcal{T}^{-1} = \Sigma_{\mathcal{G}} \otimes \Sigma_{\mathcal{D}}, \tag{7.24}$$

Here, $\Sigma_{\mathcal{G}} := \operatorname{diag}\{\sigma_1, \sigma_2, \cdots, \sigma_{N-1}\}$, and $\Sigma_{\mathcal{D}} := \operatorname{diag}\{\tau_1, \tau_2, \cdots, \tau_n\}$, where $\sigma_1 \geq \sigma_2 \geq \cdots \geq \sigma_{N-1}$, and $\tau_1 \geq \tau_2 \geq \cdots \geq \tau_n$ are corresponding to the square roots of the spectrum of XY and $K_M^{-1}K_m$, respectively.

Proof. The LMI (7.22) follows from the KYP condition in Lemma 2.4 as $\mathbf{\Sigma_i}$ in (7.1) is passive. We verify that

$$\begin{aligned}
&\Phi\mathcal{X} + \mathcal{X}\Phi^T + (\bar{F} \otimes B)(\bar{F}^T \otimes B^T) \\
=&(X \otimes AK_M^{-1} - \bar{\Lambda}X \otimes BCK_M^{-1}) \\
&+ (X \otimes K_M^{-1}A^T - X\bar{\Lambda} \otimes K_M^{-1}C^T B^T) + \bar{F}\bar{F}^T \otimes BB^T \\
=&X \otimes (AK_M^{-1} + K_M^{-1}A^T) \\
&\qquad + (-\bar{\Lambda}X - X\bar{\Lambda} + \bar{F}\bar{F}^T) \otimes BB^T \preccurlyeq 0,
\end{aligned}$$

where the inequality holds due to (7.19a) and K_M being a solution of (7.22). Similarly, it can be verify that $\mathcal{Y}$ in (7.23) satisfies the inequality in (7.16b). Thus, by Definition (7.1), $\mathcal{X}$ and $\mathcal{Y}$ in (7.23) characterize the generalized Gramians of $\mathbf{\Sigma_s}$. Next, by the standard balancing theorem [7], there exists nonsingular matrices $T_{\mathcal{G}}$ and $T_{\mathcal{D}}$ such that

$$T_{\mathcal{G}} X T_{\mathcal{G}}^T = \Sigma_{\mathcal{G}} = T_{\mathcal{G}}^{-T} Y T_{\mathcal{G}}^{-1}, \tag{7.25a}$$

$$T_{\mathcal{D}} K_M^{-1} T_{\mathcal{D}}^T = \Sigma_{\mathcal{D}} = T_{\mathcal{D}}^{-T} K_m T_{\mathcal{D}}^{-1}. \tag{7.25b}$$

Thus, a balancing transformation for $\mathbf{\Sigma_s}$ is given by

$$\mathcal{T} = T_{\mathcal{G}} \otimes T_{\mathcal{D}}, \tag{7.26}$$

which can be verified to satisfy (7.24). Moreover, due to

$$\begin{aligned} T_{\mathcal{G}} X Y T_{\mathcal{G}}^{-1} &= T_{\mathcal{G}} X T_{\mathcal{G}}^{T} T_{\mathcal{G}}^{-T} Y T_{\mathcal{G}}^{-1} = \Sigma_{\mathcal{G}}^2, \\ T_{\mathcal{D}} K_M^{-1} K_m T_{\mathcal{D}}^{-1} &= T_{\mathcal{D}} K_M^{-1} T_{\mathcal{D}}^{T} T_{\mathcal{D}}^{-T} K_m T_{\mathcal{D}}^{-1} = \Sigma_{\mathcal{D}}^2, \end{aligned}$$

the singular values in $\Sigma_{\mathcal{G}}$ and $\Sigma_{\mathcal{D}}$ are characterized by the square roots of the spectrum of XY and $K_M^{-1}K_m$, respectively. □

There exist multiple choices of generalized Gramians as the solutions of (7.16a) and (7.16b). This chapter specifically selects the pair of Gramians in (7.23) with the Kronecker product structure such that the balancing transformation $\mathcal{T}$ in (7.26) is composed of $T_{\mathcal{G}}$ and $T_{\mathcal{D}}$, which are generated from the network topology part (7.17) and agent dynamics (7.1) independently. Therefore, the topology part (7.17) and each subsystem (7.1) can be balanced and reduced independently (see (7.27)), allowing the resulting reduced-order model to preserve a network interpretation as well as the passivity of subsystems.

Remark 7.3. *The inequality in (7.22) characterizes the passivity of a linear system without a direct feed-through. The LMI tools such as YALMIP, LMILAB (a toolbox of MATLAB), etc. can be applied to compute K_m and K_M, which then define the available storage $\frac{1}{2}\langle x, K_m x\rangle$ and the required supply $\frac{1}{2}\langle x, K_M x\rangle$ of the agent system [174]. Any $K \succ 0$ satisfying (7.22) will lie between the two extremal solutions, i.e., $0 \prec K_m \preccurlyeq K \preccurlyeq K_M$, and $\frac{1}{2}\langle x, Kx\rangle$ is a quadratic storage function as defined in (2.9). Besides, it is noted that the solution of (7.22) may be unique, i.e., $K_M = K_m$, e.g., when the system (7.1) is lossless [169] or B is square and nonsingular [174]. In this case, we have $\Sigma_{\mathcal{D}} = I_n$ meaning that the subsystems are not suitable for reduction. If $K_M \neq K_m$, it can be verified that the diagonal entries of $\Sigma_{\mathcal{D}}$ in (7.24) satisfy $\tau_i \leq 1$, $i = 1, 2, \cdots, n$.*

In the balanced system of $\mathbf{\Sigma_s}$, the diagonal entries of $\Sigma_{\mathcal{G}} \otimes \Sigma_{\mathcal{D}}$ are the GHSVs in Definition 7.1, and the states are ordered in a descending order accordingly, thus allowing the following matrix partitions:

$$\begin{aligned} T_{\mathcal{D}} A T_{\mathcal{D}}^{-1} &= \begin{bmatrix} \tilde{A}_{11} & \tilde{A}_{12} \\ \tilde{A}_{21} & \tilde{A}_{22} \end{bmatrix}, \; T_{\mathcal{G}} \bar{\Lambda} T_{\mathcal{G}}^{-1} = \begin{bmatrix} \tilde{\Lambda}_{11} & \tilde{\Lambda}_{12} \\ \tilde{\Lambda}_{21} & \tilde{\Lambda}_{22} \end{bmatrix}, \\ T_{\mathcal{D}}^{-1} B &= \begin{bmatrix} \tilde{B}_1 \\ \tilde{B}_2 \end{bmatrix}, \qquad T_{\mathcal{G}}^{-1} \bar{F} = \begin{bmatrix} \tilde{F}_1 \\ \tilde{F}_2 \end{bmatrix}, \\ C T_{\mathcal{D}} &= \begin{bmatrix} \tilde{C}_1 & \tilde{C}_2 \end{bmatrix}, \qquad \bar{H} T_{\mathcal{G}} = \begin{bmatrix} \tilde{H}_1 & \tilde{H}_2 \end{bmatrix}, \end{aligned} \tag{7.27}$$

where $\tilde{\Lambda}_{11} \in \mathbb{R}^{(k-1)\times(k-1)}$, $\tilde{F}_1 \in \mathbb{R}^{(k-1)\times p}$, and $\tilde{H}_1 \in \mathbb{R}^{q\times(k-1)}$. The reduced-order agent dynamics is denoted by the minimal realization of the triplet $(\tilde{A}_{11}, \tilde{B}_1, \tilde{C}_1)$:

$$\hat{\mathbf{\Sigma}}_{\mathbf{i}} := (\hat{A}, \hat{B}, \hat{C}), \tag{7.28}$$

such that $\hat{A} \in \mathbb{R}^{r\times r}$, $\hat{B} \in \mathbb{R}^{r\times m}$, $\hat{C} \in \mathbb{R}^{m\times r}$. Consequently, the reduced-order model of the stable system $\mathbf{\Sigma_s}$ in (7.13) is presented as

$$\hat{\mathbf{\Sigma}}_{\mathbf{s}} : \begin{cases} \dot{\hat{z}}_s = (I_{k-1} \otimes \hat{A} - \bar{\Lambda}_{11} \otimes \hat{B}\hat{C})\hat{z}_s + (\bar{F}_1 \otimes \hat{B})u, \\ \hat{y}_s = (\bar{H}_1 \otimes \hat{C})\hat{z}_s. \end{cases} \tag{7.29}$$

Furthermore, the reduced-order subsystem $\hat{\mathbf{\Sigma}}_{\mathbf{i}}$ yields a lower-dimensional average module as

$$\hat{\mathbf{\Sigma}}_{\mathbf{a}} : \begin{cases} \dot{\hat{z}}_a = \hat{A}\hat{z}_a + \dfrac{1}{\sqrt{N}}(\mathbb{1}_N^T F \otimes \hat{B})u, \\ \hat{y}_a = \dfrac{1}{\sqrt{N}}(H\mathbb{1}_N \otimes \hat{C})\hat{z}_a. \end{cases} \tag{7.30}$$

Remark 7.4. *The triplet $(\tilde{A}_{11}, \tilde{B}_1, \tilde{C}_1)$ is not necessarily minimal. (Actually, $(\tilde{A}_{11}, \tilde{B}_1, \tilde{C}_1)$ is minimal when the original subsystem $\mathbf{\Sigma_i}$ is strictly passive, see [72].) However, we can always replace $\hat{\mathbf{\Sigma}}_{\mathbf{i}}$ by its minimal realization as in [137], and it can be verified that this replacement does not change the transfer functions of $\hat{\mathbf{\Sigma}}_{\mathbf{s}}$ and $\hat{\mathbf{\Sigma}}_{\mathbf{a}}$.*

Notice that, by (7.24), the accompanying system (7.17) reflecting the interconnection topology is generalized balanced, while the subsystems $\mathbf{\Sigma_i}$ are essentially positive real balanced, as the solutions of (7.22) are used to compute the balancing transformation for the subsystems. See more details about positive real balancing in e.g., [7, 72, 144]. Hence, the passivity of the reduced-order agent dynamics is preserved.

Next, by combining the average module $\hat{\mathbf{\Sigma}}_{\mathbf{a}}$ and the obtained $\hat{\mathbf{\Sigma}}_{\mathbf{s}}$, a lower-dimensional approximation of the overall system $\mathbf{\Sigma}$ is formulated as

$$\tilde{\mathbf{\Sigma}} : \begin{cases} \dot{\hat{z}} = (I_k \otimes \hat{A} - \mathcal{N} \otimes \hat{B}\hat{C})\hat{z} + (\mathcal{F} \otimes \hat{B})u, \\ \hat{y} = (\mathcal{H} \otimes \hat{C})\hat{z}. \end{cases} \tag{7.31}$$

where

$$\mathcal{N} = \begin{bmatrix} \bar{\Lambda}_{11} & \\ & 0 \end{bmatrix}, \mathcal{F} = \begin{bmatrix} \bar{F}_1 \\ \dfrac{1}{\sqrt{N}}\mathbb{1}^T F \end{bmatrix}, \mathcal{H} = \begin{bmatrix} \bar{H}_1 & \dfrac{1}{\sqrt{N}}H\mathbb{1} \end{bmatrix}.$$

Here, $\mathcal{N}$ is not yet a Laplacian matrix, which prohibits the interpretation of $\tilde{\mathbf{\Sigma}}$ as a network system. This provides the motivation to study the properties of $\mathcal{N}$ in the following lemma.

Lemma 7.2. *The matrix $\mathcal{N}$ in (7.31) has only one zero eigenvalue at the origin and all the other eigenvalues are positive real.*

Proof. The eigenvalue property of $\mathcal{N}$ heavily relies on the structures of $\bar{\Lambda}$ in (7.18) and Y in (7.20), by which we verify that $Y\bar{\Lambda} = Y^{1/2}\bar{\Lambda}Y^{1/2}$. The reduced matrix $\bar{\Lambda}_{11}$ in (7.31) is obtained by the following standard projection

$$\begin{aligned}\tilde{\Lambda}_{11} &= \left[(V_1^T Y V_1)^{-1} V_1^T Y\right] \bar{\Lambda} V_1 \\ &= (V_1^T Y V_1)^{-1} V_1^T Y^{1/2} \bar{\Lambda} Y^{1/2} V_1,\end{aligned} \tag{7.32}$$

where $V_1 \in \mathbb{R}^{N\times k}$ is the left projection matrix obtained by the singular value decomposition of $X^{1/2}Y^{1/2}$, see [7] for more details. As V_1 is full column rank, (7.32) implies that $\tilde{\Lambda}_{11}$ is similar to the matrix

$$(V_1^T Y V_1)^{-1/2} V_1^T Y^{1/2} \bar{\Lambda} Y^{1/2} V_1 (V_1^T Y V_1)^{-1/2},$$

which is positive definite. Thus, $\tilde{\Lambda}_{11}$ only has positive and real eigenvalues, which yields the spectrum property of $\mathcal{N}$. □

Remark 7.5. *Generally, balanced truncation does not preserve the realness of eigenvalues. Lemma 7.2 is the result of using a generalized observability Gramian Y with a special structure as in (7.20). As mentioned in Remark 7.2, we may also exchange the equality and inequality in (7.19) because of duality. Then, the eigenvalue realness of $\tilde{\Lambda}_{11}$ is also guaranteed due to the similar reasoning as in the proof of Lemma 7.2. In sum, for the eigenvalue property of $\tilde{\Lambda}_{11}$, either the generalized controllability Gramian X or the generalized observability Gramian Y should be in a block diagonal form as (7.20).*

7.3.3 Network Realization

Now we show that the reduced-order model $\tilde{\boldsymbol{\Sigma}}$ in (7.31) can be interpreted as a network system again. This result is due to the following Theorem.

Theorem 7.2. *A real square matrix $\mathcal{N}$ is similar to a Laplacian matrix $\mathcal{L}$ associated with an undirected connected graph, if and only if $\mathcal{N}$ is diagonalizable and has exactly one zero eigenvalue while all the other eigenvalues are real positive.*

Proof. The "only if" part can be seen from Lemma 2.1. The rest of the proof shows the "if" part. Let $\mathcal{N} \in \mathbb{R}^{n\times n}$ be diagonalizable, and denote its eigenvalues as

$$\lambda_1 \geq \lambda_2 \geq \cdots \geq \lambda_{n-1} > \lambda_n = 0. \tag{7.33}$$

Then, there exists a spectral decomposition $\mathcal{N} = T_1 D_1 T_1^{-1}$ with

$$D_1 = \mathrm{diag}(\lambda_1, \lambda_2, \cdots, \lambda_n)$$

.

On the other hand, any undirected graph Laplacian $\mathcal{L}$ can be written in the form of

$$\mathcal{L} = \begin{bmatrix} \alpha_1 & -w_{1,2} & \cdots & -w_{1,n} \\ -w_{2,1} & \alpha_2 & \cdots & -w_{2,n} \\ \vdots & \vdots & \ddots & \vdots \\ -w_{n,1} & -w_{n,2} & \cdots & \alpha_n \end{bmatrix}, \tag{7.34}$$

where $w_{i,j} = w_{j,i} \geq 0$ denotes the weight of edge (i, j), which is the same with w_{ij} in (7.2). The sum of the off-diagonal entries in the i-th row (or column) of $\mathcal{L}$ is denoted by α_i, i.e.,

$$\alpha_i = \sum_{j=1, j\neq i}^{n} w_{i,j}. \tag{7.35}$$

There exists a spectral decomposition $\mathcal{L} = T_2 D_2 T_2^{-1}$. If $D_1 = D_2$, the we have the following similarity transformation

$$\mathcal{L} = (T_2 T_1^{-1}) \mathcal{N} (T_2 T_1^{-1})^{-1}. \tag{7.36}$$

Hence, it is sufficient to prove that there always exists a set of weights $w_{i,j}$ such that the resulting Laplacian matrix $\mathcal{L}$ in (7.34) and $\mathcal{N}$ have the same eigenvalues (7.33).

Consider the characteristic polynomial of $\mathcal{L}$, i.e.,

$$|\mathcal{L} - \lambda I_n| = \begin{vmatrix} \alpha_1 - \lambda & -w_{1,2} & \cdots & -w_{1,n-1} & -w_{1,n} \\ -w_{1,2} & \alpha_2 - \lambda & \cdots & -w_{2,n-1} & -w_{2,n} \\ \vdots & \vdots & \ddots & \vdots & \vdots \\ -w_{1,n-1} & -w_{2,n-1} & \cdots & \alpha_{n-1} - \lambda & -w_{n-1,n} \\ -w_{1,n} & -w_{2,n} & \cdots & -w_{n-1,n} & \alpha_n - \lambda \end{vmatrix}.$$

As elementary row operations do not change the determinant, we sum all rows to the final row to obtain

$$|\mathcal{L} - \lambda I_n| = \begin{vmatrix} \alpha_1 - \lambda & -w_{1,2} & \cdots & -w_{1,n-1} & -w_{1,n} \\ -w_{1,2} & \alpha_2 - \lambda & \cdots & -w_{2,n-1} & -w_{2,n} \\ \vdots & \vdots & \ddots & \vdots & \vdots \\ -w_{1,n-1} & -w_{2,n-1} & \cdots & \alpha_{n-1} - \lambda & -w_{n-1,n} \\ -\lambda & -\lambda & \cdots & -\lambda & -\lambda \end{vmatrix},$$

where the expression in (7.35) is applied.

Using a similar argument, adding the last column to all other columns then leads to (7.37). Note that the eigenvalues of $\mathcal{L}$ are determined by the roots of $|\mathcal{L} - \lambda I_n| = 0$, and we can assign the eigenvalues of $\mathcal{L}$ by manipulating the weights $w_{i,j}$.

$$|\mathcal{L}-\lambda I| = \begin{vmatrix} \alpha_1 + w_{1,n} - \lambda & w_{1,n} - w_{1,2} & \cdots & w_{1,n} - w_{1,n-1} & -w_{1,n} \\ w_{2,n} - w_{1,2} & \alpha_2 + w_{2,n} - \lambda & \cdots & w_{2,n} - w_{2,n-1} & -w_{2,n} \\ \vdots & \vdots & \ddots & \vdots & \vdots \\ w_{n-1,n} - w_{1,n-1} & w_{n-1,n} - w_{2,n-1} & \cdots & \alpha_{n-1} + w_{n-1,n} - \lambda & -w_{n-1,n} \\ 0 & 0 & \cdots & 0 & -\lambda \end{vmatrix}. \tag{7.37}$$

When $n = 2$, we have a special case, and therefore it is considered separately. Equation (7.37) becomes

$$|\mathcal{L}-\lambda I_2| = \begin{vmatrix} \alpha_1 + w_{1,2} - \lambda & -w_{1,2} \\ 0 & -\lambda \end{vmatrix} = \begin{vmatrix} 2w_{1,2} - \lambda & -w_{1,2} \\ 0 & -\lambda \end{vmatrix}.$$

To match the eigenvalues $0, \lambda_1$, we let $w_{1,2} = 0.5\lambda_1$, which yields a Laplacian matrix as

$$\mathcal{L} = \begin{bmatrix} 0.5\lambda_1 & -0.5\lambda_1 \\ -0.5\lambda_1 & 0.5\lambda_1 \end{bmatrix}, \tag{7.38}$$

and proves the desired result for $n = 2$.

Now we continue the proof for the case $n > 2$. To match the eigenvalues of $\mathcal{L}$ with the desired ones in (7.33), we let the off-diagonal entries in the lower triangular part of the determinant in (7.37) be zero and use the diagonal entries to match the eigenvalues λ_i ($i = 1, 2, \cdots, n$). Specifically, the weights $w_{i,j}$ in (7.34) need to satisfy

$$\begin{cases} w_{2,n} = w_{1,2} \\ w_{3,n} = w_{1,3} = w_{2,3} \\ w_{4,n} = w_{1,4} = w_{2,4} = w_{3,4} \\ \qquad \vdots \\ w_{n-1,n} = w_{1,n-1} = w_{2,n-1} = \cdots = w_{n-2,n-1}. \end{cases} \tag{7.39}$$

and

$$\alpha_i + w_{i,n} = \lambda_i, \ \forall i \in \{1, 2, \cdots, n-1\}. \tag{7.40}$$

Hereafter we prove that the equations (7.39) and (7.40) produce a unique set of nonnegative real weights $w_{i,j}$, which is an essential property of a Laplacian matrix, see Lemma 2.1.

For simplicity, we denote

$$a_l = w_{n-l,n}, \ l = 1, 2, \cdots, n-1. \tag{7.41}$$

For any $1 \leq l \leq n-2$, it follows from (7.39) and the symmetry of $\mathcal{L}$ that

$$a_l = w_{k,n-l} = w_{n-l,k},\ \forall k \in \{1, \cdots, n-l-1\}. \tag{7.42}$$

Furthermore, denote the sum of the above series as

$$S_l := \sum_{k=1}^{l} a_k,\ l = 1, 2, \cdots, n-1. \tag{7.43}$$

From the equation (7.40) and the expression (7.35), we have

$$\begin{aligned} \lambda_i &= (w_{i,1} + \cdots + w_{i,i-1}) \\ &\quad + (w_{i,i+1} + \cdots + w_{i,n-1}) + 2w_{i,n} \\ &= (i-1)a_{n-i} + (a_{n-i-1} + \cdots + a_1) + 2a_{n-i} \\ &= (i+1)a_{n-i} + S_{n-i-1}, \end{aligned} \tag{7.44}$$

for $i = 1, 2, \cdots, n-2$. Here, the first equality follows from (7.42) (with $i = n-l$ for the first term) and the definition (7.41). The latter equation is the result of the definition (7.43).

Rewriting (7.44) for $l = n - i$ leads to

$$a_l = \frac{1}{n-l+1}\left(\lambda_{n-l} - S_{l-1}\right). \tag{7.45}$$

Now, we prove that $a_l > 0, \forall l \in \{1, 2, \cdots, n-1\}$. To do so, we consider the cases $l = 1$ and $l = 2$ explicitly and then proceed by induction.

For $l = 1$, it follows from (7.35) and the last equation in (7.39) that (7.40) can be written as $nw_{n-1,n} = \lambda_{n-1}$, which leads to

$$a_1 = \frac{\lambda_{n-1}}{n} = S_1 > 0, \tag{7.46}$$

by the definitions in (7.41) and (7.43).

For $l = 2$, (7.45) gives

$$\begin{aligned} a_2 &= \frac{1}{n-1}\left(\lambda_{n-2} - S_1\right) \\ &\geq \frac{1}{n-1}\left(\lambda_{n-1} - S_1\right) = \frac{\lambda_{n-1}}{n} > 0, \end{aligned} \tag{7.47}$$

where the inequality follows from the ordering of the eigenvalues in (7.33).Then, using the definition (7.43), it follows that

$$S_2 = S_1 + a_2 = \frac{\lambda_{n-2}}{n-1} + \frac{(n-2)\lambda_{n-1}}{n(n-1)}. \tag{7.48}$$

Note that

$$\frac{1}{n-m}+\frac{m(n-m-1)}{n(n-m)}=\frac{m+1}{n},\ \forall m\neq n, n\neq 0. \tag{7.49}$$

Using the above equation with $m=1$ and the inequality $\lambda_{n-2}\geq\lambda_{n-1}$, we show bounds on S_2 as

$$\begin{aligned} S_2 &\geq \left[\frac{1}{n-1}+\frac{(n-2)}{n(n-1)}\right]\lambda_{n-1}=\frac{2\lambda_{n-1}}{n}, \\ S_2 &\leq \left[\frac{1}{n-1}+\frac{(n-2)}{n(n-1)}\right]\lambda_{n-2}=\frac{2\lambda_{n-2}}{n}. \end{aligned} \tag{7.50}$$

To proceed with induction on l for $l>2$, we assume both $a_l>0$ and

$$\frac{l\lambda_{n-1}}{n}\leq S_l\leq\frac{l\lambda_{n-l}}{n}, \tag{7.51}$$

for $2<l<n-1$. Then, we obtain from (7.45) and (7.51) that

$$\begin{aligned} a_{l+1} &= \frac{1}{n-l}\left(\lambda_{n-l-1}-S_l\right) \\ &\geq \frac{1}{n-l}\left(\lambda_{n-l-1}-\frac{l\lambda_{n-l}}{n}\right)\geq\frac{\lambda_{n-l}}{n}>0, \end{aligned} \tag{7.52}$$

after which the first line in (7.52) yields

$$S_{l+1}=S_l+a_{l+1}=\frac{\lambda_{n-l-1}}{n-l}+\frac{(n-l-1)S_l}{n-l}. \tag{7.53}$$

The upper and lower bounds on S_{l+1} are implied by (7.51) as

$$\begin{aligned} S_{l+1} &\geq \frac{\lambda_{n-l-1}}{n-l}+\frac{l(n-l-1)\lambda_{n-1}}{(n-l)n}, \\ S_{l+1} &\leq \frac{\lambda_{n-l-1}}{n-l}+\frac{l(n-l-1)\lambda_{n-l}}{(n-l)n}. \end{aligned} \tag{7.54}$$

Using the relation $\lambda_{n-l-1}\geq\lambda_{n-l}\geq\lambda_{n-1}$ and the equation (7.49) with $m=l$, we obtain

$$\frac{(l+1)\lambda_{n-1}}{n}\leq S_{l+1}\leq\frac{(l+1)\lambda_{n-l-1}}{n}. \tag{7.55}$$

Consequently, by induction, we now verify that $a_l>0, \forall l\in\{1,2,\cdots,n-1\}$. As the parameters a_l uniquely characterize all the the weights $w_{i,j}$ in (7.34) through (7.41) and (7.42), it follows that $w_{i,j}>0$ for all (i,j).

In summary, there always exist a set of weights $w_{i,j}>0$ such that $\mathcal{L}$ in (7.34) has the eigenvalues matching the desired spectrum $\lambda_1\geq\cdots\geq\lambda_{n-1}>\lambda_n=0$. The

matrix $\mathcal{L}$ satisfies all properties stated in Lemma 2.1 and can indeed be regarded as the Laplacian matrix of an undirected graph. Therefore, we conclude that if $\mathcal{N}$ is diagonalizable and has a single zero eigenvalue while all the other eigenvalues are real positive, then there always exists a similarity transformation between $\mathcal{N}$ and a Laplacian matrix. This finalizes the proof of Theorem 7.2. □

The proof of Theorem 7.2 provides a procedure to construct a Laplacian matrix $\mathcal{L}$ for a given matrix $\mathcal{N}$. Here, we illustrate this procedure by means of an example in 4-dimension.

Example 7.1. *Given a diagonalizable matrix $\mathcal{N}$, whose eigenvalues are $\lambda_1 \geq \lambda_2 \geq \lambda_3 > \lambda_4 = 0$. The goal is to find an undirected graph Laplacian matrix $\mathcal{L}$ whose spectrum exactly matches the given one. Let $w_{i,j}$ be the weight of the edge linking agents i and j, such that the Laplacian matrix can be explicitly expressed as*

$$\mathcal{L} = \begin{bmatrix} \alpha_1 & -w_{12} & -w_{13} & -w_{14} \\ -w_{12} & \alpha_2 & -w_{23} & -w_{24} \\ -w_{13} & -w_{23} & \alpha_3 & -w_{34} \\ -w_{14} & -w_{24} & -w_{34} & \alpha_4 \end{bmatrix}, \tag{7.56}$$

where $w_{ij} = w_{ji} \geq 0$ and $\alpha_i = \sum_{j=1,j\neq i}^{4} w_{ij}$. Furthermore, the eigenvalues of $\mathcal{L}$ are computed as the roots of the equation

$$|\mathcal{L} - \lambda I_4| = 0. \tag{7.57}$$

Following (7.37), the algebraic manipulation of (7.57) then leads to

$$\begin{vmatrix} \alpha_1 + w_{14} - \lambda & w_{14} - w_{12} & w_{14} - w_{13} & -w_{14} \\ w_{24} - w_{12} & \alpha_2 + w_{24} - \lambda & w_{24} - w_{23} & -w_{24} \\ w_{34} - w_{13} & w_{34} - w_{23} & \alpha_3 + w_{34} - \lambda & -w_{34} \\ 0 & 0 & 0 & -\lambda \end{vmatrix} = 0.$$

The strategy is to let the lower triangular part to be zero and use the diagonal entries to match the desired eigenvalues. Precisely, we have

$$\begin{cases} w_{24} - w_{12} = 0, \\ w_{34} - w_{13} = 0, \\ w_{34} - w_{23} = 0, \\ w_{12} + w_{13} + 2w_{14} = \lambda_1, \\ w_{12} + w_{23} + 2w_{24} = \lambda_2, \\ w_{13} + w_{23} + 2w_{34} = \lambda_3, \end{cases} \Rightarrow \begin{cases} w_{34} = w_{23} = w_{13} = \dfrac{1}{4}\lambda_3, \\ w_{24} = w_{12} = \dfrac{1}{3}\left(\lambda_2 - \dfrac{1}{4}\lambda_3\right), \\ w_{14} = \dfrac{1}{2}\left(\lambda_1 - \dfrac{1}{3}\lambda_2 - \dfrac{1}{6}\lambda_3\right). \end{cases}$$

For instance, when $\lambda_1 = 3$, $\lambda_2 = \lambda_3 = 2$, $\lambda_4 = 0$, the Laplacian matrix is given by

$$\mathcal{L} = \begin{bmatrix} 2 & -0.5 & -0.5 & -1 \\ -0.5 & 1.5 & -0.5 & -0.5 \\ -0.5 & -0.5 & 1.5 & -0.5 \\ -1 & -0.5 & -0.5 & 2 \end{bmatrix}. \tag{7.58}$$

Finally, we note that the obtained $\mathcal{L}$ satisfies all the properties in Lemma 2.1 as expected.

Remark 7.6. *Note that reduced Laplacian matrices obtained by the procedure in Theorem 7.2 represent undirected complete graphs, since all the weights are strictly positive. However, the matrix $\mathcal{N}$ in (7.31) may very well be similar to a Laplacian matrix of an incomplete graph, though there are examples where $\mathcal{N}$ can only be similar to a complete graph Laplacian. We illustrate this by an example of 3 dimension. Suppose vertex 2 is not adjacent to vertex 3, i.e., $w_{23} \equiv 0$. Then, the Laplacian matrix is given by*

$$\mathcal{L} = \begin{bmatrix} w_{12} + w_{13} & -w_{12} & -w_{13} \\ -w_{12} & w_{12} & 0 \\ -w_{13} & 0 & w_{13} \end{bmatrix} \tag{7.59}$$

whose characteristic polynomial is

$$|\lambda I_3 - \mathcal{L}| = \lambda \left[\lambda^2 - 2(w_{12} + w_{13})\lambda + 3w_{12}w_{13}\right].$$

Let $\lambda_1 \geq \lambda_2 > \lambda_3 = 0$ be the desired eigenvalues. We then obtain

$$2(w_{12} + w_{13}) = \lambda_1 + \lambda_2, \tag{7.60a}$$

$$3w_{12}w_{13} = \lambda_1\lambda_2. \tag{7.60b}$$

Expressing w_{12} as a function of w_{13} using (7.60a) and substitution of the result in (7.60b) gives

$$\begin{aligned} & w_{13}^2 - \frac{1}{2}(\lambda_1 + \lambda_2)w_{13} + \frac{1}{3}\lambda_1\lambda_2 = 0 \\ \Leftrightarrow \ & \left[w_{13} - \frac{1}{4}(\lambda_1 + \lambda_2)\right]^2 - \frac{\lambda_1^2 + \lambda_2^2}{16} + \frac{5\lambda_1\lambda_2}{24} = 0. \end{aligned} \tag{7.61}$$

Obviously, it has a real solution if and only if

$$3(\lambda_1^2 + \lambda_2^2) \leq 10\lambda_1\lambda_2. \tag{7.62}$$

Therefore, when $\lambda_1 \leq 3\lambda_2$, we can find suitable weights w_{12} and w_{13} such that the eigenvalues of the incomplete graph Laplacian $\mathcal{L}$ in (7.59) match the given real spectrum λ_1, λ_2, and λ_3. However, if $\lambda_1 > 3\lambda_2$, then it is impossible to find a set of suitable weights.

In this chapter, we can only guarantee to find a network realization of the system $\tilde{\mathbf{\Sigma}}$ with a complete graph topology. Observe that $\mathcal{N}$ in (7.31) is diagonalizable, and Lemma 7.2 implies that it has only one eigenvalue at the origin and all the other poles are real and strictly positive. Therefore, by Theorem 7.2, there exists a Laplacian matrix $\hat{L}$ which has the same spectrum as $\mathcal{N}$. In other words, we can find a nonsingular matrix $\mathcal{T}_n$ such that

$$\hat{L} = \mathcal{T}_n^{-1}\mathcal{N}\mathcal{T}_n. \tag{7.63}$$

Here, $\hat{L}$ is a Laplacian matrix representing a reduced connected undirected graph $\hat{\mathcal{G}}$, which contains k nodes.

Applying a coordinate transform $\hat{z} = (\mathcal{T}_n \otimes I_r)\hat{x}$ to the system $\tilde{\mathbf{\Sigma}}$ in (7.31) yields a reduced-order network model

$$\hat{\mathbf{\Sigma}} : \begin{cases} \dot{\hat{x}} = (I_k \otimes \hat{A} - \hat{L} \otimes \hat{B}\hat{C})\hat{x} + (\hat{F} \otimes \hat{B})u, \\ \hat{y} = (\hat{H} \otimes \hat{C})\hat{x}, \end{cases} \tag{7.64}$$

with $\hat{F} = \mathcal{T}_n^{-1}\mathcal{F}$ and $\hat{H} = \mathcal{H}\mathcal{T}_n$. We show in the following theorem that the reduced-order network $\hat{\mathbf{\Sigma}}$ is also synchronized for $u = 0$. The proof is a direct application of Lemma 7.1, as the reduced subsystem $(\hat{A}, \hat{B}, \hat{C})$ is passive and minimal.

Theorem 7.3. *The reduced networked passive system $\hat{\mathbf{\Sigma}}$ preserves the synchronization, i.e., when $u = 0$, for any initial condition, it holds that*

$$\lim_{t\to\infty} [\hat{x}_i(t) - \hat{x}_j(t)] = 0, \quad \forall i, j \in \{1, 2, \cdots, k\}. \tag{7.65}$$

7.3.4 Error Analysis

Following the separation of the multi-agent system $\mathbf{\Sigma}$ in Section 7.3.1, we analyze the approximation error for the overall system as follows.

$$\begin{aligned} \|\mathbf{\Sigma} - \hat{\mathbf{\Sigma}}\|_{\mathcal{H}_\infty} &= \|(\mathbf{\Sigma_s} + \mathbf{\Sigma_a}) - (\hat{\mathbf{\Sigma}}_\mathbf{s} + \hat{\mathbf{\Sigma}}_\mathbf{a})\|_{\mathcal{H}_\infty} \\ &\leq \|\mathbf{\Sigma_s} - \hat{\mathbf{\Sigma}}_\mathbf{s}\|_{\mathcal{H}_\infty} + \|\mathbf{\Sigma_a} - \hat{\mathbf{\Sigma}}_\mathbf{a}\|_{\mathcal{H}_\infty}. \end{aligned} \tag{7.66}$$

The overall approximation error can be evaluated based on the reduction results of the stable system $\mathbf{\Sigma_s}$ and the average module $\mathbf{\Sigma_a}$.

First, the *a priori* bound on the approximation error of the stable part is provided as follows.

Lemma 7.3. *Consider the original stable system $\mathbf{\Sigma_s}$ in (7.13) and its truncated model $\hat{\mathbf{\Sigma}}_\mathbf{s}$ in (7.7). The approximation error has an upper bound as*

$$\|\mathbf{\Sigma_s} - \hat{\mathbf{\Sigma}}_\mathbf{s}\|_{\mathcal{H}_\infty} \leq \gamma, \tag{7.67}$$

where

$$\gamma = 2\sum_{i=k}^{N-1}\sum_{j=1}^{n}\sigma_i\tau_j + 2\sum_{i=1}^{k-1}\sum_{j=r+1}^{n}\sigma_i\tau_j. \tag{7.68}$$

with σ_i and τ_i the diagonal entries of $\Sigma_{\mathcal{G}}$ and $\Sigma_{\mathcal{D}}$ in (7.24), respectively.

Proof. The GHSVs of the balanced system of $\mathbf{\Sigma_s}$ are ordered and located in the diagonal of $\Sigma_{\mathcal{G}} \otimes \Sigma_{\mathcal{D}}$, forming the structure as

$$\Sigma_{\mathcal{G}} \otimes \Sigma_{\mathcal{D}} = \mathsf{blkdiag}\left(\sigma_1 \begin{bmatrix}\tau_1 & & \\ & \ddots & \\ & & \tau_n\end{bmatrix}, \cdots, \sigma_{N-1}\begin{bmatrix}\tau_1 & & \\ & \ddots & \\ & & \tau_n\end{bmatrix}\right). \tag{7.69}$$

Then, recall the standard error bound for balanced truncation based on generalized Gramians in [58], we obtain a $\mathcal{H}_\infty$ bound as

$$\|\mathbf{\Sigma_s} - \hat{\mathbf{\Sigma}}_\mathbf{s}\|_{\mathcal{H}_\infty} \le \gamma. \tag{7.70}$$

The constant γ is computed as (7.67) since we truncate the system according to the block diagonal structure of $\Sigma_{\mathcal{G}} \otimes \Sigma_{\mathcal{D}}$ as in (7.69). □

The approximation error on the average module of the network system is then discussed. From (7.12) and (7.30), we write the transfer function of $\mathbf{\Sigma_a} - \hat{\mathbf{\Sigma}}_\mathbf{a}$ as

$$\begin{aligned}\Delta_a(s) =& \frac{1}{N}(H\mathbb{1}_N \otimes C)(sI_n - A)^{-1}(\mathbb{1}_N^T F \otimes B)\\ &- \frac{1}{N}(H\mathbb{1}_N \otimes \hat{C})(sI_r - \hat{A})^{-1}(\mathbb{1}_N^T F \otimes \hat{B}).\end{aligned}$$

Using the properties of Kronecker products, it then leads to

$$\Delta_a(s) = \frac{H\mathbb{1}_N\mathbb{1}_N^T F}{N} \otimes \Delta_i(s), \tag{7.71}$$

where $\Delta_i(s) := C(sI_n - A)^{-1}B - \hat{C}(sI_r - \hat{A})^{-1}\hat{B}$ is the transfer function of $\mathbf{\Sigma_i} - \hat{\mathbf{\Sigma}}_\mathbf{i}$. Hence, the approximation error on the average module is actually bounded if and only if the error between the original and reduced agent dynamics is bounded. However, since the agent system in (7.1) is not necessarily asymptotically stable, $\Delta_i(s)$ may not have an $\mathcal{H}_\infty$-norm bound, so does $\Delta_a(s)$. If $\|\Delta_i(s)\|_{\mathcal{H}_\infty}$ exists, we can take the $\mathcal{H}_\infty$-norm of $\Delta_a(s)$ and obtain

$$\|\mathbf{\Sigma_a} - \hat{\mathbf{\Sigma}}_\mathbf{a}\|_{\mathcal{H}_\infty} \le \frac{\gamma_a}{N}\|\mathbf{\Sigma_i} - \hat{\mathbf{\Sigma}}_\mathbf{i}\|_{\mathcal{H}_\infty} \tag{7.72}$$

by triangular inequality of norms, where $\gamma_a := \|H\mathbb{1}_N\mathbb{1}_N^T F\|_2$. Note that $\hat{\mathbf{\Sigma}}_\mathbf{i}$ is essentially obtained from positive real balancing of $\mathbf{\Sigma_i}$. Generally, there does not exist an *a priori* bound on $\|\mathbf{\Sigma_i} - \hat{\mathbf{\Sigma}}_\mathbf{i}\|_{\mathcal{H}_\mathbf{2}}$. Nevertheless, *a posteriori* bound can be obtained, see [72].

In the rest of this section, three special cases are discussed where *a priori* error bounds on $\|\mathbf{\Sigma} - \hat{\mathbf{\Sigma}}\|_{\mathcal{H}_\infty}$ in (7.66) can be obtained.

The first case is when we only reduce the dimension of the network while the agent dynamics are untouched as in [21, 122]. Then, we have the following result.

Theorem 7.4. *Consider the network system $\mathbf{\Sigma}$ with N agents and its reduced-order model $\hat{\mathbf{\Sigma}}$ with k agents. If the agent system $\mathbf{\Sigma_i}$ is not reduced, the error bound*

$$\|\mathbf{\Sigma} - \hat{\mathbf{\Sigma}}\|_{\mathcal{H}_\infty} = \|\mathbf{\Sigma_s} - \hat{\mathbf{\Sigma}}_\mathbf{s}\|_{\mathcal{H}_\infty} \le 2\sum_{i=k}^{N-1}\sum_{j=1}^{n}\sigma_i\tau_j, \tag{7.73}$$

holds, where σ_i and τ_i are defined in Theorem 7.1.

Proof. If the agent dynamics are untouched, we have $\|\mathbf{\Sigma_a} - \hat{\mathbf{\Sigma}}_\mathbf{a}\|_{\mathcal{H}_\infty} = \mathbf{0}$ due to (7.72). Then, the error bound straightforwardly follows from (7.66) and (7.67). Even though the agent dynamics are retained, τ_j, $j = 1, 2, \cdots, n$ still show up because of (7.69). □

The second case is when the average module is not observable from the outputs of the overall system $\mathbf{\Sigma}$ or uncontrollable by the external inputs. Specifically, we have

$$H\mathbb{1} = 0, \text{ or } \mathbb{1}^T F = 0, \tag{7.74}$$

which implies $\|\mathbf{\Sigma_a} - \hat{\mathbf{\Sigma}}_\mathbf{a}\|_{\mathcal{H}_\infty} = \mathbf{0}$ from (7.71). In practice, this means that we only observe or control the differences between the agents due to the coupling. Such differences usually play a crucial role in distributed control of networks, since they indicate whether two nodes or two clusters of nodes are synchronized as time evolves. A typical example can be found in [122, 125, 126] where H in (7.4) is the *incidence matrix* of the underlying network. If (7.74) holds, the following result is obtained immediately.

Corollary 7.1. *Consider the network system $\mathbf{\Sigma}$ with N agents and its reduced-order network model $\hat{\mathbf{\Sigma}}$ with k agents. If $H\mathbb{1}_N = 0$ or $\mathbb{1}_N^T F = 0$, the approximation between $\mathbf{\Sigma}$ and $\hat{\mathbf{\Sigma}}$ is bounded by*

$$\|\mathbf{\Sigma} - \hat{\mathbf{\Sigma}}\|_{\mathcal{H}_\infty} = \|\mathbf{\Sigma_s} - \hat{\mathbf{\Sigma}}_\mathbf{s}\|_{\mathcal{H}_\infty} \le \gamma,$$

where γ is given in (7.67).

The third case is when A in (7.1) is Hurwitz, and both K_M and K_m satisfy

$$A^T K + KA + \beta C^T C \preccurlyeq 0 \tag{7.75}$$

with $\beta := 1/N \cdot \min\{\mathbb{1}^T F F^T \mathbb{1}, \mathbb{1}^T H^T H \mathbb{1}\}$. Thereby, K_M^{-1} and K_m can be interpreted as the generalized Gramians of the average system $\mathbf{\Sigma_a}$. Consequently, standard results apply and an *a priori* bound on $\|\mathbf{\Sigma_a} - \hat{\mathbf{\Sigma}}_\mathbf{a}\|_{\mathcal{H}_\infty}$ in (7.66) can be evaluated by the GHSVs of $\mathbf{\Sigma_a}$, namely τ_i. Then the following bound is obtained.

$$\|\mathbf{\Sigma} - \hat{\mathbf{\Sigma}}\|_{\mathcal{H}_\infty} \leq \gamma + 2 \sum_{i=r+1}^{n} \tau_i, \tag{7.76}$$

where γ is given in (7.67).

7.4 Illustrative Example

To demonstrate the feasibility of the proposed method, we consider networked robotic manipulators as a multi-agent system example.

Following [50], the dynamics of each rigid robot manipulator is described as a standard mechanical system in the form (7.1) with

$$A = \begin{bmatrix} \mathbf{0} & M^{-1} \\ -I & -DM^{-1} \end{bmatrix}, \; C = B^T c \cdot \begin{bmatrix} I & \mathbf{0} \\ \mathbf{0} & M^{-1} \end{bmatrix}, \tag{7.77}$$

where $D \geq 0$ and $M > 0$ are the system damping and mass-inertia matrices, respectively. By Lemma 2.4, each manipulator agent is passive since there exists a positive definite matrix $P := \mathsf{blkdiag}(I, M^{-1})$ satisfying the KYP condition in (2.12).

In this example, the system parameters in (7.77) are specified as $M = \frac{1}{2} I_4$, $B = [0, 0, 0, 0, 1, 0, 0, 0]^T$, and

$$D = \begin{bmatrix} 2 & -1 & 0 & 0 \\ -1 & 4 & -2 & 0 \\ 0 & -2 & 4 & -1 \\ 0 & 0 & -1 & 2 \end{bmatrix}.$$

which yields the dynamics of each individual agent with state and input dimensions as $n = 8$ and $m = 1$.

Furthermore, the agents communicate according to an undirected cyclic graph depicted in Fig. 7.3a, which contains $N = 6$ agents. Suppose that nodes 1 and 2 are actuated, and the output error between the nodes 1 and 3 are the external

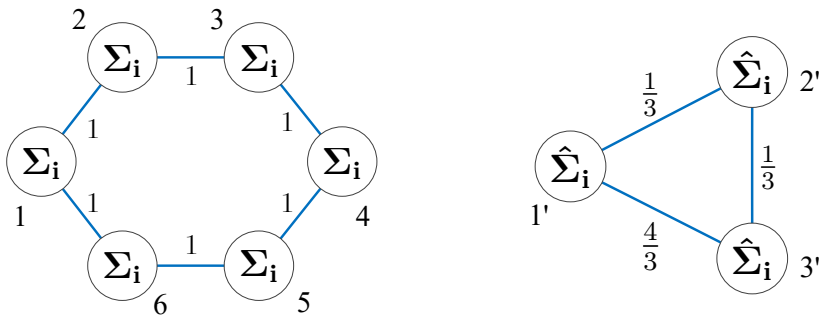

Figure 7.3: (a) and (b) illustrate the original and reduced communication graph, respectively.

measurement. Then, the Laplacian matrix and external input and output matrices are given by

$$L = \begin{bmatrix} 2 & -1 & 0 & 0 & 0 & -1 \\ -1 & 2 & -1 & 0 & 0 & 0 \\ 0 & -1 & 2 & -1 & 0 & 0 \\ 0 & 0 & -1 & 2 & -1 & 0 \\ 0 & 0 & 0 & -1 & 2 & -1 \\ -1 & 0 & 0 & 0 & -1 & 2 \end{bmatrix}, F = \begin{bmatrix} 1 \\ 0.5 \\ 0 \\ 0 \\ 0 \\ 0 \end{bmatrix}, H^T = \begin{bmatrix} 1 \\ 0 \\ -1 \\ 0 \\ 0 \\ 0 \end{bmatrix}.$$

It can be verified that the subsystems $\mathbf{\Sigma_i}$ is minimal. Thus, the original network system is synchronized as time evolves by Lemma 7.1.

Note that the nonzero eigenvalues of L are $\lambda_1 = 4, \lambda_2 = \lambda_3 = 3, \lambda_4 = \lambda_5 = 1$. Solving the LMI (7.19b) by minimizing the trace of Y, we obtain the generalized observability Gramian of the accompanying system in (7.17) as

$$Y = \mathsf{blkdiag}\left(\begin{bmatrix} 0.0120 & 0.0964 \\ 0.0964 & 0.7766 \end{bmatrix}, \begin{bmatrix} 0.3416 & 0.1972 \\ 0.1972 & 0.1139 \end{bmatrix}, 2.23 \cdot 10^{-5} \right).$$

Moreover, the controllability Gramian X of (7.17) and the maximal and minimal real symmetric solutions, K_M and K_m, of the LMI in (7.22) are computed. The results show that, in this example, $K_M \neq K_m$.

The goal is to reduce the dimension of the agent systems to $r = 2$ and the number of nodes to $k = 3$. Applying the generalized balanced truncation discussed in Section

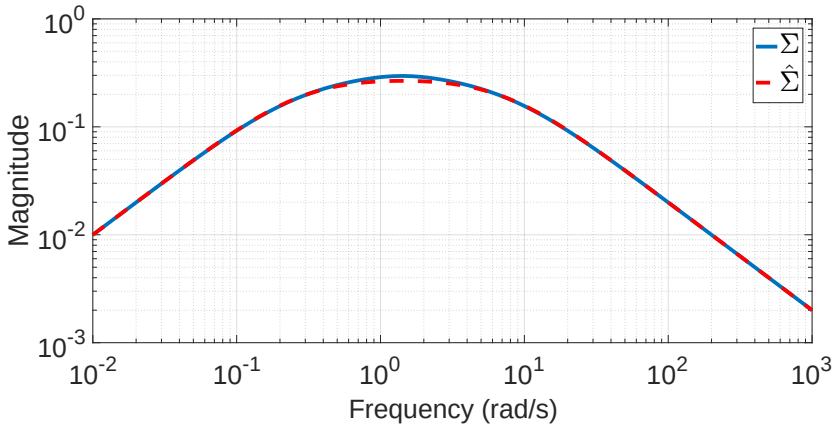

Figure 7.4: The Bode magnitude plots of the original and reduced multi-agent systems, which are represented by the solid and dashed lines in the plot respectively.

7.3.2, we obtain the reduced-order dynamics of the agents $\hat{\mathbf{\Sigma}}_\mathbf{i}$ as

$$\hat{A} = \begin{bmatrix} 0 & -1.4142 \\ 1.4142 & -4 \end{bmatrix}, \hat{B} = \hat{C}^T = \begin{bmatrix} 0 \\ -1.4142 \end{bmatrix}.$$

Furthermore, by the network realization method presented in Section 7.3.3, the lower-dimensional Laplacian matrix and external input and output matrices can be computed as

$$\hat{L} = \frac{1}{3}\begin{bmatrix} 5 & -1 & -4 \\ -1 & 2 & -1 \\ -4 & -1 & 5 \end{bmatrix}, \hat{F} = \begin{bmatrix} -0.9270 \\ 1.1380 \\ 0.8496 \end{bmatrix}, \hat{H}^T = \begin{bmatrix} -0.4939 \\ 0.4249 \\ 0.0690 \end{bmatrix}.$$

Note that $\hat{L}$ represents a reduced interconnection network as shown in Fig. 7.3b, which consists of 3 fully connected reduced agents. We observe that $\hat{\mathbf{\Sigma}}_\mathbf{i}$ is passive and minimal. Therefore, the reduced-order multi-agent system preserves the synchronization property.

Next, to compare the input-output behavior of the reduced-order network to the original one, we compute the actual model reduction error: $\|\mathbf{\Sigma} - \hat{\mathbf{\Sigma}}\|_{\mathcal{H}_\infty} \approx 0.0295$. Since $H\mathbb{1}_6 = 0$, we then obtain the *a priori* error bound by Corollary 7.1 as $\|\mathbf{\Sigma} - \hat{\mathbf{\Sigma}}\|_{\mathcal{H}_\infty} \leq 0.0773$. Therefore, the original network is well approximated by the reduced-order model. This conclusion can been seen from the plots of both systems in Fig. 7.4 as well.

7.5 Concluding Remarks

In this chapter, we have developed a novel structure-preserving model reduction method for networked passive systems. The identical agents are assumed to be linear time-invariant systems, and the communication topology is connected and undirected. The observability and passivity of each agent guarantee the synchronization of networks. Balanced truncation based on generalized Gramians is applied to reduce the dimension of each subsystem and the scale of the network in a unified framework. The resulting model can be converted to a new representation of Laplacian dynamics, which again has a network interpretation. Moreover, an *a priori* error bound on the multi-agent system has been provided. Finally, the proposed model reduction scheme was demonstrated by a numerical example. The simulation results indicate that the reduced-order model approximates the original one with a high accuracy.

Based on the balancing method, this chapter first proposes a unified framework to reduce the network topology and agent dynamics. In contrast to the other network reduction methods, the mechanism of balanced truncation potentially allows for a better approximation accuracy and also provides an *a priori* error bound, but obtaining a complete reduced graph that is less correlated with the original one is the corresponding price. Namely, the balancing transformation does not enforce a restriction on the structure of projection matrix as in the clustering-based approaches. For future works, multi-agent systems with heterogeneous agents are of interest, and the extensions to nonlinear agent dynamics and communication protocols can be further investigated.

CHAPTER 8

Balanced Truncation of Robustly Synchronized Lur'e Networks

This chapter considers a model order reduction problem that reduces the complexity of interconnected Lur'e-type subsystems while simultaneously preserving the synchronization property of the network. Differently from the previous chapters, the system in this chapter is nonlinear which consists of multiple identical Lur'e systems. A sufficient condition of the robust synchronization of the Lur'e network is first related to the passivity of a linear time-invariant auxiliary system. Consequently, a passivity preserving model reduction scheme is applied to the auxiliary system, leading to reduced-order Lur'e subsystems, and the resulting reduced network system is still robustly synchronized. In addition, an *a prior* error bound is established to compare the behaviors of the full-order and reduced-order Lur'e subsystem. Finally, the proposed method is illustrated by means of an example.

8.1 Introduction

In Chapter 5 and Chapter 7, a network of multiple interconnected subsystems is considered, whose behavior is a collection of responses from all individual subsystems and their interactions on a certain communication network. However, the methods used in Chapter 5 and Chapter 7 are developed only for linear dynamic networks. In this chapter, we consider a network of identical nonlinear Lur'e-type dynamics, and partial information of the subsystems is exchanged through a static output-feedback

protocol such that all the subsystems may achieve a common solution. This is called network *synchronization*, which is an important property of networks, and the synchronization problem of networks with linear subsystems have been extensively studied, see [145] and the references therein. In [49,106,180], the results are extended to Lur'e subsystems.

Lur'e systems is an important class of nonlinear engineering systems consisting of linear dynamics with static nonlinearities in the feedback loop. Examples can be found in Chua's circuits or some hyper-chaotic systems [99]. In a Lur'e network, when the dynamic order of each Lur'e-type subsystem becomes large, the overall network system will be of high complexity, which hinders fast prediction and transient analysis of the network states. Applications, such as controller design and fault diagnosis will also be inefficient. Hence, it is desired to apply some model reduction techniques to generate much smaller-sized models of the Lur'e subsystems that can approximate the input-output relation of the original subsystems. Meanwhile, we require the reduction process to preserve the synchronization property in the reduced network system.

There are a variety of methods developed for model order reduction. For example, moment matching and proper orthogonal decomposition, as efficient numerical techniques, can be applied to both linear and nonlinear systems [8,10,143]. However, they, in general, do not guarantee the stability of the reduced-order model and the bound on the approximation error. In contrast, balanced truncation and optimal Hankel norm approximation are well-known for their properties of stability preservation and error boundedness and have been intensively studied in stable linear time-invariant systems, see [7,66,70] for an overview. These methods rely on the controllability and observability energy functionals of the system, i.e., the Gramian matrices. These concepts then have been extended to nonlinear balancing, see [25,65,156] and the references therein. In general, implementing nonlinear balancing is expensive, as it requires the solutions of a large-scale nonlinear partial differential equation, namely the Hamilton-Jacobi equation. Moreover, as the other methods for model reduction of nonlinear systems, the truncated model from nonlinear balancing lacks an error bound on the approximation.

For linear network system, balanced truncation has only recently been studied. For example, [40] applies balanced truncation based on generalized Gramians to simplify the network topology. Some pioneering results in [125,152] present methods to approximate network systems by reducing the complexity of linear subsystems. In this chapter, we attempt to adopt balanced truncation to networked nonlinear systems, whose subsystems are identical and cast in Lur'e-type form. In [22], a reduction procedure is presented for absolutely stable Lur'e systems. The method essentially applies balanced truncation to the linear component of a Lur'e system

and therefore is computationally cheap. Furthermore, both stability and the error bound for the reduced-order model are guaranteed.

However, in this chapter, as the preservation of network synchronization is needed, we can not directly apply standard balanced truncation to each Lur'e subsystem. Instead, we establish a linear time-invariant auxiliary system associating the Lur'e network, and relate the robust synchronization condition to the passivity of this auxiliary system. Consequently, a passivity preserving model reduction on the auxiliary system yields reduced-order Lur'e subsystems and a synchronized reduced network system. Furthermore, the *a priori* bound on the approximation error is established to compare the behaviors of the full-order and reduced-order Lur'e subsystem.

This chapter is organized as follows. Section 8.2 introduces the balanced truncation method and the model of a Lur'e network. Section 8.3 then presents the proposed method for synchronization preserving model reduction of Lur'e networks, and Section 8.4 gives the analysis of the approximation error on each subsystem. The proposed method is illustrated in Section 8.5 by an example. Finally, Section 8.6 concludes the chapter.

8.2 Problem Formulation

We present the mathematical model of a Lur'e network. Consider a weighted graph is defined by a triplet $\mathcal{G} = (\mathcal{V}, \mathcal{E}, \mathcal{W})$. The sets $\mathcal{V}$ and $\mathcal{E} \subseteq \mathcal{V} \times \mathcal{V}$ present the sets of nodes and edges, respectively. $\mathcal{W}$ is called *weighted adjacency matrix*. The (i, j)-th entry of $\mathcal{W}$, denoted by w_{ij}, is positive if edge $(i, j) \in \mathcal{E}$, and $w_{ij} = 0$ otherwise. The *Laplacian matrix* of graph $\mathcal{G}$, denoted by L, is then introduced with the (i, j)-th entry as

$$L_{ij} = \begin{cases} \sum_{j=1, j\neq i}^{n} w_{ij}, & i = j \\ -w_{ij}, & \text{otherwise.} \end{cases} \tag{8.1}$$

Assumption 8.1. *We assume, in this chapter, the network is defined on an* ***undirected connected graph*** *consisting of N ($N \geq 2$) nodes. In this case, we have $L = L^T \succcurlyeq 0$, and the eigenvalues of L are $0 = \lambda_1 < \lambda_2 \leq \lambda_3 \leq \cdots \leq \lambda_N$.*

The dynamics of nodes on the network are described by identical nonlinear dynamical systems as follows.

$$\mathbf{\Sigma_i} : \begin{cases} \dot{x}_i = Ax_i + Bu_i + Ez_i \\ y_i = Cx_i \\ z_i = -\phi(y_i, t) \end{cases} , i = 1, 2, \cdots, N, \tag{8.2}$$

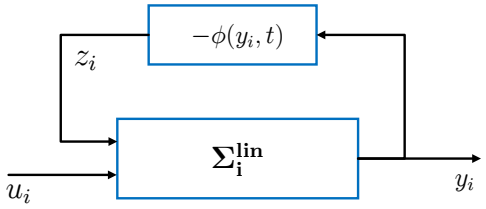

Figure 8.1: The illustration of a Lur'e subsystem

where $x_i \in \mathbb{R}^n$, $u_i, y_i, z_i \in \mathbb{R}$. The subsystem $\boldsymbol{\Sigma}_\mathbf{i}$ is in the Lur'e-type form, whose structure is illustrated in Fig. 8.1. Each Lur'e subsystem consists of a linear part $\boldsymbol{\Sigma}_\mathbf{i}^\mathbf{lin}$ formulated by

$$\boldsymbol{\Sigma}_\mathbf{i}^\mathbf{lin}: \begin{cases} \dot{x}_i = Ax_i + \begin{bmatrix} B & E \end{bmatrix} \begin{bmatrix} u_i \\ z_i \end{bmatrix} \\ y_i = Cx_i \end{cases}, i = 1, 2, \cdots, N, \tag{8.3}$$

and a continuous static output-dependent nonlinearity $\phi(y_i) : \mathbb{R} \times \mathbb{R} \mapsto \mathbb{R}$.

Assumption 8.2. *We assume that the uncertain feedback nonlinearity $\phi(\cdot)$ in (8.2) is **slope-restricted** as*

$$0 \leq \frac{\phi(y_a) - \phi(y_b)}{y_a - y_b} \leq \mu, \tag{8.4}$$

*for all $y_a, y_b \in \mathbb{R}$ and $y_a \neq y_b$, where $\mu > 0$ and $\phi(0) = 0$. Furthermore, the Lur'e dynamics $\boldsymbol{\Sigma}_\mathbf{i}$ is assumed to be **absolutely stable**, i.e., A is Hurwitz, and the linear transfer function from z_i to y_i fulfills*

$$\|C(sI_n - A)^{-1}E\|_{\mathcal{H}_\infty} < \mu^{-1}. \tag{8.5}$$

We refer to [49, 99] and the references therein for the definitions of absolute stability and slope-restrictedness, respectively.

All the subsystems on the network are interconnected according to the following static output-feedback protocol.

$$u_i = \sum_{j=1}^{N} w_{ij}(y_i - y_j),\ i = 1, 2, \cdots, N, \tag{8.6}$$

where $w_{ij} \in \mathbb{R} \geq 0$ is the (i, j)-th entry of weighted adjacency matrix of the underlying graph and stands for the intensity of the coupling between subsystem i and j. Then, combining (8.6) and (8.2) leads to a compact form of the Lur'e dynamical network as

$$\boldsymbol{\Sigma}: \begin{cases} \dot{x} = (I_N \otimes A - L \otimes BC)\, x - (I_N \otimes E)\, \Phi(y), \\ y = (I_N \otimes C)\, x, \end{cases} \tag{8.7}$$

where $x \in \mathbb{R}^{Nn}$ and $y \in \mathbb{R}^N$ are the collections of the states and outputs of the N subsystems.

$$x = \begin{bmatrix} x_1 \\ x_2 \\ \vdots \\ x_N \end{bmatrix}, \; y = \begin{bmatrix} y_1 \\ y_2 \\ \vdots \\ y_N \end{bmatrix}, \text{ and } \Phi(y) := \begin{bmatrix} \phi(y_1) \\ \phi(y_2) \\ \vdots \\ \phi(y_N) \end{bmatrix}.$$

The matrix L is the graph Laplacian of underlying network, see the definition in Section 2.1.

In the context of networks, *synchronization* is one of the important properties, which substantially means that the states of the subsystems can achieve a common value. For a Lur'e network system in (8.7), the definition of *robust synchronization* is given as follows.

Definition 8.1. *[145, 180] A Lur'e network system in form of (8.7) are called robustly synchronized if*

$$\lim_{t\to\infty} (x_i(t) - x_j(t)) = 0, \; \forall i, j = 1, 2, \cdots, N,$$

for all initial conditions and all uncertain nonlinearities $\phi(\cdot, t)$ satisfying (8.4).

Moreover, if the nonlinear function $\phi(\cdot)$ in (8.2) is slope-restricted as in (8.4), then it is also *incremental passive* [136]. Thus, a sufficient condition for robust synchronization of the Lur'e network as in (8.7) can be obtained from [180] as follows.

Lemma 8.1. *Consider the Lur'e network $\mathbf{\Sigma}$ as in (8.7) with a slope-restricted nonlinear function $\phi(\cdot)$. If there exists a matrix $Q \succ 0$ such that*

$$QE = C^T \tag{8.8}$$

and

$$(A + \lambda_i BC)^T Q + Q(A + \lambda_i BC) \prec 0, \tag{8.9}$$

for all $i = 2, \cdots, N$, then $\mathbf{\Sigma}$ robustly synchronize. In (8.9), λ_i are the eigenvalues of the Laplacian matrix L.

8.3 Synchronization Preserving Model Reduction

In this section, the original Lur'e network $\mathbf{\Sigma}$ is assumed to be synchronized, and then we reduce the dimension of each subsystem in (8.2) such that synchronization is preserved in the reduced-order network.

First, the robust synchronization condition of the Lur'e network $\mathbf{\Sigma}$ is reinterpreted by the passivity of a set of auxiliary linear systems as follows.

$$\mathbf{\Gamma}(\lambda_i) : \begin{cases} \dot{\xi} = (A - \lambda_i BC)\xi + E\nu, \\ \eta = C\xi, \end{cases} \tag{8.10}$$

where $\xi \in \mathbb{R}^n$, $\nu, \eta \in \mathbb{R}$, and λ_i is the i-th smallest eigenvalue of the Laplacian matrix L in (8.7). Note that $\mathbf{\Gamma}(\lambda_i)$ is a single-input and single-output system. If the synchronization condition of the multi-agent system $\mathbf{\Sigma}$ in Lemma 8.1 is satisfied, then $A - \lambda_i BC$ is Hurwitz for all $i = 2, 3, \cdots, N$, due to (8.9). That is the auxiliary system $\mathbf{\Gamma}(\lambda_i)$ being asymptomatically stable.

Furthermore, following [174], the conditions in (8.8) and (8.9) coincide with the (strict) *passivity* of $\mathbf{\Gamma}(\lambda_i)$. Therefore, it provides us a way to preserve the robust synchronization in the reduced-order Lur'e network. That is firstly reducing the auxiliary system $\mathbf{\Gamma}(\lambda_i)$ with passivity preservation and then substituting the reduced system matrices to the network framework in (8.7) to generate the reduced-order network system.

Before implementing the above procedure, we introduce the following lemma, where the synchronization condition in Lemma 8.1 is further relaxed by only considering the largest eigenvalue λ_N.

Lemma 8.2. *If there exists a positive definite matrix $\mathcal{Q}$ such that*

$$\begin{bmatrix} A^T\mathcal{Q} + \mathcal{Q}A + C^TC & \lambda_N\mathcal{Q}B & \mathcal{Q}E - C^T \\ \lambda_N B^T\mathcal{Q} & -I & 0 \\ E^T\mathcal{Q} - C & 0 & 0 \end{bmatrix} \prec 0, \tag{8.11}$$

with λ_N is the largest eigenvalue of L in (8.7), then the auxiliary linear system $\mathbf{\Gamma}(\lambda_i)$ in (8.10) is positive real for all $\lambda_i \leq \lambda_N$, and hence the Lur'e network $\mathbf{\Sigma}$ robustly synchronizes.

Proof. The above LMI is equivalent to

$$A^T\mathcal{Q} + \mathcal{Q}A + \lambda_N^2\mathcal{Q}BB^T\mathcal{Q} + C^TC \prec 0, \ \mathcal{Q}E = C^T. \tag{8.12}$$

For a matrix $\mathcal{Q} \succ 0$, we have

$$\begin{aligned} &(A - \lambda_i BC)^T\mathcal{Q} + \mathcal{Q}(A - \lambda_i BC) \\ &= A^T\mathcal{Q} + \mathcal{Q}A - \lambda_i(B^TC^T\mathcal{Q} + \mathcal{Q}BC). \end{aligned} \tag{8.13}$$

Note that

$$\begin{aligned} &\lambda_i(B^TC^T\mathcal{Q} + \mathcal{Q}BC) \\ &= (\lambda_i B^T\mathcal{Q} + C)^T(\lambda_i B^T\mathcal{Q} + C) - \lambda_i^2\mathcal{Q}BB^T\mathcal{Q} - C^TC. \end{aligned} \tag{8.14}$$

For any $\lambda_i \leq \lambda_N$, it then leads to

$$\begin{aligned}
&(A-\lambda_i BC)^T\mathcal{Q}+\mathcal{Q}(A-\lambda_i BC)\\
&\preccurlyeq A^T\mathcal{Q}+\mathcal{Q}A+\lambda_i^2\mathcal{Q}BB^T\mathcal{Q}+C^TC\\
&\preccurlyeq A^T\mathcal{Q}+\mathcal{Q}A+\lambda_N^2\mathcal{Q}BB^T\mathcal{Q}+C^TC\prec 0
\end{aligned} \tag{8.15}$$

where the facts that $(B^T\mathcal{Q}+\lambda_N C)^T(B^T\mathcal{Q}+\lambda_N C)\succcurlyeq 0$ and $\mathcal{Q}BB^T\mathcal{Q}\succcurlyeq 0$ are used. Together with the relation $\mathcal{Q}E=C^T$ in (8.12), we conclude that the system $\mathbf{\Gamma}(\lambda_i)$ with the dynamics in (8.10) is passive for all $\lambda_i \leq \lambda_N$. □

Remark 8.1. *Lemma 8.2 is convenient to be applied as a sufficient condition to check the robust synchronization of the Lur'e network $\mathbf{\Sigma}$, since one just need to show the existence of $\mathcal{Q}$ in (8.11) rather than the solutions of (8.8) and (8.9) for all λ_i with $i=2,\cdots,N$. Furthermore, only using the solutions of the LMI in (8.11), we can reduce the dimension of the auxiliary system $\mathbf{\Gamma}(\lambda_i)$, for any $\lambda_i \leq \lambda_N$.*

The passivity-preserving model reduction is now introduced in the framework of balanced truncation. Let K_M and K_m be the maximum and minimal solutions of (8.11). Let T be a nonsingular coordinate transformation such that

$$TK_M^{-1}T^T=T^{-T}K_mT^{-1}=\Theta=\text{diag}(\theta_1,\theta_2,\cdots,\theta_n), \tag{8.16}$$

with $\theta_1\geq\theta_2\geq\cdots\geq\theta_n>0$. We define the balanced system of $\mathbf{\Gamma}(\lambda_i)$ by $\bar{\mathbf{\Gamma}}(\lambda_i):=(\bar{A}-\lambda_i\bar{B}\bar{C},\bar{E},\bar{C})$, where

$$\bar{A}:=TAT^{-1},\ \bar{B}:=TB,\ \bar{E}:=TE,\ \text{and}\ \bar{C}:=CT^{-1}. \tag{8.17}$$

Now, we truncate the $n-k$ states corresponding to the smallest θ_i of the balanced system $\bar{\mathbf{\Gamma}}(\lambda_i)$. To do so, we consider the following matrix partitions.

$$\begin{aligned}
&\bar{A}=\begin{bmatrix}A_{11}&A_{12}\\A_{21}&A_{22}\end{bmatrix},\bar{B}=\begin{bmatrix}B_1\\B_2\end{bmatrix},\bar{E}=\begin{bmatrix}E_1\\E_2\end{bmatrix},\\
&\bar{C}=\begin{bmatrix}C_1&C_2\end{bmatrix},\Theta=\begin{bmatrix}\Theta_1&\\&\Theta_2\end{bmatrix},
\end{aligned} \tag{8.18}$$

where $A_{11}\in\mathbb{R}^{k\times k}$, $B_1\in\mathbb{R}^k$, $E_1\in\mathbb{R}^k$, $C_1\in\mathbb{R}^{1\times k}$, and $\Sigma_1:=\text{diag}(\theta_1,\theta_2,\cdots,\theta_k)$. Hereafter, denote

$$\hat{A}=A_{11},\ \hat{B}=B_1,\ \hat{E}=E_1,\ \text{and}\ \hat{C}=C_1. \tag{8.19}$$

It can be shown that the matrix $\hat{A}-\lambda_i\hat{B}\hat{C}$ is the k-th order principal submatrix of the system matrix, $\bar{A}-\lambda_i\bar{B}\bar{C}$, in the balanced system $\bar{\mathbf{\Gamma}}(\lambda_i)$. Thus, the truncated model

of $\mathbf{\Gamma}(\lambda_i)$ is presented as

$$\hat{\mathbf{\Gamma}}(\lambda_i) : \begin{cases} \dot{\hat{\xi}} = (\hat{A} - \lambda_i \hat{B}\hat{C})\hat{\xi} + \hat{E}\nu, \\ \hat{\eta} = \hat{C}\hat{\xi}, \end{cases} \tag{8.20}$$

where $\hat{\xi} \in \mathbb{R}^k$ and $\hat{\eta} \in \mathbb{R}$.

Remark 8.2. *Lemma 8.2 actually requires a stricter synchronization condition than Lemma 8.1. However, this is computationally cheaper, as it only need to check the feasibility of (8.11). Moreover, the same pair K_M and K_m can be used for balanced truncation of the linear system $\mathbf{\Gamma}(\lambda_i)$ for all $\lambda_i \leq \lambda_N$.*

Then, the reduced-order dynamics of each agent is constructed by substituting the truncated matrices $\hat{A}$, $\hat{B}$, $\hat{E}$, and $\hat{C}$ to the Lur'e form as in (8.2).

$$\hat{\mathbf{\Sigma}}_\mathbf{i} : \begin{cases} \dot{\hat{x}}_i = \hat{A}\hat{x}_i + \hat{B}u_i + \hat{E}\hat{z}_i \\ \hat{y}_i = \hat{C}\hat{x}_i \\ \hat{z}_i = -\phi(\hat{y}_i) \end{cases} , i = 1, 2, \cdots, N, \tag{8.21}$$

with $\hat{x}_i \in \mathbb{R}^k$, and $\hat{z}_i, \hat{y}_i \in \mathbb{R}$. Consequently, it leads to reduced-order Lur'e network dynamics as

$$\hat{\mathbf{\Sigma}} : \begin{cases} \dot{\hat{x}} = (I_N \otimes \hat{A} - L \otimes \hat{B}\hat{C})\hat{x} - (I_N \otimes \hat{E})\Phi(\hat{y}), \\ \hat{y} = (I_N \otimes \hat{C})\hat{x}, \end{cases} \tag{8.22}$$

comparing to (8.7).

The following theorem shows that the synchronization property is preserved after the above reduction process.

Theorem 8.1. *Consider the full-order Lur'e network $\mathbf{\Sigma}$ in (8.7) and its reduced-order model $\hat{\mathbf{\Sigma}}$ in (8.22). If $\mathbf{\Sigma}$ robustly synchronizes due to Lemma 8.2, then $\hat{\mathbf{\Sigma}}$ also robustly synchronizes.*

Proof. By Lemma 8.1, the system $\hat{\mathbf{\Sigma}}$ robustly synchronizes if the auxiliary system of $\hat{\mathbf{\Sigma}}$ is passive. Therefore, it is sufficient to prove that $\hat{\mathbf{\Gamma}}(\lambda_i)$ in (8.20) is passive for all $\lambda_i \leq \lambda_N$.

Lemma 8.2 implies that the auxiliary system $\mathbf{\Gamma}(\lambda_i)$ is passive, so does the balanced system $\bar{\mathbf{\Gamma}}(\lambda_i)$. It means that

$$(\bar{A} - \lambda_i \bar{B}\bar{C})^T\Theta + \Theta(\bar{A} - \lambda_i \bar{B}\bar{C}) \prec 0, \text{ and } \Theta\bar{E} = \bar{C}^T, \tag{8.23}$$

for $i = 2, 3, \cdots, N$, where Θ is given in (8.16), and $\bar{A}$, $\bar{B}$, $\bar{E}$, and $\bar{C}$ are defined in (8.17). Expanding (8.23) using the partitions as in (8.18) then yields

$$(\hat{A} - \lambda_i \hat{B}\hat{C})^T\Theta_1 + \Theta_1(\hat{A} - \lambda_i \hat{B}\hat{C}) \prec 0, \text{ and } \Theta_1\hat{E} = \hat{C}^T.$$

for $i = 2, 3, \cdots, N$. Hence, the reduced auxiliary system is also passive, which gives the synchronization of the reduced-order model $\hat{\mathbf{\Sigma}}$ by Lemma 8.1. □

8.4 Error Analysis

We start with the analysis of the approximation of the linear dynamics $\mathbf{\Sigma_i^{lin}}$ in (8.3). The linear part of the reduced-order Lur'e subsystem truncation in (8.21) is given by

$$\mathbf{\hat{\Sigma}_i^{lin}}: \begin{cases} \dot{\hat{x}}_i = \hat{A}\hat{x}_i + \begin{bmatrix} \hat{B} & \hat{E} \end{bmatrix} \begin{bmatrix} u_i \\ \hat{z}_i \end{bmatrix} \\ \hat{y}_i = \hat{C}\hat{x}_i \end{cases}, i = 1, 2, \cdots, N. \tag{8.24}$$

For simplicity, we hereafter denote

$$\begin{aligned} &g_B(s) := C(sI_n - A)^{-1}B,\ g_E(s) := C(sI_n - A)^{-1}E, \\ &\hat{g}_B(s) := \hat{C}(sI_k - \hat{A})^{-1}\hat{B},\ \hat{g}_E(s) := \hat{C}(sI_k - \hat{A})^{-1}\hat{E}. \end{aligned} \tag{8.25}$$

Then, we provide the *a priori* error bounds on the linear part in the following lemma.

Lemma 8.3. *Consider the following transfer functions in (8.25) corresponding to the linear parts of the full-order and reduced-order Lur'e subsystems,* $\mathbf{\Sigma_i^{lin}}$ *and* $\mathbf{\hat{\Sigma}_i^{lin}}$*, respectively. The following error bounds hold.*

$$\|g_B(s) - \hat{g}_B(s)\|_{\mathcal{H}_\infty} \leq \frac{2}{\lambda_N} \sum_{k=r+1}^{n} \theta_k, \tag{8.26a}$$

$$\|g_E(s) - \hat{g}_E(s)\|_{\mathcal{H}_\infty} \leq 2 \sum_{k=r+1}^{n} \theta_k, \tag{8.26b}$$

where θ_k *are defined in (8.16).*

Proof. The minimal solution of (8.11), K_m, satisfies

$$K_m \succ 0,\ A^T K_m + K_m A + C^T C \prec 0. \tag{8.27}$$

Analogously, the maximum solution of (8.11), $K_M \succ 0$, satisfies (8.12), which is reformulated as

$$\begin{aligned} &AK_M^{-1} + K_M^{-1}A^T + K_M^{-1}C^T C K_M^{-1} + \lambda_N^2 BB^T \prec 0, \\ &E = K_M^{-1}C^T. \end{aligned} \tag{8.28}$$

Substituting the latter equation into the inequality yields

$$AK_M^{-1} + K_M^{-1}A^T + EE^T + \lambda_N^2 BB^T \prec 0. \tag{8.29}$$

Thus, the following two Lyapunov inequalities hold.

$$AK_M^{-1} + K_M^{-1}A^T + \lambda_N^2 BB^T \prec 0, \tag{8.30a}$$

$$AK_M^{-1} + K_M^{-1}A^T + EE^T \prec 0. \tag{8.30b}$$

Recall the definitions of generalized Gramians in Chapter 2. From (8.27), (8.30a) and (8.30b), the pair K_M^{-1}, K_m can be regarded as generalized Gramians of the systems $\lambda_N \cdot g_B(s)$ and $g_E(s)$. Since the reduced matrices $\hat{A}$, $\hat{B}$, $\hat{E}$ and $\hat{C}$ in the reduced-order models in (8.25) are obtained by the balanced truncation based on the pair K_M^{-1} and K_m. Application of (2.30) in Chapter 2 then leads to the error bounds in (8.26a) and (8.26b). □

Moreover, the approximation error for $\mathbf{\Sigma_i^{lin}}$ in (8.3) is also bounded.

Proposition 8.1. *Let $\mathbf{\Sigma_i^{lin}}$ and $\hat{\mathbf{\Sigma}}_\mathbf{i}^{\mathbf{lin}}$ be the linear parts of the full-order and reduced-order Lur'e subsystems, respectively. The approximation error between the two system is bounded by*

$$\|\mathbf{\Sigma_i^{lin}} - \hat{\mathbf{\Sigma}}_\mathbf{i}^{\mathbf{lin}}\|_{\mathcal{H}_\infty} \leq \frac{2}{\min\{\lambda_N, 1\}} \sum_{k=r+1}^{n} \theta_k, \tag{8.31}$$

with θ_k given in (8.16).

Proof. It then follows from (8.29) that

$$AK_M^{-1} + K_M^{-1}A + \min\{\lambda_N^2, 1\} \begin{bmatrix} B & E \end{bmatrix} \begin{bmatrix} B^T \\ E^T \end{bmatrix} \prec 0. \tag{8.32}$$

Therefore, K_M^{-1} and K_m in (8.27) are generalized Gramians for the linear system $\min\{\lambda_N, 1\} \cdot \mathbf{\Sigma_i^{lin}}$. Following the same reasoning in the proof of Lemma 8.3, we obtain (8.31). □

Now, we investigate the approximation error of each Lur'e subsystem with uncertain nonlinearity $\phi(\cdot)$. Following the procedure in [22], the condition of absolute stability of the reduced-order Lur'e system $\hat{\mathbf{\Sigma}}_\mathbf{i}$ is first discussed.

Proposition 8.2. *By performing the balanced truncation in Section 8.3, the reduced Lur'e-type agent $\hat{\mathbf{\Sigma}}_\mathbf{i}$ in (8.21) is absolutely stable if*

$$\|g_E(s)\|_{\mathcal{H}_\infty} < \mu^{-1} - 2 \sum_{k=r+1}^{n} \theta_k, \tag{8.33}$$

where μ is defined in (8.4).

Proof. The result follows from [22]. If the equation (8.33) holds, then it can be shown that $\|\hat{g}_E(s)\|_{\mathcal{H}_\infty} < \mu^{-1}$. With a Hurwitz $\hat{A}$ matrix in $\hat{\mathbf{\Sigma}}_\mathbf{i}$, we conclude that $\hat{\mathbf{\Sigma}}_\mathbf{i}$ is absolutely stable. □

Then, by assuming that $\hat{\mathbf{\Sigma}}_\mathbf{i}$ in (8.21) is absolutely stable, namely satisfying (8.33), we explore an error bound for the reduction of Lur'e subsystems $\mathbf{\Sigma_i}$. The proof of the following theorem outline is inspired by [22]. Differently, an *a priori* error bound is provided.

Theorem 8.2. *Consider the full-order Lur'e system $\mathbf{\Sigma_i}$ in (8.2) satisfying the slope-restrictedness condition in Assumption 8.2 and the synchronization condition in Lemma 8.2. Denote the reduced-order model of $\mathbf{\Sigma_i}$ by $\hat{\mathbf{\Sigma}}_\mathbf{i}$ in (8.21), which satisfies the absolute stability condition in (8.33). Then, the error of the outputs of $\mathbf{\Sigma_i}$ and $\hat{\mathbf{\Sigma}}_\mathbf{i}$ is bounded by*

$$\|y_i(t) - \hat{y}_i(t)\|_2 \leq \frac{\delta(1+\delta+\epsilon)}{\lambda_N \mu \epsilon(\delta+\epsilon)} \|u_i(t)\|_2, \tag{8.34}$$

where $\delta = 2\sum_{k=r+1}^{n} \theta_k$ and $\epsilon := \mu^{-1} - \delta - \|g_E(s)\|_{\mathcal{H}_\infty} > 0$.

Proof. Taking the Laplace transform of the differential equations in (8.2) and (8.21), respectively, we first obtain

$$y_i(s) = \begin{bmatrix} g_B(s)u_i(s) \\ g_E(s)z_i(s) \end{bmatrix}, \; \hat{y}_i(s) = \begin{bmatrix} \hat{g}_B(s)u_i(s) \\ \hat{g}_E(s)\hat{z}_i(s) \end{bmatrix}, \tag{8.35}$$

where the transfer functions $g_B(s)$, $g_E(s)$, $\hat{g}_B$ and $\hat{g}_E(s)$ are defined in (8.25). Thus, the output error in Laplace domain is presented as

$$y_i(s) - \hat{y}_i(s) = \begin{bmatrix} [g_B(s) - \hat{g}_B(s)]\, u_i(s) \\ g_E(s)z_i(s) - \hat{g}_E(s)\hat{z}_i(s) \end{bmatrix}, \tag{8.36}$$

which leads to

$$\begin{aligned} \|y_i(t) - \hat{y}_i(t)\|_2 \leq\; & \|g_B(s) - \hat{g}_B(s)\|_{\mathcal{H}_\infty} \|u_i(t)\|_2 \\ & + \|g_E(s) - \hat{g}_E(s)\|_{\mathcal{H}_\infty} \|z_i(t)\|_2 \\ & + \|\hat{g}_E(s)\|_{\mathcal{H}_\infty} \|z_i(t) - \hat{z}_i(t)\|_2. \end{aligned} \tag{8.37}$$

Hereafter, we analyze the bound for each component in (8.37) as follows.

First, the transfer function of $y_i(s)$ implies

$$\|y_i(t)\|_2 \leq \|g_B(s)\|_{\mathcal{H}_\infty} \|u_i(t)\|_2 + \|g_E(s)\|_{\mathcal{H}_\infty} \|z_i(t)\|_2, \tag{8.38}$$

and the slope-restrictedness on the uncertain function $\phi(\cdot)$ gives

$$\|z_i(t)\|_2 \leq \mu \|y_i(t)\|_2. \tag{8.39}$$

Substituting (8.38) to (8.39) then yields a bound on $z_i(t)$ as

$$\|z_i(t)\|_2 \leq \frac{\|g_B(s)\|_{\mathcal{H}_\infty}}{\mu^{-1} - \|g_E(s)\|_{\mathcal{H}_\infty}} \|u_i(t)\|_2. \tag{8.40}$$

Following [58], the Riccati inequality (8.12) implies that the transfer function $g_B(s)$ is bounded by $\|g_B(s)\|_{\mathcal{H}_\infty} \leq \lambda_N^{-1}$. Together with the $\mathcal{H}_\infty$ bound on $g_E(s)$ assumed in (8.33), we further obtain

$$\|z_i(t)\|_2 \leq \lambda_N^{-1}(\delta+\epsilon)^{-1}\|u_i(t)\|_2. \tag{8.41}$$

Second, using the slope-restrictedness of $\phi(\cdot)$, we obtain

$$\begin{aligned}
&\|\hat{g}_E(s)\|_{\mathcal{H}_\infty}\|z_i(t)-\hat{z}_i(t)\|_2 \\
&\leq (\|\hat{g}_E(s)-g_E(s)\|_{\mathcal{H}_\infty}+\|g_E(s)\|_{\mathcal{H}_\infty})\cdot\mu\|y_i(t)-\hat{y}_i(t)\|_2 \\
&\leq \left[\delta+(\mu^{-1}-\delta-\epsilon)\right]\cdot\mu\|y_i(t)-\hat{y}_i(t)\|_2 \\
&= (1-\mu\epsilon)\|y_i(t)-\hat{y}_i(t)\|_2.
\end{aligned} \tag{8.42}$$

Now, consider the bounds in Lemma 8.3. Substitution of (8.26a), (8.26b), (8.41) and (8.42) in (8.37) then leads to

$$\begin{aligned}
&\|y_i(t)-\hat{y}_i(t)\|_2 \\
&\leq \lambda_N^{-1}\delta\|u_i(t)\|_2+\lambda_N^{-1}\delta(\delta+\epsilon)^{-1}\|u_i(t)\|_2 \\
&\quad +(1-\mu\epsilon)\|y_i(t)-\hat{y}_i(t)\|_2,
\end{aligned} \tag{8.43}$$

which gives the bound in (8.34). □

Remark 8.3. *The error bound in (8.34) indicates the $\mathcal{H}_\infty$-norm of the error between two Lur'e systems $\mathbf{\Sigma_i}$ and $\hat{\mathbf{\Sigma}}_\mathbf{i}$, see [170].*

8.5 Illustrative Example

The feasibility of the proposed method is illustrated through a simulation, which considers a network consisting of 4 Lur'e subsystems. The interconnection topology is given in Fig 8.2. The dynamics of Lur'e subsystems $\mathbf{\Sigma_i}$ are in (8.2) are given by matrices

$$A = \begin{bmatrix}
0 & 0 & 0 & 0 & 1 & 0 & 0 & 0 \\
0 & 0 & 0 & 0 & 0 & 0.25 & 0 & 0 \\
0 & 0 & 0 & 0 & 0 & 0 & 0.5 & 0 \\
0 & 0 & 0 & 0 & 0 & 0 & 0 & 1 \\
-1 & 0 & 0 & 0 & -3 & 0.25 & 0 & 0 \\
0 & -1 & 0 & 0 & 1 & -1 & 1 & 0 \\
0 & 0 & -1 & 0 & 0 & 0.5 & -2 & 1 \\
0 & 0 & 0 & -1 & 0 & 0 & 0.5 & -2
\end{bmatrix},$$

$$B = \begin{bmatrix} 0 & 0 & 0 & 0 & 0 & 1 & -2 & 2 \end{bmatrix}^T,$$

$$C = E^T = \begin{bmatrix} 0 & 0 & 0 & 0 & 1 & 0 & 0 & 0 \end{bmatrix},$$

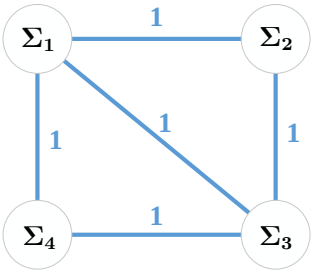

Figure 8.2: Interconnection topology of the Lur'e network

and a nonlinearity

$$\phi(y) = 0.5\left(|y+1| - |y-1|\right). \tag{8.44}$$

By (8.4), we have $\mu = 1$. Therefore, each subsystem is absolutely stable, due to the fact that

$$\|g_E(s)\|_{\mathcal{H}_\infty} = \|C(sI-A)^{-1}E\|_{\mathcal{H}_\infty} = 0.3606 < \mu^{-1} = 1$$

It can be checked that the LMI in (8.11) is feasible, i.e., the solutions of (8.11) exists. Thus, by Lemma 8.2, the original Lur'e network in form of (8.7) synchronizes under the interconnection topology as in Fig. 8.2.

Then, solving the LMI in (8.11) gives maximum and minimal solutions K_M and K_m, which can be simultaneously digitalized as

$$TK_M^{-1}T^T = T^{-T}K_mT^{-1} = \Theta =$$
$$\text{diag}(1, 1, 0.1149, 0.1126, 0.0493, 0.0425, 0.0225, 0.0098).$$

Using the balanced truncation procedure of Section 8.3 to eliminate the last four states in the balanced system leads to the following reduced matrices.

$$A = \begin{bmatrix} 0 & -1 & 0 & 0 \\ 1 & -3 & -1.0742 & 0.7406 \\ 0 & -0.1943 & -1.1737 & 0.3472 \\ 0 & 0.1412 & 1.2461 & -0.5473 \end{bmatrix},$$
$$B = \begin{bmatrix} 0 & 0 & -0.1248 & 0.0841 \end{bmatrix}^T,$$
$$C = E^T = \begin{bmatrix} 0 & 1 & 0 & 0 \end{bmatrix},$$

Therefore, the reduced Lur'e subsystems $\hat{\mathbf{\Sigma}}_\mathbf{i}$ are obtained. For comparison, we show the Bode magnitude plots of the transfer functions $g_B(s)$, $\hat{g}_B(s)$, $g_E(s)$, and $\hat{g}_E(s)$ in Fig 8.3, which indicates that the approximation error on the linear part of

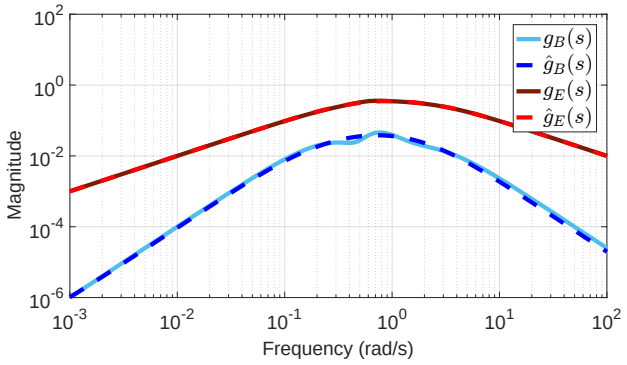

Figure 8.3: The comparison of the Bode magnitude plots of linear parts in the full-order and reduced-order Lur'e subsystems, which show that the linear part of each Lur'e subsystem is well-approximated.

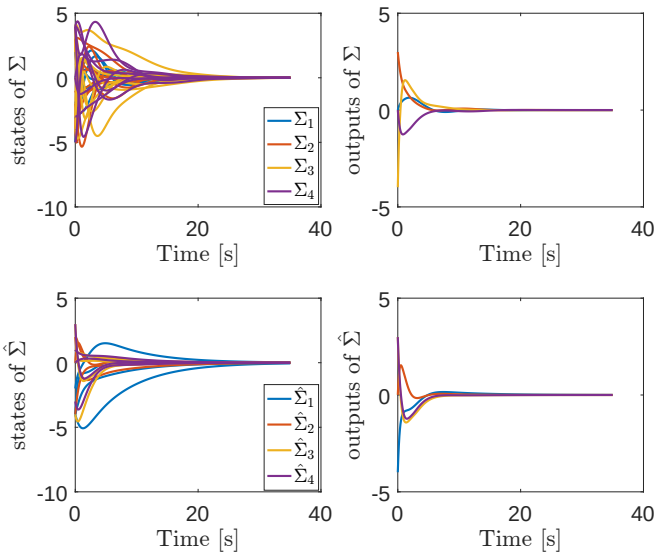

Figure 8.4: The trajectories of the states and outputs of the full-order Lur'e network (in the top two figures) and reduced-order network (in the bottom two figures). The initial states are set to random values for both systems. It shows that both full-order and reduced-order networks are synchronized.

each Lur'e subsystem is small. Moreover, we measure the linear reduction errors by $\mathcal{H}_\infty$ norm as $\|g_B(s) - \hat{g}_B(s)\|_{\mathcal{H}_\infty} \approx 0.0112$, and $\|g_E(s) - \hat{g}_E(s)\|_{\mathcal{H}_\infty} \approx 0.0183$, which using Lemma 8.3, the a priori bounds are obtained as 0.0620 and 0.2481, respectively.

Next, with the dynamics of the reduced-order Lur'e subsystems $\hat{\boldsymbol{\Sigma}}_{\mathbf{i}}$, we construct the a lower-dimensional Lur'e network as in (8.22). Note that both original and reduced Lur'e network in (8.7) and ((8.22)) are autonomous. To investigate the synchronization phenomenon in both systems, we stimulate both systems by assigning random values as their initial states. The trajectories of the states and outputs of both networks are then plotted in Fig. 8.4. We can see that, by the proposed model reduction scheme, the reduced-order Lur'e network preserves the synchronization property.

8.6 Conclusions

In this chapter, we have investigated the problem of model order reduction for Lur'e networks. The proposed method aims at preserving the robust synchronization through the reduction process. To this end, a sufficient condition for robust synchronization of Lur'e networks was presented, which relates to the passivity of a linear auxiliary system. Using the maximum and minimum solutions of (8.11), we reduce the auxiliary system and then obtain the reduced system matrices for Lur'e subsystems. An *a priori* error bound for the Lur'e subsystems can be obtained since the reduction process can also be regarded as Lyapunov balanced truncation based on generalized Gramians for the linear part of each Lur'e subsystem. In the time domain, an *a priori* bound on the input-output error between the full-order and reduced-order Lur'e subsystems is established using the error bound for the linear part and the slope-restrictedness of the uncertain nonlinear function.

CHAPTER 9

Conclusions and Future Research

This thesis has discussed the structure preserving model reduction problem of dynamic network systems. This final chapter summarizes the main results presented in Chapter 3 - 8 and provide an outlook on some potential directions for future research.

9.1 Conclusions

In science and engineering, dynamical systems with interconnection structures are ubiquitous. Since their dynamics are often complex due to large-scale underlying networks and high-dimensional vertex dynamics, this thesis developed model reduction methods to approximate their behaviors by simpler models. The proposed solutions use two methodologies, namely clustering-based projection and generalized balanced truncation, which can reduce the complexity of the network topology and vertex dynamics, respectively. Meanwhile, we also have shown that the proposed methods preserve certain properties of network systems, e.g., synchronization, passivity, and stability throughout the approximation. Therefore, applying the results of this thesis captures the essential properties of interest of large-scale networks and leads to simpler analysis and control design of large-scale interconnected systems.

The framework of clustering-based projection has been developed in Part I, which can be applied to effectively reduce the complexity of different kinds of network systems, e.g., second-order networks, controlled power networks, multi-agent systems, and directed networks. The method provides an effective way of reducing the

number of vertices in dynamic networks and shows a great potential for retaining network structures, namely, obtained reduced-order models can be always interpreted as smaller-sized network systems. In the clustering-based approach, the concept of vertex dissimilarity plays an important role, as it characterizes how different two vertices in a network behave with respect to the external control inputs. With this notation, graph clustering algorithms, that are adapted from data ming or computer graphics [94], can be performed to aggregate the vertices with smaller dissimilarities. Therefore, the results in Part I have extended the domain of clustering problems from static graphs or data to dynamic networks. In Part I, we also introduced the pseudo Gramians for general semistable linear networks. We have shown how one can use them to efficiently evaluate the vertex dissimilarities and then choose an appropriate graph clustering for a large-scale network.

To reduce the dimensions of the subsystems, we have proposed a method based on a conventional model reduction technique, namely, balanced truncation in Part II. First, linear networked passive systems are studied. It is the first time that the celebrated balancing method is used for simultaneously reducing the network topology and nodal dynamics of a network system in a structure preserving manner. Based on two selected generalized Gramians, the balanced truncation is applied to reduce the network structure and agent dynamics in a unified framework. Moreover, we have shown that the synchronization of the network system is preserved, and the approximation error is computed *a priori*, i.e., independent of the dynamics of the reduced-order network model. Furthermore, the generalized balanced truncation has been applied to model reduction of nonlinear Lur'e networks. We have shown that by carefully choosing the generalized Gramian matrices, the linear component of each Lur'e subsystem can be reduced and the robust synchronization property of overall Lur'e networks can be preserved. The idea used in this method provides meaningful insights into the robust synchronization preserving model reduction of networks with nonlinear dynamics.

9.2 Future Research

The clustering-based model reduction approach proposed in this thesis is applied to different types of linear network systems. The reason for that is for linear systems we are able to capture the dynamics of vertices by transfer functions and characterize the vertex dissimilarities by system norms. Moreover, for a linear time-invariant system, the pairwise dissimilarities can be calculated via the Gramian matrices effectively, as shown in Part I. These benefits may not exist when time-variant or nonlinear network dynamics are considered. The nonlinearity of a network can come from two aspects: nonlinear subsystems and nonlinear coupling among the subsystems,

see e.g., [63, 109–111, 147, 176, 179] for more details. Nonlinearities in a network may cause much difficulty with the analysis of graph clustering. The first problem that needs to be tackled is how to design a metric for evaluating the dissimilarities of vertex dynamics. Indeed, in the time domain, $\mathcal{L}_2$ or $\mathcal{L}_\infty$ can be the candidate for the evaluation. However, computing the dissimilarities of every pair of vertices in a large-scale network will be a formidable task. Generally, the further extension to nonlinear networks is still an open question.

The method based on the generalized balanced truncation potentially allows for a better approximation accuracy and also provides an *a priori* error bound, but the price to pay is losing more structure information in the reduced-order model. Although the method in Chapter 7 recovers a network interpretation from the obtained simplified model, the new network is fully connected, i.e., is a complete graph, and the relation between the reduced network and the original one is not clear. Thus, how to design a method that produces sparser reduced networks is another possible research direction. Furthermore, the results in Chapter 8 can be further extended to more general nonlinear systems. For instance, instead of slope-restricted functions, we can consider incremental sector bounded nonlinear functions as the static feedback [38, 180]. Moreover, we may further replace the static nonlinearity with nonlinear dynamics [23, 24], and as a general framework for describing nonlinearities and system uncertainty, we also may use the integral quadratic constraints (IQC), see [5, 115]. This framework includes a number of well-known constraints such as passivity and norm bounds. By exploring the synchronization condition, generalized balanced truncation may be applied.

Bibliography

[1] R. AGAEV AND P. CHEBOTAREV, *On the spectra of nonsymmetric Laplacian matrices*, Linear Algebra and its Applications, 399 (2005), pp. 157–168.

[2] C. C. AGGARWAL AND C. K. REDDY, *Data Clustering: Algorithms and Applications*, CRC press, 2013.

[3] T. AHSENDORF, F. WONG, R. EILS, AND J. GUNAWARDENA, *A framework for modelling gene regulation which accommodates non-equilibrium mechanisms*, BMC Biology, 12 (2014), p. 102.

[4] J. ANDERSON AND A. PAPACHRISTODOULOU, *A decomposition technique for nonlinear dynamical system analysis*, IEEE Transactions on Automatic Control, 57 (2012), pp. 1516–1521.

[5] L. ANDERSSON, A. RANTZER, AND C. BECK, *Model comparison and simplification*, International Journal of Robust and Nonlinear Control, 9 (1999), pp. 157–181.

[6] M. ANDREASSON, E. TEGLING, H. SANDBERG, AND K. H. JOHANSSON, *Coherence in synchronizing power networks with distributed integral control*, in Proceedings of 2017 IEEE 56th Annual Conference on Decision and Control (CDC), Dec 2017, pp. 6327–6333.

[7] A. C. ANTOULAS, *Approximation of large-scale dynamical systems*, vol. 6, SIAM, 2005.

[8] A. ASTOLFI, *Model reduction by moment matching for linear and nonlinear systems*, IEEE Transactions on Automatic Control, 55 (2010), pp. 2321–2336.

[9] B. AVRAMOVIC, P. V. KOKOTOVIC, J. R. WINKELMAN, AND J. H. CHOW, *Area decomposition for electromechanical models of power systems*, Automatica, 16 (1980), pp. 637–648.

[10] Z. BAI, *Krylov subspace techniques for reduced-order modeling of large-scale dynamical systems*, Applied Numerical Mathematics, 43 (2002), pp. 9–44.

[11] Z. BAI AND Y. SU, *Dimension reduction of large-scale second-order dynamical systems via a second-order arnoldi method*, SIAM Journal on Scientific Computing, 26 (2005), pp. 1692–1709.

[12] J. BANASIAK, M. MOKHTAR-KHARROUBI, ET AL., *Evolutionary Equations with Applications in Natural Sciences*, Springer, 2015.

[13] A.-L. BARABÁSI, *Network Science*, Cambridge University Press, 2016.

[14] R. H. BARTELS AND G. W. STEWART, *Solution of the matrix equation* $AX + XB = C$, Communications of the ACM, 15 (1972), pp. 820–826.

[15] A. BEAULIEU, J. DE WILDE, AND J. M. A. SCHERPEN, *Smart Grids from a Global Perspective*, Springer, 2016.

[16] P. BENNER, *Factorized solution of sylvester equations with applications in control*, in Proceedings of the 16th International Symposium on: Mathematical Theory of Network and Systems, Leuven, Belgium, 2004, pp. 1–10.

[17] A. R. BERGEN AND D. J. HILL, *A structure preserving model for power system stability analysis*, IEEE Transactions on Power Apparatus and Systems, PAS-100 (1981), pp. 25–35.

[18] A. BERMAN AND R. J. PLEMMONS, *Nonnegative Matrices in the Mathematical Sciences*, vol. 9, SIAM, 1994.

[19] D. S. BERNSTEIN AND S. P. BHAT, *Lyapunov stability, semistability, and asymptotic stability of matrix second-order systems*, Journal of Mechanical Design, 117 (1995), pp. 145–153.

[20] B. BESSELINK, H. SANDBERG, AND K. H. JOHANSSON, *Model reduction of networked passive systems through clustering*, in Proceedings of the 2014 European Control Conference, Strasbourg, France, 2014, pp. 1069–1074.

[21] B. BESSELINK, H. SANDBERG, AND K. H. JOHANSSON, *Clustering-based model reduction of networked passive systems*, IEEE Transactions on Automatic Control, 61 (2016), pp. 2958–2973.

[22] B. BESSELINK, N. VAN DE WOUW, AND H. NIJMEIJER, *An error bound for model reduction of Lur'e-type systems*, in Proceedings of the 48th IEEE Conference on Decision and Control, 2009 held jointly with the 2009 28th Chinese Control Conference, IEEE, 2009, pp. 3264–3269.

[23] ——, *Model reduction for a class of convergent nonlinear systems*, IEEE Transactions on Automatic Control, 57 (2012), pp. 1071–1076.

[24] ——, *Model reduction for nonlinear systems with incremental gain or passivity properties*, Automatica, 49 (2013), pp. 861–872.

[25] B. BESSELINK, N. VAN DE WOUW, J. M. A. SCHERPEN, AND H. NIJMEIJER, *Model reduction for nonlinear systems by incremental balanced truncation*, IEEE Transactions on Automatic Control, 59 (2014), pp. 2739–2753.

[26] E. BIYIK AND M. ARCAK, *Area aggregation and time-scale modeling for sparse nonlinear networks*, Systems & Control Letters, 57 (2008), pp. 142–149.

[27] S. BOCCALETTI, V. LATORA, Y. MORENO, M. CHAVEZ, AND D.-U. HWANG, *Complex networks: Structure and dynamics*, Physics Reports, 424 (2006), pp. 175–308.

[28] S. BOYD, L. EL GHAOUI, E. FERON, AND V. BALAKRISHNAN, *Linear Matrix Inequalities in System and Control Theory*, SIAM, 1994.

[29] F. BULLO, J. CORTES, AND S. MARTINEZ, *Distributed Control of Robotic Networks: A Mathematical Approach to Motion Coordination Algorithms*, Princeton University Press, 2009.

[30] S. Y. CALISKAN AND P. TABUADA, *Towards Kron reduction of generalized electrical networks*, Automatica, 50 (2014), pp. 2586–2590.

[31] Y. CHAHLAOUI, D. LEMONNIER, A. VANDENDORPE, AND P. VAN DOOREN, *Second-order balanced truncation*, Linear algebra and its applications, 415 (2006), pp. 373–384.

[32] W.-K. CHEN, *Applied Graph Theory*, vol. 13, Elsevier, 2012.

[33] X. CHENG, Y. KAWANO, AND J. M. A. SCHERPEN, *Clustering-based model reduction of network systems with error bounds*, in Proceedings of 22nd International Symposium on Mathematical Theory of Networks and Systems, Minnesota, the USA, 2016, pp. 90–95.

[34] ——, *Graph structure-preserving model reduction of linear network systems*, in Proceedings of 2016 European Control Conference, Aalborg, Denmark, 2016, pp. 1970–1975.

[35] ——, *Reduction of second-order network systems with structure preservation*, IEEE Transactions on Automatic Control, 62 (2017), pp. 5026 – 5038.

[36] ——, *Model reduction of multi-agent systems using dissimilarity-based clustering*, To appear in IEEE Transactions on Automatic Control, (2018).

[37] X. CHENG, J. SCHERPEN, AND B. BESSELINK, *Balanced truncation of networked linear passive systems*, arXiv preprint arXiv:1710.03455, (2017).

[38] X. CHENG, J. SCHERPEN, AND F. ZHANG, *Reduction of robustly synchronized lur'e networks with incrementally sector bounded nonlinearities*, Submitted, (2018).

[39] X. CHENG AND J. M. A. SCHERPEN, *Introducing network Gramians to undirected network systems for structure-preserving model reduction*, in Proceedings of IEEE 55th Conference on Decision and Control, Las Vegas, the USA, Dec 2016, pp. 5756–5761.

[40] X. CHENG AND J. M. A. SCHERPEN, *Balanced truncation approach to model order reduction of Laplacian dynamics*, in Proceedings of the 20th World Congress of the International Federation of Automatic Control (IFAC), Toulouse, France, 2017, pp. 2506–2511.

[41] X. CHENG AND J. M. A. SCHERPEN, *A new controllability Gramian for semistable systems and its application to approximation of directed networks*, in Proceedings of IEEE 56th Conference on Decision and Control, Melbourne, Australia, Dec 2017, pp. 3823–3828.

[42] X. CHENG AND J. M. A. SCHERPEN, *Clustering approach to model order reduction of power networks with distributed controllers*, To appear in Advances in Computational Mathematics, (2018).

[43] ——, *Gramian-based model reduction of directed networks*, Submitted, (2018).

[44] ——, *Robust synchronization preserving model reduction of Lur'e networks*, in Proceedings of the 16th annual European Control Conference (ECC), Limassol, Cyprus, June 2018, pp. 2254–2259.

[45] X. CHENG, J. M. A. SCHERPEN, AND Y. KAWANO, *Model reduction of second-order network systems using graph clustering*, in Proceedings of IEEE 55th Conference on Decision and Control, Las Vegas, the USA, Dec 2016, pp. 7471–7476.

[46] J. H. CHOW, *Power System Coherency and Model Reduction*, Springer, 2013.

[47] J. H. CHOW, R. GALARZA, P. ACCARI, AND W. W. PRICE, *Inertial and slow coherency aggregation algorithms for power system dynamic model reduction*, IEEE Transactions on Power Systems, 10 (1995), pp. 680–685.

[48] S. P. CORNELIUS, W. L. KATH, AND A. E. MOTTER, *Realistic control of network dynamics*, Nature Communications, 4 (2013), p. 1942.

[49] P. DELELLIS AND M. DI BERNARDO, *Adaptive pinning control of complex networks of Lur'e systems*, in Proceedings of the IEEE 51st Annual Conference on Decision and Control (CDC), IEEE, 2012, pp. 6060–6064.

[50] D. A. DIRKSZ AND J. M. A. SCHERPEN, *Port-Hamiltonian and power-based integral type control of a manipulator system*, in Proceedings of the 18th World Congress of the International Federation of Automatic Control (IFAC), Milano, Italy, 2011, pp. 13450–13455.

[51] F. DÖRFLER AND F. BULLO, *Topological equivalence of a structure-preserving power network model and a non-uniform kuramoto model of coupled oscillators*, in Proceedings of IEEE 50th Conference on Decision and Control and European Control Conference (CDC-ECC), Orlando, the USA, 2011, IEEE, pp. 7099–7104.

[52] ——, *Kron reduction of graphs with applications to electrical networks*, IEEE Transactions on Circuits and Systems I: Regular Papers, 60 (2013), pp. 150–163.

[53] ——, *Synchronization in complex networks of phase oscillators: A survey*, Automatica, 50 (2014), pp. 1539–1564.

[54] F. DÖRFLER, M. R. JOVANOVIC, M. CHERTKOV, AND F. BULLO, *Sparsity-promoting optimal wide-area control of power networks*, IEEE Transactions on Power Systems, 29 (2014), pp. 2281–2291.

[55] ——, *Sparsity-promoting optimal wide-area control of power networks*, IEEE Transactions on Power Systems, 29 (2014), pp. 2281–2291.

[56] F. DÖRFLER, J. W. SIMPSON-PORCO, AND F. BULLO, *Breaking the hierarchy: Distributed control and economic optimality in microgrids*, IEEE Transactions on Control of Network Systems, 3 (2016), pp. 241–253.

[57] G.-R. DUAN AND R. J. PATTON, *A note on Hurwitz stability of matrices*, Automatica, 34 (1998), pp. 509–511.

[58] G. E. DULLERUD AND F. PAGANINI, *A Course in Robust Control Theory: A Convex Approach*, Springer, New York, the USA, 2013.

[59] L. FARINA AND S. RINALDI, *Positive Linear Systems: Theory and Applications*, vol. 50, John Wiley & Sons, 2011.

[60] Y. FENG AND M. YAGOUBI, *Robust Control of Linear Descriptor Systems*, Springer, 2017.

[61] S. FIAZ, D. ZONETTI, R. ORTEGA, J. M. A. SCHERPEN, AND A. J. VAN DER SCHAFT, *A port-hamiltonian approach to power network modeling and analysis*, European Journal of Control, 19 (2013), pp. 477–485.

[62] D. M. FORRESTER, *Arrays of coupled chemical oscillators*, Scientific reports, 5 (2015), p. 16994.

[63] M. FRASCA, L. V. GAMBUZZA, A. BUSCARINO, AND L. FORTUNA, *Synchronization in Networks of Nonlinear Circuits: Essential Topics with MATLAB Code*, Springer, 2018.

[64] R. W. FREUND, *Model reduction methods based on krylov subspaces*, Acta Numerica, 12 (2003), pp. 267–319.

[65] K. FUJIMOTO AND J. M. A. SCHERPEN, *Balanced realization and model order reduction for nonlinear systems based on singular value analysis*, SIAM Journal on Control and Optimization, 48 (2010), pp. 4591–4623.

[66] K. GLOVER, *All optimal hankel-norm approximations of linear multivariable systems and their L_∞-error bounds*, International Journal of Control, 39 (1984), pp. 1115–1193.

[67] C. GODSIL AND G. F. ROYLE, *Algebraic Graph Theory*, vol. 207, Springer Science & Business Media, 2013.

[68] G. GOLUB, S. NASH, AND C. VAN LOAN, *A hessenberg-schur method for the problem $AX + XB = C$*, IEEE Transactions on Automatic Control, 24 (1979), pp. 909–913.

[69] E. J. GRIMME, D. C. SORENSEN, AND P. VAN DOOREN, *Model reduction of state space systems via an implicitly restarted lanczos method*, Numerical algorithms, 12 (1996), pp. 1–31.

[70] S. GUGERCIN AND A. C. ANTOULAS, *A survey of model reduction by balanced truncation and some new results*, International Journal of Control, 77 (2004), pp. 748–766.

[71] S. GUGERCIN, A. C. ANTOULAS, AND C. BEATTIE, *H_2 model reduction for large-scale linear dynamical systems*, SIAM Journal on Matrix Analysis and Applications, 30 (2008), pp. 609–638.

[72] C. GUIVER AND M. R. OPMEER, *Error bounds in the gap metric for dissipative balanced approximations*, Linear Algebra and its Applications, 439 (2013), pp. 3659–3698.

[73] J. GUNAWARDENA, *A linear framework for time-scale separation in nonlinear biochemical systems*, PloS one, 7 (2012), p. e36321.

[74] GUOSHAN ZHANG, SHUPING WANG, WANQUAN LIU, AND ZHIQIANG ZUO, *H_∞ norm computation for descriptor symmetric systems*, in 7th Asian Control Conference(ASCC), 2009, pp. 636–641.

[75] H. HAMANN, *Swarm Robotics: A Formal Approach*, Springer, 2018.

[76] T. HATANAKA, N. CHOPRA, M. FUJITA, AND M. W. SPONG, *Passivity-Based Control and Estimation in Networked Robotics*, Springer, 2015.

[77] S. HEO AND P. DAOUTIDIS, *Control-relevant decomposition of process networks via optimization-based hierarchical clustering*, AIChE Journal, 62 (2016), pp. 3177–3188.

[78] S. HEO, W. A. MARVIN, AND P. DAOUTIDIS, *Automated synthesis of control configurations for process networks based on structural coupling*, Chemical Engineering Science, 136 (2015), pp. 76–87.

[79] D. J. HIGHAM, *Modeling and simulating chemical reactions*, SIAM Review, 50 (2008), pp. 347–368.

[80] E. HOGAN, E. COTILLA-SANCHEZ, M. HALAPPANAVAR, S. WANG, P. MACKEY, P. HINES, AND Z. HUANG, *Towards effective clustering techniques for the analysis of electric power grids*, in Proceedings of the 3rd International Workshop on High Performance Computing, Networking and Analytics for the Power Grid, ACM, 2013, p. 1.

[81] F. HORN AND R. JACKSON, *General mass action kinetics*, Archive for Rational Mechanics and Analysis, 47 (1972), pp. 81–116.

[82] T. C. IONESCU, A. ASTOLFI, AND P. COLANERI, *Families of moment matching based, low order approximations for linear systems*, Systems and Control Letters, 64 (2014), pp. 47–56.

[83] T. ISHIZAKI AND J. I. IMURA, *Clustered model reduction of interconnected second-order systems*, Nonlinear Theory and Its Applications, IEICE, 6 (2015), pp. 26–37.

[84] T. ISHIZAKI, K. KASHIMA, A. GIRARD, J.-I. IMURA, L. CHEN, AND K. AIHARA, *Clustered model reduction of positive directed networks*, Automatica, 59 (2015), pp. 238–247.

[85] T. ISHIZAKI, K. KASHIMA, J. I. IMURA, AND K. AIHARA, *Model reduction and clusterization of large-scale bidirectional networks*, IEEE Transactions on Automatic Control, 59 (2014), pp. 48–63.

[86] T. ISHIZAKI, R. KU, AND J.-I. IMURA, *Clustered model reduction of networked dissipative systems*, in Proceedings of 2016 American Control Conference, IEEE, 2016, pp. 3662–3667.

[87] A. J. VAN DER SCHAFT, *On model reduction of physical network systems*, in Proceedings of 21st International Symposium on Mathematical Theory of Networks and Systems, Groningen, The Netherlands, 2014, pp. 1419–1425.

[88] ——, *Modeling of physical network systems*, Systems & Control Letters, 101 (2017), pp. 21 – 27.

[89] A. J. VAN DER SCHAFT, G. ESCOBAR, S. STRAMIGIOLI, AND A. MACCHELLI, *Beyond passivity: port-Hamiltonian systems*, NOLCOS, 2007.

[90] A. J. VAN DER SCHAFT AND B. M. MASCHKE, *Port-hamiltonian systems on graphs*, SIAM Journal on Control and Optimization, 51 (2013), pp. 906–937.

[91] A. J. VAN DER SCHAFT, S. RAO, AND B. JAYAWARDHANA, *Complex and detailed balancing of chemical reaction networks revisited*, Journal of Mathematical Chemistry, 53 (2015), pp. 1445–1458.

[92] A. JADBABAIE, J. LIN, AND A. S. MORSE, *Coordination of groups of mobile autonomous agents using nearest neighbor rules*, IEEE Transactions on automatic control, 48 (2003), pp. 988–1001.

[93] I. M. JAIMOUKHA AND E. M. KASENALLY, *Krylov subspace methods for solving large lyapunov equations*, SIAM Journal on Numerical Analysis, 31 (1994), pp. 227–251.

[94] A. K. JAIN, M. N. MURTY, AND P. J. FLYNN, *Data clustering: a review*, ACM Computing Surveys (CSUR), 31 (1999), pp. 264–323.

[95] C. R. JOHNSON, *Matrix Theory and Applications*, vol. 40, American Mathematical Society, 1990.

[96] H.-J. JONGSMA, P. MLINARIĆ, S. GRUNDEL, P. BENNER, AND H. L. TRENTELMAN, *Model reduction of linear multi-agent systems by clustering with H_2 and H_∞ error bounds*, Mathematics of Control, Signals, and Systems, 30 (2018), p. 6.

[97] T. KACZOREK, *Externally and internally positive time-varying linear systems*, International Journal of Applied Mathematics and Computer Science, 11 (2001), pp. 957–964.

[98] L. KAUFMAN AND P. J. ROUSSEEUW, *Finding groups in data: an introduction to cluster analysis*, vol. 344, John Wiley & Sons, 2009.

[99] H. K. KHALIL, *Nonlinear Systems*, Prentice Hall, New Jersey, the USA, 1996.

[100] J. P. KOELN AND A. G. ALLEYNE, *Stability of decentralized model predictive control of graph-based power flow systems via passivity*, Automatica, 82 (2017), pp. 29–34.

[101] P. V. KOKOTOVIC, R. E. O'MALLEY JR, AND P. SANNUTI, *Singular perturbations and order reduction in control theory—an overview*, Automatica, 12 (1976), pp. 123–132.

[102] P. KUNDUR, N. J. BALU, AND M. G. LAUBY, *Power System Stability and Control*, vol. 7, McGraw-hill New York, 1994.

[103] G. K. LARSEN, N. D. VAN FOREEST, AND J. M. A. SCHERPEN, *Power supply–demand balance in a smart grid: An information sharing model for a market mechanism*, Applied Mathematical Modelling, 38 (2014), pp. 3350–3360.

[104] V. LESSER, C. L. ORTIZ JR, AND M. TAMBE, *Distributed sensor networks: A multiagent perspective*, vol. 9, Springer Science & Business Media, 2012.

[105] J.-R. LI AND J. WHITE, *Low rank solution of lyapunov equations*, SIAM Journal on Matrix Analysis and Applications, 24 (2002), pp. 260–280.

[106] Z. LI, Z. DUAN, AND G. CHEN, *Global synchronised regions of linearly coupled Lur'e systems*, International Journal of Control, 84 (2011), pp. 216–227.

[107] Z. LI, Z. DUAN, G. CHEN, AND L. HUANG, *Consensus of multiagent systems and synchronization of complex networks: a unified viewpoint*, IEEE Transactions on Circuits and Systems I: Regular Papers, 57 (2010), pp. 213–224.

[108] F.-L. LIAN, J. MOYNE, AND D. TILBURY, *Network design consideration for distributed control systems*, IEEE Transactions on Control Systems Technology, 10 (2002), pp. 297–307.

[109] W. LIU AND J. HUANG, *Adaptive leader-following consensus for a class of higher-order nonlinear multi-agent systems with directed switching networks*, Automatica, 79 (2017), pp. 84–92.

[110] X. LIU AND T. CHEN, *Exponential synchronization of nonlinear coupled dynamical networks with a delayed coupling*, Physica A: Statistical Mechanics and its Applications, 381 (2007), pp. 82–92.

[111] ——, *Synchronization of nonlinear coupled networks via aperiodically intermittent pinning control*, IEEE transactions on neural networks and learning systems, 26 (2015), pp. 113–126.

[112] Y. LIU AND B. D. ANDERSON, *Singular perturbation approximation of balanced systems*, International Journal of Control, 50 (1989), pp. 1379–1405.

[113] R. LOZANO, B. BROGLIATO, O. EGELAND, AND B. MASCHKE, *Dissipative Systems Analysis and Control: Theory and Applications*, Springer Science & Business Media, 2013.

[114] O. MAIMON AND L. ROKACH, *Data Mining and Knowledge Discovery Handbook*, Springer-Verlag New York, Inc., Secaucus, NJ, USA, 2005.

[115] A. MEGRETSKI AND A. RANTZER, *System analysis via integral quadratic constraints*, IEEE Transactions on Automatic Control, 42 (1997), pp. 819–830.

[116] H. MEHRJERDI, S. LEFEBVRE, D. ASBER, AND M. SAAD, *Graph partitioning of power network for emergency voltage control*, in Control Conference (ASCC), 2013 9th Asian, IEEE, 2013, pp. 1–6.

[117] M. MESBAHI AND M. EGERSTEDT, *Graph Theoretic Methods in Multiagent Networks*, Princeton University Press, 2010.

[118] D. G. MEYER AND S. SRINIVASAN, *Balancing and model reduction for second-order form linear systems*, IEEE Transactions on Automatic Control, 41 (1996), pp. 1632–1644.

[119] C. MICHELE, S. TRIP, C. D. PERSIS, X. CHENG, A. FERRARA, AND A. V. D. SCHAFT, *A robust consensus algorithm for current sharing and voltage regulation in dc microgrids*, To appear in IEEE Transactions on Control Systems Technology, (2018).

[120] I. MIRZAEV AND J. GUNAWARDENA, *Laplacian dynamics on general graphs*, Bulletin of Mathematical Biology, 75 (2013), pp. 2118–2149.

[121] P. MLINARIĆ, S. GRUNDEL, AND P. BENNER, *Efficient model order reduction for multi-agent systems using QR decomposition-based clustering*, in Proceedings of 54th IEEE Conference on Decision and Control (CDC), Dec 2015, pp. 4794–4799.

[122] ——, *Clustering-based model order reduction for multi-agent systems with general linear time-invariant agents*, in Proceedings of 22nd International Symposium on Mathematical Theory of Networks and Systems (MTNS), 2016, pp. 230–235.

[123] N. MONSHIZADEH, C. DE PERSIS, A. J. VAN DER SCHAFT, AND J. M. A. SCHERPEN, *A novel reduced model for electrical networks with constant power loads*, IEEE Transactions on Automatic Control, (2017).

[124] N. MONSHIZADEH AND A. J. VAN DER SCHAFT, *Structure-preserving model reduction of physical network systems by clustering*, in Proceedings of 53rd IEEE Conference on Decision and Control, IEEE, 2014, pp. 4434–4440.

[125] N. MONSHIZADEH, H. L. TRENTELMAN, AND M. K. CAMLIBEL, *Stability and synchronization preserving model reduction of multi-agent systems*, Systems & Control Letters, 62 (2013), pp. 1–10.

[126] N. MONSHIZADEH, H. L. TRENTELMAN, AND M. K. CAMLIBEL, *Projection-Based Model Reduction of Multi-Agent Systems Using Graph Partitions*, IEEE Transactions on Control of Network Systems, 1 (2014), pp. 145–154.

[127] N. MONSHIZADEH AND A. VAN DER SCHAFT, *Structure-preserving model reduction of physical network systems by clustering*, in IEEE 53rd Annual Conference on Decision and Control (CDC), IEEE, 2014, pp. 4434–4440.

[128] B. C. MOORE, *Principal component analysis in linear systems: Controllability, observability, and model reduction*, IEEE Transactions on Automatic Control, 26 (1981), pp. 17–32.

[129] A. E. MOTTER, S. A. MYERS, M. ANGHEL, AND T. NISHIKAWA, *Spontaneous synchrony in power-grid networks*, Nature Physics, 9 (2013), p. 191.

[130] M. NEWMAN, *Networks: An Introduction*, Oxford university press, 2010.

[131] M. E. NEWMAN, *The structure and function of complex networks*, SIAM Review, 45 (2003), pp. 167–256.

[132] M. E. NEWMAN, *Modularity and community structure in networks*, Proceedings of the national academy of sciences, 103 (2006), pp. 8577–8582.

[133] M. E. NEWMAN AND M. GIRVAN, *Finding and evaluating community structure in networks*, Physical Review E, 69 (2004), p. 026113.

[134] D. B. NGUYEN, J. M. A. SCHERPEN, AND F. BLIEK, *Distributed optimal control of smart electricity grids with congestion management*, IEEE Transactions on Automation Science and Engineering, 14 (2017), pp. 494–504.

[135] G. A. PAGANI AND M. AIELLO, *The power grid as a complex network: a survey*, Physica A: Statistical Mechanics and its Applications, 392 (2013), pp. 2688–2700.

[136] A. PAVLOV AND L. MARCONI, *Incremental passivity and output regulation*, Systems & Control Letters, 57 (2008), pp. 400–409.

[137] R. POLYUGA AND A. VAN DER SCHAFT, *Structure preserving model reduction of port-Hamiltonian systems*, in 18th International Symposium on Mathematical Theory of Networks and Systems, Blacksburg, the USA, 2008.

[138] G. D. POOLE, *Generalized m-matrices and applications*, Mathematics of Computation, 29 (1975), pp. 903–910.

[139] G. C. PYO, J. W. PARK, AND S. I. MOON, *A new method for dynamic reduction of power system using pam algorithm*, in IEEE PES General Meeting, July 2010, pp. 1–7.

[140] A. RANTZER, *Distributed control of positive systems*, in Proceedings of 2011 50th IEEE Conference on Decision and Control and European Control Conference, Dec 2011, pp. 6608–6611.

[141] C. R. RAO AND S. K. MITRA, *Generalized Inverse of Matrices and its Applications*, Wiley New York, 1971.

[142] S. RAO, A. J. VAN DER SCHAFT, AND B. JAYAWARDHANA, *A graph-theoretical approach for the analysis and model reduction of complex-balanced chemical reaction networks*, Journal of Mathematical Chemistry, 51 (2013), pp. 2401–2422.

[143] M. RATHINAM AND L. R. PETZOLD, *A new look at proper orthogonal decomposition*, SIAM Journal on Numerical Analysis, 41 (2003), pp. 1893–1925.

[144] T. REIS AND T. STYKEL, *Positive real and bounded real balancing for model reduction of descriptor systems*, International Journal of Control, 83 (2010), pp. 74–88.

[145] W. REN, R. W. BEARD, AND E. M. ATKINS, *A survey of consensus problems in multi-agent coordination*, in Proceedings of the 2005 American Control Conference, IEEE, 2005, pp. 1859–1864.

[146] H. J. R. RICHARD A. BRUALDI, *Combinatorial Matrix Theory*, Cambridge University Press, 1991.

[147] F. A. RODRIGUES, T. K. D. PERON, P. JI, AND J. KURTHS, *The kuramoto model in complex networks*, Physics Reports, 610 (2016), pp. 1–98.

[148] D. ROMERES, F. DÖRFLER, AND F. BULLO, *Novel results on slow coherency in consensus and power networks*, in Proceedings of the 2013 European Control Conference, Zürich, Switzerland, 2013, IEEE, pp. 742–747.

[149] M. RUBENSTEIN, A. CORNEJO, AND R. NAGPAL, *Programmable self-assembly in a thousand-robot swarm*, Science, 345 (2014), pp. 795–799.

[150] M. G. SAFONOV AND R. CHIANG, *A schur method for balanced-truncation model reduction*, IEEE Transactions on Automatic Control, 34 (1989), pp. 729–733.

[151] B. SALIMBAHRAMI AND B. LOHMANN, *Order reduction of large scale second-order systems using Krylov subspace methods*, Linear Algebra and its Applications, 415 (2006), pp. 385–405.

[152] H. SANDBERG AND R. M. MURRAY, *Model reduction of interconnected linear systems*, Optimal Control Applications and Methods, 30 (2009), pp. 225–245.

[153] G. SCARCIOTTI AND A. ASTOLFI, *Data-driven model reduction by moment matching for linear and nonlinear systems*, Automatica, 79 (2017), pp. 340–351.

[154] S. E. SCHAEFFER, *Graph clustering*, Computer Science Review, 1 (2007), pp. 27–64.

[155] C. SCHERER AND S. WEILAND, *Linear matrix inequalities in control*, Lecture Notes, Dutch Institute for Systems and Control, Delft, The Netherlands, 3 (2000).

[156] J. M. A. SCHERPEN, *Balancing for nonlinear systems*, Systems & Control Letters, 21 (1993), pp. 143–153.

[157] ——, *H_∞ balancing for nonlinear systems*, International Journal of Robust and Nonlinear Control, 6 (1996), pp. 645–668.

[158] J. SCHIFFER, D. GOLDIN, J. RAISCH, AND T. SEZI, *Synchronization of droop-controlled microgrids with distributed rotational and electronic generation*, in Proceedings of 2013 IEEE 52nd Annual Conference on Decision and Control (CDC), IEEE, 2013, pp. 2334–2339.

[159] G. SCUTARI, S. BARBAROSSA, AND L. PESCOSOLIDO, *Distributed decision through self-synchronizing sensor networks in the presence of propagation delays and asymmetric channels*, IEEE Transactions on Signal Processing, 56 (2008), pp. 1667–1684.

[160] B. SINOPOLI, C. SHARP, L. SCHENATO, S. SCHAFFERT, AND S. S. SASTRY, *Distributed control applications within sensor networks*, Proceedings of the IEEE, 91 (2003), pp. 1235–1246.

[161] S. H. STROGATZ, *Exploring complex networks*, Nature, 410 (2001), p. 268.

[162] K. TAN AND K. M. GRIGORIADIS, *Stabilization and H_∞ control of symmetric systems: an explicit solution*, Systems & Control Letters, 44 (2001), pp. 57–72.

[163] M. THOMSON AND J. GUNAWARDENA, *Unlimited multistability in multisite phosphorylation systems*, Nature, 460 (2009), pp. 274–277.

[164] I. TOTONCHI, H. AL AKASH, A. AL AKASH, AND A. FAZA, *Sensitivity analysis for the ieee 30 bus system using load-flow studies*, in 3rd International Conference on Electric Power and Energy Conversion Systems (EPECS), IEEE, 2013, pp. 1–6.

[165] S. TRIP, M. BÜRGER, AND C. DE PERSIS, *An internal model approach to (optimal) frequency regulation in power grids with time-varying voltages*, Automatica, 64 (2016), pp. 240–253.

[166] S. TRIP, R. HAN, M. CUCUZZELLA, X. CHENG, J. M. A. SCHERPEN, AND J. GUERRERO, *Distributed averaging control for voltage regulation and current sharing in dc microgrids: Modelling and experimental validation*, in 7th IFAC Workshop on Distributed Estimation and Control in Networked Systems (NecSys18), Groningen, The Netherlands, pp. 242–247.

[167] S. TRIP, C. MICHELE, X. CHENG, AND J. M. A. SCHERPEN, *Distributed averaging control for voltage regulation and current sharing in dc microgrids*, IEEE Control Systems Letters, 3 (2018), pp. 174 – 179.

[168] S. TRIP, C. MICHELE, C. D. PERSIS, X. CHENG, AND A. FERRARA, *Sliding modes for voltage regulation and current sharing in dc microgrids*, in Proceedings of the 2018 American Control Conference (ACC), Milwaukee, The USA, June 2018, pp. 6778–6783.

[169] A. VAN DER SCHAFT, *Balancing of lossless and passive systems*, IEEE Transactions on Automatic Control, 53 (2008), pp. 2153–2157.

[170] A. J. VAN DER SCHAFT, *L_2-Gain and Passivity Techniques in Nonlinear Control*, vol. 2, Springer, 2000.

[171] O. VERMESAN AND P. FRIESS, *Internet of Things: Converging Technologies for Smart Environments and Integrated Ecosystems*, River Publishers, 2013.

[172] E. VOS, J. M. SCHERPEN, AND A. VAN DER SCHAFT, *Equal distribution of satellite constellations on circular target orbits*, Automatica, 50 (2014), pp. 2641–2647.

[173] D. J. WATTS AND S. H. STROGATZ, *Collective dynamics of 'small-world' networks*, Nature, 393 (1998), pp. 440–442.

[174] J. C. WILLEMS, *Dissipative dynamical systems part II: Linear systems with quadratic supply rates*, Archive for Rational Mechanics and Analysis, 45 (1972), pp. 352–393.

[175] C. W. WU, *Algebraic connectivity of directed graphs*, Linear and Multilinear Algebra, 53 (2005), pp. 203–223.

[176] ——, *Synchronization in Complex Networks of Nonlinear Dynamical Systems*, World Scientific, 2007.

[177] G. XU AND V. VITTAL, *Slow coherency based cutset determination algorithm for large power systems*, IEEE Transactions on Power Systems, 25 (2010), pp. 877–884.

[178] Y. XU, S. M. SALAPAKA, AND C. L. BECK, *Aggregation of graph models and markov chains by deterministic annealing*, IEEE Transactions on Automatic Control, 59 (2014), pp. 2807–2812.

[179] T. YANG, Z. MENG, G. SHI, Y. HONG, AND K. H. JOHANSSON, *Network synchronization with nonlinear dynamics and switching interactions*, IEEE Transactions on Automatic Control, 61 (2016), pp. 3103–3108.

[180] F. ZHANG, H. L. TRENTELMAN, AND J. M. A. SCHERPEN, *Fully distributed robust synchronization of networked Lur'e systems with incremental nonlinearities*, Automatica, 50 (2014), pp. 2515–2526.

[181] K. ZHOU, J. C. DOYLE, AND K. GLOVER, *Robust and optimal control*, vol. 40, Prentice hall New Jersey, 1996.

Summary

This thesis is devoted to the model reduction of network systems. Generally, the study aims to find a low-dimensional approximation with a network structure for a given large-scale dynamical network system. The proposed solutions are developed using two methodologies, namely clustering-based projection and generalized balanced truncation, which are presented in separated parts of this thesis.

A novel reduction method using graph clustering is proposed in Part I to simplify different types of networks. First, interconnected second-order systems are studied. The proposed framework is based on the Petrov-Galerkin projection constructed by graph clustering. The notion of vertex dissimilarity is introduced to characterize how differently the vertices behave with respect to the external control inputs. Then graph clustering is then performed to aggregate the vertices with smaller dissimilarities. The resulting reduced-order model has shown to preserve not only the second-order form but also the network structure. The second network model considered in this thesis is a controlled power network with distributed controllers, which contains two layers: physical transmission links and a communication network interconnecting power generators. The proposed method reduces the two networks simultaneously, and the reduced-order model inherits a network interpretation for the interconnections of the power units and the communication among the generators. Third, we extend the reduction framework of structure preserving model reduction to multi-agent systems, where the subsystems are of higher-dimensions. By comparing the outputs of the agents with respect to external control inputs, we characterize the dissimilarities of the agents. Then, the clustering-based model reduction is applied to obtain a reduced-order model that can be interpreted as a multi-agent system but with fewer agents. At last, we investigate directed network systems that obey locally consensus protocols and have semistable dynamics. The notion of clusterability is proposed to classify the groups of vertices that can be aggregated to guarantee a bounded approximation error. The pairwise dissimilarity, quantifying the difference between two clusterable vertices, is now with respect to both inputs and outputs.

Part II switches our focus to a conventional model reduction technique, balanced truncation, and discusses the possibility of applying this technique to the structure preserving model reduction of network systems. First, we consider networked passive systems, where vertex dynamics are identical and linear time-invariant. Two generalized Gramians that are structured by the Kronecker product are selected such that the balanced truncation is applied to reduce the network structure and agent dynamics in a unified framework. The resulting model can be converted to a new representation of Laplacian dynamics, which again has a network interpretation. We propose a necessary and sufficient condition of a matrix being similar to a Laplacian matrix. Using this result, the reduction process is designed to preserve the Laplacian structure in the reduced network. The method guarantees the a priori computation of a bound on the approximation error with respect to external inputs and outputs. Second, we study another application of generalized balanced truncation to nonlinear Lur'e networks. We aim to reduce the dimension of each nonlinear subsystem and meanwhile preserve the synchronization property of the overall network. The robust synchronization of a Lur'e network can be characterized by a linear matrix inequality, whose solutions then are treated as generalized Gramians for the balanced truncation of the linear component of each Lur'e subsystem. It is verified that, with the same communication topology, the resulting reduced-order network system is still robustly synchronized, and the a priori bound on the approximation error is guaranteed to compare the behaviors of the full-order and reduced-order Lur'e subsystems.

Samenvatting

Dit proefschrift is gewijd aan modelreductie van netwerksystemen. In het algemeen wordt getracht een lage-orde benadering van een gegeven groot-schalige dynamische netwerksysteem te vinden. De voorgedragen oplossingen zijn ontwikkeld met behulp van twee methodologieën: clustervorming-gebaseerde projectie en de gegeneraliseerde balanced truncation (gebalanceerde afkappingsmethode). Deze komen aan de orde in aparte delen van dit proefschrift.

In deel I wordt op basis van graaf clustervorming een nieuwe reductie methode voorgedragen voor het vereenvoudigen van verschillende typen netwerken. Allereerst worden tweede-orde systemen bestudeerd. De voorgedragen methode is gebaseerd op de Petrov-Galerkin projectie die geconstrueerd wordt op basis van graaf clustervorming. We introduceren hierbij het begrip knoop ongelijkheid om het verschillende gedrag van de knopen ten opzichte van externe regel inputs te karakteriseren. Graaf clustervorming is toegepast om knopen met minimaal verschillend gedrag bijeen te voegen. Het wordt aangetoond dat in het verkregen gereduceerde-orde model zowel de tweede-orde vorm als de netwerkstructuur behouden worden.

Het tweede netwerk model dat bestudeerd wordt in dit proefschrift is energie netwerk met gedistribueerde regelaars die uit twee lagen bestaan: een fysieke laag, bestaande uit transmissie verbindingen, en een communicatie laag voor het verbinden van energie generatoren. De voorgedragen methode reduceert beide netwerken tegelijkertijd, en het gereduceerde-orde model heeft een netwerk interpretatie voor de verbindingen tussen de krachtbronnen en communicatie tussen de generatoren.

Als derde breiden we de structuur behoudend modelreductie methode uit naar multi-agent systemen met hoge-orde deelsystemen. Door de outputs van de agenten ten opzichte van de externe regel inputs met elkaar te vergelijken, kan het verschillende gedrag van de agenten gekarakteriseerd worden. Hierna kan de op clustervorming-gebaseerde modelreductie toegepast worden om een gereduceerd-orde model te verkrijgen die geïnterpreteerd kan worden als een multi-agent systeem,

maar dan met minder agenten.

Als laatst bestuderen we gerichte netwerksystemen die zich aan lokale consensus protocollen houden en semistabiele dynamica hebben. Het begrip van clusterbaarheid is voorgesteld om knoop groepen te classificeren die bijeengebracht kunnen worden waarbij een begrensde reductiefout gegarandeerd is. De ongelijkheid van een paar knopen kwantificeert het verschil tussen twee clusterbare knopen nu ten opzichte van zowel de inputs als de outputs.

Deel II is gericht op de klassieke modelreductie techniek balanced truncation (gebalanceerde afkapping). We bestuderen de mogelijkheid voor het toepassen van deze techniek voor structuur behoudend modelreductie van netwerksystemen. Allereerst focussen we op netwerk passieve systemen, waarbij de knoop dynamica identiek en lineair tijds-invariant zijn. Twee gegeneraliseerde Gramians, die gestructureerd zijn door het Kronecker product, zijn geselecteerd opdat de gebalanceerde afkapping toegepast kan worden voor het reduceren van de netwerk structuur en knoop dynamica in een uniform methode. Het verkregen model kan hierna getransformeerd worden naar een nieuwe representatie van Lapliacian dynamica met een duidelijke netwerk interpretatie. We formuleren een noodzakelijke en voldoende voorwaarde voor een matrix om overeenkomstig te zijn met een Laplacian matrix. Middels dit resultaat, wordt het reductie proces ontworpen voor behoud van de Laplacian structuur in het gereduceerde netwerk. De methode garandeert een a priori berekening van een grens voor de reductiefout ten opzichte van externe in-en outputs.

Ten tweede bestuderen we een andere toepassing van gegeneraliseerde gebalanceerde afkapping voor niet-lineaire Lur'e systemen. Ons doel hierbij is het reduceren van de orde van alle individuele niet-lineaire deelsysteem dusdanig dat het synchronisatie karakter van het gehele netwerk behouden blijft. De robuuste synchronisatie van een Lur'e netwerk kan gekarakteriseerd worden door een lineaire matrix ongelijkheid, wiens oplossingen aangemerkt kunnen worden als gegeneraliseerde Gramians voor de gebalanceerde afkapping van het lineaire component van elk Lur'e systeem. Het is geverifieerd dat, met dezelfde communicatie topologie, het verkregen gereduceerde-orde netwerk systeem nog steeds robuust gesynchroniseerd is, en dat de a priori grens voor de reductiefout kan worden berekend om het gedrag van de originele en de gereduceerde-orde Lur'e deelsystemen met elkaar te vergelijken.